TECHNISCHE UNIVERSITÄT MÜNCHEN

TUM School of Life Sciences

Biofilm formation by *Staphylococcus xylosus*

Carolin Josephina Schiffer

Vollständiger Abdruck der von der TUM School of Life Sciences der Technischen Universität München zur Erlangung des akademischen Grades einer

Doktorin der Naturwissenschaften (Dr. rer. nat.)

genehmigten Dissertation.

Vorsitzender:	Prof. Dr. Wilfried Schwab
Prüfende der Dissertation:	1. Prof. Dr. Rudi F. Vogel
	2. Prof. Dr. J. Philipp Benz
	3. Prof. Dr. Friedrich Götz

Die Dissertation wurde am 03.02.2022 bei der Technischen Universität München eingereicht und durch die TUM School of Life Sciences am 02.05.2022 angenommen.

Biofilm formation by *Staphylococcus xylosus*

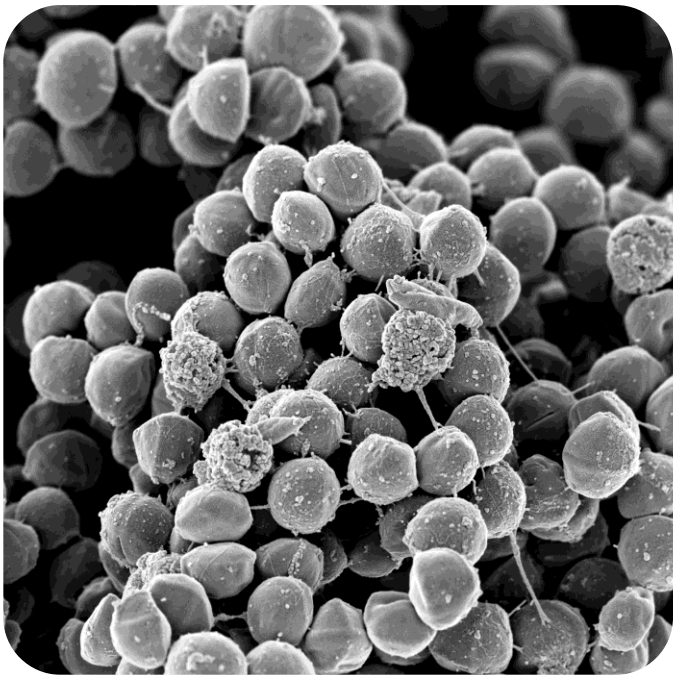

Carolin Josephina Schiffer

Doctoral thesis

Freising, 2022

*Electron microscopy of *S. xylosus* TMW 2.1523; Picture credit: Dr. Christoph Schaudinn

Abbreviations

Aap	accumulation-associated protein
Agr	accessory gene regulator
ANI	average nucleotide identity
Atl	Autolysin
BADGE	Blast diagnostic gene finder
***bap*/Bap**	biofilm-associated protein
BHI	brain heart infusion
BLAST	basic local alignment search tool
BM	basic medium
bp	base pairs
BRIG	BLAST Ring Image Generator
°C	degree Celsius
cas	CRISPR-associated endonucleases
cfu	colony forming units
CM	chloramphenicol
cna	Collagen-binding adhesin
CoNS	coagulase-negative staphylococci
CRA	congo red agar
CRISPR	clustered regularly interspaced short palindromic repeat systems
DNA	deoxyribonucleic acid
dH_2O	deionized water
E.	*Escherichia*
ECM	extracellular matrix
eDNA	extracellular DNA
EDTA	Ethylenediaminetetraacetic acid
Fnbp	Fibronectin-binding protein
HGT	horizontal gene transfer
iBAQ	Intensity-based absolute quantification
ica	intracellular adhesion
IPD	interpulse duration
LB	lysogenic broth
LFQ	Label-free quantification
MATH	microbial adhesion to hydrocarbons
MALDI-TOF MS	Matrix-assisted laser desorption/ionization-time of flight mass spectrometry
MGE	mobile genetic element
MSCRAMMs	microbial surface components recognizing adhesive matrix molecules
n.d.	not determined
NaCl	sodium chloride
NCBI	National Center for Biotechnology Information
OD_{600}	optical density at 600 nm wavelength
ORF	open reading frame
PBS	Phosphate buffered saline
PCR	polymerase chain reaction
PGAP	NCBI prokaryotic genome annotation pipeline

PIA	polysaccharide intercellular adhesin
PNAG	poly-β-(1-6)-N-acetylglucosamine
PSM	phenol-soluble modulin
QS	quorum sensing
RAST	rapid annotation using subsystem technology
RM	restriction modification
S.	*Staphylococcus*
sbp	small basic protein
SD proteins	serine-aspartate repeat-containing proteins
SDS-PAGE	Sodium dodecyl sulfate-polyacrylamide gel electrophoresis
SE	standard error
SMRT	single-molecule real-time
***sxs*A/SxsA**	*Staphylococcus xylosus* surface protein A
***sxs*B/SxSB**	*Staphylococcus xylosus* surface protein B
TMW	Technische Mikrobiologie Weihenstephan
TSA/TSB	tryptic soy agar/broth
vs.	*versus*

Table of contents

List of figures

List of tables

Abstract

The present work encompasses a holistic approach to better understand biofilm formation in *Staphylococcus (S.) xylosus*, a coagulase-negative organism that colonizes human and animal skin as a commensal bacterium and can reach high numbers in fermented foods. To elucidate the molecular mechanisms of biofilm formation and their influence on the occupation and persistence in natural and man-made habitats, five different *S. xylosus* strains were tested for their adhesion behavior. Their genomes were screened for gene homologs that have been described as involved in biofilm formation of other staphylococcal species before. In this context, it was found that in *S. xylosus,* adhesion and exopolymer biosynthesis are mostly polysaccharide (*ica*) independent but rather characterized by eDNA and especially (surface-) proteins. Furthermore, biofilm formation was found to be strain-specific and positively affected by environmental factors such as (fermentation induced) pH decrease, the hydrophilicity of the adhesion surface, and calcium. Comparative genomics predicted a wide range of biofilm-associated homologs previously described for *S. aureus* and *S. epidermidis* as absent in the genomes of *S. xylosus*. Nonetheless, all analyzed strains encode the biofilm-associated gene Bap, with the biofilm negative strain TMW 2.1602 carrying a truncated version of the gene. However, by performing detailed sequence comparisons complemented with phenotypic tests, we could show that *S. xylosus* biofilms differed in key characteristics (i.e. calcium and pH influence) from Bap-mediated *S. aureus* / *S. epidermidis* biofilms. In detail, the protein induces biofilm formation in Bap-positive *S. aureus* strains when low calcium concentrations (< 10 mM) and a low pH value (< 5) are present. Additionally, the deletion of Bap diminished the biofilm positive phenotype of these strains. In contrast, *S. xylosus* encodes a Bap homolog, yet after deletion of the corresponding gene, the phenotype remained biofilm positive. Furthermore, *S. xylosus* is unable to grow below pH values of 5, and calcium was shown to be essential rather than inhibiting for biofilm formation of the organism. Thus, we were able to show that, in contrast to bovine, Bap-positive *S. aureus* isolates, biofilm formation of *S. xylosus* is not mediated by Bap and is induced under different environmental conditions. Therefore, we postulated that another protein should be responsible for adhesion and biofilm formation of the species. By screening the *S. xylosus* genomes in a generic approach for genes harboring characteristic attributes of adherence-mediating surface proteins like an YSIRK-G/S motif signal peptide, an LPxTG cell wall anchor, an extensive repeat region, and a domain folding into structures with high amyloidogenic potential, we were able to identify a new, hitherto not described protein mediating *S. xylosus* biofilm formation. The protein was subsequently characterized and given the name *Staphylococcus xylosus*

surface protein A (SxsA). Hereby, both macro-and microscopic analyses revealed that SxsA mutants exhibit a reduced multicellular behavior and a reduced biofilm forming phenotype. Again, SxsA deletion has a different effect on the two investigated strains; while both strains showed impaired biofilm formation, a reduction in adherence to polystyrene of around 90 - 100% was obtained for *S. xylosus* TMW 2.1523, compared to a reduction of up to 50% in TMW 2.1023 (reduction values depend on the type of support and medium composition used in the experiments). Since TMW 2.1023 encodes an additional surface protein with a predictively similar function on one of its plasmids, we suggest that this might be the cause of the only partially observed reduction. Again, this emphasizes how a heterogenic genetic background impacts strain-specific phenotypes of a species. As the results of this work were largely based on genetic manipulation experiments, a part of this work was dedicated to restriction modification systems and barriers of horizontal gene transfer. Hereby, we were able to show that *S. xylosus* harbors strong barriers to the introduction of plasmid DNA. In this context, the methylome of *S. xylosus* was characterized, a novel variant of type I restriction modification (RM) systems that requires two instead of one specificity subunits for specific DNA methylation (*hsd*RSMS) was identified, and the respective DNA motif recognition sequences were determined. In a last step, this study presents some insights into metabolic changes of cells that are part of a biofilm compared to cells grown in planktonic culture. In this regard, changes associated with fermentative energy gain of sessile cells were most prominent. We also found that phenol-soluble modulins (PSMs) were highly expressed in planktonic samples. PSMs are a group of amphipathic peptides known to structure biofilms and promote cell dissemination through their biofilm-destructive properties. All in all, we could show that cells under biofilm conditions are exposed to different stressors (such as low oxygen and pH) to which they can adapt through several different metabolic changes.

In summary, this work contributes to a better understanding of the biofilm formation mechanisms of the species *S. xylosus* and presents additional, previously unknown factors that critically shape attachment and cell aggregation behavior within the species.

Zusammenfassung

Die vorliegende Arbeit dient dem verbesserten Verständnis der Biofilmbildung bei *Staphylococcus (S.) xylosus*, einem koagulase-negativen Organismus, der als kommensales Bakterium die Haut von Menschen und Tieren besiedelt und in hohen Zellzahlen in Lebensmittelfermentationen auftritt. Zur Aufklärung der molekularen Mechanismen der Biofilmbildung und ihres Einflusses auf die Besiedlung und Persistenz in natürlichen und menschgemachten Lebensräumen, wurden fünf verschiedene *S. xylosus* Stämme auf ihr Adhäsionsverhalten analysiert. Dabei wurden ihre Genome auf Gene untersucht, von denen bekannt ist, dass sie an der Biofilmbildung anderer Staphylokokken beteiligt sind. Es zeigte sich, dass Adhäsion und Exopolymerbiosynthese bei *S. xylosus* weitestgehend Polysaccharid-unabhängig sind und vielmehr durch eDNA und vor allem (Oberflächen-)Proteine geprägt werden. Darüber hinaus konnte festgestellt werden, dass die Biofilmbildung stammspezifisch ist und positiv von Umweltfaktoren wie der (fermentationsbedingten) pH-Absenkung, Hydrophilie der Adhäsionsoberfläche und Kalzium abhängt. Vergleichende genomische Analysen ergaben, dass eine Vielzahl von Biofilm-assoziierten Homologen, die zuvor für *S. aureus* und *S. epidermidis* beschrieben wurden, in den Genomen von *S. xylosus* fehlen. Dennoch kodieren alle untersuchten Stämme das Biofilm-assoziierte Gen Bap, wobei der Biofilm-negative Stamm TMW 2.1602 jedoch eine mutierte Version des Gens trägt. Über einen detaillierten Sequenzvergleich und ergänzende phänotypische Tests, konnte gezeigt werden, dass sich *S. xylosus* Biofilme in wichtigen Merkmalen (Kalzium- und pH-Einfluss) von Bap-vermittelten *S. aureus* / *S. epidermidis*-Biofilmen unterscheiden. Besser gesagt bestimmt das Protein die Biofilmbildung in Bap-positiven *S. aureus*-Stämmen nur dann, wenn niedrige Kalziumkonzentrationen (< 10 mM) und ein niedriger pH-Wert (< 5) vorliegen. Wichtiger aber ist, dass die Bakterien nach Ausknocken von Bap, ihre Fähigkeit einen Biofilm zu bilden, verlieren. *S. xylosus* codiert zwar ein Bap-Homolog, jedoch blieb nach Deletion des entsprechenden Gens der Phänotyp Biofilm-positiv. Ebenfalls ist *S. xylosus* nicht in der Lage, in einer Umgebung mit einem pH-Wert kleiner 5 zu wachsen. Außerdem ist Kalzium für die Biofilmbildung des Organismus essenziell statt hemmend. Das zeigt, dass die Biofilmbildung von *S. xylosus* im Gegensatz zu *S. aureus* Isolaten aus Rindern nicht durch Bap bestimmt wird. Folglich nahmen wir an, dass ein anderes Protein für Adhäsion und Biofilmbildung bei *S. xylosus* verantwortlich sein muss. Durch Screening der *S. xylosus* Genome auf Gene, die charakteristische Merkmale von Adhäsions-vermittelnden Oberflächenproteinen aufweisen, wie z.B. ein YSIRK-G/S-Signalpeptid, ein LPxTG-Zellwandanker, eine Region mit Sequenzwiederholungen und eine Domäne, die sich zu Strukturen mit hohem amyloidogenem

Potenzial faltet, konnten wir ein neues, bisher nicht beschriebenes Protein identifizieren, das die Biofilmbildung von *S. xylosus* maßgeblich mitbestimmt. Das Protein wurde anschließend umfassend charakterisiert und erhielt den Namen *Staphylococcus xylosus* surface protein A (SxsA). Dabei zeigten sowohl makro- als auch mikroskopische Analysen, dass SxsA-Mutanten ein vermindertes Aggregationsverhalten sowie eine verringerte Biofilmbildung aufweisen. Auch hier hat die Deletion von SxsA einen unterschiedlichen Effekt auf die beiden verwendeten Stämme; während beide Stämme in ihrer Biofilmbildung beeinträchtigt waren, wurde bei *S. xylosus* TMW 2.1523 eine Reduktion der Anheftung an Polystyrol von etwa 90 - 100% erreicht, verglichen mit einer Reduktion von < 50% bei TMW 2.1023 (die Werte hängen von der Art des Trägermaterials und der Zusammensetzung des Wachstumsmediums ab). Da TMW 2.1023 auf einem seiner Plasmide ein zusätzliches Oberflächenprotein mit einer möglicherweise ähnlichen Funktion kodiert, vermuten wir, dass dies die Ursache für die partielle Verringerung des Biofilms sein könnte. Dies unterstreicht abermals den heterogenen genetischen Hintergrund und die stammspezifischen Phänotypen der Art. Da die Ergebnisse dieser Arbeit größtenteils auf Experimenten beruhen, die Genmodifikationen benötigen, wurden Restriktionsmodifikationssystemen und Barrieren gegenüber horizontalen Gentransfers, näher untersucht. Dabei konnten wir zeigen, dass *S. xylosus* starke Barrieren gegenüber der Aufnahme von Plasmid-DNA aufweist. Zusätzlich charakterisieren wir das Methylom von *S. xylosus*. Dabei wurde ein neuartiges Typ I Restriktionsmodifikationssystem (RM) identifiziert, welches zwei Spezifitätsuntereinheiten für eine spezifische DNA-Methylierung benötigt (*hsd*RSMS). Zuletzt bietet diese Arbeit einen Einblick in die metabolischen Veränderungen von Zellen, die entweder Teil eines Biofilms sind oder in Flüssigkultur gewachsen. Hierbei sind in den Biofilmzellen Veränderungen, die im Zusammenhang mit der fermentativen Energiegewinnung stehen, am ausgeprägtesten. Ebenfalls konnten wir zeigen, dass „Phenol-soluble modulins (PSM)“ in Flüssigproben deutlich häufiger vorkommen. PSMs sind eine Gruppe amphipathischer Peptide und dafür bekannt, dass sie Biofilme strukturieren und die Verbreitung von Zellen durch ihre biofilmzerstörenden Eigenschaften fördern. Insgesamt konnten wir zeigen, dass Zellen unter Biofilm-Bedingungen verschiedenen Stressfaktoren (wie niedrigem Sauerstoff und pH-Wert) ausgesetzt sind, an die sie sich mit verschiedensten metabolischen Veränderungen anpassen können.

Zusammenfassend trägt diese Arbeit zu einem besseren Verständnis der Mechanismen der Biofilmbildung der Spezies *S. xylosus* bei und zeigt zusätzliche, bisher unbekannte Faktoren auf, die das Anheftungs- und Zellaggregationsverhalten innerhalb der Spezies entscheidend mitbestimmen.

1 Introduction

1.1 *Staphylococcus xylosus*

Staphylococcus (S.) xylosus are Gram-positive, catalase-positive cocci that were first described by Schleifer and Kloos in 1975 and that belong to the large group of coagulase-negative staphylococci (CoNS). CoNS are a very heterogeneous, constantly expanding group of species that preferentially colonize the skin and mucous parts of humans and animals (Becker et al., 2020). *S. xylosus* is also recognized as a commensal of mammalian skin, constituting a prominent commensal, especially of farm animals and small mammals (Kloos et al., 1976; Nagase et al., 2002). The species is furthermore of high biotechnological value as it is commonly used as a starter organism in food fermentations, especially in raw sausage fermentations in which it contributes to aroma formation and color stabilization (Stahnke, 1994; Vos et al., 2009; Toldrá, 2015; Leroy et al., 2017). The latter is mediated by the reduction of nitrate to nitrite (nitrate reductase activity), which results in the formation of nitrosylmyoglobin, a substance responsible for the red color of meat products (Gøtterup et al., 2007; Vermassen et al., 2014). Other reasons for using *S. xylosus* as a starter culture in food fermentations include its ability to outcompete the autochthonous microbiota, i.e. undesired species such as *S. equroum* and *S. saprophyticus*, thereby contributing to a stable and controlled fermentation process (Hutkins, 2006; Toldrá, 2015; Laranjo et al., 2019). Controlled fermentations serve not only to suppress unwanted and pathogenic bacteria but also to control for the production of biogenic amines, the prevalence of transmissible antibiotic-resistance genes, and a reduced likelihood of off-flavors (Leroy et al., 2006; Resch et al., 2008; Seitter et al., 2011; Laranjo et al., 2019). Factors that determine the ability of an organism to outcompete the autochthonous microbiota during fermentation processes include an increased tolerance to the hurdles provided by the fermented product, the production of antimicrobial compounds, faster depletion of growth substrates as well as to colonize the cavities of a given matrix, occupying the niche, and thereby repressing any unwanted organisms. Hurdles that have to be faced by staphylococci during raw sausage fermentations include a low pH induced by lactic acid bacteria, low a_w values caused by the drying process, as well as nitrosative and oxidative stress due to the presence of curing salts and reactive oxygen species (Vermassen et al., 2014; Toldrá, 2015; Vermassen et al., 2016; Leroy et al., 2017). The occupation of natural habitats and the associated suppression of undesirable microorganisms is also known as colonization resistance, a principle of high value in intestinal research (Lawley and Walker, 2013). First insights into factors that promote the assertiveness and/or expression

of colonization resistance in fermented foods have been reported for lactobacilli in previous studies on sausage fermentations (Janßen et al., 2018). Hereby, the principle of cooperation (Eisenbach et al., 2019), inhibition by bacteriocins (Janßen et al., 2020), and adhesive functions that can be mediated by surface glycosyltransferases (Widenmann et al., 2022) were described. None of these principles has yet been described for *S. xylosus*. Biofilm formation is of lesser importance in lactobacilli but the preferred lifestyle of staphylococci. For the latter, it can promote niche occupancy and persistence in stressful environments.

An emerging research topic over the past years has been the evaluation of the virulence of coagulase-negative staphylococci, bringing up some good reviews, summarizing the presence of virulence factors among the different species (Otto, 2004; Rogers et al., 2009; Heilmann et al., 2019; França et al., 2021). They mainly discuss clinical studies that have isolated CoNS from infections and address the occurrence of antibiotic resistance, hemolysis, and enterotoxin genes, as well as the species' ability to form biofilms. Special focus is usually on *S. epidermidis*, which is by far the most prominent CoNS species with the highest clinical importance. Due to its natural occurrence on mammal skin combined with its strong ability to form biofilms and adhere to surfaces, *S. xylosus* has been repeatedly associated with infections in the past as well, in particular mastitis infections (Gozalo et al., 2010; Supré et al., 2011; Condas et al., 2017; Brand and Rufer, 2021; Buck et al., 2021). Yet, studies hereon have to be considered with care, as it is hard to distinguish whether an organism is the causative agent of an infection or whether it is isolated from infected tissue as a contaminant because it is a commensal of the skin. In terms of the prevalence of staphylococcal enterotoxin genes among *S. xylosus* isolates, the current data available is controversial. Even though a few studies detected certain staphylococcal enterotoxin genes (*sec, seh*) among *S. xylosus* isolates, a clear connection between CoNS and food poisoning outbreaks has not been demonstrated so far (Martín et al., 2006; Zell et al., 2008; Talon and Leroy, 2011). In the end, the topic causing the deepest concern in regard to the safety evaluation of *S. xylosus* strains is the prevalence and spread of antibiotic resistance genes. Studies reported a vast variety of transmissible antibiotic resistance genes in *S. xylosus*, among them resistances to some of the main antibiotics used in human and veterinary medicine such as ampicillin, chloramphenicol, erythromycin, fosfomycin, penicillin, rifampicin, streptomycin, tetracycline, and vancomycin (Martín et al., 2006; Resch et al., 2008; Even et al., 2010; Leroy et al., 2019; Buck et al., 2021; França et al., 2021).

Eventually, the trend is towards carefully choosing starter culture strains, not just with respect to potential safety hazards but also ensuring their persistence upon sausage fermentation, limitation of unwanted autochthonous staphylococci, and considering and promoting specific functional properties such as color and aroma formation and reproducible fermentation processes.

1.2 Biofilm formation in *Staphylococcus spp.*

The ability to form biofilm is essential to almost all existing bacterial species. The term bacterial biofilm formation was first defined by Costerton et al., (1978). Per definition, a biofilm is a microbial community of sessile cells that either adhere to a surface or to each other and that are embedded into a self-produced extracellular polymeric matrix (Donlan and Costerton, 2002). The extracellular matrix usually consists of three major components, namely polysaccharides, proteins, and extracellular DNA (eDNA) with lipids, extracellular bacterial structures (e.g., flagella) and humic substances being of minor importance as well (Flemming and Wingender, 2010). Advantages of colonizing surfaces, forming a biofilm and living in a stable microbial consortium include protection against desiccation, phagocytosis, antibiotics and other antimicrobial substances (e.g., metallic cations, ultraviolet radiation) as well as escaping host defense mechanisms (Vuong et al., 2004; Otto, 2006; Flemming and Wingender, 2010; Tremblay et al., 2014). Traditionally, three major stages are associated with the biofilm cycle of bacteria, as depicted in Figure 1: (i) the initial attachment of cells mediated by hydrophobic interactions, electrostatic forces, wall teichoic acids, eDNA and/or specific adhesins (ii) biofilm accumulation and maturation including cell proliferation and the synthesis of the extracellular matrix, and (iii) cell detachment, driven by enzymes (nucleases, proteases) and phenol-soluble modulins ((PSMs), Gross et al., 2001; Qin et al., 2007; Otto, 2008; Schilcher and Horswill, 2020). The dynamics between these three stages, between planktonic and sessile cell growth as well as the biofilm matrix composition, are tightly regulated and often driven by environmental cues such as the availability of nutrients, variations within the bacterial community and experienced mechanical signals such as shear forces, temperature and osmolarity (Rachid et al., 2000a; Rachid et al., 2000b; Knobloch et al., 2001; Otto, 2008; Karatan and Watnick, 2009; Flemming and Wingender, 2010; Lawal et al., 2021)

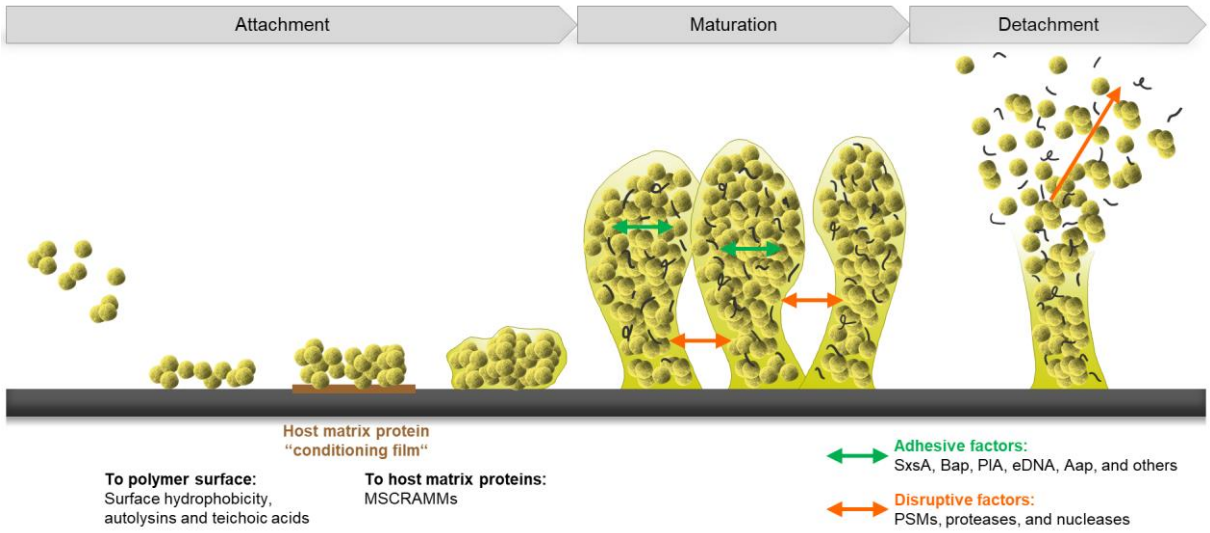

Figure 1: Traditional three stage biofilm model, describing the three phases of biofilm development. Biofilm formation starts with initial attachment of cells to a surface or the host matrix, followed by the aggregation of cells through adhesive factors and embedding cells in an extrapolymeric matrix. Channel formation in mature biofilms is mediated by disruptive factors, which also facilitates the release of cells into the environment, ready to colonize other surfaces. This figure was inspired by Otto, (2013b).

Mechanisms of biofilm formation are multifactorial, differing between organisms but also between species and strains (Tremblay et al., 2013; Schiffer et al., 2019; Lamret et al., 2021; Lawal et al., 2021). This applies to *Staphylococcus spp*. as well. The first major findings on the accumulation mechanisms of staphylococci in biofilms have been made by Mack et al., (1994) and Heilmann et al., (1996a; 1996b). Using transposon mutagenesis, they discovered that an operon (*ica*ADBCR) synthesizing an extracellular polysaccharide (polysaccharide intercellular adhesin PIA, β(1,6)-*N*-acetylglucosaminoglycan) is a major component of staphylococcal biofilm matrices. Over the years, research evolved and *ica*-negative, biofilm positive strains were reported (Cucarella et al., 2004; Tormo et al., 2005), which opened the debate for further, non-polysaccharide mediated adhesion and cell accumulation mechanisms of *Staphylococcus spp*. Hereby, two additionally important components were identified, namely proteins and eDNA. A large variety of different proteins is either involved in primary attachment and/or in biofilm accumulation (Foster et al., 2014; Speziale et al., 2014; Foster, 2020). Proteins mediating primary attachment to abiotic surfaces include sortase-attached surface proteins, such as the biofilm-associated protein Bap, the accumulation-associated protein Aap or Fibronectin-binding proteins ((FnBPs), Cucarella et al., 2001; Conlon et al., 2014; McCourt et al., 2014). Moreover, the major autolysin (AtlA, AtlE) is considered as an important factor in the attachment of cells to abiotic surfaces such as polystyrene (Heilmann et al., 1997; Biswas et al., 2006). Proteins mediating primary attachment to components of the extracellular host matrix are summarized under the term microbial surface components recognizing adhesive matrix molecules

((MSCRAMMs), Foster, 2019). MSCRAMMs are a family of proteins, which share structural similarities such as a C-terminal cell wall anchor (LPxTG), Ig-like folds and a common mechanism for ligand binding that includes the interaction of two adjacent subdomains (Foster et al., 2014; Foster, 2019). The family encompasses specific adhesins, such as the collagen adhesion protein ((Cna), Patti et al., 1992), fibronectin-binding proteins (FnBP) A and B (Jönsson et al., 1991; Hartford et al., 2001), clumping factor (Clf) A and B (McDevitt et al., 1994; Ní Eidhin et al., 1998) as well as elastin- (EbpS) and laminin- (Eno) binding proteins (Downer et al., 2002; Carneiro et al., 2004). Proteins involved in biofilm accumulation processes have been characterized in depth in the past years. Basically, two proteins underwent extensive characterization, the biofilm-associated protein Bap, first reported in *S. aureus* V329 (Cucarella et al., 2001) as well as the accumulation-associated protein Aap of *S. epidermidis* (Rohde et al., 2005) and its *S. aureus* homolog the *Staphylococcus aureus* surface protein G ((SasG), Corrigan et al., 2007). Both proteins contribute to intercellular adhesion by the formation of amyloid fibers, even though the respective mechanisms differ slightly. Bap is cleaved extracellularly and while the C-terminal part remains bound to the cell surface having a yet unknown function, N-terminal peptides self-assemble into amyloid fibers under low pH (< 5) and low calcium (< 10 mM) concentrations, thereby linking cells together (Taglialegna et al., 2016b). Aap is also processed extracellularly in the N-terminal part. Yet, in this case, the polypeptide that remains on the cell surface (exposed G5-E domains) mediates the accumulation of neighboring cells by homophilic interactions, a reaction dependent on the presence of Zn^{2+} and followed by the irreversible formation of amyloid fibers in the course of biofilm maturation (Conrady et al., 2008; Geoghegan et al., 2010; Yarawsky et al., 2020). Other proteins, which are not associated with the cell wall, can also contribute to biofilm accumulation, such as the recently characterized 18 kDa small basic protein Sbp (Decker et al., 2015) and the extracellular adherence protein Eap (Yonemoto et al., 2019).

Next to extracellular polysaccharides and proteins, eDNA was identified as highly important in biofilm formation of *Staphylococcus spp*. Reports about the origin of eDNA are controversial, but the major autolysin (AtlA/AtlE) is reported to play a dominant role in mediating lysis of a subpopulation of cells. Furthermore, phage release in biofilms with subsequent cell lysis has been reported to occur frequently (Resch et al., 2005). Released eDNA features a structural component of the matrix, supporting its stability and integrity (Qin et al., 2007; Bose et al., 2012; Okshevsky and Meyer, 2015). Besides cell lysis, active excretion of DNA is speculated to be another source for eDNA as well (Biswas et al., 2006; Qin et al., 2007; Flemming and

Wingender, 2010). In *S. xylosus* the impact of eDNA on biofilm formation was recently investigated by transcriptomic and microscopic analysis of strain C2a (Leroy et al., 2021). Thereby, the authors confirmed the critical role of eDNA in *S. xylosus* biofilm formation and proposed two mechanisms of cell lysis mediated eDNA release, namely lytic phage activity and the CidABC system. The latter encodes a holin protein, regulating murein hydrolase activity (Leroy et al., 2021).

In conclusion, much is known on biofilm forming mechanisms of staphylococcal species such as *S. aureus* and *S. epidermidis*, which have been extensively characterized by intensive research, but very little is known on the respective mechanisms in underrated species such as *S. xylosus*, *S. saprophyticus* or *S. cohnii*.

1.3 Horizontal gene transfer and genetic manipulation in *Staphylococcus spp*.

Horizontal gene transfer (HGT) generally refers to the transfer of genes among more or less closely related organisms (Koonin et al., 2001). HGT is known to shape prokaryotic evolution and the emergence of organismal phylogeny. This applies especially for microorganisms associated with the skin microbiome. Studies suggest that more than 50% of the total genes in the genomes of the human microbiota were transferred by HGT, an effect that is particularly enhanced by the physical proximity of microorganisms on human skin (Jeong et al., 2019). HGT is further an emerging topic in the field of coagulase-negative staphylococcal research as there is increasing evidence that CoNS might serve as a hidden reservoir for antibiotic and virulence genes, which can, if transferred, enhance the colonization and persistence potential of *S. aureus* during infections (Otto, 2013a; Leroy et al., 2019). Biofilms are most likely an environment in which the exchange of DNA is favored as well. Again, by the close proximity of the cells, but also due to the availability of large amounts of extracellular DNA (Abe et al., 2020). Since biofilms are usually composed of multiple species, HGT can likely occur across species levels. Recent studies on this revealed that HGT does occur in biofilms, yet at least plasmid transfer seems to be limited to the outer layers of the biofilm where bacteria are metabolically most active (Stalder and Top, 2016). Still, it is important to understand the possibilities of HGT and its mechanisms between staphylococcal species also including the protective barriers that organisms naturally possess against HGT. These include surface exclusion as well as restriction systems (Thomas and Nielsen, 2005). The latter comprises, among others, CRISPR/Cas, phosphorothioate-, BREX- and restriction modification (RM) systems (Thomas and Nielsen, 2005; Lindsay, 2019; Wang et al., 2019; Nye et al., 2020). The appearance of phosphorothioate- and

BREX systems has been predominantly described for *Streptomyces spp., Pseudomonas spp.* (Wang et al., 2019) and *Bacillus spp.* (Goldfarb et al., 2015) so far. The occurrence of CRISPR/Cas systems in CoNS is reported as low, with studies implicating only 9% of *S. epidermidis* and 3% of *S. haemolyticus* isolates harboring CRISPR/Cas systems (Rossi et al., 2017). RM systems, on the other hand, have been shown to provide an effective barrier to the uptake of exogenous DNA in *S. aureus* and *S. epidermidis* (Monk et al., 2015; Lee et al., 2019). Such barriers can be beneficial for a bacterium in its natural habitats, especially for protection against bacteriophage attacks and unwanted genetic information encoded on conjugative plasmids (metabolic burden). On the other hand, if they are too strong, the bacterium cannot profit from the evolutionary advantages transmitted DNA may provide, including the acquisition of beneficial genes enabling the colonization of new niches, survival in selective environments and an increase of overall fitness of a cell (Hall et al., 2020). Thus, HGT has advantages and disadvantages and is therefore controlled by multiple mechanisms. The extent to which HGT of resistance and virulence genes occurs in staphylococci, the role of CoNS as a potentially effective gene reservoir and whether there are differences between species in the prevalence of uptake of exogenous DNA remains controversial and requires further investigation.

For the researcher, natural barriers to HGT can become quite a challenge, a fact that was already pointed out by Falkow, who insisted that genetic manipulation is essential for the investigator to perform successful research on the role of genes, but at the same time admitted that such studies are hard to fulfill (Molecular Koch's Postulates, Falkow, 1988). Indeed, genetic manipulation of bacteria is essential for understanding gene-phenotype relations, as well as the molecular mechanisms behind observed phenotypes and metabolic processes. Yet, while laboratory strains have been selected as easy to transform since they lost a large part of their natural defense mechanisms, environmental and clinical isolates (so-called wildtype strains) are usually much harder to genetically modify. As stated above, a distinct barrier to HGT in *Staphylococcus spp.* are RM systems. They can be divided into four families (Type I – Type IV) based on their enzymatic subunit composition, cofactor requirements and target specificity sequences (Murray, 2000; Loenen et al., 2014). While type I, II and III RM systems recognize specific DNA sequences and cleave them if they are not properly methylated, type IV systems digest modified motifs only. This explains why type I, II and III RM systems consist of a methyltransferase mediating either adenine (m6A) or cytosine (m5C, m4C) methylation plus an endonuclease, while type IV systems encompass solely one to two restriction endonucleases (Loenen and Raleigh, 2014).

Gene manipulation systems have been established for *S. aureus* and *S. epidermidis* in the past, with most of the staphylococcal vectors available in public plasmid databases such as the Addgene repository (Kamens, 2015) developed for *S. aureus*. A vector that has been used successfully for genetic modification of *S. aureus* and *S. epidermidis* is pIMAY. The vector was first constructed by Monk et al., (2012) and slightly modified with pIMAY* (Schuster et al., 2019) being based on a different counter-selection mechanism (secY antisense RNA vs. PheS*) and pIMAY-Z carrying an additional Gram-positive ribosome binding site as well as *lac*Z for blue-white screening (Monk et al., 2015).

A vector map of pIMAY* is shown in Figure 2. The vector is 5,536 bps in size and its basic principle for genome engineering is based on homologous recombination using allelic exchange and subsequent counter-selection (Schuster et al., 2019). The plasmid is composed of a chloramphenicol (CM) acetyltransferase for successful selection of transformed *E. coli* and staphylococcal strains on CM supplemented agar, a temperature-sensitive replicon (*rep*BCAD) for Gram-positive bacteria (replication only at 28 °C), an origin of replication for *E. coli* (p15A, low copy) and the counter-selectable marker PheS*. Gene deletion using pIMAY* is obtained by inserting two homologous regions flanking the gene of interest into the vector and transforming it into the target cell. The vector then integrates into the chromosome due to the homologous regions in a single crossover event at a non-permissive temperature, at which the plasmid cannot replicate (37 °C) and under antibiotic selection. The second crossover event causing the deletion of the gene of interest and excision of the vector is induced by growth without antibiotic pressure at a permissive temperature (28 °C). Plasmid loss is subsequently enforced by counterselection based on *phe*S*, which encodes a mutated version of the phenylalanine tRNA synthetase. PheS* causes the incorporation of toxic *para*-chlorophenylalanine (PCPA) instead of phenylalanine into proteins. Therefore, bacterial growth on media containing PCPA is restricted if the cells still carry the plasmid, enabling the detection of plasmid-cured cells.

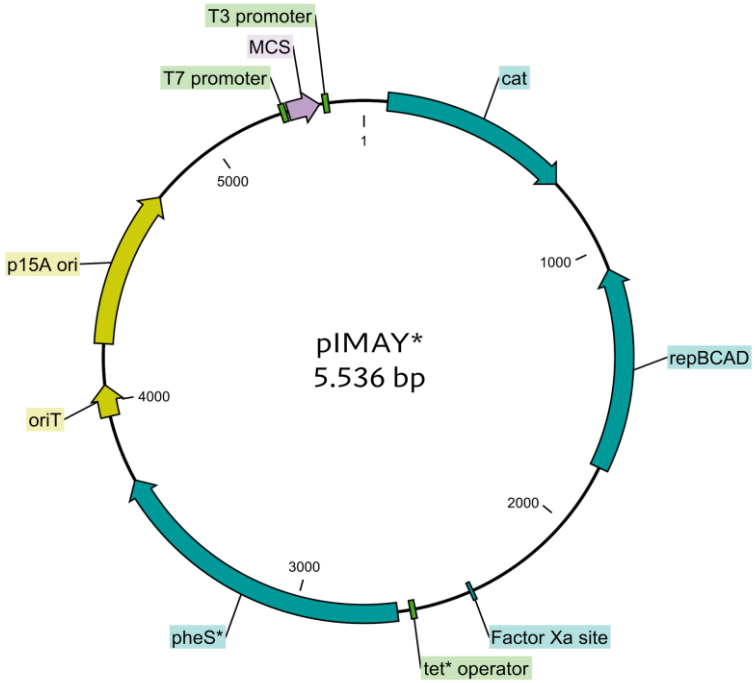

Figure 2: Vector map of the allelic exchange vector pIMAY*. Gram-positive replicon (*rep*BCAD), *E. coli* origin of replication (p15A), selection marker (chloramphenicol acetyltransferase *cat*), counterselection marker PheS* expressed from a mutated $P_{xyl/tet*}$ promotor, origin of transfer for conjugation (oriT) and the multiple cloning site (MCS) are shown.

Genetic engineering studies of other staphylococcal species are less common. Gene deletion studies on *S. xylosus* were mainly performed with *S. xylosus* C2a, a derivate of *S. xylosus* DSM 20267 that was cured of its endogenous plasmid pSX267 in the past (Götz et al., 1983; Sizemore et al., 1992; Brückner, 1997; Barrière et al., 2002). Others also used *S. xylosus* KL117 as an expression host for recombinant surface proteins (Liljeqvist et al., 1997; Samuelson et al., 2000). The exact origin of *S. xylosus* Kl117 is not clear from the literature, but the strain does not carry any plasmids either, which suggests that it has been cured of any and can probably be considered as a laboratory strain as well.

As for a long time, there was a great need to be able to genetically modify clinical strains of *S. aureus* next to a limited selection of already deeply characterized laboratory strains, Monk and colleagues worked on establishing a protocol to allow for successful gene deletion in any strain of *S. aureus*. Basically, they specified restriction modification systems (RM) as the major barrier to horizontal gene transfer in *S. aureus* and developed a strategy to circumvent them (Monk et al., 2012; Monk and Foster, 2012). Since only very few strains of *S. aureus* encode type III RM systems, they saw no need to further address them (Monk and Foster, 2012; Costa et al., 2017). Type II RM systems are also underrepresented in the species, with some strains

carrying a methyltransferase (Sau3AI) recognizing GATC motifs, which is usually circumventable by naturally occurring *dam* methylation of *E. coli* strains (Lindsay, 2014; Monk et al., 2015). To evade Type IV RM systems, *E. coli* DC10B was created, a K12 derivate lacking *dcm*, thus not being able to methylate cytosine residues (Monk et al., 2012). Finally, type I restriction modification systems, which are very strong and often present in multiple variants within one *S. aureus* strain, had to be circumvented. In this regard, a method called plasmid artificial modification (PAM) has been successfully applied for different bacteria in the past (Suzuki and Yasui, 2011; Monk et al., 2015; Lee et al., 2019). Using the example of *S. aureus*, PAM involves the expression of *S. aureus* methyltransferases in *E. coli* and the subsequent passage of vector plasmids through the respective modified *E. coli* strain to obtain the same modification pattern, thereby masking the plasmid as intrinsic for the target strain (*S. aureus*). Hereby, it is recommended to heterologously express the methyltransferases from the chromosome (Lee et al., 2019) rather than from a plasmid (Costa et al., 2017), to enhance stability and reduce the metabolic burden for the cell. To verify that the expressed methyltransferases are active in *E. coli*, the methylome of the modified *E. coli* strains can be determined using single-molecule, real-time (SMRT) sequencing technology and compared to the methylome of the corresponding target strains. The basic principle of detecting base modifications based on SMRT sequencing technology is the delayed incorporation of a nucleotide if the DNA template is modified. This results in a longer interpulse duration (IPD), meaning the space between two fluorescent pulses increases, and can subsequently be determined by computational analysis. Figure 3 visualizes the principle of detecting base modification using SMRT sequencing.

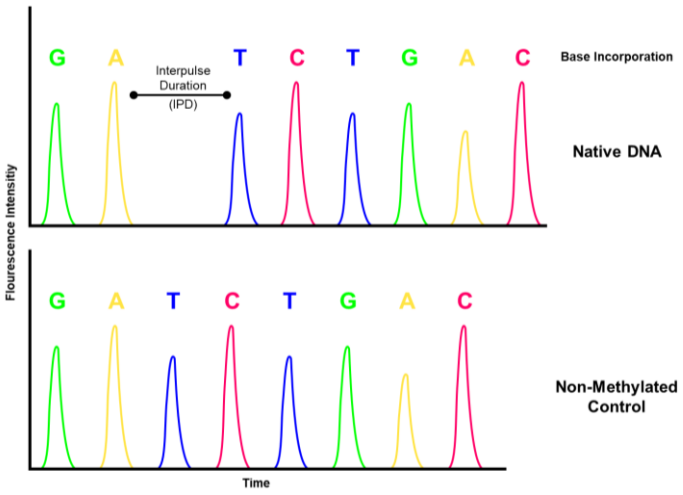

Figure 3: Principle of detecting base modification during SMRT sequencing. Kinetic signature of a template strand containing a modified base (top) compared to a template lacking any modifications (bottom). Polymerase-based incorporation of two successive bases is altered (increased IPD) if the template contains a modified base at the respective position. The Figure was inspired by Clark et al., (2012).

2 Aim of this work

The ability of bacteria to successfully multiply in a habitat and to prevail against biotic competition and abiotic stress consists of an optimal metabolic adaptation to the available substrates and minimization of self-inhibition emerging from accumulating metabolites, but also requires the ability to occupy spaces, defend them against others, expand them and ideally establish a colonization resistance. Biofilm formation can serve many of these aspects as it protects against environmental stress factors, reserves substrates in proximity, prevents intrusion of competitors and even facilitates interactions between organisms, including the transfer of genetic material. Attachment and spreading can be achieved by a sophisticated interplay between biofilm formation and cell dissolution, a property that is particularly pronounced in staphylococci. This work was designed as a holistic approach to better understand the behavior and underlying molecular mechanisms thereof, which allows *S. xylosus* to occupy and persist in its natural (mammalian mucoae/glandular tissue) and man-made (fermented food products) habitats. Hereby, the main aim of this work was to characterize surface properties, adhesive biofilm formation and aggregation behavior of *S. xylosus* on a phenotypic as well as on a molecular level. The approach chosen comprises the investigation of the influence of environmental factors on the phenotype but also provides insights into the genetic basis of adhesion and biofilm forming mechanisms within the species.

The focus of this work should be laid on basic phenotypic characterization of the ability to form biofilm under different conditions by comparing different *S. xylosus* strains. The same set of strains should further undergo a detailed genetic characterization to identify genetic determinants involved in biofilm formation of the species. In the following, the impact and function of identified genetic determinants should be characterized by the generation of knockout mutants and discussed within the context of known biofilm forming mechanisms of other staphylococcal species such as *S. aureus* and *S. epidermidis*. Finally, a proteomic study should be performed to explore the differential expression of proteins involved in metabolism and cell (surface) structure between cells grown under vigorous agitation in liquid medium (simulating planktonic growth) and sessile cells embedded in a polymeric matrix (biofilm condition).

This work was motivated by the following working hypotheses.

(i) The ability of biofilm formation by *S. xylosus* is strain-specific and depends on different surface hydrophilicities of the cells and matrices as well as environmental factors.

(ii) Genes mediating *S. xylosus* biofilm formation can be identified by comparative genomic analyses with respect to homologs described for well-characterized species such as *S. aureus* and *S. epidermidis*.

(iii) A transformation system for *S. xylosus* can be established, to facilitate the marker-free deletion of target genes and to enable the analysis of their contribution to biofilm formation.

(iv) Comparative proteomics can provide insights into the mechanisms of biofilm formation and the metabolism of sessile cells.

(v) Adhesion and biofilm formation are important fitness factors in the lifestyle of *S. xylosus*, contributing to the occupation of and persistence in natural and man-made habitats of *S. xylosus.*

3 Materials and methods

3.1 Strains, oligonucleotides and plasmids used

Table 1 lists all microorganisms used within the scope of this work. Bacteria were cryo-preserved for storage. Therefore, fresh overnight cultures were concentrated and diluted 1:1 in 80% glycerol (Carl Roth, Karlsruhe, Germany) before freezing at -80 °C. Strains were routinely checked for purity using Matrix Assisted Laser Desorption/ionization Time of Flight Mass Spectrometry (MALDI-TOF MS, Bruker Corporation, Billerica, USA). For a detailed protocol on sample preparation for MALDI-TOF MS-based bacteria identification, the reader is referred to Hilgarth, (2018).

Table 1: Bacterial strains used in this study

Strain	Description	Source/Accession (gbk)
DC10B	*E. coli* DH10B (K12 derivat), Δ*dcm*	CP000948/ Monk et al., (2012)
CM56	*E. coli* DC10B with 2.1023 *hsd*SMS integrated at 186-2 (Promotor: P_{N25})	this study
CM13	*E. coli* DC10B with 2.1324 *hsd*SMS integrated at 186-1 and 2.1324 MT integrated at λ (Promotor: P_{N25})	this study
CM57	*E. coli* DC10B with 2.1023 *hsd*MS integrated at 186-2 (Promotor: P_{N25})	this study
CM19	*E. coli* DC10B with 2.1324 *hsd*MS integrated at 186-1 and 2.1324 MT integrated at λ (Promotor: P_{N25})	this study
CM5	*E. coli* DC10B with 2.1324 *hsd*SMS integrated at 186-1 (Promotor: P_{N25})	this study
CM30	*E. coli* DC10B with 2.1324 *hsd*MS_tr integrated at 186-2, 2.1324 MT integrated at λ (Promotor: P_{N25})	this study
CM93	*E. coli* DC10B with 2.1324 MT integrated at λ (Promotor: P_{N25})	this study
CM2	*E. coli* DC10B with 2.1324 MT integrated at 186-1 (Promotor: P_{bla})	this study
DC3.1	*E. coli* resistant to *ccdB* (Type II toxin antitoxin system)	(St-Pierre et al., 2013)
E811	*E. coli* (P2 lysogen) in which the strong promotor P_E is repressed	(St-Pierre et al., 2013)
Newman	*S. aureus*, ST8, CC8, commonly used laboratory strain	AP009351 / (Duthie and Lorenz, 1952)
RP62A	*S. epidermidis*, clinical reference strain, *ica* positive	CP000029 / (Gill et al., 2005)
TMW 2.1023	*S. xylosus*, isolated from raw fermented sausages	this study, JAEMUG000000000
TMW 2.1023 Δ*bap*	Mutant of TMW 2.1023 with *bap* deletion	this study
TMW 2.1023 Δ*sxs*A	Mutant of TMW 2.1023 with *sxs*A deletion	this study
TMW 2.1023 Δ*bap*,*sxs*A	Mutant of TMW 2.1023 with *sxs*A and *bap* deletion	this study

TMW 2.1324	*S. xylosus* isolated from raw fermented sausages	this study, CP066726-CP066729
TMW 2.1521	*S. xylosus* isolated from raw fermented sausages	this study, JAEMUF000000000
TMW 2.1523	*S. xylosus* isolated from raw fermented sausages	this study, CP066721-CP066725
TMW 2.1523 Δ*bap*	Mutant of TMW 2.1523 with *bap* deletion	this study
TMW 2.1523 Δ*sxs*A	Mutant of TMW 2.1523 with *sxs*A deletion	this study
TMW 2.1523 Δ*bap*,*sxs*A	Mutant of TMW 2.1523 with *sxs*A and *bap* deletion	this study
TMW 2.1602	*S. xylosus* isolated from raw fermented sausages	this study, CP066719-CP066720
TMW 2.1693	*S. xylosus* isolated from bovine mastitis	this study, JAJAGM000000000
TMW 2.1704	*S. xylosus* isolated from bovine mastitis	this study, JAJAGL000000000
TMW 2.1780	*S. xylosus* isolated from raw fermented sausages	this study, JAJAGN000000000

3.2 Media and cultivation conditions

E. coli was routinely cultured in Lysogeny broth (LB, tryptone 10 g/l, yeast extract 5 g/l, NaCl 5 g/l, pH 7.0 ± 0.1) at 37 °C, 16 h, 200 rpm. Unless required otherwise, *Staphylococcus spp.* was cultured in trypticase soy broth, TSB_N (casein peptone 15 g/l, soy peptone 15 g/l, yeast extract 3 g/l, pH 7.2 ± 0.2) at 37 °C and 200 rpm. All media were autoclaved (121 °C, 20 min) before usage. For solid media, 1.5% agar (w/v) (Carl Roth) was added to the respective liquid media. Sugars were generally autoclaved separately. Antibiotics (all purchased from Carl Roth) were added in the concentrations 20 µg/ml (Kanamycin), 100 µg/ml (Ampicillin), 20 µg/ml (*E. coli*, Chloramphenicol) and 10 µg/ml (*Staphylococcus spp.*, Chloramphenicol) to the growth media (sterilized by filtration) whenever needed.

3.3 Biofilm formation tests

To screen for adhesive biofilm formation, a method described by Christensen et al., (1985) was slightly modified, as reported by Schiffer et al., (2019). Basically, bacterial cultures were diluted to an OD_{590} of 0.05 in the respective growth medium and incubated statically in 96-well plates for 24 hours at 37 °C. Afterwards, non-adherent cells were carefully washed off with sterile phosphate buffered saline (PBS) (NaCl 9 g/l, $Na_2HPO_4*7H_2O$ 0.795 g/l, KH_2PO_4 0.114 g/l, pH 7.2) and the adherent biofilm was fixated at 60 °C for 1 h before staining with 0.1% (w/v) safranin-O (Sigma Aldrich, St. Louis, USA) for 5 min. Unbound safranin was removed and two wash steps followed, before plates were airdried and the stain was solubilized with

ethanol (95%, v/v). In a last step, the absorbance was quantified at 490 nm in a plate reader (SpectrostarNano^{TM}, BMG Labtech, Ortenburg, Germany). In order to test the influence of different environmental conditions on biofilm formation of *S. xylosus*, biofilm formation was quantified in different cultivation media (TSB_N, TSB^+ (TSB_N + 1% glucose), $NaCl^+$ (TSB^+ + 3% NaCl), Lac^+ (TSB^+ acidified to pH 6 by 80% lactic acid)). Additionally, experiments were conducted on hydrophobic (polystyrene 96-well plates, Sarstedt Nürmbrecht, Germany) and hydrophilic support (Nunclon^{TM} delta surface 96-well plates, Thermo Fisher Scientific, Waltham, USA). For visualization purposes biofilm tests were in some cases additionally performed in small petri discs (Nunclon^{TM} delta surface tissue culture plates (Thermo Fisher Scientific)), incubated, washed, fixated, and stained in the same way as described for the 96-well assays. The discs were subsequently photographed. To screen for effects of calcium and zinc on biofilm formation, either $CaCl_2$, $ZnCl_2$ or EDTA was added to a final concentration of 20 mM, 40 µM or 0.2 mM, respectively, to the wells at t_0 whenever indicated.

Of note is that three different stains were tried during the first stages of the biofilm experiments (Figure 4), namely alcian blue (Carl Roth), crystal violet ((CV), Carl Roth) and safranin-O (Carl Roth). Alcian blue, reported to stain the polysaccharide part of the exopolymer biofilm matrix (Wu et al., 2020), was soon eliminated from the tests as staining was hardly reproducible. Crystal violet and Safranin-O both worked equally well in staining the biofilm biomass. Yet, considering the fact that CV is toxic, and Safranin-O is not, it was decided to proceed with Safranin-O (Ommen et al., 2017).

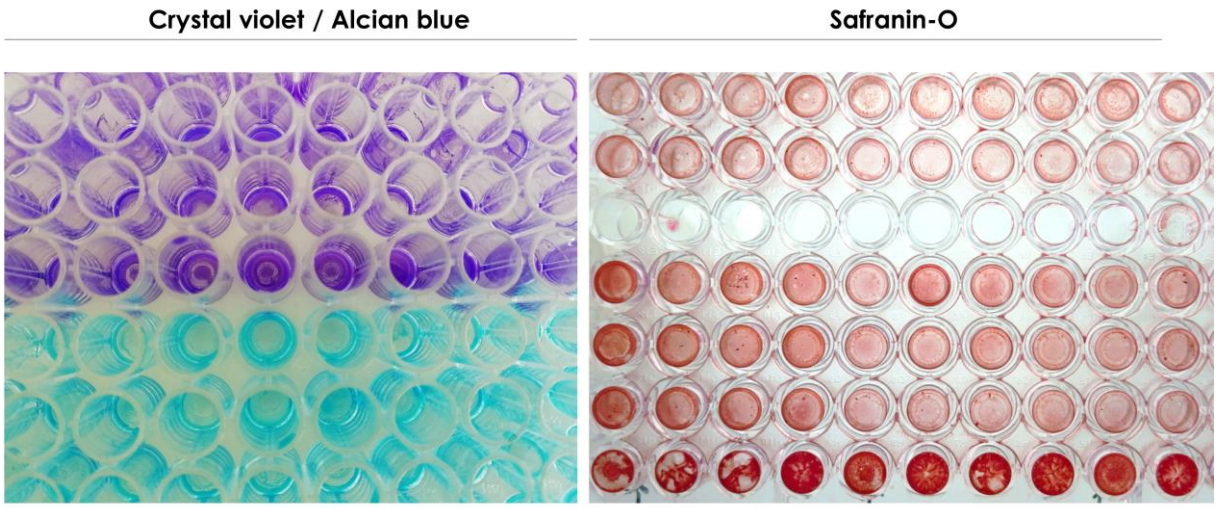

Figure 4: Traditional stains used in 96-well assays to quantify adherent biofilm formation

3.4 Cell aggregation assays

Bacterial aggregation assays are described in detail by Schiffer et al., (2021 and 2022a). Basically, overnight cultures were diluted to an OD_{600} of 0.1 and incubated in different vessels (test tubes, Erlenmeyer flasks) in different media (TSB_N / TSB^+) for one, two, five, 12 and 24 hours respectively at 37 °C (200 rpm). Cell aggregation was subsequently evaluated macroscopically. In some cases, the impact of calcium on cell aggregation was investigated, therefore $CaCl_2$ was added to a concentration of 20 mM to the liquid media.

3.5 Congo red agar assay

The congo red agar assay was first described by Freeman et al., (1989) in order to screen for slime producing organisms. It was modified by Heilmann and Götz, (1998) who distinguished PIA-positive (black phenotype) from PIA-negative (red phenotype) strains. Cucarella et al., (2001) reported the difference of colony margins between Bap-positive and Bap-negative colonies on CRA, an effect that was later ascribed to amyloid fiber formation by Bap (Taglialegna et al., 2016b). Within this work, cultures were cultivated on three different versions of CRA. In Schiffer et al., (2019) colonies were cultivated on media containing 37 g/l brain heart infusion (BHI) broth, 10 g/l agar and 50 g/l sucrose. In Schiffer et al., (2021) colony morphology was assessed on CRA based on TSA supplemented with 10 g/l glucose. In Schiffer et al., (2022a) CRA was once again modified and based on TSA only, therefore being deficient of any sugar source. Each time, the media was supplemented with a sterile solution of 0.8 g/l Congo red dissolved in water (w/v), before plates were poured. Isolates were streaked onto the plates, incubated at 37 °C for 24 hours and subsequently let stand for another one to two days at room temperature before visual screening for differences in colony morphology. Congo red is known to interact with a range of polymeric substances such as proteins and amyloidogenic structures. Usually, colony phenotypes are screened for morphology (dry or shiny), colour (black or red) and margins (smooth or rough). Differences in phenotypes are characterized and depicted in Knobloch et al., (2002) and Erskine et al., (2018).

3.6 Microbial adhesion to hydrocarbon (MATH)

To evaluate the surface hydrophobicity of bacterial cells, MATH tests were performed as described by Schiffer et al., (2019). Briefly, overnight cultures were washed and resuspended to an OD_{590} of 0.35 to 0.4 (A_B) in imidazole/phosphate buffered saline (KH_2PO_4 0.1 g/l,

$Na_2HPO_4*2H_2O$ 4.45 g/l, imidazole 1.7 g/l, pH 6.2). 5 ml of the cell suspension were subsequently overlaid with 0.4 ml n- hexadecane (Sigma Aldrich), followed by incubation at 37 °C for 10 min, vortexing for 2 min and incubation at room temperature until complete phase separation was achieved. The affinity for *n*-hexadecane (%) was then determined by measuring the absorbance (A_A) of the aqueous phase and by using the following formula:

$$affinity\ to\ n\text{-}hexadecane\ (\%) = \frac{A_B - A_A}{A_B}\ x\ 100$$

Strains can be considered as highly hydrophobic when values are over 50% and as hydrophilic when under 20%.

3.7 Growth and pH dynamics

Changes in pH over time were recorded using the icinac system (AMS Systea, Rome, Italy). Growth dynamics were monitored in a microplate reader (Spectrostar^{Nano}, BMG Labtech) over a period of 33 hours with an optical density of OD_{600} = 0.1 at t_o. Samples were measured (OD_{600}) every 30 minutes and plates were shaken double orbitally (10 min, 600 rpm) before each measurement (Schiffer et al., 2021; Schiffer et al., 2022a)

3.8 Microscopy

Microscopy was performed at the institute of advanced light and electron microscopy of the Robert Koch Institute, Berlin, Germany. Therefore, biofilm positive strain *S. xylosus* TMW 2.1523 and its isogenic *sxs*A and *bap,sxs*A mutant were sent to Dr. Christoph Schaudinn, who incubated them accordingly and prepped them for CLSM, SEM and TEM microscopy. Sample preparation and microscopic settings are described in detail in Schiffer et al., (2022a).

3.9 Genomic DNA isolation and DNA sequencing

High-molecular-weight DNA was isolated from liquid cultures using the E.Z.N.A® kit (Omega Bio-Tek Inc., Norcross, USA) according to the manufacture's instruction but lysostaphin (0.5 mg/ml) was included into the lysis buffer to weaken the cell wall. Whole genome sequencing was performed using PacBio Single molecule real time sequencing (SMRT), library construction and sequencing parameters are described in Schiffer et al., (2019) and Schiffer et al., (2022a). Some strains (TMW 2.1023, TMW 2.1324, TMW 2.1521, TMW 2.1523, TMW

2.1602) were additionally sequenced using next generation sequencing (NGS) technology on a MiSeq sequencing platform (Illumina, Inc. San Diego, CA, USA) at Eurofins Genomics (Ebersberg, Germany). *S. xylosus* TMW strains 2.1693, 2.1704 and 2.1780 were sequenced using PacBio technology only, at the research unit for environmental genomic Munich (Helmholtz Zentrum München). *E. coli* strains, heterologously expressing methyltransferases (CMx strains) were sequenced at the functional genomics center Zurich. PCR products were purified as described below and sequenced at Eurofins Genomics.

3.10 PCR amplification and purification

Polymerase chain reactions (PCR) were performed using the Taq DNA Core Kit 10 (MP Biomedicals, Irvine, USA) for routine screenings and Q5 or Phusion for cloning experiments. Cycling conditions were chosen based on the instructions provided by the manufacturer, depending on which primers and which polymerase was used. Oligonucleotides/Primers and plasmids used within the scope of this work are listed in the respective publications (Schiffer et al., 2021; Schiffer et al., 2022b; Schiffer et al., 2022a). All oligonucleotides were purchased at Eurofins Genomics. Plasmids were obtained from Addgene (Watertown, USA). PCR products were purified using the NEB PCR & DNA Cleanup kit, excised PCR fragments from an agarose gel were purified using the NEB DNA gel extraction kit. Plasmids were generally isolated and purified using the NEB Monarch plasmid DNA miniprep kit (all NEB products from New England BioLabs Inc., Ipswich, USA).

3.11 Gel electrophoresis

Agarose gel electrophoresis

Samples subjected to agarose gel electrophoresis were mixed with 6 x loading dye (Thermo Fisher Scientific) and applied to an 0.8% (w/v) agarose gel when DNA sizes were expected above 1 kb, and to an 1.2% (w/v) agarose gel when DNA fragments were below the size of 1 kb. Agarose was diluted in 1 x TAE buffer (40 mM Tris, 20 mM acetic acid, 1 mM EDTA, pH 8.2). As reference a 1 kb DNA ladder (Thermo Fisher Scientific) was generally applied to the gel as well. Gels were stained in a dimidium bromide (Carl Roth) bath for 20 min following electrophoresis and subsequently kept in washing solution (dH_2O) for another 15 min before being visualized on an UVT-28M transilluminator (Herolab, Wiesloch, Germany).

SDS-PAGE analysis

Bacteria were grown in TSB_N for about 12 hours until they reached early stationary phase (37 °C, 200 rpm). 5 ml of the cell culture were harvested, washed twice with ice-cold PBS and resuspended in 150 µl digestion Buffer (PBS + 30% (w/v) raffinose (Sigma Aldrich)). 7 µl lysostaphin (1 mg/ml, Sigma Aldrich) and 3 µl DNAseI (1 mg/ml, Sigma Aldrich) were added to the mixture which was then incubated at 37 °C for 2 h. Protoplasts were sedimented at 8000 x g for 30 min. Supernatants were mixed with 2x Laemmli sample buffer (Sigma Aldrich), denatured at 95 °C for 5 min and subsequently subjected to sodium dodecyl sulfate polyacrylamide gel electrophoresis (SDS-PAGE), (10% (w/v) resolving, 4% (w/v) stacking gel, 1 mm spacer plate). The NEB P7719S ladder served as molecular weight reference ladder. The analysis was performed in a Mini-PROTEAN Tetra Cell Electrophoresis chamber (Bio-Rad Laboratories, Hercules, USA) for approximately 60 min at 120 V using a 1 x Tris-glycine running buffer (3 g/l Tris base, 14.4 g/l glycine, 1 g/l SDS). Protein staining was performed using ROTI®Blue (Carl Roth) according to the manufacturer's instructions.

3.12 Vector assembly and gene replacement / gene expression

Three major genetic engineering projects were part of this dissertation. The first one was to delete the *bap* gene in TMW 2.1023 and TMW 2.1523 (Schiffer et al., 2021), the second one was to delete the chromosomal *sxs*A gene in the same strains as well as to create double mutant strains (Schiffer et al., 2022a) and the third project encompassed the heterologous expression of staphylococcal methyltransferases and type I modification systems in *E. coli* (Schiffer et al., 2022b). The construction of the respective cloning vectors is described in the following, adapted from the just cited publications.

For chromosomal deletion of *bap*, pIMAY* was used, a vector which is based on allelic replacement of the gene of interest. Firstly, two regions flanking the to be deleted sequence were amplified using primer bap1F and bap2R as well as bap3F and bap4R. Hereby, primers were designed to match sequence of both strains, TMW 2.1023 and TMW 2.1523. In the following, pIMAY* was linearized using the restriction enzymes SacI and PstI (NEB) and PCR fragments were ligated into pIMAY* by Gibson Assembly (Gibson Assembly Master Mix, NEB). The assembly mixture was then transformed into *E. coli* DC10B by electroporation and plated on LB 20CM to select for successful transformants. Correct assembly of the vector was verified by sequencing. The vector was transformed into *S. xylosus* wildtype strains TMW 2.1023 and TMW 2.1523.

The *sxs*A vector construct was built by amplifying regions up-and downstream of the to be deleted sequence using primers sxsA1F and sxsA2R as well as sxsA3F and sxsA4R. Again, primer sequences were designed to match the target sequence in both *S. xylosus* strains. After purification of the PCR fragments, primers sxsA1F and sxsA4R were used in another PCR reaction for overamplification. The corresponding DNA fragment was excised from an agarose gel and purified. PIMAY* was digested using PstI-HF and XhoI-HF (NEB) and the insert was ligated (T4 DNA Ligase, Thermo Fisher Scientific) into the vector. The ligation approach was transformed into *E. coli* DC10B and successful transformants were selected on LB 20CM. Correct assembly of the vector was verified by sequencing again. The *sxs*A vector was transformed in *S. xylosus* TMW 2.1023, TMW 2.1523 and their respective Δ*bap* mutants to yield double mutant (Δ*bap,* Δ*sxs*A) strains. For allelic replacement of the chromosomal genes, we followed the step-by-step protocol provided by Schuster et al., (2019). Successful gene deletion and allelic replacement of the genes of interest as well as loss of pIMAY* were verified in the end by colony PCR as well as loss of chloramphenicol resistance was verified by replica plating.

Vector assembly for heterologous expression of *S. xylosus* methyltransferases from the *E. coli* chromosome was performed as described in the following. Basically, a method called clonetegration was used which ensures site-specific insertion of genes into locations of the chromosome, in a single cloning and chromosomal integration step. The method was first described by St-Pierre et al., (2013). The expression of methyltransferases from the chromosome rather than multicopy plasmids, results in a reduced metabolic burden for the cell, and therefore a stable expression and complete base modification. The applied method relies on bacteriophage integrases that mediate site-specific insertions of any gene into prokaryotic chromosomes at the respective *att*B sites. Within the scope of our studies, we used the integrases of coliphages λ (pOSIP-KL) and 186 (pOSIP-KO). Primers PN25_MT_F and RS_MT_R were used to amplify the type II methyltransferase of *S. xylosus* TMW 2.1324. A PCR reaction consisting of the methyltransferase sequence, the dimerized oligosaccharides of promoter P_{N25} and primers PN25_MT_F and RS_MT_R, followed. Successfully amplified promoter-gene constructs were purified from an agarose gel and ligated into the restricted (SacI/PstI) vector pOSIP-KL. Type I modification systems of TMW 2.1023 and TMW 2.1324 (*hsd*SMS/*hsd*MS/*hsd*MS_{tr}) were ligated into vector pOSIP-KO (KpnI/SphI) the same way, but primer pairs PN25_*hsd*SMS_F / PN25_*hsd*MS_F and RS_*hsd*S_R / RS_*hsd*S_tr_R were used at first, followed by overamplification with RS_PN25_F and RS_*hsd*S_R / RS_*hsd*S_tr_R, respectively. The P_{Bla}-MTase construct was built by amplifying P_{Bla} from plasmid pE-Flp using primers vec_pBla_1F and Bla_Mtase_1R as well as amplifying the type II methyltransferase of TMW 2.1324 using the

overlapping primers Bla_Mtase_2F and Mtase_186_2R. Gibson assembly was used to assemble all PCR products into the linearized vector pOSIP-KO (KpnI/PstI). All assembled vector constructs were transformed into *E. coli* DC10B by electroporation, site-specific integration of the respective genes into the *E. coli* chromosome followed and FLP-mediated excision of the vector backbone was performed by transforming cells with plasmid pE-FLP. A step-by-step protocol provided by Cui and Shearwin, (2017) describes in detail the single steps performed during integration, selection for successful transformation, excision, and final screening.

3.13 Transformation protocol for *E. coli*

E. coli strains were transformed using electrocompetent cells that were prepared according to standard protocols. Briefly, 100 ml of bacterial liquid culture was harvested at mid-exponential phase (OD_{600} 0.5 - 0.7), chilled on ice for 10 minutes and centrifuged at 5000 x g, 4 °C for 10 minutes. The supernatant was decanted, and the pellet was resuspended in 100 ml 10% (v/v) glycerol. Centrifugation and resuspension steps were repeated twice with decelerating volumes of resuspension buffer until cells were finally resuspended in 500 µl of 10% glycerol. Transformation was performed in a 0.1 cm cuvette (Gene pulser MicroPulser cuvette) at 1.8 kV using a MicroPulser electroporator (Bio-Rad Laboratories).

3.14 Transformation protocol for *Staphylococcus spp*.

Staphylococcus spp. (*S. xylosus, S. aureus*) cells were grown in 10 ml BHI for approximately 14 hours before they were diluted to an OD_{600} of 0.5 in fresh basic medium (1% peptone, 0.5% yeast extract, 0.5% NaCl, 0.1% Glucose, 0.1% K_2HPO_4). Incubation of the cultures for another 30 - 40 minutes (OD_{600}: 0.7 - 0.8) at 37 °C and 200 rpm followed before cells were transferred to a centrifugation tube and chilled on ice for 10 min. Cells were harvested at 6000 x g for 5 minutes, washed twice with ice-cold dH_2O and twice with 10% glycerol in decelerating volumes (1/10, 1/25). Finally, cells were resuspended in 1/200 volume 10% glycerol + 500 mM sucrose (sterile filtrated) and directly subjected to electroporation. For electroporation 50 µl of competent cells were carefully mixed with 1 - 1.5 µg of plasmid and kept at room temperature for 15 min before cells were transformed in a 0.2 cm cuvette at 2.5 kV and immediately resuspended in 1 ml BHI + 200 mM sucrose after electroporation. For recovery, cells were incubated at 28 °C under slowly shaking conditions for one hour before they were plated on BHI 10CM and incubated at 28 °C for two days. Of note is that this protocol only yields very low tansformation efficiencies for *S. xylosus* TMW 2.1023 (10 ± 2 cfu/µg DNA) and TMW 2.1523 (1 ±

0.5 cfu/µg DNA). Many attempts to increase the transformation efficiency, including transforming TMW 2.1324 remained unsuccessful. Hereby, various parameters known to affect the electrotransformation efficiency were tested, such as cell growth (medium, growth phase), washing procedure (temperature, cycles, wash solution), *E. coli* strains, prepulse incubation time, electroporation conditions (voltage field strength, cell density, volume, plasmid concentration), vector (pCasSA vs. pIMAY), incubation at 56 °C before transformation, outgrowth media, length incubation and selection media/conditions. None of them resulted in higher transformation rates.

3.15 Full proteome analysis

Full proteome analysis was performed to investigate differences in protein expression of cells grown planktonically compared to cells grown under sessile conditions. Moreover, successful gene deletion in mutant strains (Δ*bap*, Δ*sxs*A) was confirmed by determining the whole proteome of the strains. Therefore, overnight cultures were diluted (0.1%, v/v) in fresh Lac^+ and incubated under shaking conditions (planktonic samples, 200 rpm, 5 ml) or statically (sessile samples, 2 ml) in Nunclon^{TM} delta surface tissue culture plates (Thermo Fisher Scientific) at 35 °C for 24 hours. Planktonic cells were harvested (5000 x g, 4 °C, 4 min), washed twice with ice-cold PBS and resuspended in 100 µl Trifluoroacetic acid (TFA). For sessile sample preparation, the supernatant was decanted, non-adherent cells were removed by washing the plates twice with ice-cold PBS and the biofilm was resuspended in 100 µl TSA. TFA-cell suspensions were neutralized to pH 8.1 - 8.3 by adding nine volumes of Tris buffer (2 M). Cells were subsequently incubated for 5 min, at 55 °C and 450 rpm and shortly centrifuged. Protein concentrations were determined using Bradford assay according to manufacturer's instructions (B6916, SigmaAldrich) and sent to the Bavarian Biomolecular Mass Spectrometry Center (BayBioMS) to identify the proteins of the samples and measure abundance changes between the different samples. A detailed description of how the samples were processed and processed at BayBioMS is provided in Schiffer et al., (2021). Full proteome analysis of planktonic and sessile samples incubated in Lac^+ was performed for TMW strains 2.1023, 2.1324, 2.1521, 2.1523, 2.1602 as well as TMW 2.1523 was also sampled in TSB_N. Mutant strains TMW 2.1023Δ*bap*, 2.1023Δ*sxs*A, 2.1023Δ*bap,sxs*A, 2.1523Δ*bap*, 2.1523Δ*sxs*A, 2.1523Δ*bap,sxs*A were only sampled from planktonic grown cultures.

3.16 Bioinformatic and statistical analysis

Sequencing reads obtained from PacBio sequencing were assembled using the HGAP4 script of SMRT Analysis version 7.0 (Pacific Biosciences, Menlo Park, USA). SMRT Analysis was also used to determine the methylome of all PacBio-sequenced strains (Base modification and motif analysis script). For genome assembly of Next-generation sequencing data (WGS data) the Unicycler assembly tool of the galaxy project (Galaxy Version 0.4.8.0) was used with default settings (Wick et al., 2016). Gene annotation of the sequenced genomes is based on the NCBI Prokaryotic Genome Annotation Pipeline (PGAP) and the Rapid Annotations using Subsystems Technology (RAST) Server (Aziz et al., 2008; Tatusova et al., 2016). Average nucleotide identity (ANI) values were determined by the ANIb algorithm (Goris et al., 2007) which is implemented within the JspeciesWS web service (Richter et al., 2016). A neighbor-joining distance tree was built using Molecular Evolutionary Genetics Analysis (MEGA 7) software (Kumar et al., 2016). General bioinformatic analysis and comparative genomics were performed using the Blast Diagnostic Gene finder tool (BADGE, (Behr et al., 2016)) and CLC Main Workbench 8 (CLC bio, Aarhus, Denmark). The Blast Ring Image Generator (BRIG) was used for visualization of pan-, core-, and accessory genome (Alikhan et al., 2011). The integrated CLC clustal-omega plug-in was used for sequence alignments, which then served for generation of phylogenetic trees (neighbor-joining). Protein statistics such as isoelectric point (pI) and molecular weight (MW) were computed using the Expasy server online tool (available under: https://web.expasy.org/compute_pi/, last accessed on 29th January 2022). ProScan (https://npsa-prabi.ibcp.fr/cgi-bin/npsa_automat.pl?page=/NPSA/npsa_proscan.html, last accessed on 29th January 2022), which screens against the PROSITE database, was used to determine EF-hand motifs (cut-off set to 80% protein identity). InterPro (86.0, EMBL-EBI, Cambridgeshire, UK) predicted signal peptides, transmembrane segments and cell wall anchor. Amyloidogenic parts of a given protein sequence were analyzed by comparing the results of four different amyloid finder algorithms, namely WALTZ-DB 2.0 (Louros et al., 2020), AGGRESCAN (Groot et al., 2012), TANGO (Fernandez-Escamilla et al., 2004) and FoldAmyloid (Garbuzynskiy et al., 2010). Coiled-coil motifs were predicted using MARCOIL (Delorenzi and Speed, 2002). Additionally, an overview on secondary structure was generated by the MPI bioinformatics toolkit (Gabler et al., 2020). To identify proteins harboring a C-terminal LPxTG cell wall anchor motif, whole genome sequencing data was screened using the respective Prosite algorithm, [LY]PX[TSA][GNAST]X(0,10){DEQNKRP}{DEQNKRP}{DEQNKRP}{DEQNKRP}{DEQNKRP}{DEQNKRP}{DEQNKRP}{DEQNKRP}{DEQNKRP}X(0,15)[DEQNKRH]X(0,5) (Roche et al., 2003). NCBI BLASTN and BLASTP searches

against the nucleotide / protein database were used for the analysis of sequence similarities to other genes / proteins, identification of organisms also harboring the gene and to screen for potential protein homologs. BLAST-based searches against the NCBI database were also used to estimate the prevalence of a certain gene within a bacterial species. NCBI's conserved domain database (Marchler-Bauer et al., 2015) as well as the restriction enzyme database REBASE were consulted for the analysis of restriction modification systems i.e. family affiliations, presence of motif / system in other organisms, determination of enzymatic domains and target recognition domains. Genomes were screened for the presence of mobile genetic elements i.e. genetic islands using island viewer 4 (Bertelli et al., 2017) and for prophages using the PHAge Search Tool Enhanced Release ((PHASTER), Arndt et al., 2016). Secondary structure conformation of polypeptides was predicted by the protein fold recognition server PHYRE^2 (Kelley et al., 2015). To screen the genomes for CRISPR and *cas* genes, the CRISPRCasFinder online tool was used (Couvin et al., 2018). Identified spacer sequences were blasted manually against vector sequences and the NCBI database.

Proteomic data was processed using MaxQuant (v1.6.3.4) with Andromeda for peptide identification and quantification (Cox et al., 2011). MS2 spectra were searched against the NCBI proteome database of the respective *S. xylosus* strains. Trypsin/P was selected as proteolytic enzyme, common contaminants were included into the analysis, all further parameters that were set are named in Schiffer et al., (2021). Differential protein expression was calculated using Perseus version 1.6.15.0 (Tyanova et al., 2016) and LFQ-Analyst (Shah et al., 2020). Thereby, missing label-free quantitation (LFQ) values were imputed from normal distribution. Significant differences in intensities were calculated by student's t-test (pairwise comparison) with a cutoff of the adjusted *p*-value set to 0.05. False discovery rate (FDR) correction (Benjamini Hochberg method) was applied to correct *p*-values. Differentially expressed proteins were associated to metabolic categories based on the SEED servers (Overbeek et al., 2014) and the TIGRFAMs database of protein families (Haft et al., 2003).

Experiments were usually performed in biological triplicates and data is presented as means +/- standard errors (SE) of the means, unless stated otherwise. SigmaPlot Version 12.5 (Systat Software GmbH, Erkrath, Germany) was used to test for statistical significances (Student's *t*-tests).

The proteomics dataset is accessible via ProteomeXchange (PRIDE database, Perez-Riverol et al., 2019) using the identifier PXD029728. WGS data of *S. xylosus* TMW strains has been deposited at GenBank under the respective accession numbers listed in Table 1.

4 Results

4.1 Bap and cell surface hydrophobicity are important factors in *Staphylococcus xylosus* biofilm formation

Preface: At the time of the publication not much was known on biofilm formation of other staphylococci except for *S. aureus* and *S. epidermidis*. Talon and coworkers published a study on biofilm formation of 12 *S. xylosus* strains, in which they investigated strain-specific differences in adherence to different support materials (Planchon et al., 2006) and, just recently, another study focusing on the impact of eDNA on *S. xylosus* C2a biofilms (Leroy et al., 2021). Additionally, a Chinese group published two proteomic studies in 2017 and 2018, both addressing *S. xylosus* biofilm inhibition mechanisms, by either Cefquinome (Zhou et al., 2018) or by Aspirin (Xu et al., 2017). Lastly, another study from Canada evaluated the ability of different CoNS (including *S. xylosus*) isolated from dairy farms to form biofilms (Tremblay et al., 2014). Yet, these studies are mainly descriptive and compared to the extensively characterized biofilm formation mechanisms of *S. aureus* and *S. epidermidis*, very little was known for *S. xylosus*. In particular, little was known about what influences *S. xylosus* biofilm formation and the genetic background of the species i.e. the prevalence of biofilm-associated genes. In our study, Schiffer et al., (2019), we continued with the comparison of different strains of *S. xylosus* on their ability to form biofilm. We also investigated and discussed the influence of environmental factors such as media composition as well as hydrophobicity of the cell and the attachment surface on the ability to form biofilms. The phenotypic data was complemented with detailed bioinformatic analyses on a range of biofilm-inducing genes, described for *S. aureus* and *S. epidermidis* so far and the occurrence of potential homologs in *S. xylosus* genomes. We thereby found that the biofilm negative strain TMW 2.1602 was a natural mutant of the biofilm-associated gene *bap*, and therefore postulated that Bap should be as important to *S. xylosus* biofilm formation as it is for *S. aureus* V329 (Cucarella et al., 2001) and *S. epidermidis* C533 (Tormo et al., 2005).

Author contributions: Carolin Schiffer conducted all the experiments and was in charge of the experimental design, writing of the first draft of the manuscript, visualization, and interpretation of the data as well as for detailed bioinformatic analyses. She also contributed to the refereeing process and final version of the manuscript.

frontiers in Microbiology

ORIGINAL RESEARCH
published: 25 June 2019
doi: 10.3389/fmicb.2019.01387

Bap and Cell Surface Hydrophobicity Are Important Factors in *Staphylococcus xylosus* Biofilm Formation

*Carolin Schiffer, Maik Hilgarth, Matthias Ehrmann and Rudi F. Vogel**

Lehrstuhl für Technische Mikrobiologie, Technische Universität München, Freising, Germany

Staphylococcus (S.) xylosus is a coagulase-negative *Staphylococcus* species naturally present in food of animal origin with a previously described potential for biofilm formation. In this study we characterized biofilm formation of five selected strains isolated from raw fermented dry sausages, upon different growth conditions. Four strains exhibited a biofilm positive phenotype with strain-dependent intensities. Biofilm formation of *S. xylosus* was influenced by the addition of glucose, sodium chloride and lactate to the growth medium, respectively. It was further dependent on strain-specific cell surface properties. Three strains exhibited hydrophobic and two hydrophilic cell surface properties. The biofilm positive hydrophilic strain TMW 2.1523 adhered significantly better to hydrophilic than to hydrophobic supports, whereas the differences in adherence to hydrophobic versus hydrophilic supports were not as distinct for the hydrophobic strains TMW 2.1023, TMW 2.1323, and TMW 2.1521. Comparative genomics enabled prediction of functional biofilm-related genes and link these to phenotypic variations. While a wide range of biofilm associated factors/genes previously described for *S. aureus* and *S. epidermidis* were absent in the genomes of the five strains analyzed, they all possess the gene encoding biofilm associated protein Bap. The only biofilm negative strain TMW 2.1602 showed a mutation in the *bap* sequence. This study demonstrates that Bap and surface hydrophobicity are important factors in *S. xylosus* biofilm formation with potential impact on the assertiveness of a starter strain against autochthonous staphylococci by competitive exclusion during raw sausage fermentation.

Keywords: *Staphylococcus xylosus*, biofilm, biofilm associated protein (Bap), surface hydrophobicity, coagulase negative staphylococci

OPEN ACCESS

Edited by:
Rosanna Tofalo,
University of Teramo, Italy

Reviewed by:
Régine Talon,
Institut National de la Recherche Agronomique (INRA), France
Krzysztof Skowron,
Nicolaus Copernicus University in Toruń, Poland

****Correspondence:***
Rudi F. Vogel
rudi.vogel@tum.de;
rudi.vogel@wzw.tum.de

Specialty section:
This article was submitted to Food Microbiology, a section of the journal Frontiers in Microbiology

Received: *26 April 2019*
Accepted: *03 June 2019*
Published: *25 June 2019*

Citation:
Schiffer C, Hilgarth M, Ehrmann M and Vogel RF (2019) Bap and Cell Surface Hydrophobicity Are Important Factors in Staphylococcus xylosus Biofilm Formation. Front. Microbiol. 10:1387. doi: 10.3389/fmicb.2019.01387

INTRODUCTION

Staphylococcus (S.) xylosus is a Gram-positive, coagulase negative species often found on mammal skin. *S. xylosus* is also widely used as starter organism in raw sausage fermentations (Vos et al., 2009) and has been described as biofilm producer in the past (Planchon et al., 2006; Xu et al., 2017). This ability can be positively associated with food fermentation processes, as adhesion and biofilm formation may increase the assertiveness of a starter organism against the autochthonous

microbiota by concomitant induction of colonization resistance in a particular ecological niche. Additionally, biofilms offer a physical protection to bacteria against stress factors including antimicrobial substances (An and Friedman, 2010). In general, the lifecycle of a biofilm can be divided into the stages attachment, maturation and detachment (Otto, 2008). Thereby the first two stages are the main steps of the biofilm formation process, in which multiple factors are involved, and which is often dependent on environmental factors and availability of nutrients (Götz, 2002). Primarily, adherence to a certain support is mediated by nonspecific and/or specific adhesion factors. The latter are termed microbial surface components recognizing adhesive matrix molecules (MSCRAMMS), comprising adhesins on the cell surface of bacteria that bind specifically to extracellular matrix proteins, such as collagen, fibronectin or elastin (An and Friedman, 2010). Following initial adhesion, biofilm accumulation sets in with cells adhering to each other and producing a matrix in which they are embedded in. This extracellular matrix is usually composed of polysaccharides, proteins, and eDNA (Flemming and Wingender, 2010). The multifactorial mechanisms involved in biofilm formation of staphylococci have been described extensively for *S. aureus* and *S. epidermidis* in the past (Götz, 2002; Fey and Olson, 2010), often focusing on two important gene loci with functional redundancy, i.e., presence of either one correlates with strong biofilm production (Moretro et al., 2003; Cucarella et al., 2004; Tormo et al., 2005). The polysaccharide intercellular adhesin (PIA), which is synthesized by the products of the *ica* operon (Cramton et al., 1999) and the biofilm associated protein (Bap). Members of the Bap family are known to be involved in adhesion and biofilm forming processes (Latasa et al., 2006) and comprise among others Bhp, a surface protein often found in *S. epidermidis* (Tormo et al., 2005) and Esp, a surface protein found in *Enterococcus faecalis* (Shankar et al., 1999).

This study aimed to characterize phenotypic variations among different strains of *S. xylosus* regarding their ability to form biofilms, investigate factors influencing biofilm formation, and employed comparative genomic analysis to further comprehend primary adhesion and biofilm accumulation mechanisms in *S. xylosus*.

MATERIALS AND METHODS

Bacterial Strains and Culture Conditions

Five *S. xylosus* strains from the strain collection of Technische Mikrobiologie Weihenstephan (TMW), which were originally isolated from raw fermented sausages, and *S. epidermidis* RP62A obtained from DSMZ were selected for all experiments. Unless otherwise indicated, strains were grown from cryocultures in tryptic soy broth (TSB, casein peptone 15 g/l, soy peptone 15 g/l, yeast extract 3 g/l) aerobically cultivated until stationary phase (approximately 18 h) at 37°C and shaken at 200 rpm until further use.

Congo Red Agar Assay

To screen for slime production, the congo red agar test was performed as described by Freeman et al. (1989). Briefly, cultures were cultivated on a mixture of 37 g/l brain heart infusion broth (Carl Roth, Germany), 10 g/l agar and 50 g/l sucrose. The medium was supplemented with a solution of separately autoclaved 0.8 g/l of Congo Red (Carl Roth, Germany). After incubation of the isolates on the plates for 24 h at 37°C and 12 h at room temperature, plates were screened for differences in colony morphology. Black and dry crystalline colonies reveal slime producer, while non-slime producer usually develop pink and smooth colonies. Pictorial examples for different kinds of phenotypes is given in Knobloch et al. (2002).

Quantitative Biofilm Formation Assay on Hydrophilic and Hydrophobic Support in Different Cultivation Media

Biofilm formation was tested according to Christensen et al. (1985), with some minor modifications. Basically, overnight cultures of the selected strains were washed and diluted to an OD_{590} of 0.05 in medium. 200 µl of the adjusted cultures were pipetted into the wells of a 96-well plate and statically incubated for 24 h. After incubation, OD_{590} was measured again to confirm adequate cell growth in all wells. The wells were carefully decanted and plates were washed twice with sterile phosphate buffered saline (PBS) (NaCl 9 g/l, $Na_2HPO_4{}^*7H_2O$ 0.795 g/l, KH_2PO_4 0.114 g/l, pH 7.2). For biofilm fixation, plates were dried in an inverted position in a heat chamber (60°C) for at least 1 h. Adherent biofilm was stained with 200 µl 0.1% safranin-O (Sigma Aldrich, United States) for 5 min. Unbound safranin was removed, and plates were washed again twice with PBS. After air drying of the plates, the stain was solubilized with ethanol (95%) and absorbance was quantified at 490 nm.

In order to test dependence of phenotypic variations and expression of a biofilm positive phenotype on the presence of certain substances, the biofilm assay was performed using different cultivation media (TSB, TSB + 1% glucose, TSB + 1% glucose + 3% sodium chloride, using lactic acid). Additionally, two different supports were used, polystyrene 96-well plates (Sarstedt, Germany) and Nunclon™ delta surface 96-well plates (Thermo Fisher Scientific, United States) as hydrophobic and hydrophilic representatives, respectively.

Experiments were conducted in at least three independent biological replicates. Each biological replicate was performed in technical triplicates. Wells containing sterile medium only, served as a control in every experiment performed. *S. epidermidis* RP62A described as a strong biofilm producer and commonly used as model strain (Mack et al., 1992; Conlon et al., 2002) was included as a positive control for biofilm formation into the experiments.

Microbial Adhesion to Hydrocarbon (MATH)

For determining the surface hydrophobicity of cells, the adherence of bacteria to *n*-hexadecane was measured as described by Rosenberg (2006). Cells from overnight cultures were

washed and resuspended in imidazole/PBS (KH_2PO_4 0.1 g/l, $Na_2HPO_4{}^*2H_2O$ 4.45 g/l, imidazole 1.7 g/l, pH 6.2) to an OD_{590} of 0.35 to 0.4 (A_B). 5 ml of the cell suspension were overlaid with 0.4 ml *n*-hexadecane (Sigma Aldrich, United States) and incubated for 10 min at 37°C. Mixtures were then vortexted for 2 min and statically incubated for another 15 min at room temperature until phase separation was completed. The absorbance (A_A) of the aqueous phase was measured and the affinity for *n*-hexadecane (%) determined by using the following formula:

$$affinity\ to\ n\text{-hexadecane}\ (\%) = \frac{A_B - A_A}{A_B}\ x\ 100$$

If values were over 50%, strains were considered as highly hydrophobic, if values were under 20%, as hydrophilic. Each experiment was conducted in three independent runs.

DNA Isolation, Sequencing and Bioinformatics Analysis

For isolation of high-molecular-weight DNA from liquid (tryptic soy broth) bacterial overnight cultures, the E.Z.N.A®kit (Omega Bio-Tek Inc., United States) was used. Whole genome sequencing followed using SMRT (Single molecule real time) sequencing technology (PacBio RS II). The sequencing was carried out at GATC Biotech (Konstanz, Germany). For library creation an insert size of 8 to 12 kb was constructed, delivering at least 200 Mb of raw data from one to two SMRT cells (1 × 120-min movies), when P4-C2 chemistry is applied. SMRT Analysis version 2.2.0.p2 and the hierarchical genome assembly process (HGAP) were used for *de novo* assembly (Chin et al., 2013). Completion by manual processing according to PacBio instructions followed. Annotation of the genomes was based on the NCBI Prokaryotic Genome Annotation Pipeline (PGAP) and the Rapid Annotations using Subsystems Technology (RAST) Server (Aziz et al., 2008; Tatusova et al., 2016). Bioinformatic analysis and comparative genomics were performed using CLC Main Workbench 8 software (CLC bio, Denmark). To determine strain diversity, average nucleotide identity (ANI) values were calculated using additionally available whole genome sequencing data of four other *S. xylosus* strains (C2A (LN554884), S170 (CP013922), HKUOPL8 (CP007208), and SMQ-121 (CP008724)). Therefore, the ANIb algorithm (Goris et al., 2007) which is implemented within JspeciesWS web service (Richter et al., 2016) was applied and a neighbor-joining distance tree was built using MEGA7 software.

Statistical Analysis

For statistical analysis, Shapiro–Wilk test was performed to assure normal distribution of data. Means of the technical triplicates were determined first, followed by calculating the means of the biological triplicates including error propagation, which were then used for subsequent statistical comparison of differences. Two-tailed Student's *t*-tests assuming unequal variances were performed using SigmaPlot Version 12.5 (Systat Software GmbH, Germany). A difference of means was considered as being significant if *p*-values were less than 0.05 ($P < 0.05$). Student's *t*-test were performed to compare biofilm intensities of the strains on hydrophilic vs. hydrophobic support and in TSB supplemented with glucose compared to TSB, TSB supplemented with 3% NaCl + 1% glucose compared to TSB + 1% glucose as well as TSB + 1% glucose + lactate (pH 6) compared to TSB + 1% glucose.

RESULTS

Surface Hydrophobicity

According to the MATH test, only two of the tested strains possess hydrophilic surface properties (TMW 2.1523, TMW 2.1602). All other strains expressed a decisive affinity for the hydrocarbon phase, thus can be considered as strongly hydrophobic (**Table 1**).

Behavior of Colonies in the Congo Red Agar Assay

All *S. xylosus* isolates were tested negative for slime production by the congo red agar test. Colonies were mostly smooth, shiny and pink. Yet, changes to a darker color in parts where colonies were in close proximity to each other were observed for TMW 2.1523. The colonies of TMW 2.1523 also showed a rough instead of a smooth surface and a lobate margin. A dry surface with a lobate margin was observed for TMW 2.1521 as well. However, the typical overall black and dry crystalline morphology of a slime producer couldn't be detected for any of the *S. xylosus* strains. *S. epidermidis* RP62A served as positive control.

Influence of Support Hydrophobicity on Biofilm Formation

Adherence potential of *S. xylosus* to either hydrophobic or hydrophilic supports differed as shown in **Figure 1**. Among the strains that proved to be of hydrophobic nature, TMW 2.1023 and TMW 2.1521 weakly ($A_{490} < 1.5$) adhered to both supports, TMW 2.1324 adhered slightly better to hydrophobic than to hydrophilic support and *S. epidermidis* RP62A formed significantly more biofilm on hydrophilic than on hydrophobic support. Among the two hydrophilic strains, TMW 2.1602

TABLE 1 | Surface hydrophobicity of *S. xylosus* TMW strains and *S. epidermidis* RP62A.

Strain	Affinity for *n*-hexadecane (%)	Degree of Hydrophobicity
S. xylosus TMW 2.1023	95.0 ± 0.2	strong
S. xylosus TMW 2.1324	89.7 ± 3.1	strong
S. xylosus TMW 2.1521	93.4 ± 2.7	strong
S. xylosus TMW 2.1523	0.6 ± 1.1	weak
S. xylosus TMW 2.1602	0.9 ± 1.9	weak
S. epidermidis RP62A	95.6 ± 1.7	strong

Mean ± SE.

adhered to neither of the supports ($A_{490} < 0.5$), while TMW 2.1523 produced significantly more biofilm on hydrophilic compared to the hydrophobic support. In general, relations of biofilm formation on the two tested supports were similar in TSB and TSB + 1% glucose (compare **Figures 1A,B**), implicating that medium composition had no major influence on the adherence preference of the examined strains to either of the supports. Moreover, *S. xylosus* proved to be able to form comparable intensities of biofilm as the well characterized biofilm producer *S. epidermidis* RP62A.

Influence of Media Composition on Biofilm Formation

Media composition was found to influence adherence potential in a strain dependent matter (**Figure 2**). *S. xylosus* strain TMW 2.1602 proved again to be a non-biofilm producer regardless of which additive the media contained ($A_{490} < 0.5$).

S. xylosus TMW strains 2.1324 and 2.1521 as well as *S. epidermidis* RP62A displayed significantly enhanced biofilm formation on both supports tested upon the addition of 1% glucose to the culture medium. On the contrary, biofilm formation was significantly reduced by the presence of glucose in TMW 2.1523 on hydrophilic support. In weak biofilm producer TMW 2.1023, supplementation of glucose had no significant effect on adherence potential. Upon the addition of 3% NaCl to the culture medium, no clear pattern was identifiable for TMW strains 2.1023, 2.1324, and 2.1521. However, biofilm formation was significantly enhanced with NaCl present in TMW 2.1523 and significantly reduced in *S. epidermidis* RP62A on both supports, respectively. Acidification to pH 6 by lactate had a significantly enhancing effect on biofilm formation of TMW 2.1521 and 2.1523 while it significantly reduced biofilm formation of RP62A. The promoting effect of lactate on biofilm formation was especially distinct in TMW 2.1521, as the strain displayed a weak biofilm phenotype in TSB, TSB enriched with glucose and TSB enriched with a combination of glucose and NaCl. Using lactic acid, however, enhanced the strains biofilm formation to a degree that was comparable to the strong biofilm formers *S. xylosus* TMW 2.1324, 2.1523 and *S. epidermidis* RP62A ($A_{490} > 2.0$).

General Genome Features

Supplementary Table S1 summarizes the main genome features of the sequenced strains as well as the respective accession numbers. All five sequenced *S. xylosus* strains possess a single circular chromosome with sizes ranging from 2.8 to 2.9 Mbp, a GC content of 32.7 – 32.9 mol% and a strain-dependent plasmid quantity. The calculated ANI values (**Supplementary Figure S1**) confirmed genomic diversity among the isolates and revealed certain groups within the species *S. xylosus*. One comprising most of the TMW strains as well as *S. xylosus* C2A, originating from human skin (Götz et al., 1983) and *S. xylosus* SMQ-121, a starter used in the fermentation of processed meat (Labrie et al., 2014). Within this group, the strains TMW 2.1023 and TMW 2.1521 show the lowest genomic distance, while TMW 2.1523 seems to be considerably different from all the other *S. xylosus* strains. The second group comprised TMW 2.1602 and two additional *S. xylosus* strains that were both isolated in Asia, S170 from leaf vegetables (Hong and Roh, 2018) and HKUOPL8 from feces of healthy panda (Ma et al., 2014).

Genetic Screening for Adhesion and Biofilm Formation Related Factors

To further investigate the observed phenotypic differences, sequenced genomes of the five *S. xylosus* isolates were screened for the presence of genes that have been described to be associated with adhesion and biofilm formation processes of well characterized biofilm producers *S. epidermidis* and *S. aureus* (**Table 2**). *S. xylosus* carries only a small fraction of the described genes, among them autolysin *atl*/*atlE*, known to be involved in unspecific adhesion, MCSCRAMMs such as *ebpS*, *eno*, *fnb* as well as *bap*, a protein important in the biofilm accumulation process. Other genes, also associated with biofilm accumulation, such as *aap* and the *ica*-operon are lacking in all *S. xylosus* strains. Solely TMW 2.1602 carries parts of the *ica* operon, however, *icaD* is missing and only *icaR*, *icaC*, *icaB*, and *icaA* are present in the genome. Moreover, six out of eight genes of the *ess* cluster, encoding the ESAT-6 secretion system (ESS), were detected in TMW 2.1523 (*esxA*, *esaA*, *essA*, *esaB*, *essB*, *essC*, and A2I72_12780-12805). Compared to the *ess* cluster of *S. aureus* Newman (Burts et al., 2008), only *esaC* and *esxB* are missing in TMW 2.1523, both of which encode secreted polypeptides. All biofilm related genes analyzed in this study are located on the chromosome of the corresponding *S. xylosus* strains and not on their plasmids.

Two truncated genes related to biofilm formation were found in the investigated *S. xylosus* genomes. In TMW 2.1602 the *bap* gene encoding the biofilm associated protein carries a mutation. In TMW 2.1324, *fnb*, responsible for the synthesis of a fibronectin binding protein is truncated. TMW 2.1324 additionally lacks the *gehD* – lipase gene, which has been described for being involved in adhesion to collagen (Bowden et al., 2002).

Structural Analysis of the Biofilm Associated Protein (Bap) in *S. xylosus*

In *ica*-negative strains, Bap plays a major role in biofilm formation. Thus, a detailed *in situ* structural analysis of the Bap sequence was performed (**Figure 3**). General structural features were adapted from Cucarella et al. (2001), and Tormo et al. (2005), and Bap structure of *S. aureus* V329 (GenBank: AY220730.1) was included into the analysis. The *bap* gene is present in the genomes of all five *S. xylosus* isolates. However, the bap sequence of strain TMW 2.1602 contains a stop codon after 94 amino acids (aa) indicating an early termination during translation. All other Bap protein sequences show typical structural characteristics. At the N-terminal site of *S. xylosus* Bap, the YSIRK signal sequence (45 aa) for extracellular secretion is followed by region A (315 aa) which contains two short repeats of 5 aa. The signal sequence is missing in the NCBI-defined open reading frame (ORF) of strains TMW 2.1023 and TMW 2.1521,

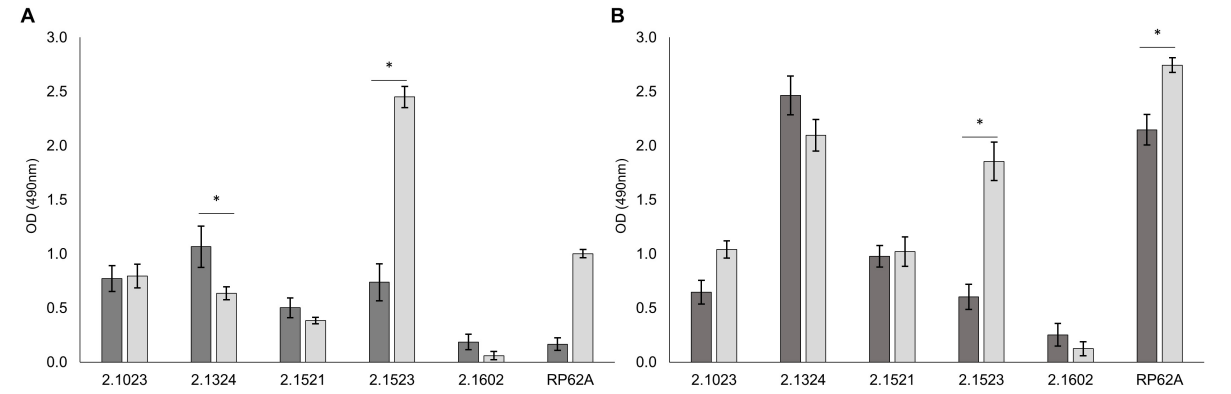

FIGURE 1 | Biofilm formation is dependent on surface hydrophobicity of the support. Biofilm formation on hydrophobic (■) and hydrophilic (□) support in TSB **(A)** and TSB + 1% glucose **(B)**. Significant differences of mean are marked by *. Mean ± SE.

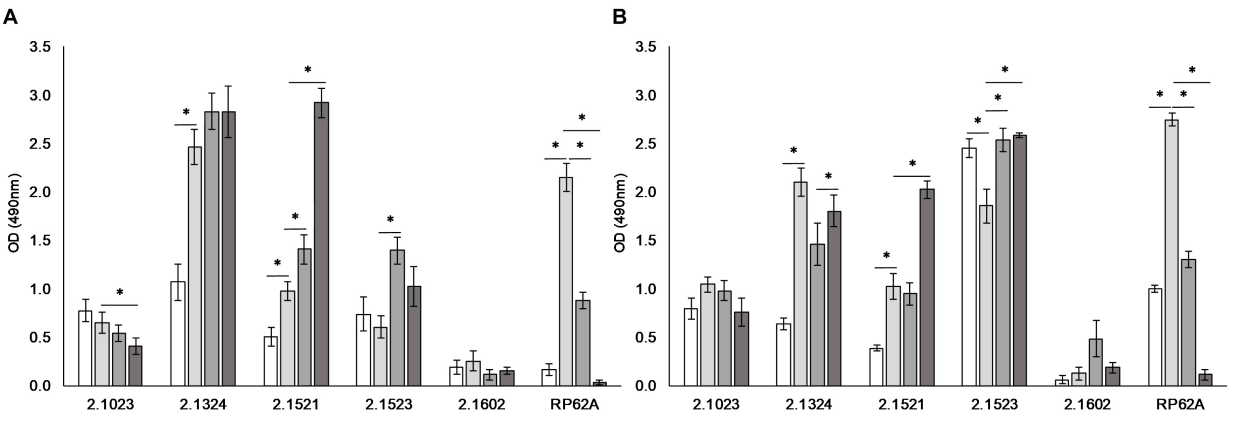

FIGURE 2 | Biofilm formation is dependent on environmental conditions. Biofilm formation on hydrophobic **(A)** and hydrophilic **(B)** support when incubated in TSB (□), TSB + 1% glucose (□), TSB + 1% glucose + 3% NaCl (■), and TSB + 1% glucose + lactate (pH 6) (■). Significant differences of mean are marked by *. Mean ± SE.

however, the missing sequence is present in the unprocessed consensus sequence indicating a false delimitation of the ORF. Region B (458 aa) possesses the most conserved part of the protein as it shows the highest sequence identity among the *S. xylosus* strains (protein identity 98.7 – 100%) as well as 80% identity to the B region of *S. aureus* V329 Bap. Region C starts with a short spacer region (48 aa) followed by a long core section which encompasses a varying number of Ig-like domain repeats (83 – 86 aa). The highest number of C repeats is present in the genome of *S. xylosus* TMW 2.1523 (13), followed by TMW strains 2.1324 (10), 2.1023 (7), and 2.1521 (7). The carboxy-terminal region D is characterized by differing numbers (12 – 17) of nearly identical 6 aa tandem repeats. Additionally, it contains an LPxTG motif, which is a well-known cell wall anchor sequence in Gram-positive bacteria. Regarding Bap of TMW 2.1602, not just the early stop codon indicates a truncation of the protein, also the B region misses 73 aa, the spacer region is much shorter and the sequence of the C and D repeats is different than in the other *S. xylosus* strains, where the repeating sequence was homolog and only the amount of repeats differed among the strains. Compared to *S. aureus* V329, the biggest difference in the organization of Bap in *S. xylosus* involves the number of C and D repeats, as size and amino acid sequence differ.

DISCUSSION

This study investigated variations in the biofilm forming capacity of five *S. xylosus* strains isolated from raw fermented sausages in dependence of different supports and media compositions. It was demonstrated that *S. xylosus* strains with hydrophobic surface properties (TMW 2.1023, TMW 2.1324, and TMW 2.1521) adhered equally well or with minor differences to the two supports tested (hydrophobic, hydrophilic). The only hydrophilic biofilm positive *S. xylosus* strain (TMW 2.1523) on the other hand adhered distinctly better to hydrophilic than to the hydrophobic support. This is in accordance with previous studies, which have proven that bacteria with hydrophobic surface properties adhere generally well to both kinds of supports while hydrophilic strains prefer hydrophilic supports (Heilmann et al., 1996a; Planchon et al., 2006). Hydrophobic

interactions are an important factor for adhesion, and cell surface hydrophobicity is influenced by a combination of the activity of autolysins such as AtlE, teichoic acids, cell surface structures, and surface net charge as well as components of the growth medium (Heilmann et al., 1997; Gross et al., 2001; An and Friedman, 2010). In this study it was further proven that biofilm formation is affected by additives to the growth medium, i.e., glucose, NaCl and lactate. The tested additives had no general stimulating or inhibitory effect on biofilm formation of all strains, but rather displayed varying strain-dependent effects. The here reported controversial effect of glucose on biofilm formation of *S. xylosus* has been reported for other staphylococci in previous studies (Hennig et al., 2007; Potter et al., 2009). For certain strains, such as *S. epidermidis* RP62A, addition of 1% glucose is essential for biofilm formation (Mack et al., 1992), which could be confirmed in this study. A generally positive effect on biofilm formation by addition of sodium chloride, previously reported for *S. epidermidis* and *S. aureus* (Rachid et al., 2000; Moretro et al., 2003) was not as distinct in the investigated *S. xylosus* strains.

Generally, the impact of glucose, sodium chloride and lactate on biofilm formation of *Staphylococcus* spp. has been mainly associated with changes in physicochemical interactions between cell and surface (Planchon et al., 2006) as well as differential expression of the *ica* operon upon stress exposure (Rachid et al., 2000; Knobloch et al., 2001). Since *S. xylosus* is *ica* negative, biofilm formation should be differently regulated by environmental stimuli. Therefore, it seems more likely that the

TABLE 2 | Analysis of adhesion and biofilm associated genes, described for *S. aureus* and *S. epidermidis* regarding their presence in the sequenced genomes of *S. xylosus* TMW 2.1023, TMW 2.1324, TMW 2.1521, TMW 2.1523, and TMW 2.1602.

Gene	Product	*S. aureus*	*S. epidermidis*	2.1023	2.1324	2.1521	2.1523	2.1602
aap/*sas*G	Accumulation associated protein	Corrigan et al., 2007	Schaeffer et al., 2015	–	–	–	–	–
atl/*atl*E	Autolysin	Bose et al., 2012	Heilmann et al., 1997	A2I69_ 04060	A2I70_ 04320	A2I71_ 09220	A2I72_ 04315	A2I73_ 09055
bap	Biofilm associated protein	Cucarella et al., 2001	Tormo et al., 2005	A2I69_ 12090	A2I70_ 12670	A2I71_ 01190	A2I72_ 12310	truncated A2I73_ 01165
bhp	Bap homolog protein	–	Tormo et al., 2005	–	–	–	–	–
*clf*A, *clf*B	Clumping factors A and B	McDevitt et al., 1994; Ní Eidhin et al., 1998	–	–	–	–	–	–
cna	Collagen adhesion protein	Patti et al., 1992	–	–	–	–	–	–
eap/*map*	Extracellular adhesion protein	Jönsson et al., 1995; Palma et al., 1999	–	–	–	–	–	–
ebh/*embp*	Extracellular matrix binding protein	Clarke et al., 2002	Williams et al., 2002	–	–	–	–	–
*ebp*S	Elastin binding protein	Downer et al., 2002	–	A2I69_ 06275	A2I70_ 06530	A2I71_ 07005	A2I72_ 06515	A2I73_ 06955
efb (*fib*	Fibronectin / fibrinogen adhesin	Palma et al., 1998	–	–	–	–	–	–
eno	Laminin binding protein	Carneiro et al., 2004	–	A2I69_ 03160	A2I70_ 03175	A2I71_ 10410	A2I72_ 03065	A2I73_ 10075
fbe (*sdr*G)	Fibronectin binding protein	–	Hartford et al., 2001	–	–	–	–	–
*fmt*A	methicillin resistance protein	Tu Quoc et al., 2007	–	A2I69_ 04085	A2I70_ 04345	A2I71_ 09195	A2I72_ 04340	A2I73_ 09030
fnb	Fibronectin binding protein	Jönsson et al., 1991	–	A2I69_ 01875	truncated A2I70_ 01890 – 95	A2I71_ 11695	A2I72_ 01805	A2I73_ 11285
*geh*D	Lipase	–	Bowden et al., 2002	A2I69_ 12875	–	A2I71_ 00405	A2I72_ 01015	A2I73_ 02855
ica ADBCR	Polysaccharide intercellular adhesin (PIA)	Heilmann et al., 1996b	Cramton et al., 1999	–	–	–	–	Incomplete A2I73_ 00825 – 00840
*mec*A	PBP2A	Côrtes et al., 2015	Petrelli et al., 2006	–	–	–	–	–
*sdr*C,D,E	SD-repeat containing proteins	Josefsson et al., 1998	–	–	–	–	–	–
*sdr*F,G,H	SD-repeat containing proteins	–	McCrea et al., 2000	–	–	–	–	–

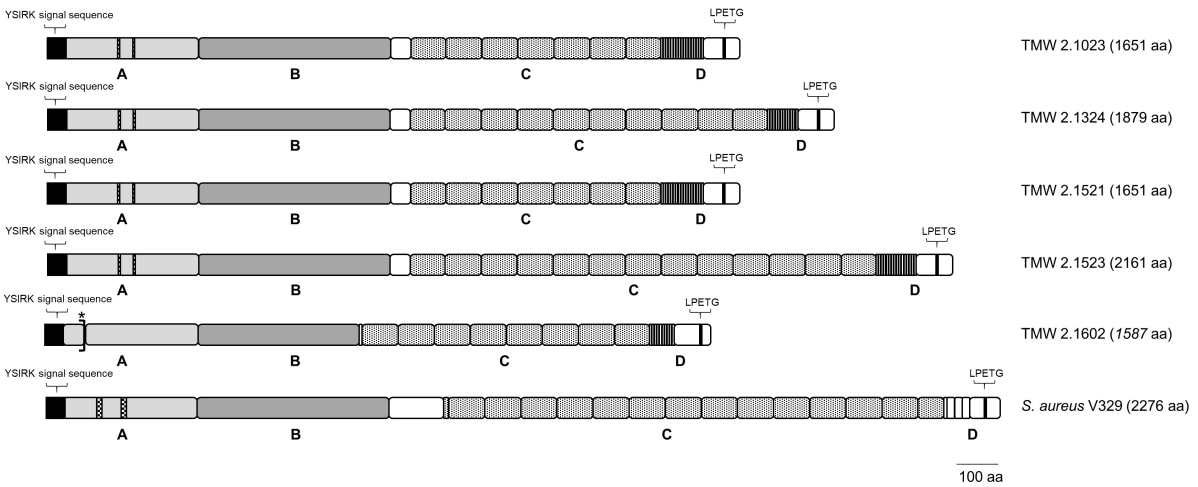

FIGURE 3 | Bap structure of *S. xylosus* and *S. aureus*. The positions of the YSIRK signal sequence, the LPxTG cell wall anchor motif as well as the four domains (A–D) of the protein are shown; asterisk indicates early translation termination due to a stop codon in the aa sequence of TMW 2.1602.

addition of glucose or sodium chloride to the culture medium or the change of pH by lactic acid influences the physiochemical surface properties such as the surface charge of the *S. xylosus* cells (Briandet et al., 1999). These changes, can impair the cell surface hydrophobicity, change electrostatic forces between support and cell, and therefore interfere with adhesion. Quorum sensing is another regulatory factor, often discussed in context with staphylococcal biofilm formation (Vuong et al., 2003). It appears that quorum sensing effects don't account for differences in biofilm phenotypes in this study though, as growth rates did not differ significantly in the tested media among the five *S. xylosus* strains (Data not shown). This is in contrary to the growth enhancing effects of 20 g/l NaCl addition that Planchon et al. (2006) reported. We solely observed a significantly higher growth rate and OD_{max} in TSB + 1% glucose compared to TSB lacking glucose for *S. epidermidis* RP62A (Data not shown).

Staphylococci that are *ica*-positive and thus are able to synthesize PIA often display a slime-positive phenotype on congo red agar (Petrelli et al., 2006). In this study, none of the analyzed *S. xylosus* strains showed a positive phenotype in the CRA tests, which confirmed the *in silico* analysis of *S. xylosus* being *ica* negative. It also confirms the hypothesis that *S. xylosus* TMW 2.1602 is most likely not synthesizing PIA despite carrying some genes of the *ica* operon. However, as Götz (2002) has also reported, *icaD* is of importance for PIA expression and *icaD* is missing in TMW 2.1602. TMW 2.1523 showed some characteristics of a CRA-positive phenotype by part of the colonies turning dark, rough and undulated instead of remaining round and shiny. This might be related to congo red being able to not only interact with exopolysaccharides but also proteins (Cucarella et al., 2001). Thus, either the presence of the *ess* cluster in the genome of TMW 2.1523, which mediates the excretion of certain polypeptides (Burts et al., 2008) or extracellular Bap might cause the reported phenotypic change on CRA. In general, the impact of the *ess* cluster encoded ESAT-6 secretion system on biofilm formation of *S. aureus* has been questioned in the past (Wang et al., 2016), yet for *Mycobacterium marinum* a correlation between ESAT-6 and biofilm formation has been reported (Lai et al., 2018). Therefore, the secreted polypeptides might be part of the biofilm matrix of TMW 2.1523.

To address the question of biofilm intensity formed by *S. xylosus*, *S. epidermidis* RP62A, known for being a strong biofilm producer, was taken into account as a reference strain in this study. Hereby, it was shown that *ica*-negative *S. xylosus* strains are able to form similar intensities of biofilm as the *ica*-positive *S. epidermidis* RP62A strain does. In order to investigate the mechanism of *S. xylosus* biofilm formation, a comparative genomic analysis of the *S. xylosus* strains was performed and genomes were screened for presence or absence of genes, which have previously been identified as being involved in biofilm formation of *S. aureus* and *S. epidermidis*. Bap seems to be a major factor in *S. xylosus* biofilm formation, as other well-known biofilm accumulation factors such as the *ica* operon and *aap* were absent in the analyzed genomes. Additionally, the physiological data support the thesis that Bap plays a major role in *S. xylosus* biofilm formation, as the biofilm negative strain TMW 2.1602 carried a truncated *bap* sequence. The importance of Bap in *ica*-negative strains has been described for other staphylococci before, e.g., Tormo et al. (2005), have proven that *ica* negative strains lose their ability to form biofilm once the *bap* gene is disrupted. It is possible though, that other, yet unknown mechanisms can contribute to biofilm formation. Comparison of the Bap sequences in *S. xylosus* demonstrated variations in the number of C and D repeats of the protein. However, it has been assumed that at least a varying number of C repeats does not influence the functionality of Bap, as for instance Cucarella et al. (2004) could not identify a correlation between number of C repeats and bap-mediated biofilm formation of *S. aureus* isolates. Furthermore, Bap has been described as being carried on the pathogenicity island SaPIbov2 in *S. aureus* (Ubeda et al., 2003). Yet, for *S. xylosus* no indicators were found that the bap locus was carried on or within a mobile genetic element.

Biofilm formation may contribute to fitness and survival of starter cultures in a particular ecological niche. This assumption is based on the principle of colonization resistance, a phenomenon well known from the human intestine where the microbiota prevents inflammation by occupying all niches along the intestinal tract (Lawley and Walker, 2013). In the sausage matrix, starters with high adhesion and biofilm forming potential may occupy microniches within the meat matrix during fermentation and thus increase their assertiveness against autochthonous staphylococci. The knowledge obtained in this study can be used to explain strain-specific differences of assertiveness in raw sausage fermentation previously identified (Vogel et al., 2017). Screening for a defined set of marker genes derived from the reported comparative genomics results may support the choice of assertive biofilm formers among *S. xylosus*. Taken together, this study demonstrated variability in biofilm formation of different *S. xylosus* strains and analyzed for the first time, which adhesion and biofilm related genes are present and absent among different *S. xylosus* strains displaying distinct phenotypes.

DATA AVAILABILITY

The datasets generated for this study can be found in Genbank, CP015538, CP015539 – CP015541, CP015542 – CP015545, CP015546 – CP015551, and CP015555 – CP015556.

AUTHOR CONTRIBUTIONS

CS conducted all the experiments, evaluated the data, generated the figures and tables, and wrote the first draft of the manuscript. MH helped in the bioinformatics analyses. ME supervised the work of CS and helped with biofilm tests. RV initiated the project, leaded the design of the study, and supervised CS. All authors contributed to manuscript revision, read, and approved the submitted version.

FUNDING

Part of this work was funded by the German Federal Ministry for Economic Affairs and Energy via the German Federation of Industrial Research Associations (AiF) and the Forschungskreis der Ernährungsindustrie E.V. (FEI), projects AiF17897N and 19690N. Publication of this work was supported by the Technische Universität München as part of the funding program Open Access Publishing.

SUPPLEMENTARY MATERIAL

The Supplementary Material for this article can be found online at: https://www.frontiersin.org/articles/10.3389/fmicb.2019.01387/full#supplementary-material

REFERENCES

An, Y. H., and Friedman, R. J. (eds) (2010). *Handbook of Bacterial Adhesion: Principles, Methods, and Applications*. Totowa, NJ: Humana Press.

Aziz, R. K., Bartels, D., Best, A. A., DeJongh, M., Disz, T., Edwards, R. A., et al. (2008). The RAST server: rapid annotations using subsystems technology. *BMC Genomics* 9:75. doi: 10.1186/1471-2164-9-75

Bose, J. L., Lehman, M. K., Fey, P. D., and Bayles, K. W. (2012). Contribution of the *Staphylococcus aureus* Atl AM and GL murein hydrolase activities in cell division, autolysis, and biofilm formation. *PLoS One* 7:e42244. doi: 10.1371/journal.pone.0042244

Bowden, M. G., Visai, L., Longshaw, C. M., Holland, K. T., Speziale, P., and Hook, M. (2002). Is the GehD lipase from *Staphylococcus epidermidis* a collagen binding adhesin? *J. Biol. Chem.* 277, 43017–43023. doi: 10.1074/jbc.M207921200

Briandet, R., Meylheuc, T., Maher, C., and Bellon-Fontaine, M. N. (1999). *Listeria monocytogenes* scott a: cell surface charge, hydrophobicity, and electron donor and acceptor characteristics under different environmental growth conditions. *Appl. Environ. Microbiol.* 65, 5328–5333.

Burts, M. L., DeDent, A. C., and Missiakas, D. M. (2008). EsaC substrate for the ESAT-6 secretion pathway and its role in persistent infections of *Staphylococcus aureus*. *Mol. Microbiol.* 69, 736–746. doi: 10.1111/j.1365-2958.2008.06324.x

Carneiro, C. R. W., Postol, E., Nomizo, R., Reis, L. F. L., and Brentani, R. R. (2004). Identification of enolase as a laminin-binding protein on the surface of *Staphylococcus aureus*. *Microbes Infect.* 6, 604–608. doi: 10.1016/j.micinf.2004.02.003

Chin, C.-S., Alexander, D. H., Marks, P., Klammer, A. A., Drake, J., Heiner, C., et al. (2013). Nonhybrid, finished microbial genome assemblies from long-read SMRT sequencing data. *Nat. Methods* 10, 563–569. doi: 10.1038/nmeth.2474

Christensen, G. D., Simpson, W. A., Younger, J. J., Baddour, L. M., Barrett, F. F., Melton, D. M., et al. (1985). Adherence of coagulase-negative staphylococci to plastic tissue culture plates: a quantitative model for the adherence of staphylococci to medical devices. *J. Clin. Microbiol.* 22, 996–1006.

Clarke, S. R., Harris, L. G., Richards, R. G., and Foster, S. J. (2002). Analysis of Ebh, a 1.1-megadalton cell wall-associated fibronectin-binding protein of *Staphylococcus aureus*. *Infect. Immun.* 70, 6680–6687.

Conlon, K. M., Humphreys, H., and O'Gara, J. P. (2002). icaR encodes a transcriptional repressor involved in environmental regulation of ica operon expression and biofilm formation in *Staphylococcus epidermidis*. *J. Bacteriol.* 184, 4400–4408.

Corrigan, R. M., Rigby, D., Handley, P., and Foster, T. J. (2007). The role of *Staphylococcus aureus* surface protein SasG in adherence and biofilm formation. *Microbiology* 153, 2435–2446. doi: 10.1099/mic.0.2007/006676-0

Côrtes, M. F., Beltrame, C. O., Ramundo, M. S., Ferreira, F. A., and Figueiredo, A. M. S. (2015). The influence of different factors including *fnb*A and *mec*A expression on biofilm formed by MRSA clinical isolates with different genetic backgrounds. *Int. J. Med. Microbiol.* 305, 140–147. doi: 10.1016/j.ijmm.2014.11.011

Cramton, S. E., Gerke, C., Schnell, N. F., Nichols, W. W., and Götz, F. (1999). The intercellular adhesion (*ica*) locus is present in *Staphylococcus aureus* and is required for biofilm formation. *Infect. Immun.* 67, 5427–5433.

Cucarella, C., Solano, C., Valle, J., Amorena, B., Lasa, I., and Penadés, J. R. (2001). Bap, a *Staphylococcus aureus* surface protein involved in biofilm formation. *J. Bacteriol.* 183, 2888–2896. doi: 10.1128/JB.183.9.2888-2896.2001

Cucarella, C., Tormo, M. A., Ubeda, C., Trotonda, M. P., Monzon, M., Peris, C., et al. (2004). Role of biofilm-associated protein Bap in the pathogenesis of bovine *Staphylococcus aureus*. *Infect. Immun.* 72, 2177–2185. doi: 10.1128/IAI.72.4.2177-2185.2004

Downer, R., Roche, F., Park, P. W., Mecham, R. P., and Foster, T. J. (2002). The elastin-binding protein of *Staphylococcus aureus* (EbpS) is expressed at the cell surface as an integral membrane protein and not as a cell wall-associated protein. *J. Biol. Chem.* 277, 243–250. doi: 10.1074/jbc.M107621200

Fey, P. D., and Olson, M. E. (2010). Current concepts in biofilm formation of *Staphylococcus epidermidis*. *Future Microbiol.* 5, 917–933. doi: 10.2217/fmb.10.56

Flemming, H. C., and Wingender, J. (2010). The biofilm matrix. *Nat. Rev. Microbiol.* 8, 623–633. doi: 10.1038/nrmicro2415

Freeman, D. J., Falkiner, F. R., and Keane, C. T. (1989). New method for detecting slime production by coagulase negative staphylococci. *J. Clin. Pathol.* 42, 872–874.

Goris, J., Konstantinidis, K. T., Klappenbach, J. A., Coenye, T., Vandamme, P., and Tiedje, J. M. (2007). DNA-DNA hybridization values and their relationship to whole-genome sequence similarities. *Int. J. Syst. Evol. Microbiol.* 57, 81–91. doi: 10.1099/ijs.0.64483-0

Götz, F. (2002). Staphylococcus and biofilms. *Mol. Microbiol.* 43, 1367–1378. doi: 10.1046/j.1365-2958.2002.02827.x

Götz, F., Zabielski, J., Philipson, L., and Lindberg, M. (1983). DNA homology between the arsenate resistance plasmid pSX267 from *Staphylococcus xylosus* and the penicillinase plasmid pI258 from *Staphylococcus aureus*. *Plasmid* 9, 126–137. doi: 10.1016/0147-619X(83)90015-X

Gross, M., Cramton, S. E., Götz, F., and Peschel, A. (2001). Key role of teichoic acid net charge in *Staphylococcus aureus* colonization of artificial surfaces. *Infect. Immun.* 69, 3423–3426. doi: 10.1128/IAI.69.5.3423-3426.2001

Hartford, O., O'Brien, L., Schofield, K., Wells, J., and Foster, T. J. (2001). The Fbe (SdrG) protein of *Staphylococcus epidermidis* HB promotes bacterial adherence to fibrinogen. *Microbiology* 147, 2545–2552. doi: 10.1099/00221287-147-9-2545

Heilmann, C., Gerke, C., Perdreau-Remington, F., and Götz, F. (1996a). Characterization of Tn917 insertion mutants of *Staphylococcus epidermidis* affected in biofilm formation. *Infect. Immun.* 64, 277–282.

Heilmann, C., Schweitzer, O., Gerke, C., Vanittanakom, N., Mack, D., and Götz, F. (1996b). Molecular basis of intercellular adhesion in the biofilm-forming *Staphylococcus epidermidis*. *Mol. Microbiol.* 20, 1083–1091. doi: 10.1111/j.1365-2958.1996.tb02548.x

Heilmann, C., Hussain, M., Peters, G., and Götz, F. (1997). Evidence for autolysin-mediated primary attachment of *Staphylococcus epidermidis* to a polystyrene surface. *Mol. Microbiol.* 24, 1013–1024. doi: 10.1046/j.1365-2958.1997.4101774.x

Hennig, S., Nyunt Wai, S., and Ziebuhr, W. (2007). Spontaneous switch to PIA-independent biofilm formation in an *ica*-positive *Staphylococcus epidermidis* isolate. *Int. J. Med. Microbiol.* 297, 117–122. doi: 10.1016/j.ijmm.2006.12.001

Hong, J., and Roh, E. (2018). Complete genome sequence of biofilm-producing strain *Staphylococcus xylosus* S170. *Korean J. Micobiol.* 54, 167–168. doi: 10.7845/kjm.2018.54.3.308

Jönsson, K., McDevitt, D., McGavin, M. H., Patti, J. M., and Höök, M. (1995). *Staphylococcus aureus* expresses a major histocompatibility complex class II analog. *J. Biol. Chem.* 270, 21457–21460.

Jönsson, K., Signas, C., Müller, H.-P., and Lindberg, M. (1991). Two different genes encode fibronectin binding proteins in *Staphylococcus aureus*. The complete nucleotide sequence and characterization of the second gene. *Eur. J. Biochem.* 202, 1041–1048. doi: 10.1111/j.1432-1033.1991.tb16468.x

Josefsson, E., McCrea, K. W., Ní Eidhin, D., O'Connell, D., Cox, J., Höök, M., et al. (1998). Three new members of the serine-aspartate repeat protein multigene family of *Staphylococcus aureus*. *Microbiology* 144(Pt 12), 3387–3395. doi: 10.1099/00221287-144-12-3387

Knobloch, J. K., Bartscht, K., Sabottke, A., Rohde, H., Feucht, H. H., and Mack, D. (2001). Biofilm formation by *Staphylococcus epidermidis* depends on functional RsbU, an activator of the sigB operon: differential activation mechanisms due to ethanol and salt stress. *J. Bacteriol.* 183, 2624–2633. doi: 10.1128/JB.183.8.2624-2633.2001

Knobloch, J. K.-M., Horstkotte, M. A., Rohde, H., and Mack, D. (2002). Evaluation of different detection methods of biofilm formation in *Staphylococcus aureus*. *Med. Microbiol. Immunol.* 191, 101–106. doi: 10.1007/s00430-002-0124-3

Labrie, S. J., El Haddad, L., Tremblay, D. M., Plante, P.-L., Wasserscheid, J., Dumaresq, J., et al. (2014). First complete genome sequence of *Staphylococcus xylosus*, a meat starter culture and a host to propagate *Staphylococcus aureus* phages. *Genome Announc.* 2:e0671-14. doi: 10.1128/genomeA.00671-14

Lai, L.-Y., Lin, T.-L., Chen, Y.-Y., Hsieh, P.-F., and Wang, J.-T. (2018). Role of the *Mycobacterium marinum* ESX-1 secretion system in sliding motility and biofilm formation. *Front. Microbiol.* 9:1160. doi: 10.3389/fmicb.2018.01160

Latasa, C., Solano, C., Penadés, J. R., and Lasa, I. (2006). Biofilm-associated proteins. *C. R. Biol.* 329, 849–857. doi: 10.1016/j.crvi.2006.07.008

Lawley, T. D., and Walker, A. W. (2013). Intestinal colonization resistance. *Immunology* 138, 1–11. doi: 10.1111/j.1365-2567.2012.03616.x

Ma, A. P. Y., Jiang, J., Tun, H. M., Mauroo, N. F., Yuen, C. S., and Leung, F. C.-C. (2014). Complete genome sequence of *Staphylococcus xylosus* HKUOPL8, a potential opportunistic pathogen of mammals. *Genome Announc.* 2:e0653-14. doi: 10.1128/genomeA.00653-14

Mack, D., Siemssen, N., and Laufs, R. (1992). Parallel induction by glucose of adherence and a polysaccharide antigen specific for plastic-adherent *Staphylococcus epidermidis*: evidence for functional relation to intercellular adhesion. *Infect. Immun.* 60, 2048–2057.

McCrea, K. W., Hartford, O., Davis, S., Eidhin, D. N., Lina, G., Speziale, P., et al. (2000). The serine-aspartate repeat (Sdr) protein family in *Staphylococcus epidermidis*. *Microbiology* 146(Pt 7), 1535–1546. doi: 10.1099/00221287-146-7-1535

McDevitt, D., Francois, P., Vaudaux, P., and Foster, T. J. (1994). Molecular characterization of the clumping factor (fibrinogen receptor) of *Staphylococcus aureus*. *Mol. Microbiol.* 11, 237–248.

Moretro, T., Hermansen, L., Holck, A. L., Sidhu, M. S., Rudi, K., and Langsrud, S. (2003). Biofilm formation and the presence of the intercellular adhesion locus *ica* among staphylococci from food and food processing environments. *Appl. Environ. Microbiol.* 69, 5648–5655. doi: 10.1128/AEM.69.9.5648-5655.2003

Ní Eidhin, D., Perkins, S., Francois, P., Vaudaux, P., Höök, M., and Foster, T. J. (1998). Clumping factor B (ClfB), a new surface-located fibrinogen-binding adhesin of *Staphylococcus aureus*. *Mol. Microbiol.* 30, 245–257. doi: 10.1046/j.1365-2958.1998.01050.x

Otto, M. (2008). Staphylococcal biofilms. *Curr. Top. Microbiol. Immunol.* 322, 207–228.

Palma, M., Haggar, A., and Flock, J. I. (1999). Adherence of *Staphylococcus aureus* is enhanced by an endogenous secreted protein with broad binding activity. *J. Bacteriol.* 181, 2840–2845.

Palma, M., Wade, D., Flock, M., and Flock, J. I. (1998). Multiple binding sites in the interaction between an extracellular fibrinogen-binding protein from *Staphylococcus aureus* and fibrinogen. *J. Biol. Chem.* 273, 13177–13181.

Patti, J. M., Jonsson, H., Guss, B., Switalski, L. M., Wiberg, K., Lindberg, M., et al. (1992). Molecular characterization and expression of a gene encoding a *Staphylococcus aureus* collagen adhesin. *J. Biol. Chem.* 267, 4766–4772.

Petrelli, D., Zampaloni, C., D'Ercole, S., Prenna, M., Ballarini, P., Ripa, S., et al. (2006). Analysis of different genetic traits and their association with biofilm formation in *Staphylococcus epidermidis* isolates from central venous catheter infections. *Eur. J. Clin. Microbiol. Infect. Dis.* 25, 773–781. doi: 10.1007/s10096-006-0226-8

Planchon, S., Gaillard-Martinie, B., Dordet-Frisoni, E., Bellon-Fontaine, M. N., Leroy, S., Labadie, J., et al. (2006). Formation of biofilm by *Staphylococcus xylosus*. *Int. J. Food Microbiol.* 109, 88–96. doi: 10.1016/j.ijfoodmicro.2006.01.016

Potter, A., Ceotto, H., Giambiagi-Demarval, M., Dos Santos, K. R. N., Nes, I. F., and Bastos Mdo, C. (2009). The gene *bap*, involved in biofilm production, is present in *Staphylococcus* spp. Strains from nosocomial infections. *J. Microbiol.* 47, 319–326. doi: 10.1007/s12275-009-0008-y

Rachid, S., Ohlsen, K., Wallner, U., Hacker, J., Hecker, M., and Ziebuhr, W. (2000). Alternative transcription factor sigma B is involved in regulation of biofilm expression in a *Staphylococcus aureus* mucosal isolate. *J. Bacteriol.* 182, 6824–6826. doi: 10.1128/JB.182.23.6824-6826.2000

Richter, M., Rosselló-Móra, R., Oliver Glöckner, F., and Peplies, J. (2016). JSpeciesWS: a web server for prokaryotic species circumscription based on pairwise genome comparison. *Bioinformatics* 32, 929–931. doi: 10.1093/bioinformatics/btv681

Rosenberg, M. (2006). Microbial adhesion to hydrocarbons: twenty-five years of doing MATH. *FEMS Microbiol. Lett.* 262, 129–134. doi: 10.1111/j.1574-6968.2006.00291.x

Schaeffer, C. R., Woods, K. M., Longo, G. M., Kiedrowski, M. R., Paharik, A. E., Büttner, H., et al. (2015). Accumulation-associated protein enhances *Staphylococcus epidermidis* biofilm formation under dynamic conditions and is required for infection in a rat catheter model. *Infect. Immun.* 83, 214–226. doi: 10.1128/IAI.02177-14

Shankar, V., Baghdayan, A. S., Huycke, M. M., Lindahl, G., and Gilmore, M. S. (1999). Infection-derived *Enterococcus faecalis* strains are enriched in *esp*, a gene encoding a novel surface protein. *Infect. Immun.* 67, 193–200.

Tatusova, T., DiCuccio, M., Badretdin, A., Chetvernin, V., Nawrocki, E. P., Zaslavsky, L., et al. (2016). NCBI prokaryotic genome annotation pipeline. *Nucleic Acids Res.* 44, 6614–6624. doi: 10.1093/nar/gkw569

Tormo, M. A., Knecht, E., Götz, F., Lasa, I., and Penades, J. R. (2005). Bap-dependent biofilm formation by pathogenic species of *Staphylococcus*: evidence of horizontal gene transfer? *Microbiology* 151, 2465–2475. doi: 10.1099/mic.0.27865-0

Tu Quoc, P. H., Genevaux, P., Pajunen, M., Savilahti, H., Georgopoulos, C., Schrenzel, J., et al. (2007). Isolation and characterization of biofilm formation-defective mutants of *Staphylococcus aureus*. *Infect. Immun.* 75, 1079–1088. doi: 10.1128/IAI.01143-06

Ubeda, C., Tormo-Mas, M. A., Cucarella, C., Trotonda, P., Foster, T. J., Lasa, I., et al. (2003). Sip, an integrase protein with excision, circularization and integration activities, defines a new family of mobile *Staphylococcus aureus* pathogenicity islands. *Mol. Microbiol.* 49, 193–210. doi: 10.1046/j.1365-2958.2003.03577.x

Vogel, R. F., Lechner, A., Ruhland, K., and Ehrmann, M. A. (2017). "Assertiveness of *Staphylococcus carnosus* and *Staphylococcus xylosus* in sausage fermentation," in *Proceedings of the 3rd International Symposium on Fermented Meats* (France: Clermont-Ferrand), 15.

Vos, P., de Garrity, G. M., and Jones, D. (eds) (2009). *Bergey's Manual of Systematic Bacteriology: Volume 3: The Firmicutes*. Dordrecht: Springer.

Vuong, C., Gerke, C., Somerville, G. A., Fischer, E. R., and Otto, M. (2003). Quorum-sensing control of biofilm factors in *Staphylococcus epidermidis*. *J. Infect. Dis.* 188, 706–718. doi: 10.1086/377239

Wang, Y., Hu, M., Liu, Q., Qin, J., Dai, Y., He, L., et al. (2016). Role of the ESAT-6 secretion system in virulence of the emerging community-associated *Staphylococcus aureus* lineage ST398. *Sci. Rep.* 6:25163. doi: 10.1038/srep25163

Williams, R. J., Henderson, B., Sharp, L. J., and Nair, S. P. (2002). Identification of a fibronectin-binding protein from *Staphylococcus epidermidis*. *Infect. Immun.* 70, 6805–6810. doi: 10.1128/IAI.70.12.6805-6810.2002

Xu, C.-G., Yang, Y.-B., Zhou, Y.-H., Hao, M.-Q., Ren, Y.-Z., Wang, X.-T., et al. (2017). Comparative proteomic analysis provides insight into the key proteins as possible targets involved in aspirin inhibiting biofilm formation of *Staphylococcus xylosus*. *Front. Pharmacol.* 8:543. doi: 10.3389/fphar.2017.00543

Conflict of Interest Statement: The authors declare that the research was conducted in the absence of any commercial or financial relationships that could be construed as a potential conflict of interest.

4.2 Bap-independent biofilm formation in *Staphylococcus xylosus*

Preface: In a first study (Schiffer et al., 2019) we concluded that the biofilm-associated protein Bap could be important for biofilm formation in *S. xylosus* since a natural *bap* defective strain had shown to be unable to form a biofilm. In the following, we sought to go deeper into the biofilm forming mechanisms of *S. xylosus* and reevaluate our hypothesis that Bap is essential for *S. xylosus* biofilm formation. Therefore, we constructed *S. xylosus* knockout mutants of two *S. xylosus* strains, TMW 2.1023 and TMW 2.1523. Of note is that previously reported biofilm- and Bap- positive strains TMW 2.1521 and TMW 2.1324 could not be included in the study, as the first harbors a chloramphenicol resistance gene interfering with the selection marker of the chosen vector system and the latter not being transformable by electroporation (compare Schiffer et al., 2022b). *S. xylosus* mutants deficient in *bap*, have hitherto not been described in the literature. Thus, we were the first to investigate the role of the protein in staphylococcal species other than *S. aureus* and *S. epidermidis*. Interestingly, subsequent phenotypic tests on adherence to hydrophilic and hydrophobic supports showed that mutant strains behaved mostly like wildtype strains and no differences were observable. Furthermore, studies characterizing Bap in *S. aureus* have shown that calcium addition diminished Bap mediated biofilm formation (Arrizubieta et al., 2004), an effect we were not able to reproduce for *S. xylosus* in this work either. To understand the phenotypic results and find possible explanations for the impact of Bap on biofilm formation of different staphylococci, the respective protein sequences of *S. aureus* V329 and *S. xylosus* were compared and analyzed. Sequence analysis revealed major differences between the two proteins, which might explain the different phenotypes of the gene homologs in these two species.

In this study, we were the first to describe that Bap homologs do not necessarily have the same function that is described for *S. aureus*, in other staphylococci and that care should be taken when gene functions are extrapolated from one organism to another. By showing that Bap is not essential for biofilm formation of the species, we have opened the debate that other proteins must be involved in multicellular behavior and biofilm formation of *S. xylosus*.

Author contributions: Carolin Schiffer was responsible for conceptualization of the study and performed all experiments. She prepared the proteomic samples for analysis by BayBioMS and conducted detailed bioinformatic analyses. She also wrote the original draft of the manuscript and co-edited the final version. Furthermore, she acted as corresponding author in the submission process and responded to the reviewers' suggestions.

microorganisms

MDPI

Article

Bap-Independent Biofilm Formation in *Staphylococcus xylosus*

Carolin J. Schiffer [1,*], Miriam Abele [2], Matthias A. Ehrmann [1] and Rudi F. Vogel [1]

[1] Lehrstuhl für Technische Mikrobiologie, Technische Universität München, 85354 Freising, Germany; matthias.ehrmann@tum.de (M.A.E.); rudi.vogel@tum.de (R.F.V.)
[2] Bayerisches Zentrum für Biomolekulare Massenspektrometrie (BayBioMS), 85354 Freising, Germany; m.abele@tum.de
* Correspondence: carolin.schiffer@tum.de

Abstract: The biofilm associated protein (Bap) is recognised as the essential component for biofilm formation in *Staphylococcus aureus* V329 and has been predicted as important for other species as well. Although Bap orthologs are also present in most *S. xylosus* strains, their contribution to biofilm formation has not yet been demonstrated. In this study, different experimental approaches were used to elucidate the effect of Bap on biofilm formation in *S. xylosus* and the motif structure of two biofilm-forming *S. xylosus* strains TMW 2.1023 and TMW 2.1523 was compared to Bap of *S. aureus* V329. We found that despite an identical structural arrangement into four regions, Bap from *S. xylosus* differs in key factors to Bap of *S. aureus*, i.e., isoelectric point of aggregation prone Region B, protein homology and type of repeats. Disruption of *bap* had no effect on aggregation behavior of selected *S. xylosus* strains and biofilm formation was unaffected (TMW 2.1023) or at best slightly reduced under neutral conditions (TMW 2.1523). Further, we could not observe any typical characteristics of a *S. aureus* Bap-positive phenotype such as functional impairment by calcium addition and rough colony morphology on congo red agar (CRA). A dominating role of Bap in cell aggregation and biofilm formation as reported mainly for *S. aureus* V329 was not observed. In contrast, this work demonstrates that functions of *S. aureus* Bap cannot easily be extrapolated to *S. xylosus* Bap, which appears as non-essential for biofilm formation in this species. We therefore suggest that biofilm formation in *S. xylosus* follows different and multifactorial mechanisms.

Keywords: *Staphylococcus xylosus*; knockout; Bap; biofilm; aggregation

Citation: Schiffer, C.J.; Abele, M.; Ehrmann, M.A.; Vogel, R.F. Bap-Independent Biofilm Formation in *Staphylococcus xylosus*. *Microorganisms* **2021**, *9*, 2610. https://doi.org/10.3390/microorganisms9122610

Academic Editor: Edward Fox

Received: 30 November 2021
Accepted: 15 December 2021
Published: 17 December 2021

1. Introduction

Staphylococcus (S.) xylosus is a Gram-positive, coagulase-negative commensal of mammal skin with a biotechnological relevance, as it is commonly used as a starter organism for raw sausage fermentation [1]. For persistence in such environments, surface colonization and the formation of biofilms are anticipated as important traits. Biofilm formation is a common property of many bacteria and describes a state where cells are embedded in an extracellular matrix, mainly consisting of exopolysaccharides, proteins and extracellular DNA [2]. Biofilm matrix composition can vary and is dependent on species-specific mechanisms as well as environmental conditions [3]. If biofilms are of a mainly proteinaceous nature, surface proteins play a prominent role in primary adhesion and biofilm maturation as they can either interact with surface structures on adjacent cells or form amyloid structures that promote cellular aggregation [4]. Known surface proteins influencing proteinaceous biofilm matrix assembly include fibronectin binding proteins (FnBPs), *Staphylococcus aureus* surface protein G (SasG) and the biofilm associated protein (Bap) [5,6]. Bap is a high molecular weight surface protein, which was first described by Cucarella et al. [7]. Bap and its homologues have been shown to mediate multicellular aggregation as well as biofilm formation in several organisms, such as staphylococci and enterococci [8,9]. In *S. aureus*, V329 Bap is extensively studied, and it has been demonstrated that its functionality is based on self-assembly of *N*-terminal peptides of the protein into amyloid fibers

under acidic conditions [9]. Furthermore, Bap-mediated biofilm formation is influenced by calcium ions in the environment, as they prevent amyloid assembly of Bap-derived peptides and subsequent intercellular aggregation [10]. Other than in the well-studied *S. aureus* V329, Bap function has only been molecularly characterized by the construction of knockout mutants in *S. epidermidis* C533 [11]. Studies addressing *bap* of biofilm-positive *S. xylosus* strains have been focusing solely on presence/absence of the gene analysed by PCR/hybridization approaches so far [11,12]. Thus, the actual function of the protein in *S. xylosus* has not been verified experimentally yet.

In a previous study, we demonstrated a strain-specific behavior in biofilm formation among different *S. xylosus* strains depending on environmental conditions as well as their individual genomic settings with respect to additional biofilm-related genes [13]. The fact that a strain in which *bap* is naturally defective displayed a biofilm negative phenotype led us to suggest an essential role of Bap in biofilm formation of *S. xylosus.* In order to test this hypothesis and to ensure that any impact of other genomic determinants is excluded, we generated isogenic *bap* knockout mutants of biofilm positive strains. Furthermore, we investigated whether *S. xylosus* and its *bap* mutants show typical phenotypic characteristics and differences, as they have been reported in Bap-positive *S. aureus* strains and its respective *bap* mutants.

2. Materials and Methods

2.1. Bacterial Strains and Culture Conditions

S. xylosus TMW 2.1023 and TMW 2.1523 are both biofilm-positive strains, isolated from raw fermented sausages [13]. *Escherichia (E.) coli* DC10B is a cytosine methyltransferase-negative derivate, often used in transformation experiments to evade type IV restriction modification systems [14].

E. coli DC10B was cultured in Lysogeny Broth (LB, tryptone 10 g/L, yeast extract 5 g/L, NaCl 5 g/L) 37 °C. Staphylococcal strains were cultured at 28 or 37 °C in Trypticase soy broth (TSB, casein peptone 15 g/L, soy peptone 15 g/L, yeast extract 3 g/L) supplemented with either no glucose (TSB_N) or 1% glucose (TSB^+), brain heart infusion (BHI) broth, or basic medium (BM, 1% peptone, 0.5% yeast extract, 0.5% NaCl, 0.1% Glucose, 0.1% K_2HPO_4). For transformation experiments, 20 µg/mL (*E. coli*) or 10 µg/mL (*S. xylosus*) of chloramphenicol (CarlRoth, Karlsruhe, Germany) were added when necessary.

2.2. DNA Manipulations and Bacterial Transformation: Mutagenesis of the Chromosomal Bap Gene by Allelic Exchange

For inactivation of *bap* in *S. xylosus*, regions up—and downstream of the sequence to be deleted were amplified using primers bap1F (5′-ACTCACTATAGGGCGAATTGGAGCT GTTATCAGCAGCTGCTAAG-3′), bap2R (5′-GTATATTGCGACACAATGTAAAGTATATC AG-3′), bap3F (5′-CTTTACATTGTGTCGCAATATACAGCTAG-3′) and bap4R (5′-GCTTGA TATCGAATTCCTGCAGCATCTATAACTTTAGCTG-3′). To be able to use the same primer set for both *S. xylosus* strains (TMW 2.1023, TMW 2.1523), primers were chosen to map on conserved regions of the gene. PCR products were purified using a Monarch PCR and DNA cleanup kit (New England Biolabs (NEB), Ipswich, United Stated). Shuttle vector pIMAY*, which was kindly provided by A. Gründling (Molecular Microbiology, Imperial College London, UK) was digested with restriction enzymes *SacI* and *PstI* and PCR fragments were ligated into the vector using Gibson Assembly (NEB). The construct was transformed into *E. coli* DC10B by electroporation and successful transformants were selected on chloramphenicol plates. Sequencing, to verify correct assembly of the vector, followed. Plasmid was isolated using the Monarch plasmid DNA miniprep kit (NEB) and transformed into electrocompetent *S. xylosus* cells as described by Monk et al. [15]. Briefly, *S. xylosus* was cultured overnight in BHI and diluted to an OD_{600} of 0.5 in BM the next morning. Cultures were then incubated at 37 °C and 200 rpm for another 40 min, harvested, washed twice with ice-cold water and another two times with 10% glycerol in decelerating volumes (1/10, 1/25). Finally, cells were resuspended in 1/200 volume 10% glycerol +

500 mM sucrose and directly subjected to electroporation. At least 1 µg of plasmid was transformed (0.2 cm, 2.5 kV) and cells were immediately suspended in 1 mL BHI + 200 mM sucrose. After one hour at 28 °C, cells were spread on BHI 20CM and incubated at 28 °C for two days. Colonies were picked and allelic replacement was performed as described by Schuster et al. [16]. Lastly, successful allele replacement of the chromosomal *bap* sequence as well as plasmid loss were verified by colony PCR using primers bap1F and bap4R.

2.3. Colony Morphology on CRA

Colony morphology of wildtype and mutant strains on congo red agar (CRA, 10 g/L glucose, 0.8 g/L congo red) was assessed as previously described [17]. As congo red interacts with proteins and proteinaceous structures, strains with rough colony margins were considered as Bap positive, whereas Bap negative strains usually retain smooth colony margins.

2.4. Biofilm Formation Assays

Biofilm formation was quantified in 96-well plates as described by Schiffer et al. [13]. Strains were cultured in different media (TSB_N, TSB^+ (pH 7.2), Lac^+ (TSB^+ acidified with lactic acid to pH 6.0) and on different supports (hydrophobic (Sarstedt, Nürmbrecht, Germany), hydrophilic (Nunclon™ delta, Thermo scientific, Waltham, MA, USA)). The media chosen, represent the three media found in a previous study to influence biofilm formation of the selected strains the most [13]. Lactic acid was used instead of an inorganic acid, as it is a prevalent acid found in one of the habitats of the species *S. xylosus* (raw fermented sausages). To determine whether calcium influences biofilm formation, $CaCl_2$ was added to the wells to a final concentration of 20 mM when indicated.

2.5. Bacterial Aggregation Assay

Bacterial aggregation was determined by growing cell suspensions (OD_{600} at t_0: 0.1) in test tubes for 24 h at 37 °C, 200 rpm in either TSB_N or TSB^+. Aggregation behavior was evaluated macroscopically. To investigate whether calcium has an impact on cellular aggregation behavior, $CaCl_2$ was added to a concentration of 20 mM when indicated.

2.6. Growth and pH Dynamics

pH changes of *S. xylosus* strains in TSB^+ were monitored using the icinac system (AMS Systea, Rome, Italy). Growth curves were recorded by determining the optical density over a period of 33 h in a Microplate Reader (Spectrostar^{Nano}, BMG Labtech, Ortenburg, Germany).

2.7. SDS Page of Protein Extracts

Bacteria were grown in TSB_N until early stationary phase (37 °C, 200 rpm, 12 h). Then, 5 mL of cell culture were harvested (4 °C, 5000× *g*), washed twice with ice-cold phosphate-buffered saline (PBS) and resuspended in 150 µL PBS + 30% [wt/vol] raffinose (SigmaAldrich, St. Louis, MI, USA). Afterwards, 7 µL lysostaphin (1 mg/mL, SigmaAldrich, St. Louis, MI, USA) and 3 µL of DNAseI (1 mg/mL, SigmaAldrich, St. Louis, MI, USA) were added and after incubation at 37 °C for 2 h, protoplasts were sedimented at 8000× *g* for 30 min with slow deceleration. Supernatants were stored at −20 °C until subjection to SDS-PAGE analysis (10% resolving, 4% stacking gel).

2.8. Full Proteome Analysis

For full proteome analysis of *S. xylosus* cells, 0.1% of overnight cultures were diluted in fresh Lac^+ and incubated in Erlenmeyer flasks under agitation (planktonic, 5 mL) or statically in Nunclon™ delta surface (Thermo scientific, Waltham, MA, USA) tissue culture plates (sessile, 2 mL) for 24 h at 37 °C. Cell lysis and in-solution digest were performed with minor changes according to the SPEED protocol [18]. Shortly, 2 mL of planktonic cells were harvested, washed twice with ice-cold PBS and resuspended in 100 µL of

absolute Trifluoroacetic acid (TFA). Sessile cells were also washed twice with ice-cold PBS to remove any non-adherent cells as well as to remove as many media proteins as possible, and dissolvement of adherent cells was performed by carefully resuspending the biofilm in 100 µL (TFA). All TFA cell suspensions were neutralized to pH 8.1–8.3 by adding nine volumes of Tris (2 M, pH not adjusted). Incubation in a thermomixer for 5 min at 55 °C and 450 rpm (ThermoMixerC, Eppendorf, Hamburg, Germany) as well as short centrifugation followed. Protein concentrations were determined using Bradford assay (B6916, SigmaAldrich, St. Louis, MI, USA) according to manufacturer's instructions. Then, 15 µg of total protein amount were reduced, alkylated (10 mM Tris-(2-carboxyethyl)-phosphin, 40 mM 2-Chloroacetamide; 5 min, 95 °C) and afterwards diluted with water (1:1). Trypsin digest was performed in an enzyme to protein ratio of 1:50 overnight at 30 °C with mild agitation (400 rpm) and then stopped with 3% Formic acid (FA). Three discs of Empore C18 (3 M, Saint Paul, Minnesota, United States) material were packed in 200 µL pipette tips. The resulting desalting columns were conditioned (100% acetonitrile, can) and equilibrated (40% ACN/0.1% FA followed by 2% ACN/0.1% FA). Peptides were loaded, washed (2% ACN/0.1% FA) and eluted (40% ACN/0.1% FA). For the determination of expression levels of Bap in sessile versus planktonic cultures, around 250 ng peptides of three biological replicates were subjected to an Ultimate 3000 RSLCnano system coupled to a Q-Exactive HF-X mass spectrometer (Thermo Fisher Scientific, Waltham, MA, USA). All acquisition parameters were the same as described by Kolbeck et al. [19]. Proteomic analysis of the mutant strains was done in single measurements. Around 250 ng of peptides were subjected to an Ultimate 3000 RSLCnano system coupled to a Fusion Lumos Tribrid mass spectrometer (Thermo Fisher Scientific, Waltham, MA, USA). All parameters were set as described by Bechtner et al. [20].

Since TMW 2.1523 is a well biofilm former in TSB_N [13], it was chosen that planktonic as well as sessile data was sampled for this particular strain not just in Lac^+ but also in TSB_N.

2.9. Bioinformatic and Statistical Analysis

Bioinformatic analysis and comparative genomics were performed using CLC Main Workbench 8 software (CLC bio, Aarhus, Denmark). Isoelectric point (pI) and molecular weight (MW) were computed using the respective tool from the Expasy server (available under: https://web.expasy.org/compute_pi/, accessed on 29 November 2021), InterPro (86.0) was used to predict signal peptide, transmembrane regions and cell wall anchor and ProScan (screens against PROSITE database) was used to scan for EF-hand motifs (cut off was set to 80% protein identity). Amyloidogenic regions in protein sequences were analyzed by using the amyloid finder tools FoldAmyloid [21], Aggrescan [22], Waltz-DB 2.0 [23] and Tango [24].

Peptide identification and quantification were performed using MaxQuant (v1.6.3.4) with Andromeda[97] [25,26]. MS2 spectra were searched against the NCBI proteome databaste of *S. xylosus* 2.1023 and 2.1523, respectively; common contaminants were included (built-in option in MaxQuant). Trypsin/P was specified as proteolytic enzyme. Precursor tolerance was set to 4.5 ppm and fragment ion tolerance to 20 ppm. Results were adjusted to 1% false discovery rate (FDR) on peptide spectrum match level and protein level employing a target-decoy approach using reversed protein sequences. Minimal peptide length was defined as 7 amino acids; the "match-between-run" function disabled. Carbamidomethylated cysteine was set as fixed and oxidation of methionine and *N*-terminal protein acetylation as variable modifications. Perseus version 1.6.15.0 [27] and LFQ-Analyst [28] were used for data analysis. Missing label-free quantitation (LFQ) values were imputed from normal distribution. Significant differences in intensities between the conditions chosen, were calculated by student's t-test with α set to 0.05 FDR correction (Benjamini Hochberg method) was applied to correct *p*-values. Data are, if not otherwise indicated, presented as means +/− standard errors of the means. Student's *t*-tests were performed using Perseus Version 1.6.15.0.

3. Results

3.1. Protein Motif Structural Organization of S. xylosus Bap

To allow conclusions on structure-function correlations, the protein structures of *S. xylosus* and *S. aureus* Bap were compared. To get an idea of the conservation of the protein along the full sequence length, each region was aligned separately. Hereby, we sticked to the four major regions of the protein which were defined previously [7,13]. Bap of *S. xylosus* TMW 2.1023 and TMW 2.1523 share high sequence similarities, with 99.4% (Region A), 99.4% (Region B), 79.5% (Region C) and 98.4% (Region D) protein identity, respectively. Strain specific differences of *S. xylosus* Bap mainly rely on the number of C-Repeats, which have previously been shown to have no impact on the biofilm function of Bap [30]. Therefore, both *S. xylosus* sequences are referred to as Bap_{XYL} in this paragraph and compared to the sequence of the phenotypically well-characterized, Bap-positive strain *S. aureus* V329 (Bap_{AUR}).

Bap_{XYL} as well as Bap_{AUR} are both high molecular weight proteins fulfilling typical criteria of surface proteins such as a 44 amino acid (aa) long *N*-terminal signal sequence (YSIRK motif) as well as a C-terminal hydrophobic transmembrane segment and the LPxTG cell wall anchor motif. However, deeper sequence comparison of Bap of these two species revealed some notable differences (Table 1).

While the predicted pI of the full protein sequences is almost identical (~3.9), it is noticeably lower in Bap_{XYL} when the aggregation prone Region B ($BapB_{AUR}$: 4.6, $BapB_{XYL}$: 4.4) is considered only. Further, repeating sequence patterns differ remarkably between the proteins of both species. While Bap_{AUR} carries two large repeating sequences in region A, $BapA_{XYL}$ contains only two short tandem repeats. Similar applies for region D repeats. $BapD_{AUR}$ repeats are rich in serine and aspartate, while $BapD_{XYL}$ repeats are not just shorter but also lacking these amino acids and are rather rich in glycine. Another difference is the type of repeats in the C Region of the protein described for both species. For $BapC_{XYL}$ repeats are predicted to be ig-like domain type 6 repeats, while for $BapC_{AUR}$ repeats are characterized as ig-like domain type 3 repeats. It is also noteworthy that Bap_{XYL} carries almost twice as many predicted EF hand binding motifs than Bap_{AUR}. However, EF hand motifs EF2 and EF3 displayed by Region B of the protein, which have been shown to have a regulating effect on the activity of the protein [10], are identical in both species.

Several online tools were employed to predict amyloidogenic regions of the three protein sequences. All proteins share a region with high amyloidogenic potential, roughly between amino acid 400 and 900 (Figure 1).

However, while this region seems to be the only one with amyloidogenic potential in *S. aureus* V329, results are less conclusive for Bap_{XYL}, as, especially in TMW 2.1523, regions with amyloidogenic structural characteristics are also predicted in the C-terminal part of the protein. For Bap_{AUR}, two peptides (I: $_{487}$TVGNIISNAG$_{496}$, II: $_{579}$GIFSYS$_{584}$) are characterized as displaying significant amyloidogenic potential [9]. *S. xylosus* harbors similar peptide sequences in its Bap sequence, however, not identical (I: $_{490}$TVANILNNAG$_{499}$, II: $_{582}$GVFSYS$_{587}$). To ensure that the sequences of our selected *S. xylosus* strains are representative for the species, we compared them to a range of other *S. xylosus bap* sequences as well (see Figure S1). In this context we also included the sequence of *S. epidermidis* C533 into the alignments, as Tormo et al. [11] have previously reported a biofilm negative phenotype for this strain upon deletion of *bap*. Sequence analysis confirmed that *S. aureus* and *S. epidermidis* Bap are closely related and share high sequence homologies in all parts of the protein. *S. xylosus bap* sequences on the other hand, share high homologies among themselves, but differ from *S. aureus* and *S. epidermidis bap* genes in some functionally important parts. Namely, they lack long amino acid repeats in region A, harbor slightly different amyloidprone peptide sequences in region B, carry different types of C-repeats and are rather composed of G-rich as to SD-repeats in region D. It is further worth noting that we found a high range of truncated Bap sequences among *S. xylosus* strains, and also in biofilm positive strains ([12], e.g., *S. xylosus* C2a, accession: WP_144404228.1). This

substantiates our hypothesis that the protein is non-essential for biofilm formation by this species.

Table 1. Sequence comparison of Bap originating from *S. xylosus* TMW 2.1023, TMW 2.1523 and *S. aureus* V329. Different characteristics such as protein size, length of each region of the multidomain protein, molecular weight (MW), isoelectric point (pI) as well as number (#) of repeats and EF-hand motifs are listed.

Bap	***S. xylosus* 2.1023**	***S. xylosus* 2.1523**	***S. aureus* V329**
Accession	JGY91_02455	JGY88_01140-45	AAK38834
Length total (aa)	1651	2161	2276
YSIRK Signal Peptide	1–44	1–44	1–44
Region A	316	316	316
Region B	458	458	458
Region C (incl. spacer)	644	1160	1321
Region D (incl LPXTG)	189	183	137
TM helix	1624–1641	2134–2151	2249–2266
MW (kDa)	173.1	224.3	238.5
pI_Bap	4.01	3.90	3.90
pI_BapB	4.41	4.39	4.61
# RepeatsA	2	2	2
sequence	TAEDN	TAEDN	AQDDDNIKEDSNTQEESTN TSSQSSEVPQTKK
# RepeatsC	7	13	14
type of C repeats	ig-like domain type 6	ig-like domain type 6	ig-like domain type 3
# RepeatsD	17	16	7
sequence	13× GTGENP, 1× GKGENP, 1× GGGENP, 1× GIGENP, 1× GTGENT	14× GTGENP, 1× GAGENP, 1× GTGENT	2× SDDNSDNGNN 1× SDDNSGNGDN 1× SDDNSDN 1× SGAGDTSD 2× SGAGDNSD
%p.identity_Xyl vs Aur	45.13	58.97	-
%p.identity_B_Xyl vs Aur	80.18	79.96	-
# EF motifs	7	7	4
seq_EF2	DYDKDGLLDRYER	DYDKDGLLDRYER	DYDKDGLLDRYER
seq_EF3	DTDGDGKNDGDEV	DTDGDGKNDGDEV	DTDGDGKNDGDEV
%p.identity EF2_Xyl vs. Aur	100	100	-
%p.identity EF3_Xyl vs. Aur	100	100	-

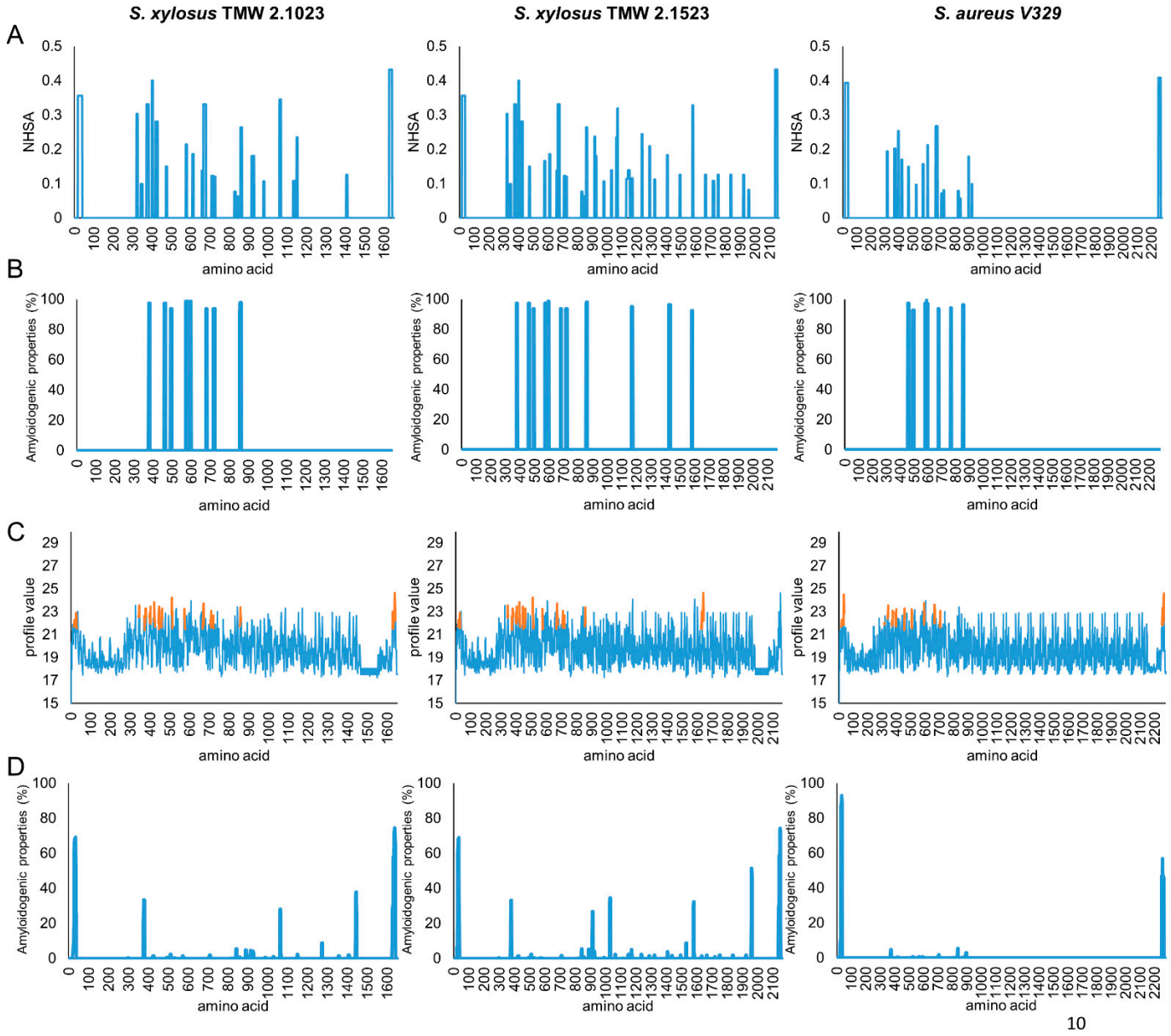

Figure 1. Amyloidogenic structure prediction of different protein sequences from *S. xylosus* TMW 2.1023, TMW 2.1523 and *S. aureus* V329. Prediction based on aggrescan (**A**), waltz (**B**), fold amyloid (**C**) and tango (**D**).

3.2. Mutagenesis of the Chromosomal Bap Gene

For mutagenesis of the chromosomal *bap* gene, 452 nt of the *bap* promotor region as well as the first 1427 nt of the *N*-terminal part of the protein in *S. xylosus* strains TMW 2.1023 and TMW 2.1523 were deleted. To confirm successful knockout of the protein, cell extracts were at first subjected to SDS-PAGE analysis. For TMW 2.1523 a weak band was visible at the expected position for Bap (224 kDa) in the wildtype strain (indicated by arrow) but not in the mutant strain (Figure S2). For TMW 2.1023 no band was detectable at the position of Bap (173 kDa) in neither wildtype nor mutant strain.

Since visibility of *S. xylosus* Bap on SDS gels was poor and inconclusive namely for strain TMW 2.1023, a high-sensitivity mass-spectrometric analysis of the full proteome was performed. Bap deletion was confirmed by comparing the peptide sequences mapping to Bap in wildtype in contrast to mutant samples. No peptide, except for one in TMW 2.1023 mutant, was found in the full proteome analysis (Table S1). This result confirmed successful knockout of *bap*.

3.3. Growth Dynamics of Wildtype and Mutant Strains

To ensure that the transformation procedure led to no growth defects as well as to investigate whether Bap deletion has an impact on the growth behavior of *S. xylosus*, growth curves in different media were recorded. Figure 2 shows the growth dynamics for both strains in TSB_N (pH 7.2), TSB^+ (pH 7.2), Lac^+ (pH 6) and TSB^+-HCl (pH 6). While wildtype and mutant strains behave very similar in TSB_N and TSB^+, curves show higher variation when the growth medium is acidified to pH 6 by either the addition of lactic acid or HCl from the very beginning. However, in general one cannot ascribe any growth deficiencies to the *bap* mutant strains.

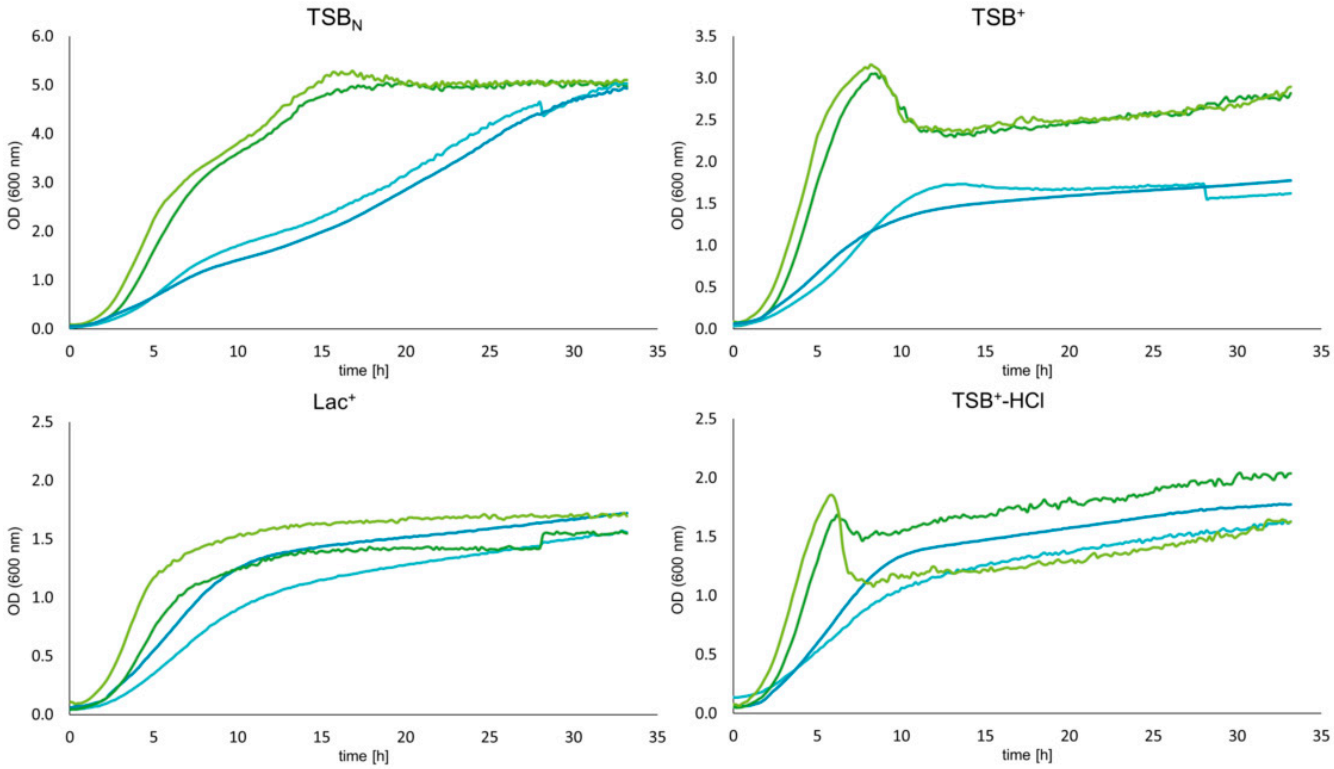

Figure 2. Growth curves of wildtype and mutant strains of *S. xylosus* TMW 2.1023 and TMW 2.1523 in different growth media (as indicated). Curves were recorded in 96-well plates in a plate reader (37 °C, aerobic conditions) every 30 min over a period of 33 h— – 023-WT, – 023-mut, – 523-WT, – 523-mut. Data are shown as mean of three biological replicates.

3.4. Biofilm Formation of Bap Wildtypes and Mutants

To determine the impact of Bap on biofilm formation of *S. xylosus*, we tested the biofilm forming capacities of two wildtype strains and their respective mutants in a 96-well plate assay. Tests were performed on hydrophilic and hydrophobic supports as well as in three different growth media that have previously been shown to promote biofilm formation to various extents in these strains [13]. The results of the biofilm assay are depicted in Figure 3. A significant reduction of biofilm formation on both supports was detectable with strain TMW 2.1523 in TSB_N only, thus in a medium where no sugar is present and therefore no pH decrease occurs upon growth. For strain TMW 2.1023, no differences in biofilm formation between wildtype and *bap* mutant strain were observed.

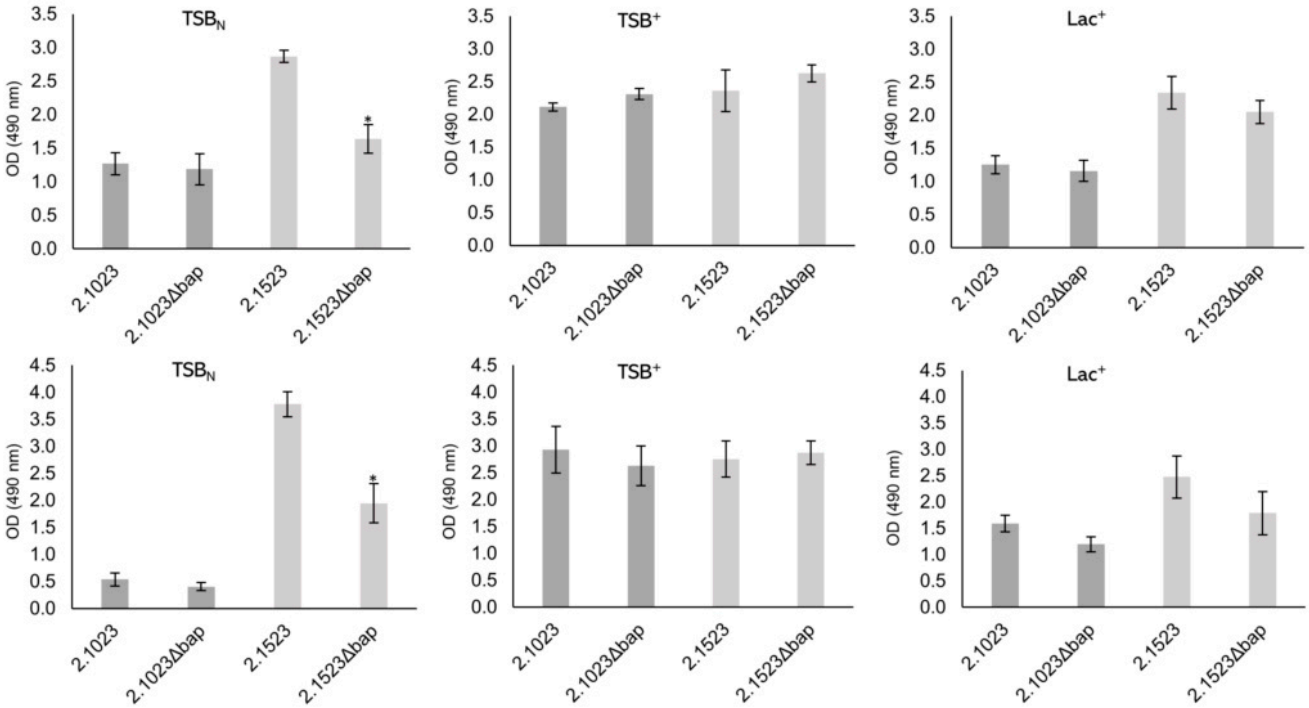

Figure 3. Biofilm formation of *S. xylosus* strains TMW 2.1023 and TMW 2.1523 and its *bap* mutants on hydrophilic (upper row) and hydrophobic (lower row) support in TSB_N, TSB^+ and Lac^+ (as indicated). Significant differences of means are marked by * (p-value < 0.05). Mean ± SE.

3.5. Colony Morphology of Bap Wildtype and Mutant Strains on Congo Red Agar

A typical characteristic of Bap positive *S. aureus* strains is their rough colony morphology on congo red agar as the dye interacts with proteinaceous, fibrillar structures [31]. Loss of Bap causes a transformation of their rough colony morphologies to a smooth type [7]. As shown in Figure 4, we could not observe any differences in colony morphology between wildtype and mutant strains on congo red agar in *S. xylosus*. Even after a couple of days of inoculation, no switches to Bap positive phenotypes (rough colonies) were observable and colony margins remained smooth.

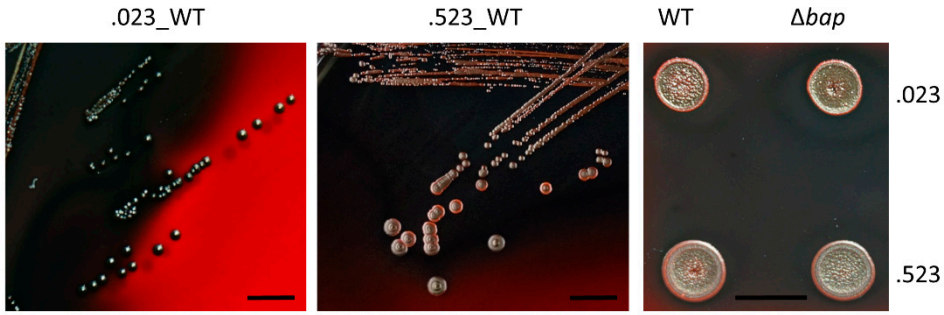

Figure 4. Colony morphology of *S. xylosus* strains on congo red agar. Bacterial overnight cultures were either streaked out for single colonies (**left**, **middle**) or applied as drops to the agar (**right**). Scale bar indicates 10 mm.

3.6. pH Changes of S. xylosus during Growth in Glucose Supplemented Media

In *S. aureus* the formation of Bap-based amyloid structures starts with the entry of *S. aureus* cells into stationary phase when the pH drops under pH 5 [9]. The mechanism of Bap-based aggregation is very sensible to pH changes, best functioning when the environment reaches pH values close to the isoelectric point of the protein. However, pH measurements over time of *S. xylosus* strains in TSB^+ show, that *S. xylosus* is not lowering the pH below

5.0 (see Figure S3). After 24 h of pH measurement, *S. xylosus* incubated in TSB$^+$ yielded values between 5.1 ± 0.2 and 5.0 ± 0.1 for TMW 21023 and TMW 2.1523, respectively. The observed accelerated acidification of TMW 2.1023 compared to TMW 2.1523 is in concurrence with the observed, faster growth of this particular strain.

3.7. Calcium Does Not Impair Biofilm Formation of Bap Positive S. xylosus Wildtype Strains

Since calcium has been described as a negative effector on biofilm formation in *S. aureus* V329 and addition of calcium to the growth medium completely abolished Bap mediated biofilm formation [10], the role of Ca^{2+} on *S. xylosus* biofilm formation was investigated. Therefore, $CaCl_2$ was added to a concentration of 20 mM to the wells and biofilm formation was quantified again. As shown in Figure 5 (the respective staining results are shown in Figure S4), no biofilm-eradicating effect of calcium was found on neither of the tested supports nor in any of the tested growth media. This result leads us to hypothesize that Bap is not a major factor of *S. xylosus* biofilm formation in these strains.

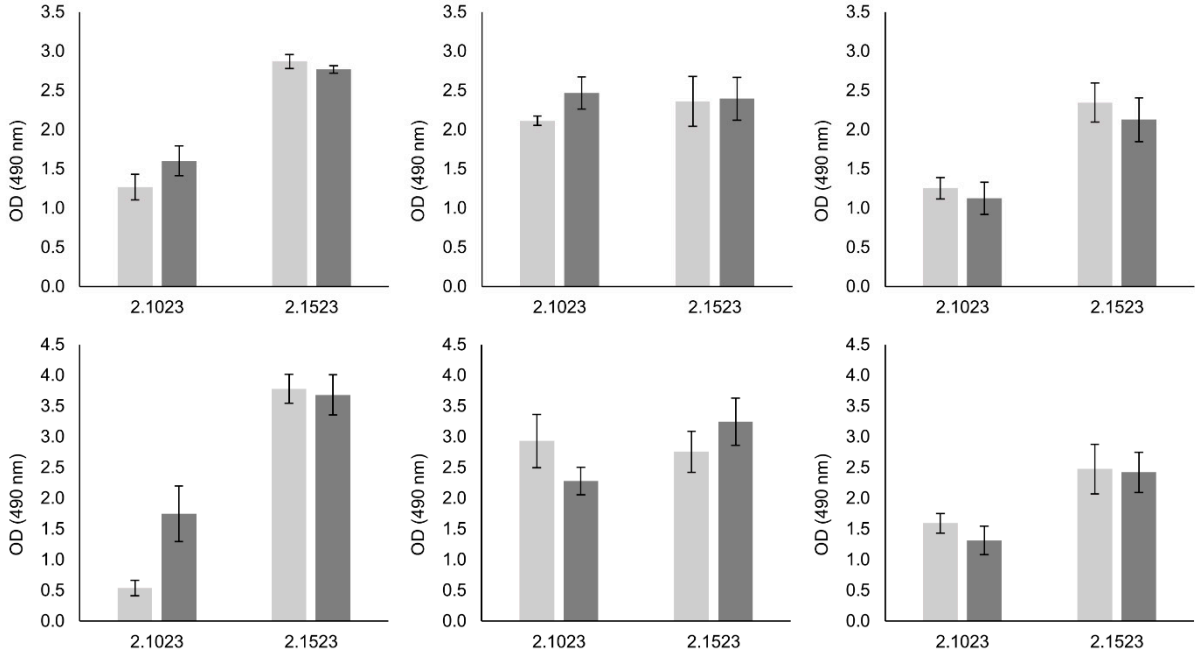

Figure 5. Effect of calcium on biofilm formation of *S. xylosus*. Biofilm formation was quantified of *S. xylosus* TMW 2.1023 and 2.1523 in three different media on hydrophilic (upper row) and hydrophobic (lower row) support. $CaCl_2$ (dark grey bars) was added to the respective growth medium to a final concentration of 20 mM.

3.8. Formation of Cell Aggregates in Wildtype and Mutant Strains

Previous studies with *S. aureus* V329 have shown that Bap is engaged in intercellular interactions, promoting aggregate formation under acidic conditions [9]. We found that *S. xylosus* is prone to aggregation in an acidic environment, too. However, neither the absence of Bap nor addition of $CaCl_2$ can impair cell aggregation as it has been described for *S. aureus* V329. As shown in Figure 6, all cultures showed heavy cell clumping with cells precipitating either at the bottom of the tube or building a top layer at the air-liquid interface when incubated in TSB$^+$.

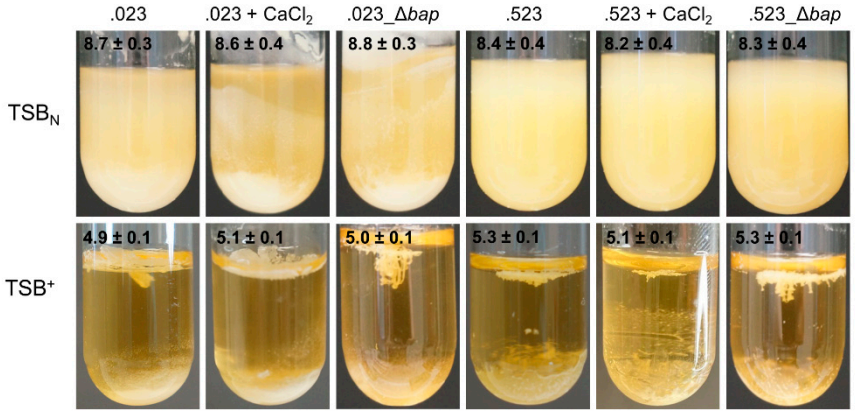

Figure 6. Aggregation behavior of *S. xylosus* TMW 2.1023 (.023), TMW 2.1523 (.523) and the corresponding *bap* mutants grown for 24 h in TSB^+ at 37 °C (200 rpm). Measured pH values are specified in the top left corner. $CaCl_2$ was added to a concentration of 20 mM when indicated.

Generally, the formation of multicellular aggregates is much weaker when strains are incubated in TSB_N, where pH remains in a neutral to basic range. Still, in neither of the media tested, any differences between wildtype and mutant strains were detectable. We further tested the aggregation and biofilm behavior of *S. xylosus* strains when incubated in medium acidified with 1 M HCl to pH 4.5. However, no growth was detectable and thus neither aggregation nor biofilm formation could be observed. Acidification to pH 4.5 of the cells, which had been grown at neutral pH, did not lead to a change to a clumping phenotype either. Cells remained in a turbid suspension, comparable to when they were grown under neutral conditions (TSB_N).

3.9. Proteomic Analysis of Expression Levels of Bap under Planktonic versus Sessile Conditions

Since visibility of Bap on SDS page was poor, we decided to use a full proteome analysis to confirm that Bap is expressed and to monitor the expression of Bap under different conditions. Therefore, we compared the measured intensity values for Bap of both *S. xylosus* strains when planktonic growth in Lac^+ occurred compared to sessile growth in the same medium. Hereby, detected Bap amounts did not change significantly (TMW 2.1023) or only to a minor degree (1.15 $\log_2$ fold, TMW 2.1523) between the two compared conditions; however, one should keep in mind that cells grown planktonically in Lac^+ show heavy cell aggregation which is closely related to biofilm formation. On the other hand, when Bap amounts are compared in cells grown in TSB_N, the protein shows a more than fivefold reduction in biofilm stages compared to planktonic growth (Table 2, Figure S4, note: TSB_N data only available for TMW 2.1523).

Further, Bap expression is significantly higher (+2.97) when TMW 2.1523 planktonic cells are grown in TSB_N compared to Lac^+.

In order to obtain a better understanding of whether Bap of *S. xylosus* is a protein with a generally low abundance in the cell, Bap intensity values were not just compared between samples obtained from cells at different growth stages but also within samples. Plotting all protein intensities measured in one sample under one condition, reveals that Bap is not a highly abundant protein such as, for example, ribosomal proteins are. However, Bap expression is not remarkably low either (compare Figure S6).

Table 2. LFQ intensities determined during full proteome analysis for two different *S. xylosus* strains in two different growth media. Indicated are $\log_2$ fold change of intensity values, adjusted (Benjamini-Hochberg method) *p*-values and whether the change in expression between the compared conditions is considered as statistically significant ($\alpha = 0.05$, True vs. False). If the $\log_2$ fold change was <2, true is written in italics.

	Biofilm Associated Protein (Bap)		
TMW 2.1023			JGY91_02455
	plankt. vs. sessile, Lac^+	$\log_2$ fold change	0.901
		p.val (adj.)	0.158
		significant	FALSE
TMW 2.1523			JGY88_01140-45
	plankt. vs. sessile, Lac^+	$\log_2$ fold change	1.15
		p.val (adj.)	0.0189
		significant	*TRUE*
	plankt. vs. sessile, TSB_N	$\log_2$ fold change	5.11
		p.val (adj.)	0.0000231
		significant	TRUE
	Lac^+ vs. TSB_N (plankt.)	$\log_2$ fold change	−2.97
		p.val (adj.)	0.000139
		significant	TRUE
	Lac^+ vs. TSB_N (sessil)	$\log_2$ fold change	0.981
		p.val (adj.)	0.0356
		significant	FALSE

4. Discussion

In this study different experimental approaches were used to evaluate the impact of Bap in *S. xylosus* on its anticipated general role in biofilm formation and multicellular behavior. Therefore two *S. xylosus* wildtype strains were chosen, that have previously been shown to display different biofilm positive phenotypes [13]. After genetic and phenotypic comparison of the two strains and their isogenic *bap* mutants we found that the role of Bap in *S. xylosus* is most likely non-essential for biofilm formation, apparently strain-specific, and predictively more diverse than anticipated. Upon deletion of *bap*, a significant reduction in biofilm formation was only observed with *S. xylosus* TMW 2.1523 under neutral pH environmental conditions. It did not affect its aggregation behavior and had no effect on any of the investigated traits of *S. xylosus* TMW 2.1023. This is in contrast to studies on *S. aureus* V329 [7] and *S. epidermidis* C533 [11], which showed that disruption of *bap* led to complete abolishment of biofilm formation. We therefore conclude that, firstly, *bap* orthologs do not necessarily have the same function in other staphylococcal species as the one previously determined for single strains of *S. aureus* and *S. epidermidis* and secondly, that biofilm formation and aggregation of *S. xylosus* involves different mechanisms. This view is supported by our previous study, which revealed that different *S. xylosus* strains encode a variable set of biofilm related genes in their genomes and display a biofilm phenotype that is dependent on environmental conditions in a strain-specific manner [13]. It is also supported by the observation that *S. xylosus* C2a has been described as a strong biofilm producer [12], even though we found that Bap is truncated by a premature stop codon in region B in this strain. Given this, it appears likely that either other factors dominate biofilm formation of the species, such as eDNA, which has been named as an important component of *S. xylosus* C2a biofilm matrix [32], or that Bap does not have a predominant role in *S. xylosus* biofilm formation, due to either low expression or functional differences of the protein.

Congo red is commonly used as amyloid dye and has been shown to interact with amyloidogenic structures formed by the *N*-terminal part of Bap [9,31] resulting in rough colony phenotypes of Bap positive strains on CRA. Loss of Bap has subsequently been shown to transform rough colonies to colonies with smooth margins [31]. Even though *S. xylosus* strains TMW 2.1023 and TMW 2.1523 are Bap positive, no colony morphology changes in wildtype versus mutant strains could be observed. Both strains and their respective mutants displayed smooth colony margins, suggesting that in contrary to Bap positive *S. aureus* strains, (Bap based-) amyloid formation seems to be different or at least under the conditions tested, not existent in *S. xylosus*. Another factor supporting a minor role of Bap in biofilm formation of *S. xylosus* is that calcium addition (20 mM) had neither an inhibiting effect on cell aggregation in culture tubes nor on biofilm formation. In *S. aureus* V329 adding as little as 6 mM calcium to the growth medium already abolishes any kind of aggregation and biofilm formation behavior [10]. If Bap binds calcium ions with low affinity, the molten globule conformation of the protein is stabilized in a way that no subsequent assembly to amyloid structures occurs. The effect of calcium binding and stabilization is attributed to EF domains 2 and 3 in the B region of the protein. However, even though Bap_{XYL} harbors the exact same EF hand motifs in its B region as Bap_{AUR}, no aggregation/biofilm reducing effects were observed upon calcium addition. On the contrary, in some cases one could rather predict a trend towards an enhancing effect on biofilm formation especially on hydrophobic support. If and to which extent the increased number of EF hand motifs found in Bap_{XYL}, compared to Bap_{AUR}, is related to this observation remains speculative.

pH plays an important factor in Bap-mediated biofilm formation, as self-assembly of the protein into amyloid fibers occurs under acidic conditions only. When *S. aureus* V329 is incubated in medium containing glucose, pH drops below 5 as soon as stationary phase is entered, thereby approaching the pI of the aggregation prone B region of the protein, which facilitates amyloid structure formation [9]. *S. xylosus* differs in two points. First, the calculated pI of Region B of $BapB_{XYL}$ is 4.4 compared to $BapB_{AUR}$ 4.6, thus, considerably lower. Secondly, *S. xylosus* is not lowering the pH below 5 in medium containing glucose. Hence, even though amyloidogenic potential of $BapB_{XYL}$ was predicted by several amyloid finders in silico, peptide self-assembly into amyloids is impeded, as a pH close to the pI of $BapB_{XYL}$ is not reached during sugar fermentation of the organism. A final pH of 5 and not lower, after glucose fermentation by *S. xylosus*, is in consistence with our observation that *S. xylosus*, contrary to *S. aureus* [9], did not show any growth in medium with pH 4.5.

While glucose has been discussed to indirectly regulate biofilm formation of *S. aureus* [33] and acidosis related to glucose metabolism is essential for biofilm formation in Bap^+ *S. aureus* strains [9], it is noteworthy that *S. xylosus* is a well biofilm former under neutral to basic conditions (TSB_N) and that pH decrease during growth is, in contrast to *S. aureus* V329, not necessary to induce biofilm formation. Additionally, the only reduction in biofilm formation between wildtype and mutant strain we observed was when strain TMW 2.1523 was grown under neutral conditions. Besides the already mentioned fact that the pH drop during growth of *S. xylosus* might not be low enough to induce Bap derived peptide aggregation, one could also argue that Bap might not be expressed in sufficient amounts, especially under acidic conditions, to promote formation of multicellular aggregates. This is substantiated by the results obtained from full proteome analysis which revealed a significantly higher amount of $Bap_{2.1523}$ in neutral (TSB_N) compared to acidic (Lac^+) medium. Moreover, even though multiple authors reported good visibility of Bap on SDS gels [7,10], *S. xylosus* Bap was poorly visible on the gel, and only a slight band was detectable for strain TMW 2.1523 when grown in TSB_N. This leads us to hypothesize that Bap_{AUR} is expressed to a higher extent than Bap_{XYL}. Whether Bap_{XYL} visibility on SDS gels is impaired by any processing that occurs, as described for Bap_{AUR} under acidic conditions [9], cannot be ruled out and should be kept in mind.

Another difference between the two species to be considered is the structural organization of the proteins. While Bap of *S. epidermidis*, *S. chromogenes*, *S. hyicus* and *S. simulans*

share almost 100% protein similarity with Bap_{AUR} [11], Bap_{XYL} and Bap_{AUR} show only around 50 (our study) to 80% [11] protein identity. Thus, different functions cannot be excluded, especially since the correlation between Bap and staphylococcal biofilm formation has mainly been studied extensively in strain *S. aureus* V329 and a function has been solely assigned to the *N*-terminal region of the protein so far. A large part of the protein (C-terminal part) remains bound to the cell surface, with a still unknown purpose for the cell. Lastly, small but predictively important sequence differences need to be considered, for example two short peptide sequences that have been predicted to show high amyloidogenic potential in Bap_{AUR} [9] are not conserved across the two species. Also, Bap_{AUR} Region D is rich in SD repeats and C-terminal SD repeats have previously been described to be an important structural attribute in staphylococcal surface adhesins [34,35]. Bap_{XYL} lacks any of those SD repeat rich regions.

Proteins containing a YSIRK signal peptide and an LPxTG cell anchor motif have been discussed in different contexts in the past and different functions including peptidase and hydrolase activity have been assigned to those proteins [36,37]. Furthermore, Bhp, a Bap homolog found in S. *epidermidis*, has been speculated to mediate biofilm formation at first [11]; however, disruption of *bhp* did not result in any biofilm reduced phenotypes [38]. Thus, we suggest that biofilm formation in *S. xylosus* does not necessarily require Bap, and that its dominant role in biofilm formation is currently rather restricted to strains of selected species such as *S. aureus* and *S. epidermidis* [9,11]. Our findings further suggest that conclusions on the function of Bap drawn from studies conducted with *S. aureus* V329 should be carefully applied to other organisms carrying Bap orthologs when experimental proof is lacking. Furthermore, it appears that other proteins/mechanisms must be involved in multicellular behavior and biofilm formation of *S. xylosus.*

Supplementary Materials: The following are available online at https://www.mdpi.com/article/10.3390/microorganisms9122610/s1, Figure S1: Bap sequence alignment of selected *S. xylosus* strains with two Bap-dependent biofilm formers: *S. epidermidis* C533 and *S. aureus* V329. Only functionally important parts of the alignment are shown. A. shows the YSIRK-Signal peptide sequence as well the difference in A-region repeat length between *S. epidermidis*/*S. aureus* and *S. xylosus*. B. shows the sequence differences between the two amyloidprone peptides (defined by Taglialegna et al. [8]) of Bap Region B (marked in yellow). C. displays the conservation across species of EF hand domains 2 and 3 (pink). D. shows the differences in D-repeats between the species. While *S. aureus* and *S. epidermidis* region D is rich in SD repeats, *S. xylosus* encodes G-rich repeats, Figure S2: Analysis of cell extract protein preparations on SDS-PAGE. Left: TMW 2.1523 wildtype (Wt) and mutant (Mt) strain, Right: TMW 2.1023 Wt and Mt. The black arrow indicates a possible location of Bap in TMW 2.1523–Wt, Figure S3: pH changes of *S. xylosus* TMW 2.1023 (grey) and 2.1523 (black) incubated in TSB^+ aerobically at 37 °C. Changes in pH were recorded over 12 h, OD_{600} at t_0 was set to 0.1. Curves display the mean of 3 biological replicates, Figure S4: Calcium (20 mM) does not impair biofilm formation of selected *S. xylosus* strains (incubated in TSB^+, 24 h, 37 °C, stained with safranin-O), Figure S5: Boxplot of log_2 transformed LFQ intensities measured for Bap in TMW 2.1023 (A) under planktonic and sessile conditions in Lac^+, for TMW 2.1523 (B) under planktonic and sessile conditions in Lac^+ and TSB_N, Figure S6: Intensity based absolute quantification (iBAQ)—intensities of proteins expressed in TMW 2.1023 under planktonic (A) or sessile (B) conditions and TMW 2.1523 under planktonic Lac^+ (A), sessile Lac^+ (B), planktonic TSB_N (C) and sessile TSB_N (D) conditions. Bap is marked in red, highly abundant ribosomal proteins (50S) are marked in green for comparison. Table S1: Identified peptide sequences (intensity values) mapping on Bap in wildtype and mutant strains of TWW strains 2.1023 and 2.1523.

Author Contributions: C.J.S.: Conceptualization, Investigation, Methodology, Software, Visualization, Writing—Original Draft preparation; M.A.: Methodology, Software, Writing—Review and Editing; M.A.E.: Conceptualization, Supervision, Writing—Review & Editing; R.F.V.: Funding Aquisition, Project Administration, Supervision, Writing—Review & Editing. All authors have read and agreed to the published version of the manuscript.

Funding: Part of this work was funded by the German Federal Ministry for Economic Affairs and Energy via the German Federation of Industrial Research Associations (AiF) and the Forschungskreis

der Ernährungsindustrie E.V. (FEI), project AiF 19690N. M. Abele was supported by the EU Horizon 2020 grant Epic-XS.

Institutional Review Board Statement: Not applicable.

Informed Consent Statement: Not applicable.

Data Availability Statement: The proteomics raw data, MaxQuant search results and used protein sequence databases have been deposited with the ProteomeXchange Consortium via the PRIDE partner repository [29] and can be accessed using the data set identifier PXD029728. Sequencing data of TMW 2.1023 and TMW 2.1523 is accessible under JAEMUG000000000 and CP066721-CP066725, respectively.

Conflicts of Interest: The authors received research grants from the AiF, which did not influence the aims or setup of this study, and declare no conflict of interest.

References

1. Leroy, S.; Vermassen, A.; Ras, G.; Talon, R. Insight into the genome of *Staphylococcus xylosus*, a ubiquitous species well adapted to meat products. *Microorganisms* **2017**, *5*, 52. [CrossRef]
2. Flemming, H.-C.; Wingender, J. The biofilm matrix. *Nat. Rev. Microbiol.* **2010**, *8*, 623–633. [CrossRef] [PubMed]
3. Götz, F. Staphylococcus and biofilms. *Mol. Microbiol.* **2002**, *43*, 1367–1378. [CrossRef]
4. Taglialegna, A.; Lasa, I.; Valle, J. Amyloid structures as biofilm matrix scaffolds. *J. Bacteriol.* **2016**, *198*, 2579–2588. [CrossRef]
5. Valle, J.; Latasa, C.; Gil, C.; Toledo-Arana, A.; Solano, C.; Penadés, J.R.; Lasa, I. Bap, a biofilm matrix protein of *Staphylococcus aureus* prevents cellular internalization through binding to GP96 host receptor. *PLoS Pathog.* **2012**, *8*, e1002843. [CrossRef]
6. Speziale, P.; Pietrocola, G.; Foster, T.J.; Geoghegan, J.A. Protein-based biofilm matrices in Staphylococci. *Front. Cell. Infect. Microbiol.* **2014**, *4*, 171. [CrossRef]
7. Cucarella, C.; Solano, C.; Valle, J.; Amorena, B.; Lasa, I.; Penadés, J.R. Bap, a *Staphylococcus aureus* surface protein involved in biofilm formation. *J. Bacteriol.* **2001**, *183*, 2888–2896. [CrossRef]
8. Taglialegna, A.; Matilla-Cuenca, L.; Dorado-Morales, P.; Navarro, S.; Ventura, S.; Garnett, J.A.; Lasa, I.; Valle, J. The biofilm-associated surface protein Esp of *Enterococcus faecalis* forms amyloid-like fibers. *NPJ Biofilms Microbiomes* **2020**, *6*, 15. [CrossRef] [PubMed]
9. Taglialegna, A.; Navarro, S.; Ventura, S.; Garnett, J.A.; Matthews, S.; Penades, J.R.; Lasa, I.; Valle, J. Staphylococcal Bap proteins build amyloid scaffold biofilm matrices in response to environmental signals. *PLoS Pathog.* **2016**, *12*, e1005711. [CrossRef]
10. Arrizubieta, M.J.; Toledo-Arana, A.; Amorena, B.; Penadés, J.R.; Lasa, I. Calcium inhibits Bap-dependent multicellular behavior in *Staphylococcus aureus*. *J. Bacteriol.* **2004**, *186*, 7490–7498. [CrossRef] [PubMed]
11. Tormo, M.A.; Knecht, E.; Götz, F.; Lasa, I.; Penades, J.R. Bap-dependent biofilm formation by pathogenic species of *Staphylococcus*: Evidence of horizontal gene transfer? *Microbiology* **2005**, *151*, 2465–2475. [CrossRef]
12. Planchon, S.; Gaillard-Martinie, B.; Dordet-Frisoni, E.; Bellon-Fontaine, M.N.; Leroy, S.; Labadie, J.; Hébraud, M.; Talon, R. Formation of biofilm by *Staphylococcus xylosus*. *Int. J. Food Microbiol.* **2006**, *109*, 88–96. [CrossRef]
13. Schiffer, C.; Hilgarth, M.; Ehrmann, M.; Vogel, R.F. Bap and cell surface hydrophobicity are important factors in *Staphylococcus xylosus* biofilm formation. *Front. Microbiol.* **2019**, *10*, 1387. [CrossRef] [PubMed]
14. Monk, I.R.; Shah, I.M.; Xu, M.; Tan, M.-W.; Foster, T.J. Transforming the Untransformable: Application of Direct Transformation To Manipulate Genetically *Staphylococcus aureus* and *Staphylococcus epidermidis*. *MBio* **2012**, *3*, e00277-11. [CrossRef]
15. Monk, I.R.; Stinear, T.P. From cloning to mutant in 5 days: Rapid allelic exchange in *Staphylococcus aureus*. *Access Microbiol.* **2021**, *3*, 1–7. [CrossRef]
16. Schuster, C.F.; Howard, S.A.; Gründling, A. Use of the counter selectable marker PheS* for genome engineering in *Staphylococcus aureus*. *Microbiology* **2019**, *165*, 572–584. [CrossRef] [PubMed]
17. Heilmann, C.; Götz, F. Further characterization of *Staphylococcus epidermidis* transposon mutants deficient in primary attachment or intercellular adhesion. *Zent. Bakteriol.* **1998**, *287*, 69–83. [CrossRef]
18. Doellinger, J.; Schneider, A.; Hoeller, M.; Lasch, P. Sample Preparation by Easy Extraction and Digestion (SPEED)—A Universal, Rapid, and Detergent-free Protocol for Proteomics Based on Acid Extraction. *Mol. Cell. Proteom.* **2020**, *19*, 209–222. [CrossRef]
19. Kolbeck, S.; Ludwig, C.; Meng, C.; Hilgarth, M.; Vogel, R.F. Comparative Proteomics of Meat Spoilage Bacteria Predicts Drivers for Their Coexistence on Modified Atmosphere Packaged Meat. *Front. Microbiol.* **2020**, *11*, 209. [CrossRef] [PubMed]
20. Bechtner, J.; Ludwig, C.; Kiening, M.; Jakob, F.; Vogel, R.F. Living the Sweet Life: How *Liquorilactobacillus hordei* TMW 1.1822 Changes Its Behavior in the Presence of Sucrose in Comparison to Glucose. *Foods* **2020**, *9*, 1150. [CrossRef]
21. Garbuzynskiy, S.O.; Lobanov, M.Y.; Galzitskaya, O.V. FoldAmyloid: A method of prediction of amyloidogenic regions from protein sequence. *Bioinformatics* **2010**, *26*, 326–332. [CrossRef]
22. De Groot, N.S.; Castillo, V.; Graña-Montes, R.; Ventura, S. AGGRESCAN: Method, application, and perspectives for drug design. *Methods Mol. Biol.* **2012**, *819*, 199–220. [CrossRef]
23. Louros, N.; Konstantoulea, K.; de Vleeschouwer, M.; Ramakers, M.; Schymkowitz, J.; Rousseau, F. WALTZ-DB 2.0: An updated database containing structural information of experimentally determined amyloid-forming peptides. *Nucleic Acids Res.* **2020**, *48*, D389–D393. [CrossRef] [PubMed]

24. Fernandez-Escamilla, A.-M.; Rousseau, F.; Schymkowitz, J.; Serrano, L. Prediction of sequence-dependent and mutational effects on the aggregation of peptides and proteins. *Nat. Biotechnol.* **2004**, *22*, 1302–1306. [CrossRef] [PubMed]
25. Cox, J.; Neuhauser, N.; Michalski, A.; Scheltema, R.A.; Olsen, J.V.; Mann, M. Andromeda: A peptide search engine integrated into the MaxQuant environment. *J. Proteome Res.* **2011**, *10*, 1794–1805. [CrossRef]
26. Tyanova, S.; Temu, T.; Cox, J. The MaxQuant computational platform for mass spectrometry-based shotgun proteomics. *Nat. Protoc.* **2016**, *11*, 2301–2319. [CrossRef]
27. Tyanova, S.; Temu, T.; Sinitcyn, P.; Carlson, A.; Hein, M.Y.; Geiger, T.; Mann, M.; Cox, J. The Perseus computational platform for comprehensive analysis of (prote)omics data. *Nat. Methods* **2016**, *13*, 731–740. [CrossRef]
28. Shah, A.D.; Goode, R.J.A.; Huang, C.; Powell, D.R.; Schittenhelm, R.B. LFQ-Analyst: An Easy-To-Use Interactive Web Platform To Analyze and Visualize Label-Free Proteomics Data Preprocessed with MaxQuant. *J. Proteome Res.* **2020**, *19*, 204–211. [CrossRef]
29. Perez-Riverol, Y.; Csordas, A.; Bai, J.; Bernal-Llinares, M.; Hewapathirana, S.; Kundu, D.J.; Inuganti, A.; Griss, J.; Mayer, G.; Eisenacher, M.; et al. The PRIDE database and related tools and resources in 2019: Improving support for quantification data. *Nucleic Acids Res.* **2019**, *47*, D442–D450. [CrossRef] [PubMed]
30. Cucarella, C.; Tormo, M.A.; Ubeda, C.; Trotonda, M.P.; Monzon, M.; Peris, C.; Amorena, B.; Lasa, I.; Penades, J.R. Role of biofilm-associated protein Bap in the pathogenesis of bovine *Staphylococcus aureus*. *Infect. Immun.* **2004**, *72*, 2177–2185. [CrossRef]
31. Tormo, M.Á.; Úbeda, C.; Martí, M.; Maiques, E.; Cucarella, C.; Valle, J.; Foster, T.J.; Lasa, Í.; Penadés, J.R. Phase-variable expression of the biofilm-associated protein (Bap) in *Staphylococcus aureus*. *Microbiology* **2007**, *153*, 1702–1710. [CrossRef]
32. Leroy, S.; Lebert, I.; Andant, C.; Micheau, P.; Talon, R. Investigating Extracellular DNA Release in *Staphylococcus xylosus* Biofilm In Vitro. *Microorganisms* **2021**, *9*, 2192. [CrossRef] [PubMed]
33. You, Y.; Xue, T.; Cao, L.; Zhao, L.; Sun, H.; Sun, B. *Staphylococcus aureus* glucose-induced biofilm accessory proteins, GbaAB, influence biofilm formation in a PIA-dependent manner. *Int. J. Med. Microbiol.* **2014**, *304*, 603–612. [CrossRef]
34. Bowden, M.G.; Chen, W.; Singvall, J.; Xu, Y.; Peacock, S.J.; Valtulina, V.; Speziale, P.; Höök, M. Identification and preliminary characterization of cell-wall-anchored proteins of *Staphylococcus epidermidis*. *Microbiology* **2005**, *151*, 1453–1464. [CrossRef] [PubMed]
35. McCrea, K.W.; Hartford, O.; Davis, S.; Eidhin, D.N.; Lina, G.; Speziale, P.; Foster, T.J.; Höök, M. The serine-aspartate repeat (Sdr) protein family in *Staphylococcus epidermidis*. *Microbiology* **2000**, *146*, 1535–1546. [CrossRef]
36. Bai, Q.; Ma, J.; Zhang, Z.; Zhong, X.; Pan, Z.; Zhu, Y.; Zhang, Y.; Wu, Z.; Liu, G.; Yao, H. YSIRK-G/S-directed translocation is required for *Streptococcus suis* to deliver diverse cell wall anchoring effectors contributing to bacterial pathogenicity. *Virulence* **2020**, *11*, 1539–1556. [CrossRef] [PubMed]
37. DeDent, A.; Bae, T.; Missiakas, D.M.; Schneewind, O. Signal peptides direct surface proteins to two distinct envelope locations of *Staphylococcus aureus*. *EMBO J.* **2008**, *27*, 2656–2668. [CrossRef]
38. Lasa, I.; Penadés, J.R. Bap: A family of surface proteins involved in biofilm formation. *Res. Microbiol.* **2006**, *157*, 99–107. [CrossRef] [PubMed]

4.3 SxsA, a novel surface protein mediating cell aggregation and adhesive biofilm formation of *Staphylococcus xylosus*

Preface: Since previous studies (Schiffer et al., 2019; Schiffer et al., 2021) had shown that our hypothesis on Bap mediating biofilm formation in *S. xylosus* could not be verified, we postulated that another protein must be responsible for autoaggregation and biofilm formation in *S. xylosus*. We therefore chose a generic approach to find potential open reading frames that could mediate the phenotype in *S. xylosus*. Basically, we used *in silico* analysis to screen the genomes of biofilm positive *S. xylosus* strains for surface proteins characterized by a YSIRK-G/S motif signal peptide and a LPxTG cell wall anchor (analogous to Bap), for proteins that were large in size and of high molecular weight and for proteins that showed a similar change in expression in proteomic experiments when comparing sessile and planktonically grown cells. Each open reading frame (ORF) of interest was analyzed in more detail for the presence of enzymatic domains and structural characteristics such as sequence repeats and amyloidogenic regions. In the end, two ORFs remained particularly interesting of one of which was present in both transformable *S. xylosus* strains i.e., TMW 2.1023 and TMW 2.1523, while the other one was only encoded in TMW 2.1023 (plasmid-based). Hence, the ORF occurring in both strains was deleted and this time mutant strains showed a clear reduction of aggregation and biofilm formation. That way, we provided data on and characterized a new and important surface protein mediating biofilm formation in *S. xylosus.* Even though homologs were also found in closely related species such as *S. nepalensis, S. saprophyticus, S. pseudoxylosus* and *S. cohnii*, their function in those species is left to be demonstrated. Still, the data provided by this study will be of broad interest in the field of staphylococcal research, given the increasing interest in coagulase-negative staphylococci other than *S. epidermidis*. Hereby, the study contributes substantially to the understanding of biofilm forming mechanisms of the species *S. xylosus*.

Author contributions: Carolin Schiffer was in charge of the conceptualization of the study and further initiated the cooperation with Dr. Christoph Schaudinn on microscopic analysis. She performed all other experiments, prepared the proteomic samples for analysis by BayBioMS and conducted detailed bioinformatic analyses on sequence structure and occurrence. She also wrote the original draft of the manuscript, co-edited the final version and handled submission and reviewer suggestions as corresponding author.

Received: 16 December 2021 | Revised: 20 January 2022 | Accepted: 20 January 2022

DOI: 10.1111/mmi.14884

RESEARCH ARTICLE

WILEY

SxsA, a novel surface protein mediating cell aggregation and adhesive biofilm formation of *Staphylococcus xylosus*

Carolin J. Schiffer[1] | **Christoph Schaudinn**[2] | **Matthias A. Ehrmann**[1] | **Rudi F. Vogel**[1]

[1]Lehrstuhl für Technische Mikrobiologie, Technische Universität München, Freising, Germany

[2]Advanced Light and Electron Microscopy, Robert Koch Institute, Berlin, Germany

Correspondence
Matthias A. Ehrmann and Carolin J. Schiffer, Lehrstuhl für Technische Mikrobiologie, Technische Universität München, Freising 85354, Germany.
Emails: matthias.ehrmann@tum.de and carolin.schiffer@tum.de

Present address
Carolin J. Schiffer and Matthias A. Ehrmann, Lehrstuhl für Mikrobiologie, Technische Universität München, Freising, Germany

Funding information
Forschungskreis der Ernährungsindustrie, Grant/Award Number: AIF19690N; German Federation of Industrial Research Associations; German Federal Ministry for Economic Affairs and Energy

Abstract

Biofilm formation of staphylococci has been an emerging field of research for many years. However, the underlying molecular mechanisms are still not fully understood and vary widely between species and strains. The aim of this study was to identify new effectors impacting biofilm formation of two *Staphylococcus xylosus* strains. We identified a novel surface protein conferring cell aggregation, adherence to abiotic surfaces, and biofilm formation. The *S. xylosus* surface protein A (SxsA) is a large protein occurring in variable sizes. It lacks sequence similarity to other staphylococcal surface proteins but shows similar structural domain organization and functional features. Upon deletion of *sxs*A, adherence of *S. xylosus* strain TMW 2.1523 to abiotic surfaces was completely abolished and significantly reduced in TMW 2.1023. Macro- and microscopic aggregation assays further showed that TMW 2.1523 *sxsA* mutants exhibit reduced cell aggregation compared with the wildtype. Comparative genomic analysis revealed that *sxs*A is part of the core genome of *S. xylosus*, *Staphylococcus paraxylosus*, and *Staphylococcus nepalensis* and additionally encoded in a small group of *Staphylococcus cohnii* and *Staphylococcus saprophyticus* strains. This study provides insights into protein-mediated biofilm formation of *S. xylosus* and identifies a new cell wall-associated protein influencing cell aggregation and biofilm formation.

KEYWORDS
amyloids, autoaggregation, biofilm, *Staphylococcus xylosus*

1 | INTRODUCTION

Staphylococcus xylosus, first described by Schleifer and Kloos (1975), belongs to the large group of coagulase-negative staphylococci (CNS). It is commonly used as a starter organism in raw sausage fermentations where its ability to reduce nitrate and its contribution to aroma formation is of high technological value (Leroy et al., 2006). Yet, CNS are also ubiquitous commensals of mammal skin and have been considered opportunistic pathogens in humans and animals (Becker et al., 2014; Michels et al., 2021). In this context, *S. xylosus* has been repeatedly associated with bovine mastitis infections (de Buck et al., 2021; Supré et al., 2011). Colonization of surfaces and biofilm formation play an important role during infections as they increase a bacterium's tolerance to host defense mechanisms and antibacterial treatments (Foster et al., 2014; Otto, 2008; Schilcher & Horswill, 2020). Biofilm formation of bacteria is a multifactorial process, often enabled by more than one mechanism. It can vary between and within bacterial species as well as it is strongly affected by environmental factors and physical conditions (Karatan & Watnick, 2009; Lawal et al., 2021; Schiffer et al., 2019). While the

understanding of molecular mechanisms, regulatory systems, and genes involved in biofilm formation processes is still growing, studies on the composition of biofilm matrices revealed that the extracellular matrix, in which the cells are embedded, is usually composed of three major constituents: polysaccharides, extracellular DNA, and proteins with lipids being involved occasionally as well (Schilcher & Horswill, 2020).

The role of proteins in biofilm formation of staphylococci is currently most widely studied in *Staphylococcus aureus* and *Staphylococcus epidermidis*. Next to secreted proteins, such as the 18 kDa small basic protein (Sbp) (Decker et al., 2015) and the extracellular adherence protein (Eap) (Yonemoto et al., 2019), cell wall-anchored proteins play a major role in the biofilm formation process. They either mediate primary attachment to surfaces and/or cell accumulation at later stages of the biofilm maturation phase (Foster, 2019; Speziale et al., 2014). Most of them comprise a C-terminal LPxTG cell wall-anchoring motif, which covalently binds them to peptidoglycan by a sortase-mediated mechanism, and an N-terminal YSIRK-G/S signal peptide, which is supposed to translocate proteins to the cross wall (Bowden et al., 2002; DeDent et al., 2008). During primary attachment of staphylococcal cells to biotic surfaces, microbial surface components recognizing matrix molecules (MSCRAMMs) that bind to host factors such as fibronectin (FnBpA, FnBpB, Embp), fibrinogen (ClfA, ClfB), and collagen (Cna, SdrF) play an essential role (Foster, 2020; Foster et al., 2014). Proteins such as autolysins and the biofilm-associated protein (Bap) on the other hand mediate attachment to abiotic surfaces (Cucarella et al., 2001; Heilmann et al., 1997). During subsequent biofilm accumulation, proteins usually contribute to cell aggregation either by interacting with surface structures on neighboring cells or by the formation of amyloid fibers (Speziale et al., 2014; Taglialegna, Lasa, et al., 2016a). Examples for staphylococcal proteins conferring biofilm accumulation include Bap and the accumulation-associated protein Aap (Rohde et al., 2005; Taglialegna, Navarro, et al., 2016b). The function of Bap is especially well characterized in *S. aureus* strain V329 and was found to be based on amyloid assembly of N-terminal peptides upon extracellular processing under acidic conditions and low Ca^{2+} concentrations (Taglialegna, Navarro, et al., 2016b). Aap of *S. epidermidis* and its homolog, *S. aureus* surface protein G (SasG), undergo extracellular proteolytic cleavage as well, resulting in different versions of truncated isoforms of the protein (Rahmdel & Götz, 2021). In the isoforms, G5-E domains of the B region are exposed and mediate intercellular adhesion in a Zn^{2+}-dependent matter (Geoghegan et al., 2010; Yarawsky et al., 2020).

Only a few studies have addressed adhesion mechanisms and biofilm matrix composition in coagulase-negative staphylococci (CNS), other than *S. epidermidis* in the past. We have previously reported that biofilm-producing *S. xylosus* strains do not encode an Aap/SasG homolog in their genome as well as that Bap is only of minor importance in biofilm formation of *S. xylosus* (Schiffer et al., 2019; Schiffer et al., 2021). We, therefore, postulate that another mechanism must be responsible for protein-mediated cell aggregation and biofilm formation in this species. In the following, we identify and characterize a new protein, influencing multicellular behavior and surface adhesion of *S. xylosus*.

2 | MATERIALS AND METHODS

2.1 | Bacterial strains and growth conditions

Staphylococcus xylosus TMW 2.1023 and TMW 2.1523 and their respective *bap*-deficient mutants are biofilm-positive strains that have been described in previous studies before (Schiffer et al., 2019; Schiffer et al., 2021). *Escherichia* (*E.*) *coli* DC10B, a cytosine methyltransferase-negative derivate of *E. coli* DH10B (Monk et al., 2012), was used for vector assembly, propagation, and purification. *E. coli* was grown in Lysogeny Broth (LB, tryptone 10 g/L, yeast extract 5 g/L, NaCl 5 g/L) at 28 and 37°C, respectively. *S. xylosus* was cultured in Trypticase soy broth (casein peptone 15 g/L, soy peptone 15 g/L, yeast extract 3 g/L, pH 7.2) which was supplemented with either no glucose (TSB_N), 1% glucose (TSB^+), or 1% glucose with additional acidification to pH 6 using either 80% lactic acid (Lac^+) or 6 N HCl (TSB^+-HCl). For transformation experiments, *S. xylosus* was cultivated in basic medium (BM, 1% peptone, 0.5% yeast extract, 0.5% NaCl, 0.1% glucose, 0.1% K_2HPO_4, pH 7.2) and brain heart infusion (BHI) broth. When necessary, 20 μg/ml (*E. coli*) or 10 μg/ml (staphylococci) of chloramphenicol (CarlRoth) was added to the respective growth medium.

2.2 | Generation of mutant strains by allelic replacement

For mutagenesis of the chromosomal *sxs*A gene in *S. xylosus*, regions up- and downstream of the to be deleted sequence (1376 nt deletion in N-terminal part of the protein) were amplified using primers *sxs*A1F (5′-TGTACTGCAGGATATAGCTGAAGTTCCTCC-3′) and *sxs*A2R (5′-GTTCCACTGTCTGGTCTAGCTCATAGCTGTCTACTTCTC-3′) as well as *sxs*A3F (5′-GAGAAGTAGACAGCTATGAGCTAGACCAGACAGTGGAAC-3′) and *sxs*A4R (5′- TCAGCTCGAGGTTCACACTATCTGGTACATC-3′). Introduced restriction sites for cloning are shown underlined. All primer sequences were chosen based on the criteria that they match the target sequence in both *S. xylosus* strains (TMW 2.1023, TMW 2.1523); thus, they were designed to map on conserved regions of the protein. The two obtained PCR products were purified using a Monarch PCR and DNA cleanup kit (New England Biolabs), and primers *sxs*A1F and *sxs*A4R were used for subsequent overamplification to generate the vector insert. Restriction digest of insert and vector using PstI-HF and XhoI-HF (NEB) followed and the insert was ligated (T4 DNA Ligase, Thermo Fisher Scientific) into the shuttle vector pIMAY* (Schuster et al., 2019). The construct was transformed into the *dcm*-negative *E. coli* strain DC10B by electroporation. Successful transformants were selected on chloramphenicol (10 μg/ml) plates. The plasmid was isolated using the Monarch plasmid DNA miniprep kit (NEB), sequenced to confirm correct assembly, and transformed

into electrocompetent *S. xylosus* cells as previously described (Monk & Stinear, 2021; Schiffer et al., 2021). Hereby, the transformation of wildtype strains was performed to obtain Δ*sxs*A mutants, as well as *bap*-deficient mutants (Schiffer et al., 2021) were transformed, to generate Δ*bap*Δ*sxs*A mutant strains. In the end, successful gene deletion and allelic replacement of the *sxs*A sequence as well as loss of pIMAY* were verified by colony PCR using primers *sxs*A1F and *sxs*A4R. Loss of chloramphenicol resistance was verified by replica plating.

2.3 | Biofilm formation and adherence to surfaces

For quantification of biofilm formation on abiotic surfaces, a 96-well plate assay based on safranin-O staining of adherent cells was used as described by Schiffer et al. (2019). Therefore, strains were cultured in different media (TSB_N, TSB^+, Lac^+) and on different supports (hydrophobic [Sarstedt], hydrophilic [Nunclon™ delta, Thermo Scientific]) for 24 h at 37°C. Adherent cells were subsequently stained with 0.1% safranin-O, and biofilm was quantified by determining the absorbance at 490 nm in a microplate reader ($Spectrostar^{Nano}$, BMG Labtech). For visualization purposes, cells were also cultured in Nucleon™ Delta-treated culture dishes (Thermo Scientific), stained the same way, and photographed. To test the impact of calcium and its respective chelating agent on biofilm formation either $CaCl_2$ (20 mM) and/or EDTA (0.2 mM) were added to the wells (Sarstedt 96-well plate) at the beginning of the incubation period. dH_2O served as the respective control. Cytotoxicity of the reagents was excluded by incubating cells overnight with/without the mentioned reagents in TSB_N and confirming similar growth by OD_{600} measurement after 24 h.

2.4 | Aggregation assays in suspension

For determination of differences in cellular aggregation, wildtype and Δ*sxs*A strains were cultivated in 50 ml of either TSB_N or TSB^+ in Erlenmeyer flasks for up to 24 h at 37°C and 200 rpm. They were removed from the shaker after 12 and 24 h, respectively, and cell aggregation was recorded visually as well as pictures were taken immediately.

To record sedimentation over time, wildtype, Δ*bap*, Δ*sxs*A, and Δ*bap*, *sxs*A strains were grown in TSB_N (37°C, 200 rpm) for 16 h and 3 ml of the cell suspension was transferred to a culture tube. Tubes remained in a steady position and pictures were taken to record cell sedimentation at time zero (t_0) and after one (t_1), two (t_2), five (t_5), and 24 (t_{24}) h, respectively.

2.5 | Colony morphology on congo red agar

Colony morphology on congo red agar (CRA) was examined for wildtype and mutant strains. Minor modifications to the protocol described in Schiffer et al. (2021) were made, since this time, CRA plates contained no glucose and were simply composed of 15 g/L casein peptone, 5 g/L soya peptone, 5 g/L NaCl, 15 g/L agar, 0.8 g/L congo red, and pH 7.2. Strains were streaked out, plates were incubated at 37°C for 24 h and remained at room temperature for another 2 days before they were visually examined. Congo red is known to interact with proteinaceous and amyloidogenic structures; red, dry, and rough colony morphologies can be considered an indicator for microbial-generated amyloid fibers (Erskine et al., 2018).

2.6 | Growth dynamics

Growth dynamics were recorded for wildtype and mutant strains in TSB_N, TSB^+, Lac^+, and TSB^+-HCl over a period of 33 h at 37°C in a microplate reader ($Spectrostar^{Nano}$, BMG Labtech). Therefore, overnight cultures of the respective strains were washed and diluted to an OD_{600} of 0.1 in the respective growth medium. Two hundred microliters of the cell suspensions were transferred to each well of a 96-well plate (Sarstedt). Growth was monitored by measuring the absorbance at 600 nm every 30 min. Before each measurement, the plate was shaken for 10 min at 600 rpm. All data were recorded in technical and biological triplicates. When necessary, colony-forming units per ml were determined by serial dilution in Ringer's solution and plating on TSA.

2.7 | SDS-PAGE analysis of whole-cell protein extracts

SDS-PAGE analysis of whole-cell protein extracts was performed as described by Schiffer et al. (2021). Basically, cells were grown in TSB_N until the early stationary phase. Five milliliters of cell suspension were harvested, washed, and lysed in an isosmotic digestion buffer (150 µl PBS + 30% [wt/vol] raffinose [Sigma], 7 µl lysostaphin [1 mg/ml, Sigma], and 3 µl DNAseI [1 mg/ml, Sigma]) at 37°C for 2 h. In the following, protoplasts were sedimented at 8000 x *g* for 30 min (slow deceleration) and supernatants were subjected to SDS-PAGE analysis (10% resolving gel, 4% stacking gel). Protein staining was performed using ROTI®Blue (CarlRoth) according to the manufacturer's instructions.

2.8 | CLSM imaging

Overnight cultures of wildtype and mutant strains were diluted (1:5 vol/vol) with TSB_N, of which 2.5 ml were transferred to ibidi dishes with glass bottom (ibidi GmbH). After incubation for 16 h at 37°C with 150 rpm, the cultures were stained with Syto60 (DNA, final concentration 5 µM) and Thioflavin T (amyloids, final concentration 20 µM) for 30 min in the dark and imaged in the CLSM (LSM 780, Carl Zeiss Microscopy).

2.9 | SEM imaging

Overnight cultures of wildtype and mutant strains were diluted (1:5 vol/vol) with TSB_N, of which 2.5 ml were transferred to the wells

of 12 well plates containing a porous glass bead each (ROBU®, VitraPOR®, Porous Glass Bead, 4.0 mm, 60 μm pore size). After incubation for 16 h at 37°C with 150 rpm the cultures were fixed (4% paraformaldehyde, 2.5% glutaraldehyde in 50 mM HEPES, pH 7.0) for 24 h, dehydrated in a graded ethanol line (30%, 50%, 70%, 90%, 95%, 100%, 100%) chemically dried (hexamethyldisilazane) overnight, mounted on aluminum stubs, sputter-coated with a 12 nm gold–palladium layer, and imaged in the SEM (ZEISS 1530 Gemini, Carl Zeiss Microscopy GmbH) operating at 3 kV and using the in-lens secondary electron detector.

2.10 | TEM imaging

Overnight cultures of wildtype and mutant strains were diluted (1:5 vol/vol) with TSB_N, of which 5 ml were transferred to 50 ml centrifugation tubes. After incubation for 16 h at 37°C at 150 rpm, the supernatant of the cultures was negatively stained with 0.5% uranyl acetate and imaged in the TEM (Tecnai 12 Spirit; FEI) at an acceleration voltage of 120 kV).

2.11 | Full proteome analysis

For confirmation of successful mutant strain generation and information on the expression of SxsA under different growth conditions, full proteome analysis was performed as described by Schiffer et al. (2021). The proteomics data set is accessible via ProteomeXchange using the identifier PXD029728.

2.12 | Bioinformatics and statistical analysis

General sequence analysis, comparisons, alignments, and phylogenetic trees were calculated using CLC Main Workbench 8 (CLC bio); for alignments, the integrated ClustalO plugin was used. EF-hand motifs (Lewit-Bentley & Réty, 2000) were predicted using ProScan (Prosite database) with a cutoff set to 80% similarity. Coiled-coil motifs were predicted using MARCOIL (Delorenzi & Speed, 2002) and confirmed with the overview generated by the MPI bioinformatics toolkit (Gabler et al., 2020). Amyloid-prone regions and peptides were identified by comparing the results generated by four different algorithms WALTZ-DB 2.0 (Louros et al., 2020), AGGRESCAN (de Groot et al., 2012), TANGO (Fernandez-Escamilla et al., 2004), and FoldAmyloid (Garbuzynskiy et al., 2010). Molecular weight (Mw) and isoelectric point (pI) were computed by the respective tool available on the Expasy server (https://web.expasy.org/compute_pi/). Genomes were screened for proteins harboring a C-terminal LPxTG cell wall-anchored motif using the respective Prosite algorithm, [LY]PX[TSA][GNAST]X(0,10){DEQNKRP}{DEQNKRP}{DEQNKRP}{DEQNKRP}{DEQNKRP}{DEQNKRP}{DEQNKRP}{DEQNKRP}{DEQNKRP}X(0,15)[DEQNKRH]X(0,5) (Roche et al., 2003). Signal peptides and hydrophobic transmembrane segments were predicted by InterPro (86.0). NCBI BLASTP searches against the protein database were used for the analysis of sequence similarities to other proteins, identification of potential homologs and to estimate the prevalence of *sxs*A within the species *S. xylosus* as well as other staphylococcal species. Genomes were screened for the presence of genetic islands using island viewer 4 (Bertelli et al., 2017). Whole-genome sequencing data of TMW 2.1023 and TMW 2.1523 have been deposited at GenBank under the accession nos. JAEMUG000000000 and CP066721-CP066725, respectively. All further *sxs*A sequences included in the analysis are available on NCBI under the indicated Locustag (Table S5). All experiments were performed in biological triplicates and data are presented as mean ± standard errors of the means, unless stated otherwise. SigmaPlot Version 12.5 (Systat Software GmbH) was used to perform Student's *t* tests.

3 | RESULTS

3.1 | Presence of YSIRK-G/S and LPxTG motif-containing proteins in the genomes of *S. xylosus* strains TMW 2.1023 and TMW 2.1523

Since surface proteins are known to be essential in adherence and biofilm formation of other coagulase-negative staphylococci (Foster, 2020; Foster et al., 2014), we have screened the genomic sequences of two *S. xylosus* strains (TMW 2.1023 and TMW 2.1523) for open-reading frames (ORFs) encoding surface proteins that could act as Bap alternatives mediating biofilm formation in this organism. Special emphasis was laid on the presence of an N-terminal YSIRK-G/S signal peptide, a C-terminal LPxTG cell wall-anchoring motif, and a hydrophobic transmembrane segment, as most surface proteins involved in biofilm formation described for other staphylococci share these motifs (Bowden et al., 2002; Mazmanian et al., 2001). Table 1 shows an overview of potential candidate proteins, which were identified in the genomes of the respective *S. xylosus* strains. All protein sequences were further subjected to the InterPro functional analysis tool, to screen for enzymatic domains, as such functional domains are commonly identified in YSIRK-G/S containing surface proteins of streptococci (Bai et al., 2020). Proteins with hydrolytic domains were excluded from further analyses as we were rather concentrating on large structural proteins. Besides Bap, a protein encoded in both *S. xylosus* strains, TMW 2.1023 (JGY91_02365) and TMW 2.1523 (JGY88_01050), and another one encoded in TMW 2.1023 only (JGY91_13535/13480) remained particularly interesting, as they comprise both motifs (YSIRK-G/S, LPxTG), thus are present on the cell surface, display no enzymatic domains, and are very large. We followed the nomenclature proposed by Mazmanian et al. (2001) for staphylococcal surface proteins and therefore named them *Staphylococcus xylosus* surface protein A (SxsA) and B (SxsB). Of note is that while *sxs*A is chromosomally encoded in both strains,

TABLE 1 Proteins of *S. xylosus* TMW 2.1023 and TMW 2.1523 harboring a YSIRK-G/S signal peptide and/or an LPxTG cell wall-anchored motif

TMW 2.1023				TMW 2.1523				
Locustag	**size (aa)**	**YSIRK**	**LPxTG**	**Locustag**	**size (aa)**	**YSIRK**	**LPxTG**	**Note**
JGY91_00380	757	YSIRK	–	JGY88_12550	721	YSIRK	–	AB hydrolase
JGY91_01665	748	YSIRK	–	–				AB hydrolase
JGY91_02365	2044	YSIRK	LPNTG	JGY88_01050	3123	YSIRK	LPNAG	SxsA
JGY91_02455	1651	YSIRK	LPETG	JGY88_01140/45	2161	YSIRK	LPETG	Bap
*JGY91_04265-70	–	FSIRK		–				AB hydrolase
JGY91_13535/ 13480^{P}	1187	FSIRK	LPNTG	–				SxsB
JGY91_12735	648	–	LPNTG	JGY88_11760	884	–	LPNTG	Fibrinogen-binding adhesin
JGY91_13335^{P}	654	–	LPDTG	JGY88_13950^{P}	654	–	LPDTG	Albumin-binding domain (GA module)
				JGY88_00260	659	-	LPDTG	

Note: Asterisk indicates truncated frames due to an internal stop, P indicates sequences that are encoded on plasmids. Some sequences are split into two different contigs in the WGS data set, however, PCR analysis confirmed their entirety as one single ORF. The last column indicates whether enzymatic domains were predicted from sequence analysis or if the protein has been described/named already.

*sxs*B is carried on a plasmid in strain TMW 2.1023 only. Additionally, we consulted the proteomic data set, we obtained from previous work (Schiffer et al., 2021) and found that SxsA shows similar intensity value changes as Bap, namely higher detectable amounts under planktonic compared with sessile growth conditions as well as higher detectable amounts when cells were grown in a neutral medium without glucose (TSB_N), in contrast to when cells were grown in glucose-containing medium additionally acidified to pH 6 by lactic acid (Lac^+). For a more detailed overview of the intensity levels determined by full proteome analysis, see Table S1.

For further investigations, we selected SxsA as a promising candidate to prove our hypothesis that another surface protein than Bap might be involved in biofilm formation of *S. xylosus*.

3.2 | Mutagenesis of the chromosomal *sxs*A gene

*Sxs*A-mutant strains (Δ*sxs*A) were generated for both *S. xylosus* strains. Furthermore, double mutants, deficient in *bap* as well as *sxs*A (Δ*bap*, *sxs*A), were also included in the project. SDS-PAGE analysis was performed to confirm the successful deletion of the respective genes. As we have already reported in Schiffer et al. (2021), Bap is hardly detectable on SDS-PAGE. SxsA, however, is visible as a distinct band at the expected size with 223 kDa for TMW 2.1023 and 338 kDa for TMW 2.1523, respectively. The band was not detectable in mutant strains as shown in Figure 1. It is highly likely that the detected band corresponds to SxsA rather than that expression of another protein decreases upon *sxs*A deletion, as in silico prediction of protein masses of proteins encoded by the two *S. xylosus* strains did not predict any other protein running at the expected size (Table S2). Yet, to confirm the results predicted by the gels, a full proteome analysis was performed. With very few exceptions that are considered as artifacts, no peptides mapping on SxsA were found in the mutant samples, confirming successful deletion of *sxs*A in both *S. xylosus* strains (Tables S3 and S4).

3.3 | Optical density-based growth curves differ between WT and mutant

To exclude that any major growth defects resulted from the transformation procedure or were caused by deleting *sxs*A, growth curves were recorded in a microtiter plate-based format over a period of 33 h. Growth curves confirmed that mutant strains mostly showed a similar growth behavior compared with their respective wildtype strains (Figure S1). Only TMW 2.1523 Δ*sxs*A strains displayed different growth dynamics, in particular, growth rates increased faster, and higher maxima ODs were obtained in some media (TSB^+, Lac^+) for mutant in contrast to wildtype strains. The measured differences in OD between wildtype and mutant strains presumably reflect different cell aggregation behaviors and are probably enhanced by the conditions of the format used (weak aeration and insufficient shaking in the microplate assay). This is also supported by data indicating

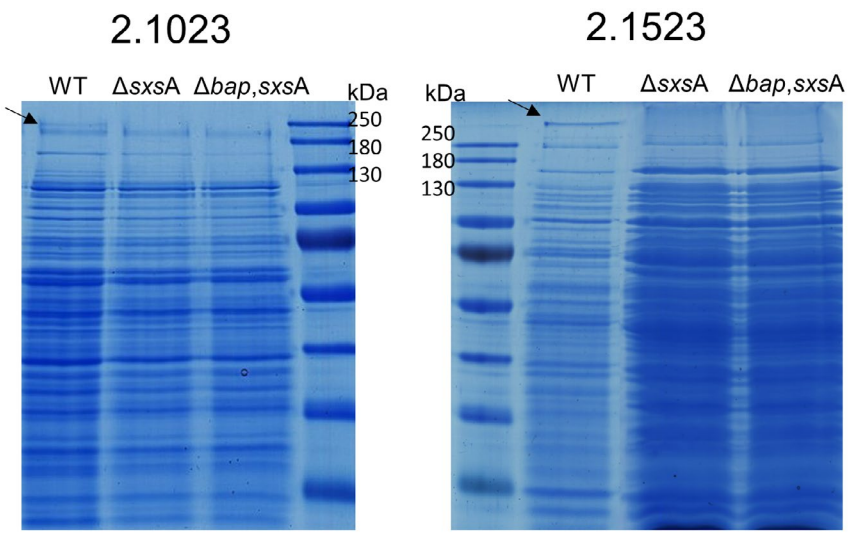

FIGURE 1 SDS-PAGE analysis of wildtype and *sxs*A-mutant strains. The arrow points to the band corresponding to SxsA (TMW 2.1023: 223 kDa, TMW 2.1523: 338 kDa)

that the difference is almost eliminated when cells are grown in the Erlenmeyer flasks under vigorous agitation (compare Section 3.5). Furthermore, almost the same high values of colony-forming units (cfu) were determined after incubation in TSB^+ for 24 h for TMW 2.1523 wildtype and Δ*sxs*A strain resulting in values of 3.4 x 10^7 and 3.5 x 10^7 cfu/ml, respectively.

3.4 | Biofilm formation on abiotic surfaces is impaired in *sxs*A mutants

Biofilm formation was quantified using a 96-well assay, based on safranin-O staining of adherent cells. Deletion of *sxs*A resulted in a complete loss of the ability to form an adherent biofilm of strain TMW 2.1523 as shown in Figure 2. Differences in staining intensities of adherent cells are also visualized in Figure S2. The effect of reduced adherence of mutant strains was regardless of the growth media (TSB_N, TSB^+, Lac^+) and the support (hydrophobic and hydrophilic) used during the experiments. In contrast to TMW 2.1523, TMW 2.1023 only showed a reduction in adherence which was especially apparent in TSB_N and TSB^+ on hydrophilic support. In summary, *sxs*A deletion has an impact on adherence and biofilm formation of *S. xylosus* on abiotic surfaces, yet, strain-specific differences occur, as the impact is much larger in strain TMW 2.1523 than in strain 2.1023. No significant additional decrease in adherence was observed in double mutants (Δ*bap*, Δ*sxs*A) compared with single mutants (Δ*sxs*A).

3.5 | *sxs*A mutants show reduced intercellular adhesion and decelerated sedimentation over time

Biofilm formation and cell aggregation are often linked closely together. To see whether SxsA impacts both phenotypes, cells were grown under shaking conditions in TSB_N until they reached stationary phase (24 h) and subsequently transferred to test tubes to allow them to settle. Figure 3 shows the sedimentation state of TMW 2.1523 at different time points. A clear difference in cell aggregation is detectable between wildtype and mutant strains. While cells of wildtype strain TMW 2.1523 had already settled to the bottom of the tubes after 1 h, *bap* mutants remained in suspension until phase separation was visible after approximately 5 h. *Sxs*A mutants had not even fully settled after 24 h. The difference in cell aggregation in liquid cultures between TMW 2.1523 wildtype and the *sxs*A-deficient strain was also very distinct when cells were grown under shaking conditions in a glucose-supplemented medium (TSB^+, Figure 4a). While wildtype cells of TMW 2.1523 form visible aggregates, especially in TSB^+, only little cell aggregation is visible for the *sxs*A-deficient mutant. However, noteworthy is that the effect demonstrated in Figure 4 between heavily clumping wildtype and little clumping-mutant strains is especially prominent during exponential and early stationary growth phase. TMW 2.1523 *sxs*A mutants grown in TSB^+ start to form visible aggregates after approximately 16 h of growth as well, at a time where they have already entered stationary phase and no pH changes occur anymore. The effect of belated visible aggregation of the *sxs*A mutant is much stronger when cells are grown in glucose-supplemented media, compared with TSB_N. The enhanced aggregation is probably pH dependent since the pH is decreasing to a larger extent when cells are grown in TSB^+ compared with TSB_N (Figure 4b). Attempts to induce visible cell aggregation the opposite way, by incubating TMW 2.1523 in a strongly basic medium (TSB_N, pH 8.5), remained unsuccessful, no differences to TSB_N were observed.

The described differences between wildtype and *sxs*A mutants in cell aggregation and settling pace could not be observed to this extent for TMW 2.1023. In general, this strain showed much less cell aggregation compared with TMW 2.1523. Clumping was only detectable, when cells were incubated in TSB^+, however, compared with the heavy aggregating cells of TMW 2.1523, the multicellular effect observed for TMW 2.1023 was much smaller (see Figures S3 and S4). To sum it up, *sxs*A impacts the multicellular behavior of *S. xylosus*. Yet, strain-specific differences should be considered environmental influences.

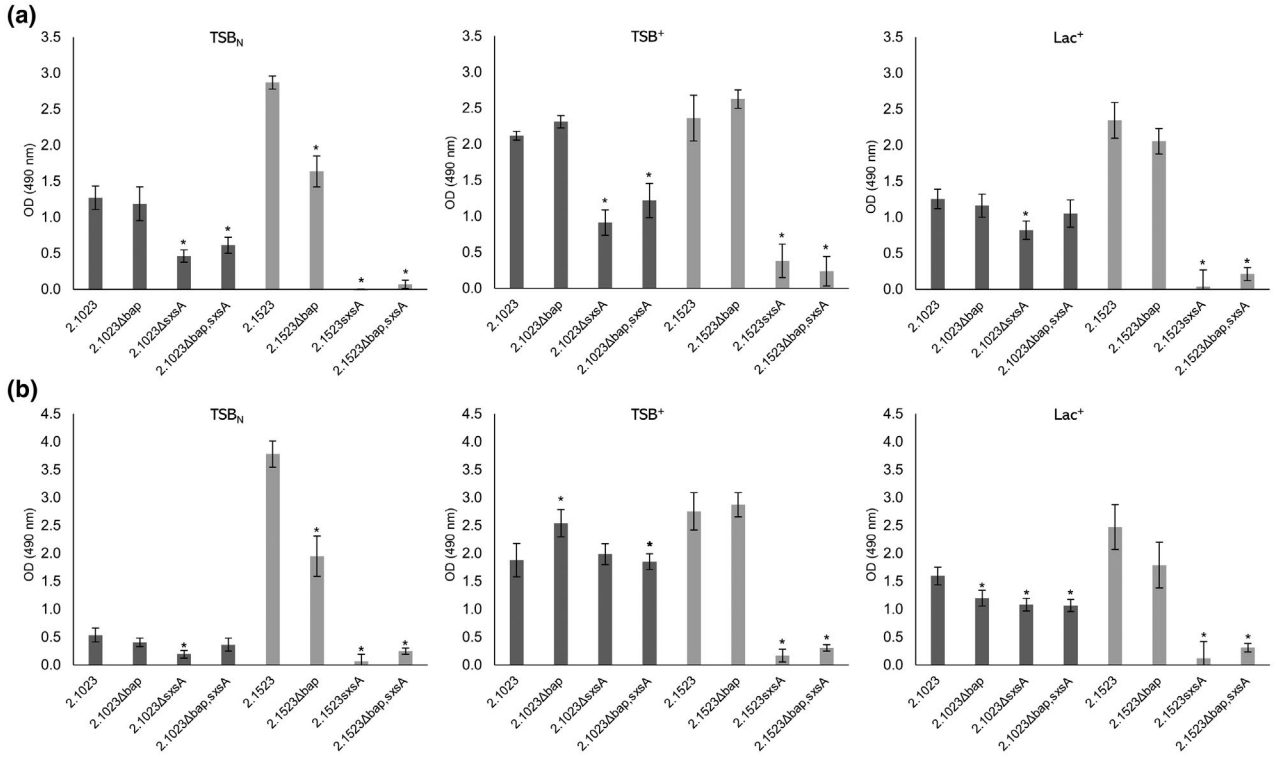

FIGURE 2 Biofilm formation of wildtype and mutant strains under different environmental conditions. Biofilm formation was quantified in a 96-well assay on hydrophilic (a) and hydrophobic (b) support in three different growth media (TSB_N, TSB^+, and Lac^+). Bars are shown as the mean of at least three independent measurements ± SE. Differences between mutant and wildtype strains that can be considered as statistically significant ($\alpha = 0.05$) are marked with asterisks (*)

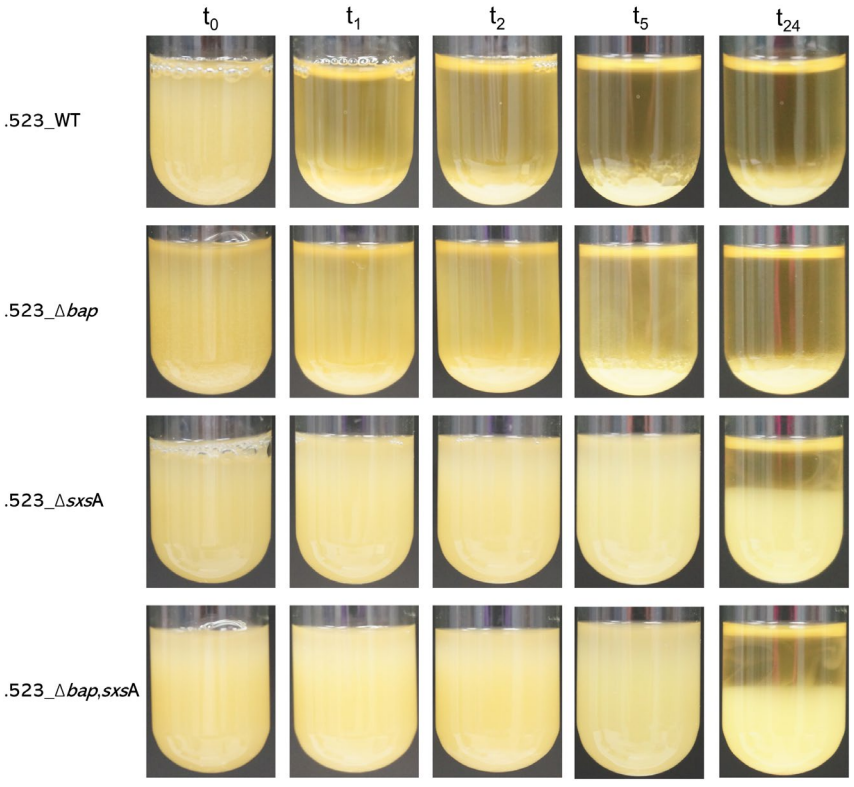

FIGURE 3 Cell sedimentation assay. Three milliliters of TMW 2.1523 cell suspensions (wildtype and mutant strains, stationary phase, TSB_N) were allowed to settle in test tubes, and pictures were taken at different time points (t_0–t_{24}). The pace of cell settlement is used as an indicator for intercellular adhesion

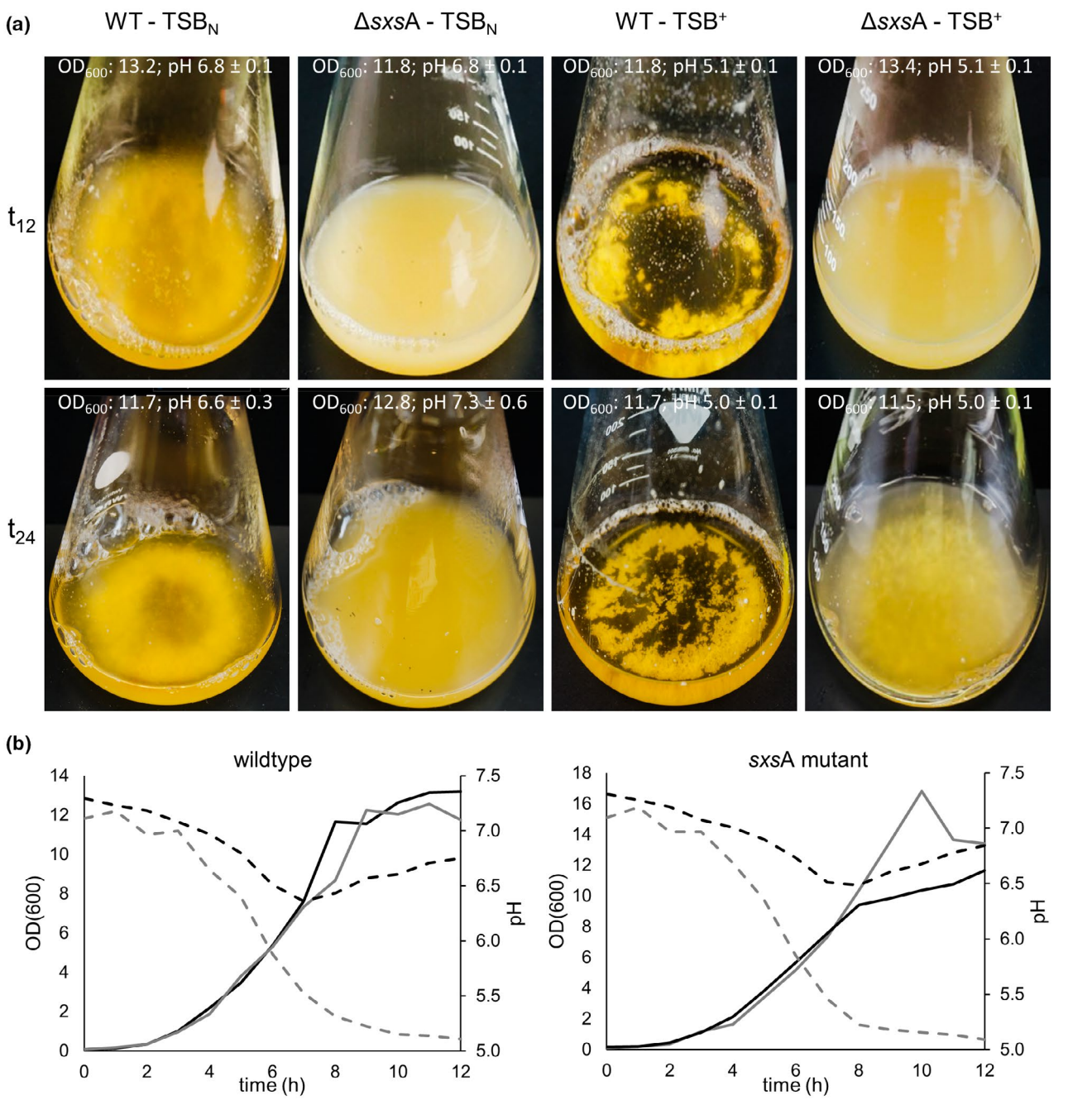

FIGURE 4 Aggregation behavior of planktonically grown wildtype and *sxs*A-mutant strains. (a) Aggregation of planktonically grown cells (TMW 2.1523 wildtype and *sxs*A mutant, 37°C, 200 rpm) was recorded after 12 and 24 h in two different growth media (TSB$_N$ and TSB$^+$). (b) Growth and pH dynamics (dashed lines) of the cultures shown in A in ●TSB$_N$ and ● TSB$^+$

3.6 | Colony morphology on congo red agar plates

Over the past years, many authors have suggested that amyloid-like fiber formation of surface proteins is a general mechanism of biofilm formation in staphylococci (Foster, 2020; Taglialegna, Lasa, et al., 2016a). Congo red (CR) dye is known to interact with amyloid structures which often leads to colony morphology changes to a red, dry, rough phenotype on CRA plates (Cucarella et al., 2001; Erskine et al., 2018). Even though CR is insufficient to confirm the presence of amyloid structures alone, as it may bind to other polymeric substances as well, it can still be a useful first indicator to see whether differences in colony morphology exist. We have previously reported that no changes in colony morphology are noticeable on CRA when the medium is supplemented with glucose (Schiffer et al., 2021). Colonies appeared black, shiny, and with smooth colony margins. In this study, we investigated colony morphologies on CRA containing no glucose. Due to the lack of glucose, the pH of the plates will not decrease during cell growth. Therefore, no changes to a darker colony color were observed on nonglucose-containing CRA plates, instead, colonies all turned red as shown in Figure S5.

While once more no differences were observable for strain TMW 2.1023, which displays in each version a red colony morphology with similar irregular, wavy colony margins, differences regarding the colony margin were noticeable between wildtype and mutant of TMW 2.1523. Again, all colonies bound the dye as well, thus appearing as red; wildtype colonies, however, showed irregular margins, while in *sxs*A mutants (Δ*sxs*A, Δ*bap*,*sxs*A), colony margins remained mostly smooth. A dry, crystalline colony consistency as reported in other studies (Cucarella et al., 2001) for *S. aureus* was not detected in the selected *S. xylosus* strains and their mutants.

3.7 | Prevalence of *sxs*A among staphylococcal species

Neither when blasting the entire SxsA sequence against the NCBI database nor when blasting parts of the protein separately, any sequence similarities to other hitherto described surface proteins (non-*sxs*A orthologs) of *S. aureus* and other staphylococci were found. Pairwise sequence comparison of SxsA and representative, well-known biofilm-associated proteins is provided in Figure S6. It confirms again that SxsA displays little homology (<10%) to other surface proteins. The BLAST-based analysis furthermore revealed that *sxs*A is likely part of the core genome of the species *S. xylosus*, *Staphylococcus pseudoxylosus*, and *Staphylococcus nepalensis* (around 60% aa identity of *S. xylosus* SxsA to other species SxsA according to BLASTp). Yet, it should be kept in mind that only limited genomic data are available on NCBI for *S. pseudoxylosus* and *S. nepalensis*, thus the data pool is limited. Other BLAST hits corresponded occasionally to genome sequences of *Staphylococcus saprophyticus*, however, no entire *sxs*A open-reading frame was found for this organism, as the sequence is split on different contigs in the few genomes in which it is encoded. Therefore, *S. saprophyticus* was not included in any of the further analyses. A higher number of hits and entirely encoded gene sequences were found for certain *Staphylococcus cohnii* isolates. In *S. cohnii*, however, *sxs*A is not part of the core genome, as it was only identified in a small group of strains, all isolated from a dairy environment/bovine mastitis infection (either SNUC strains originating from Canada or SC strains, originating from Germany). When considering a recent taxonomic revision published by Lavecchia et al. (2021), which revealed three phylogenetically distinct lines within *S. cohnii*, *sxs*A-positive isolates all correspond to group A2, a group proposed by the authors to be reclassified to *Staphylococcus cohnii* subsp. *barensis*. *Sxs*A would therefore join the list of strain-specific genes of this subspecies. Whether *sxs*A was acquired by *S. cohnii* due to horizontal gene transfer is not clearly evident. An identical shared gene synteny was found in all staphylococcal species analyzed (Figure S7). *Sxs*A is surrounded by the same set of genes, moreover, no indicators for a localization on a mobile genetic element were identifiable as no flanking transposases, integrases, recombinases, or plasmid-associated genes are located nearby. Furthermore, computational genomic island finders did not yield any hits for this region either. Thus, it appears that *sxs*A is part of the chromosome in a region with low plasticity, at least in those species in which it is part of the core genome, and it remains open whether *Staphylococcus cohnii* subsp. *barensis* has acquired the gene exogenously during speciation or if other *S. cohnii* have lost it during evolution.

3.8 | Primary sequence organization of SxsA

Domain structure analysis of SxsA was made based on the alignment of 44 different SxsA sequences, originating from four different staphylococcal species, and subsequent analysis of conserved regions and secondary structure (alpha and beta structures, coiled-coil motifs, amyloidogenic regions). Only complete open-reading frames, entirely encoded on one contig, were considered. Table S5 lists all organisms that were included in the analysis. Similar analysis of the SxsA sequences revealed a clear grouping into four different subgroups at a cutoff level of about 16% (see phylogenetic tree provided in Figure S8). This grouping partly reflects the phylogenetic relationship, as sequences of *S. cohnii* and *S. nepalensis* cluster as distinct. The two remaining groups, however, contain both *S. xylosus* and *S. pseudoxylosus* sequences.

SxsA structure can be divided into four domains, as shown in Figure 5, and as described exemplarily for TMW 2.1523 in the following. After the N-terminal signal peptide (YSIRK-G/S, 43 aa), a 286 aa long sequence follows (aa 44–329), which is rich in α-helix structure and predicted to fold into coiled-coil domains from aa 131 to 158 (Figure 5a,b). This region is designated as Region A. Of note is that some strains carry a SxsA version with short-sequence stretches that share >80% similarity with calcium-binding EF-hand motifs in their Region A (marked as a black arrow in Figure S8). Region B (aa 330–520) is rich in β-sheet secondary structure and is the most conserved region of the protein across species (Figure 5b,e). It is also the region of the protein which was computed to carry amyloidprone peptide stretches (Figure 5c). Other YSIRK-G/S, LPxTG-containing staphylococcal surface proteins, such as Bap and Aap, have been shown to mediate biofilm formation by adopting an amyloid conformation (Taglialegna, Navarro, et al., 2016b; Yarawsky et al., 2020). Therefore, special emphasis was led on the prediction and analysis of potential amyloidprone regions for SxsA as well. Similar to Bap and Aap, the amyloidogenic regions of SxsA are located within β-sheet-rich regions of the protein. Comparison of the predicted (by at least three of the four algorithms used) amino acid sequences revealed two short, conserved peptide stretches that display high amyloidogenic potential and which are present in all SxsA sequences analyzed namely $_{455}$LGYYSY$_{460}$ and $_{500}$LFGYILS$_{506}$ (aa positions are indicated for strain TMW 2.1523). Further, *S. xylosus*, *S. pseudoxylosus*, and *S. nepalensis* share a conserved amyloidogenic peptide $_{402}$VLIATMVL$_{409}$ as well as *S. nepalensis* and *S. cohnii* sequences both contain the amyloidprone segment $_{486}$VKFYISFDA$_{494}$ (S. *nep*_JS1) and *S. xylosus* and *S. pseudoxylosus* $_{482}$EFVISFDASYYI$_{493}$ (see Figure 5d and Figure S10, respectively). When referring to amyloid formation, the isoelectric point (pI) is another important parameter to consider as it is assumed that peptide assembly into amyloidogenic structures is enhanced when the environment reaches pH values close to the pI of the peptide (Taglialegna, Navarro, et al., 2016b). While the pI of the entire protein is reached

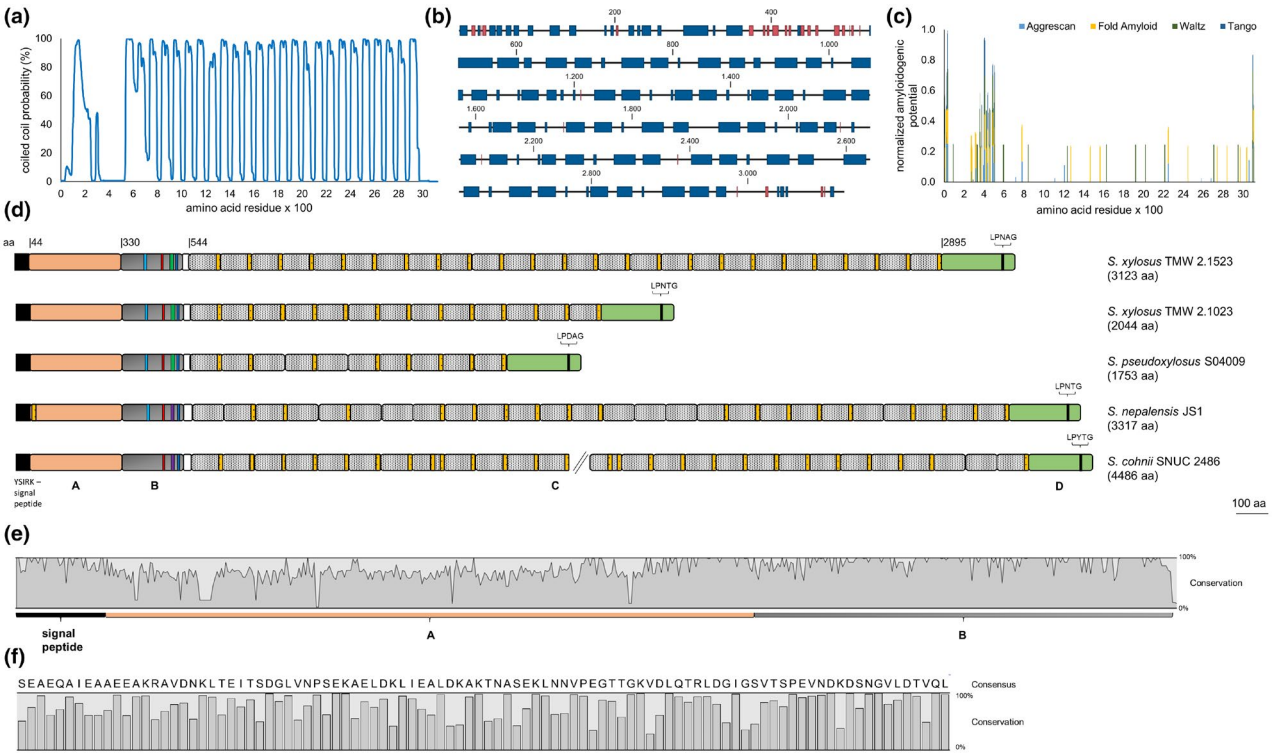

FIGURE 5 Structural organization of SxsA. (a) Prediction of coiled-coil regions (2.1523-SxsA) by MARCOIL. (b) 2.1523-SxsA secondary structure prediction, regions predicted to fold into α-helices and β-sheet are marked in blue and red, respectively. (c) Predicted amyloidogenic potential of 2.1523-SxsA. Columns represent the normalized amyloidogenic potential of SxsA by four different algorithms as Aggrescan (bright blue), FoldAmyloid (yellow), WALTZ (green), and TANGO (blue). (d) SxsA structure of four different staphylococcus species. Signal peptide, cell wall-anchor, and Regions A–D of the protein are displayed as indicated. EF-hand motifs (≥80% similarity) are shown in yellow, conserved amino acid sequences of Region B corresponding to amyloid prone peptides predicted by at least three of the algorithms used are LGYYSY (red), LFGYILS (blue), EFVISFDASYYI (green), VKFYISFDA (violet), and VLIATMVL (bright blue). SxsA of *S. cohnii* SNUC 2486 harbors 40 repeats in its C-region of which not all are shown due to space restrictions. (e) Conservation plot of the N-terminal part of the protein (SP, Regions A and B) when SxsA of 44 different strains is aligned with MUSCLE. (f) Conservation and consensus sequence when all C-repeats of all 44 analyzed SxsA sequences are aligned

under acidic conditions (4.4–4.8), the pI of SxsA Region B only is reached in the basic milieu (pI values around 8.0–9.1).

Region B is followed by a short spacer sequence after which Region C starts. Region C consists of 98 aa long repeats, not identical in their sequence but with some conserved amino acids (Figure 5f). SxsA varies in the number of repeats not only between but also within staphylococcal species. In the here performed analysis, the lowest number (4) of repeats was found in *S. xylosus* SNUC233 and the highest number (44) in *S. nepalensis* NCTC10517 and *S. xylosus* DMSX03 (Table S5). The different number of repeats is the main reason for the varying length/molecular weight of the protein among different strains. The C-repeats are further predicted to fold into coiled-coil motifs and almost every repeat sequence harbors a motif that shares more than 80% similarity with the loop consensus of Ca^{2+}-binding EF-hand motifs (Lewit-Bentley & Réty, 2000). Region D (aa 2895–3123) is at the C-terminal part of the protein and includes the LPxTG cell wall-anchor domain as well as the characteristic hydrophobic amino acid segment, often found in surface proteins with an LPxTG motif. In contrast to Bap (Cucarella et al., 2001; Schiffer et al., 2019), no repeats are identifiable in Region D of SxsA nor are serine and aspartic acid residues (SD repeats) present in any of the SxsA Region D sequences.

SxsA of all analyzed organisms shares the same structural characteristics described in this section. Coiled-coil formation, amyloidogenic potential, as well as secondary structure prediction for *S. xylosus* TMW 2.1023, *S. nepalensis* JS1, *S. pseudoxylosus* S04009, and *S. cohnii* SNUC2486 are shown in Figure S10. An overview of structural organization, number of C-repeats, and number of EF-hand motifs are provided by Figure S9.

3.9 | Microscopic analysis of biofilm matrix and cell morphology

As the phenotype of Δ*sxs*A was more distinct in TMW 2.1523 in the previously described experiments, it was decided to perform microscopic analyses with this strain and its respective *sxs*A mutants

in TSB_N, only. Microscopic analysis (CLSM and SEM) confirmed the different aggregation behavior of wildtype and *sxs*A-mutant strains. In contrast to thin layers of homogenously distributed mutant cells (single and double mutant), the wildtype strain formed compact, multilayered biofilms with densely packed cell aggregates and adhered well to the surface of porous glass beads (Figure 6a,b). Thereby, it

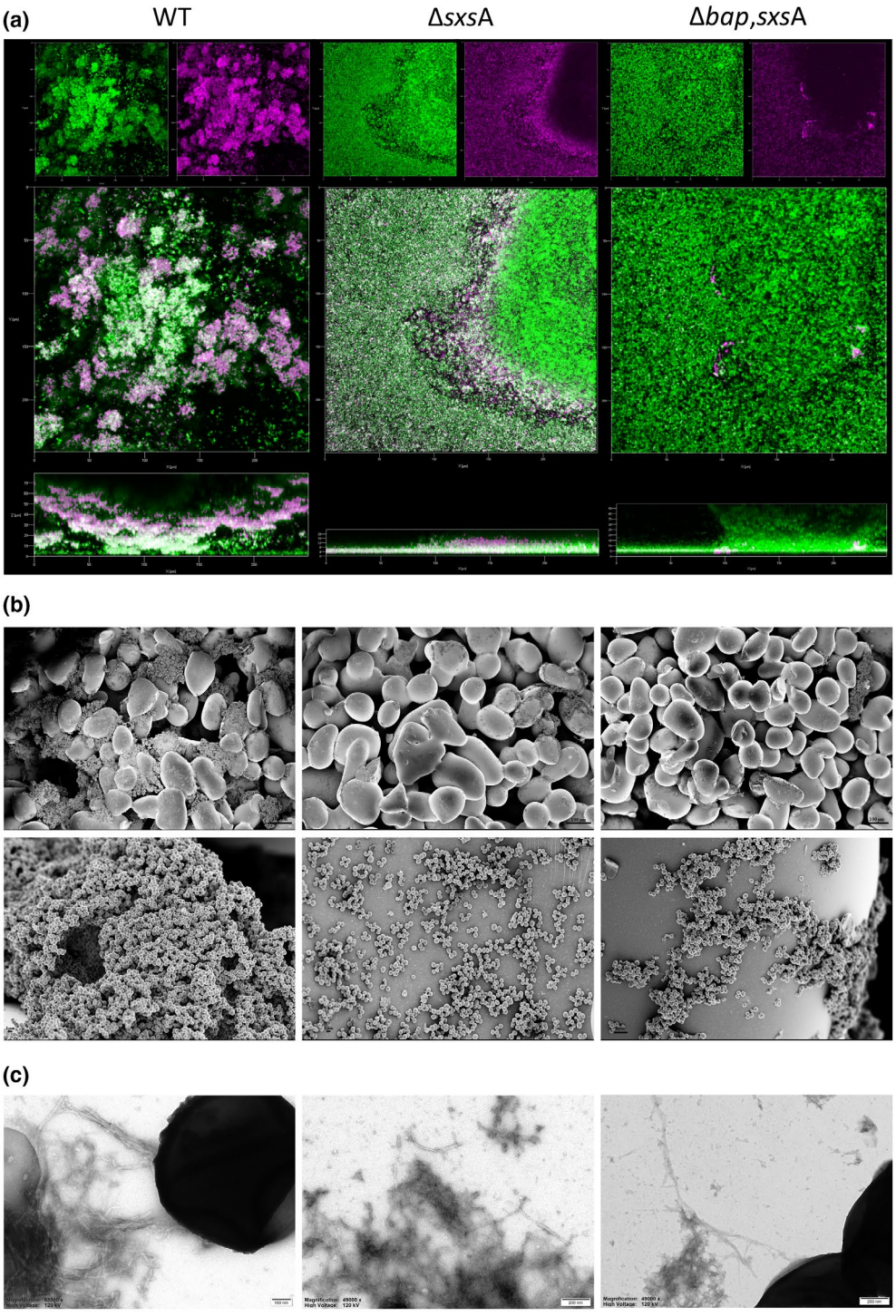

FIGURE 6 Microscopic analysis *S. xylosus* TMW 2.1523 wildtype and mutant biofilms. (a) Confocal laser scanning microscopy of *S. xylosus* TMW 2.1523 wildtype and *sxs*A single- and double-mutant biofilms/cell aggregates after 16 h of incubation (TSB_N, 150 rpm). Staining was performed using Thioflavin T (green) and Syto60 (violet). Top view single-channel images are shown on the top, the respective merged view in the middle, and merged profile (vertical) views below. (b) Scanning electron microscopy of cell aggregates adherent to porous glass beads after 16 h of incubation (TSB_N, 150 rpm). Bacteria were subjected to shear forces during incubation (150 rpm). Two different magnitudes are shown (250x, 5kx). (c) Negative-stained transmission electron micrographs to visualize fibrillar structures of *S. xylosus* cells grown for 16 h (TSB_N, 180 rpm). Scale bars are included in the figure and labeled accordingly

formed a thick biofilm layer even on the outer parts of the beads that were subjected to high shear forces during incubation.

Since literature research, bioinformatic analyses as well as preliminary results from congo red agar plates indicated that the *S. xylosus* biofilm matrix consists of amyloid fibers and that SxsA might contribute to such fiber formation, microscopic analyses were also used to further investigate the composition and structure of *S. xylosus* wildtype and mutant biofilm matrices. Amyloids are protein aggregation disorders that are often found as a structural component in biofilm matrices to provide integrity. Thioflavin T (ThT) is a fluorescent dye commonly used to stain amyloid fibrils. We found that generally large parts of the *S. xylosus* biofilm matrix responded to ThT staining (Figure 7a). Interestingly, regions responding solely to ThT staining were observed in mutant strains while in wildtype samples, most structures responded to both stains, indicating a mixture of DNA (cells/eDNA, stained by nucleic acid stain Syto60) and amyloidogenic structures (ThT staining). SEM analysis confirmed that *sxs*A mutants formed less-adherent biofilm, especially not on surfaces exposed to high shear forces, with only very few parts of the culture assembling to multicellular aggregates (Figure 6b). TEM analysis revealed the presence of at least two different fiber types surrounding the cells, which were often embedded in a slimy kind of matrix (Figure 6c). Yet again, such thin and thick fibers as well as the slimy matrix were detectable in all three sample types. All in all, microscopic analysis confirmed the presence of fibrillar structures in *S. xylosus* TMW 2.1523 biofilms. At least parts of these fibrillar structures are probably of an amyloidogenic nature since highly fluorescent complexes were visible upon ThT staining. Differences between wildtype and mutant, however, were only ascribable to their aggregation and surface adherence behavior and not to fiber type, amount, or ThT staining intensities.

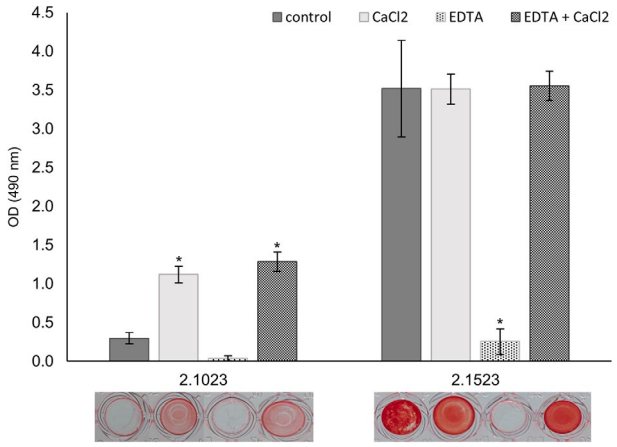

FIGURE 7 Influence of calcium on biofilm formation of *S. xylosus*. Biofilm formation was quantified in 96-well plates (hydrophobic support). Therefore, cells were incubated in TSB_N for a period of 24 h. Either 20 mM $CaCl_2$, 0.2 mM EDTA, or both reagents were added to the wells at the beginning of the incubation period

3.10 | Importance of calcium on biofilm formation of *S. xylosus*

EF-hand motifs, which bioinformatic analysis predicted to occur multiple times in the sequence of SxsA, are known to bind divalent cations such as Ca^{2+}. Such binding of cations to EF-hand motifs of proteins has been previously shown to modulate protein conformation and regulate assembly (Lewit-Bentley & Réty, 2000; Taglialegna, Navarro, et al., 2016b). Therefore, we investigated the influence of calcium on biofilm formation of *S. xylosus*. Wildtype strains TMW 2.1023 and TMW 2.1523 were screened for adhesive biofilm formation in a 96-well-based assay, this time $CaCl_2$ was added in the presence or absence of its respective chelator ethylenediaminetetraacetic (EDTA). As shown in Figure 7, biofilm formation was either unaffected or significantly enhanced when calcium was added, a result especially prevalent in strain TMW 2.1023. The addition of EDTA (0.2 μM) completely abolished biofilm formation in both strains, an effect that could be restored by adding sufficient amounts of calcium again (200 mM).

4 | DISCUSSION

Over the past years, many cell wall-anchored (CWA) proteins of *S. aureus* and *S. epidermidis* have been functionally characterized and current knowledge on staphylococcal biofilm formation is mainly based on the results obtained for these two prominent species (Foster, 2020; Foster et al., 2014; Speziale et al., 2014). Little research has been done on biofilm formation of other CNS such as *S. xylosus*, except for some valuable studies on *S. xylosus* strain C2a, focusing on the eDNA part of biofilm matrices though (Leroy et al., 2021; Planchon et al., 2006). Since the matrix composition of biofilms and mechanisms of adherence are complex and variable among staphylococci, including other species in the research will help to provide a more comprehensive picture. This is particularly relevant when considering that biofilm-mediating genes can easily migrate from CNS into highly pathogenic species such as reported for Bap into bovine strains of *S. aureus* (Tormo et al., 2005).

We have recently published that biofilm-forming mechanisms investigated for one staphylococcal species cannot easily be applied to other species, as we have shown that Bap is not conferring biofilm formation in *S. xylosus* to the same extent as it does in *S. aureus* (Schiffer et al., 2021). To our knowledge, we here present the first data of a newly discovered surface protein, occurring in *S. xylosus* and related species, which is involved in intercellular aggregation and adhesive biofilm formation on surfaces.

SxsA is a large, cell wall-anchored protein (TMW 21023: 223 kDa, TMW 21523: 338 kDa), displaying little sequence identity with other well-known staphylococcal surface proteins, yet sharing a very similar structural organization with CWA proteins such as Bap, the biofilm homologous protein Bhp, and *S. aureus* surface protein SasC (Cucarella et al., 2001; Foster, 2020; Schroeder et al., 2009; Tormo et al., 2005). Like other CWA proteins, SxsA is

organized into domains, where the N-terminal signal peptide is followed by no repeats containing sequence stretches, Regions A and B, of which Region B is highly conserved among SxsA of different species. Region B is also the part of the protein which mainly folds into β-sheet structures and which is predicted to possess high amyloidogenic potential. The core region of the protein is composed of varying numbers of imperfect tandem repeats (C-repeats) followed by the C-terminal Region D which contains the LPxTG motif, a typical cell wall anchor of staphylococcal surface adhesions (Bowden et al., 2005; Speziale et al., 2014). Region D of staphylococcal surface adhesions is often rich in SD repeats (Bowden et al., 2005), this is, however, not applicable to SxsA. The role of C-repeats in bacterial surface proteins has been controversially discussed in the past. From homophilic interactions of repeating structures on neighboring cells over immune evasion mechanisms to structural roles by maintaining proper protein conformation and/or projecting N-terminal ligand-binding domains from the cell surface up to no functional role in the molecular mechanism of biofilm formation at all (Cucarella et al., 2004; Rohde et al., 2007; Valle et al., 2012). Which function C-repeats of SxsA have, and whether the coiled-coil structure contributes to multicellular behavior remains to be discovered. Based on the data presented in the literature for other CWA proteins and the experiments conducted in this study, another mechanism of SxsA-conferring biofilm formation seems to be just as likely though. Instead of the usually extensive core region of CWA proteins, the N-terminal part of staphylococcal surface proteins is often rather substantial in the adhesion and biofilm accumulation process. Many surface adhesions display ligand-binding regions in their N-terminal part (Foster, 2019). Additionally, many CWA proteins have been shown to form amyloidogenic fibers after extracellular processing of the N-terminal part of the protein and thereby contribute to the structural integrity of biofilms (Erskine et al., 2018; Foster, 2020; Taglialegna, Lasa, et al., 2016a). The exact mechanisms of amyloid assembly differ between biofilm proteins, though. Bap and the enterococcal surface protein Esp, for instance, form amyloidogenic fibers through self-assembly of released amyloidprone peptides (Taglialegna, Navarro, et al., 2016b), while Aap-based functional amyloid fibers originate from interactions of exposed repeat-containing domains on the cell surface in the presence of Zn^{2+} (Yarawsky et al., 2020). A high potential to fold into amyloidogenic structures is predicted for Region B of SxsA as well, and red phenotypes on CRA provided a promising first indicator. The additional microscopic analysis confirmed the presence of fibers, likely of an amyloidogenic nature, in *S. xylosus* biofilms. Yet, no clear differences between wildtype and mutants were detectable in this regard. This does not necessarily mean that SxsA is not contributing to amyloid fiber formation, it rather emphasizes the multifactorial nature of *S. xylosus* biofilm formation. Furthermore, the influence of metal ions on *sxs*A-mediated biofilm formation can only be speculated at this timepoint. Divalent ions play important parts in the amyloidogenesis of peptides and protein-based cell aggregation of bacteria. Zn^{2+}, for example, has been shown to be essential for Aap- and SasG-mediated cell aggregation (Geoghegan et al., 2010; Yarawsky et al., 2020). Ca^{2+}, on the other hand, is known for inhibiting Bap-mediated biofilm formation in *S. aureus* (Arrizubieta et al., 2004). This inhibitory effect relies on the binding of the ion to EF-hand motifs in the amyloid-prone region of the protein (Taglialegna, Navarro, et al., 2016b). We have previously shown that biofilm formation of *S. xylosus* is not inhibited by Ca^{2+} addition to the growth medium but rather enhanced (Schiffer et al., 2021). Here we prove that calcium is essential for biofilm formation of *S. xylosus*, as the addition of the ion significantly enhanced adherence of TMW 2.1023 to polystyrene plates and EDTA completely abolished biofilm formation of both *S. xylosus* strains. Thus, even though SxsA carries many EF-hand motifs, an inhibiting effect of the ion through binding to EF-hand motifs and stabilization of the molten globule state thereby preventing self-assembly into amyloid fibers, can be excluded (Taglialegna, Navarro, et al., 2016b). On the contrary, we suggest that calcium rather mediates interactions of *S. xylosus* surface proteins, maybe even by interacting with SxsA, in a similar way as it is described for Aap and zinc (Conrady et al., 2008).

In this study, we found SxsA to influence multicellular behavior and adhesion to abiotic surfaces in a strain-specific manner. Biofilm formation in the 96-well assay was completely disrupted upon deletion of SxsA in *S. xylosus* strain TMW 2.1523 while it was only impaired in TMW 2.1023. This corroborates the complexity of biofilm formation in staphylococci and the high variability of mechanisms between strains. In this context, it is worth mentioning that the genetic background of the two strains is different. TMW 2.1023 carries a plasmid, encoding another CWA protein (SxsB) which shares typical characteristics of biofilm-associated surface proteins and could therefore compensate for the loss of SxsA or mask the effect in the first place. However, it might just as well be possible that the mechanism of biofilm formation in TMW 2.1023 is a completely different one and that it rather relies on other factors such as eDNA or a yet unidentified polysaccharide. Here one should also keep in mind that biofilm formation in TMW 2.1023 is generally lower than in TMW 2.1523 and while the latter tends to autoaggregate heavily, TMW 2.1023 shows no visible cell aggregation in TSB_N and only little in TSB^+.

It is known that staphylococcal biofilm matrices consist of proteins, eDNA, and polysaccharides in different proportions (Schilcher & Horswill, 2020). Our data once again demonstrate that differences in number, nature, and impact of proteinaceous components involved exist between different species and even different strains.

*Sxs*A is encoded in a group of staphylococci that have all been associated with mastitis infections in the past (Condas et al., 2017; de Buck et al., 2021). However, the potential role of SxsA in adhesion to biotic surfaces (intramammary adherence), infectious processes, and subordinate effects of biofilm formation (e.g., antimicrobial susceptibility) can currently only be speculated. Further studies on molecular mechanisms of *sxs*A-mediated biofilm formation and the role of the protein during infections are warranted.

In conclusion, this study describes a novel staphylococcal surface protein-mediating intercellular adhesion and promoting biofilm formation on abiotic surfaces.

ACKNOWLEDGMENTS

Part of this work was funded by the German Federal Ministry for Economic Affairs and Energy via the German Federation of Industrial Research Associations (AiF) and the Forschungskreis der Ernährungsindustrie E.V. (FEI), project AiF 19690 N. Open Access funding enabled and organized by Projekt DEAL.

CONFLICT OF INTEREST

The authors received a research grant from the AiF, which did not influence the aims or setup of this study, and declare no conflict of interest.

AUTHOR CONTRIBUTIONS

Carolin J. Schiffer: conceptualization, data acquisition, analysis, and interpretation, writing—original draft preparation; Christoph Schaudinn: data acquisition and analysis, writing—review and editing; Matthias A. Ehrmann: conceptualization, data analysis and interpretation, supervision, writing—review and editing; Rudi F. Vogel: funding acquisition, project administration, supervision, writing—review and editing.

DATA AVAILABILITY STATEMENT

Whole genome sequencing data of TMW 2.1023 and TMW 2.1523 have been deposited at GenBank under the accessions JAEMUG000000000 and CP066721-CP066725, respectively. The proteomics dataset is accessible via ProteomeXchange using the identifier PXD029728.

REFERENCES

Arrizubieta, M.J., Toledo-Arana, A., Amorena, B., Penadés, J.R. & Lasa, I. (2004) Calcium inhibits Bap-dependent multicellular behavior in *Staphylococcus aureus*. *Journal of Bacteriology*, *186*(22), 7490–7498. Available from: https://doi.org/10.1128/JB.186.22.7490-7498.2004

Bai, Q., Ma, J., Zhang, Z., Zhong, X., Pan, Z., Zhu, Y. et al. (2020) YSIRK--G/S-directed translocation is required for *Streptococcus suis* to deliver diverse cell wall anchoring effectors contributing to bacterial pathogenicity. *Virulence*, *11*(1), 1539–1556. Available from: https://doi.org/10.1080/21505594.2020.1838740

Becker, K., Heilmann, C. & Peters, G. (2014) Coagulase-negative staphylococci. *Clinical Microbiology Reviews*, *27*(4), 870–926. Available from: https://doi.org/10.1128/CMR.00109-13

Bertelli, C., Laird, M.R., Williams, K.P., Lau, B.Y., Hoad, G., Winsor, G.L. et al. (2017) IslandViewer 4: expanded prediction of genomic islands for larger-scale datasets. *Nucleic Acids Research*, *45*(W1), W30–W35. Available from: https://doi.org/10.1093/nar/gkx343

Bowden, M.G., Visai, L., Longshaw, C.M., Holland, K.T., Speziale, P. & Hook, M. (2002) Is the GehD lipase from *Staphylococcus epidermidis* a collagen binding adhesin? *The Journal of Biological Chemistry*, *277*(45), 43017–43023. Available from: https://doi.org/10.1074/jbc.M207921200

Bowden, M.G., Chen, W., Singvall, J., Xu, Y., Peacock, S.J., Valtulina, V. et al. (2005) Identification and preliminary characterization of cell-wall-anchored proteins of *Staphylococcus epidermidis*. *Microbiology (Reading, England)*, *151*(Pt 5), 1453–1464. Available from: https://doi.org/10.1099/mic.0.27534-0

de Buck, J., Ha, V., Naushad, S., Nobrega, D.B., Luby, C., Middleton, J.R. et al. (2021) Non-aureus staphylococci and bovine udder health: current understanding and knowledge gaps. *Frontiers in Veterinary Science*, *8*, 658031. Available from: https://doi.org/10.3389/fvets.2021.658031

Condas, L.A.Z., de Buck, J., Nobrega, D.B., Carson, D.A., Roy, J.-P., Keefe, G.P. et al. (2017) Distribution of non-aureus staphylococci species in udder quarters with low and high somatic cell count, and clinical mastitis. *Journal of Dairy Science*, *100*(7), 5613–5627. Available from: https://doi.org/10.3168/jds.2016-12479

Conrady, D.G., Brescia, C.C., Horii, K., Weiss, A.A., Hassett, D.J. & Herr, A.B. (2008) A zinc-dependent adhesion module is responsible for intercellular adhesion in staphylococcal biofilms. *Proceedings of the National Academy of Sciences*, *105*(49), 19456–19461. Available from: https://doi.org/10.1073/pnas.0807717105

Cucarella, C., Solano, C., Valle, J., Amorena, B., Lasa, I. & Penadés, J.R. (2001) Bap, a *Staphylococcus aureus* surface protein involved in biofilm formation. *Journal of Bacteriology*, *183*(9), 2888–2896. Available from: https://doi.org/10.1128/JB.183.9.2888-2896.2001

Cucarella, C., Tormo, M.A., Ubeda, C., Trotonda, M.P., Monzon, M., Peris, C. et al. (2004) Role of biofilm-associated protein Bap in the pathogenesis of bovine *Staphylococcus aureus*. *Infection and Immunity*, *72*(4), 2177–2185. Available from: https://doi.org/10.1128/IAI.72.4.2177-2185.2004

Decker, R., Burdelski, C., Zobiak, M., Büttner, H., Franke, G., Christner, M. et al. (2015) An 18 kDa scaffold protein is critical for *Staphylococcus epidermidis* biofilm formation. *PLOS Pathogens*, *11*(3), e1004735. Available from: https://doi.org/10.1371/journal.ppat.1004735

DeDent, A., Bae, T., Missiakas, D.M. & Schneewind, O. (2008) Signal peptides direct surface proteins to two distinct envelope locations of *Staphylococcus aureus*. *The EMBO Journal*, *27*(20), 2656–2668. Available from: https://doi.org/10.1038/emboj.2008.185

Delorenzi, M. & Speed, T. (2002) An HMM model for coiled-coil domains and a comparison with PSSM-based predictions. *Bioinformatics (Oxford, England)*, *18*(4), 617–625. Available from: https://doi.org/10.1093/bioinformatics/18.4.617

Erskine, E., MacPhee, C.E. & Stanley-Wall, N.R. (2018) Functional amyloid and other protein fibers in the biofilm matrix. *Journal of Molecular Biology*, *430*(20), 3642–3656. Available from: https://doi.org/10.1016/j.jmb.2018.07.026

Fernandez-Escamilla, A.-M., Rousseau, F., Schymkowitz, J. & Serrano, L. (2004) Prediction of sequence-dependent and mutational effects on the aggregation of peptides and proteins. *Nature Biotechnology*, *22*(10), 1302–1306. Available from: https://doi.org/10.1038/nbt1012

Foster, T.J. (2019) The MSCRAMM family of cell-wall-anchored surface proteins of gram-positive cocci. *Trends in Microbiology*, *27*(11), 927–941. Available from: https://doi.org/10.1016/j.tim.2019.06.007

Foster, T.J. (2020) Surface proteins of *Staphylococcus epidermidis*. *Frontiers in Microbiology*, *11*, 1829. Available from: https://doi.org/10.3389/fmicb.2020.01829

Foster, T.J., Geoghegan, J.A., Ganesh, V.K. & Höök, M. (2014) Adhesion, invasion and evasion: the many functions of the surface proteins of *Staphylococcus aureus*. *Nature Reviews Microbiology*, *12*(1), 49–62. Available from: https://doi.org/10.1038/nrmicro3161

Gabler, F., Nam, S.-Z., Till, S., Mirdita, M., Steinegger, M., Söding, J. et al. (2020) Protein sequence analysis using the MPI bioinformatics toolkit. *Current Protocols in Bioinformatics*, *72*(1), e108. Available from: https://doi.org/10.1002/cpbi.108

Garbuzynskiy, S.O., Lobanov, M.Y. & Galzitskaya, O.V. (2010) FoldAmyloid: a method of prediction of amyloidogenic regions from protein sequence. *Bioinformatics (Oxford, England)*, *26*(3), 326–332. Available from: https://doi.org/10.1093/bioinformatics/btp691

Geoghegan, J.A., Corrigan, R.M., Gruszka, D.T., Speziale, P., O'Gara, J.P., Potts, J.R. et al. (2010) Role of surface protein SasG in biofilm

formation by *Staphylococcus aureus*. *Journal of Bacteriology*, *192*(21), 5663–5673. Available from: https://doi.org/10.1128/JB.00628-10

de Groot, N.S., Castillo, V., Graña-Montes, R. & Ventura, S. (2012) AGGRESCAN: method, application, and perspectives for drug design. *Methods in Molecular Biology (Clifton, N.J.)*, *819*, 199–220. Available from: https://doi.org/10.1007/978-1-61779-465-0_14

Heilmann, C., Hussain, M., Peters, G. & Götz, F. (1997) Evidence for autolysin-mediated primary attachment of *Staphylococcus epidermidis* to a polystyrene surface. *Molecular microbiology*, *24*(5), 1013–1024. Available from: https://doi.org/10.1046/j.1365-2958.1997.4101774.x

Karatan, E. & Watnick, P. (2009) Signals, regulatory networks, and materials that build and break bacterial biofilms. *Microbiology and Molecular Biology Reviews*, *73*(2), 310–347. Available from: https://doi.org/10.1128/MMBR.00041-08

Lavecchia, A., Chiara, M., de Virgilio, C., Manzari, C., Pazzani, C., Horner, D. et al. (2021) Comparative genomics suggests a taxonomic revision of the *Staphylococcus cohnii* species complex. *Genome Biology and Evolution*, *13*(4), 1–14. Available from: https://doi.org/10.1093/gbe/evab020

Lawal, O.U., Barata, M., Fraqueza, M.J., Worning, P., Bartels, M.D., Goncalves, L. et al. (2021) *Staphylococcus saprophyticus* from clinical and environmental origins have distinct biofilm composition. *Frontiers in Microbiology*, *12*, 663768. Available from: https://doi.org/10.3389/fmicb.2021.663768

Leroy, F., Verluyten, J. & Vuyst, L.D. (2006) Functional meat starter cultures for improved sausage fermentation. *International Journal of Food Microbiology*, *106*(3), 270–285. Available from: https://doi.org/10.1016/j.ijfoodmicro.2005.06.027

Leroy, S., Lebert, I., Andant, C., Micheau, P. & Talon, R. (2021) Investigating extracellular DNA release in *Staphylococcus xylosus* biofilm in vitro. *Microorganisms*, *9*(11), 2192. Available from: https://doi.org/10.3390/microorganisms9112192

Lewit-Bentley, A. & Réty, S. (2000) EF-hand calcium-binding proteins. *Current Opinion in Structural Biology*, *10*(6), 637–643. Available from: https://doi.org/10.1016/S0959-440X(00)00142-1

Louros, N., Konstantoulea, K., de Vleeschouwer, M., Ramakers, M., Schymkowitz, J. & Rousseau, F. (2020) WALTZ-DB 2.0: an updated database containing structural information of experimentally determined amyloid-forming peptides. *Nucleic Acids Research*, *48*(D1), D389–D393. Available from: https://doi.org/10.1093/nar/gkz758

Mazmanian, S.K., Ton-That, H. & Schneewind, O. (2001) Sortase-catalysed anchoring of surface proteins to the cell wall of *Staphylococcus aureus*. *Molecular Microbiology*, *40*(5), 1049–1057. Available from: https://doi.org/10.1046/j.1365-2958.2001.02411.x

Michels, R., Last, K., Becker, S.L. & Papan, C. (2021) Update on coagulase-negative staphylococci-what the clinician should know. *Microorganisms*, *9*(4), 1–13. Available from: https://doi.org/10.3390/microorganisms9040830

Monk, I.R. & Stinear, T.P. (2021) From cloning to mutant in 5 days: rapid allelic exchange in *Staphylococcus aureus*. *Access Microbiology*, *3*(2), 1–7. Available from: https://doi.org/10.1099/acmi.0.000193

Monk, I.R., Shah, I.M., Xu, M., Tan, M.-W. & Foster, T.J. (2012) Transforming the untransformable: application of direct transformation to manipulate genetically *Staphylococcus aureus* and *Staphylococcus epidermidis*. *mBio*, *3*(2), e00277-11. Available from: https://doi.org/10.1128/mBio.00277-11

Otto, M. (2008) Staphylococcal biofilms. *Current Topics in Microbiology and Immunology*, *322*, 207–228.

Planchon, S., Gaillard-Martinie, B., Dordet-Frisoni, E., Bellon-Fontaine, M.N., Leroy, S., Labadie, J. et al. (2006) Formation of biofilm by *Staphylococcus xylosus*. *International Journal of Food Microbiology*, *109*(1-2), 88–96. Available from: https://doi.org/10.1016/j.ijfoodmicro.2006.01.016

Rahmdel, S. & Götz, F. (2021) The multitasking surface protein of *Staphylococcus epidermidis*: accumulation-associated protein (Aap). *mBio*, *12*, e0198921. Available from: https://doi.org/10.1128/mBio.01989-21

Roche, F.M., Massey, R., Peacock, S.J., Day, N.P.J., Visai, L., Speziale, P. et al. (2003) Characterization of novel LPXTG-containing proteins of *Staphylococcus aureus* identified from genome sequences. *Microbiology*, *149*(Pt 3), 643–654. Available from: https://doi.org/10.1099/mic.0.25996-0

Rohde, H., Burdelski, C., Bartscht, K., Hussain, M., Buck, F., Horstkotte, M.A. et al. (2005) Induction of *Staphylococcus epidermidis* biofilm formation via proteolytic processing of the accumulation-associated protein by staphylococcal and host proteases. *Molecular Microbiology*, *55*(6), 1883–1895. Available from: https://doi.org/10.1111/j.1365-2958.2005.04515.x

Rohde, H., Burandt, E.C., Siemssen, N., Frommelt, L., Burdelski, C., Wurster, S. et al. (2007) Polysaccharide intercellular adhesin or protein factors in biofilm accumulation of *Staphylococcus epidermidis* and *Staphylococcus aureus* isolated from prosthetic hip and knee joint infections. *Biomaterials*, *28*(9), 1711–1720. Available from: https://doi.org/10.1016/j.biomaterials.2006.11.046

Schiffer, C., Hilgarth, M., Ehrmann, M. & Vogel, R.F. (2019) Bap and cell surface hydrophobicity are important factors in *Staphylococcus xylosus* biofilm formation. *Frontiers in Microbiology*, *10*, 1387. Available from: https://doi.org/10.3389/fmicb.2019.01387

Schiffer, C.J., Abele, M., Ehrmann, M.A. & Vogel, R.F. (2021) Bap-Independent biofilm formation in *Staphylococcus xylosus*. *Microorganisms*, *9*(12), 2610. Available from: https://doi.org/10.3390/microorganisms9122610

Schilcher, K. & Horswill, A.R. (2020) Staphylococcal biofilm development: structure, regulation, and treatment strategies. *Microbiology and Molecular Biology Reviews*, *84*(3), 1–36. Available from: https://doi.org/10.1128/MMBR.00026-19

Schleifer, K.H. & Kloos, W.E. (1975) Isolation and characterization of staphylococci from human skin I. Amended descriptions of *Staphylococcus epidermidis* and *Staphylococcus saprophyticus* and descriptions of three new species: *Staphylococcus cohnii*, *Staphylococcus haemolyticus*, and *Staphylococcus xylosus*. *International Journal of Systematic Bacteriology*, *25*(1), 50–61. Available from: https://doi.org/10.1099/00207713-25-1-50

Schroeder, K., Jularic, M., Horsburgh, S.M., Hirschhausen, N., Neumann, C., Bertling, A. et al. (2009) Molecular characterization of a novel *Staphylococcus aureus* surface protein (SasC) involved in cell aggregation and biofilm accumulation. *PloS One*, *4*(10), e7567. Available from: https://doi.org/10.1371/journal.pone.0007567

Schuster, C.F., Howard, S.A. & Gründling, A. (2019) Use of the counter selectable marker PheS* for genome engineering in *Staphylococcus aureus*. *Microbiology*, *165*(5), 572–584. Available from: https://doi.org/10.1099/mic.0.000791

Speziale, P., Pietrocola, G., Foster, T.J. & Geoghegan, J.A. (2014) Protein-based biofilm matrices in Staphylococci. *Frontiers in Cellular and Infection Microbiology*, *4*, 171. Available from: https://doi.org/10.3389/fcimb.2014.00171

Supré, K., Haesebrouck, F., Zadoks, R.N., Vaneechoutte, M., Piepers, S. & de Vliegher, S. (2011) Some coagulase-negative Staphylococcus species affect udder health more than others. *Journal of Dairy Science*, *94*(5), 2329–2340. Available from: https://doi.org/10.3168/jds.2010-3741

Taglialegna, A., Lasa, I. & Valle, J. (2016a) Amyloid structures as biofilm matrix scaffolds. *Journal of Bacteriology*, *198*(19), 2579–2588. Available from: https://doi.org/10.1128/JB.00122-16

Taglialegna, A., Navarro, S., Ventura, S., Garnett, J.A., Matthews, S., Penades, J.R. et al. (2016b) Staphylococcal Bap proteins build amyloid scaffold biofilm matrices in response to environmental signals. *PLOS Pathogens*, *12*(6), e1005711. Available from: https://doi.org/10.1371/journal.ppat.1005711

Tormo, M.A., Knecht, E., Götz, F., Lasa, I. & Penades, J.R. (2005) Bap-dependent biofilm formation by pathogenic species of

Staphylococcus: evidence of horizontal gene transfer? *Microbiology (Reading, England)*, *151*(7), 2465–2475. Available from: https://doi.org/10.1099/mic.0.27865-0

Valle, J., Latasa, C., Gil, C., Toledo-Arana, A., Solano, C., Penadés, J.R. et al. (2012) Bap, a biofilm matrix protein of *Staphylococcus aureus* prevents cellular internalization through binding to GP96 host receptor. *PLOS Pathogens*, *8*(8), e1002843. Available from: https://doi.org/10.1371/journal.ppat.1002843

Yarawsky, A.E., Johns, S.L., Schuck, P. & Herr, A.B. (2020) The biofilm adhesion protein Aap from *Staphylococcus epidermidis* forms zinc-dependent amyloid fibers. *Journal of Biological Chemistry*, *295*(14), 4411–4427. Available from: https://doi.org/10.1074/jbc.RA119.010874

Yonemoto, K., Chiba, A., Sugimoto, S., Sato, C., Saito, M., Kinjo, Y. et al. (2019) Redundant and distinct roles of secreted protein eap and cell wall-anchored protein SasG in biofilm formation and pathogenicity of *Staphylococcus aureus*. *Infection and Immunity*, *87*(4), 1–15. Available from: https://doi.org/10.1128/IAI.00894-18

SUPPORTING INFORMATION

Additional supporting information may be found in the online version of the article at the publisher's website.

How to cite this article: Schiffer, C. J., Schaudinn, C., Ehrmann, M. A., & Vogel, R. F. (2022). SxsA, a novel surface protein mediating cell aggregation and adhesive biofilm formation of *Staphylococcus xylosus*. *Molecular Microbiology*, 00, 1–16. https://doi.org/10.1111/mmi.14884

4.4 Characterization of the *Staphylococcus xylosus* methylome reveals a new variant of Type I restriction modification system

Preface: The following publication seems to take a slight detour into the world of epigenetics and horizontal gene transfer. Still, these issues can be of high importance also from an ecological point of view as biofilms are usually heterogenous, multispecies communities in which gene transfer frequently occurs, particularly in the outer layers (Stalder and Top, 2016). Many bacteria try to control the uptake of exogenous DNA material to a useful minimum. This, in turn, can pose a problem to researchers, particularly if they want to modify a strain to analyze specific gene functions.

Restriction modification systems have been named as one of the major factors preventing horizontal gene transfer and impeding genetic manipulation in *S. aureus*. Monk *et al.*, (2015) has therefore developed a method to circumvent restriction modification systems of *S. aureus* by expressing the respective methyltransferases in *E. coli* and passaging vector plasmids through such modified *E. coli* strains before transforming them into *S. aureus*. The method is generally known as Plasmid Artificial Modification (PAM). We were among the first ones to genetically manipulate wildtype *S. xylosus* strains but achieved no transformants using the original protocol by Brückner, (1997) and only very low transformation efficiencies using the protocol by Monk and Stinear, (2021) despite additional variation of many different parameters. Consequently, we sought to try PAM as well. We therefore determined the methylome of eight different *S. xylosus* strains and expressed type I and type II restriction modification systems of *S. xylosus* TMW 2.1023 and TMW 2.1324 in *E. coli* DC10B. Unfortunately, transformation efficiencies could not be increased significantly by applying PAM in *S. xylosus*. Yet, during methylome and subsequent bioinformatic analyses, we were able to identify a new variant of type I restriction modification systems that has hitherto not been described in the literature. The main difference to previously known type I restriction systems (families A - E) is that the new variant requires two specificity units (*hsd*S) instead of one for proper and stable base modification. The new type I restriction modification system is described in detail in the corresponding publication and contributes substantially to the major understanding of the variety of DNA methylation systems in bacteria. This relates above all to the increasing interest in DNA modification patterns as they have been shown to be further involved in various epigenetic processes, such as phase variable gene expression of prokaryotic cells (Anton and Roberts, 2021).

Author contribution: Carolin Schiffer was responsible for the design of the study. She performed all experiments in the lab as well as bioinformatic analysis of the genes characterized within the study, including base modification and motif analysis for the *S. xylosus* strains. Carolin Schiffer further wrote the original draft of the manuscript, co-edited the final version and handled submission as corresponding author.

Note:

The manuscript has been submitted to the Journal of bacteriology on January 25th (Manuscript Number JB00040-22) and is currently under review (Status last checked: February 3rd 2022). The submitted manuscript is printed below.

Characterization of the *Staphylococcus xylosus* methylome reveals a new variant of Type I restriction modification system

Carolin J. Schiffer[1,2#], Rudi F. Vogel[1], Matthias A. Ehrmann[1,2]

[1]Technical University of Munich, TUM School of Life Sciences, Chair of Technical Microbiology, 85354 Freising, Germany

[2] present address: Technical University of Munich, TUM School of Life Sciences, Chair of Microbiology, 85354 Freising, Germany

#To whom correspondence should be addressed:

Tel: +49 8161 / 71 6100**;** carolin.schiffer@tum.de

Keywords: *Staphylococcus xylosus*, restriction modification systems, methylome

Abstract

Restriction modification (RM) systems are known for providing a strong barrier to the exchange of DNA between and within bacterial species. In the past years, staphylococcal research has identified and characterized RM systems focusing mainly on *Staphylococcus aureus* and *S. epidermidis*. We sequenced eight genomes of *S. xylosus* isolated from different environments using single-molecular, real-time (SMRT) sequencing, and subsequently analyzed their methylomes. Sequencing results were further complemented with *in silico* sequence analysis assigning the respective enzymes to the discovered modification patterns. The analysis revealed the presence of Type I, II and III restriction modification systems in *S. xylosus*. Hereby, a new variant of type I RM systems composed of two specificity subunits (*hsd*RSMS) was discovered. Different variants (*hsd*SMS/*hsd*MS/*hsd*MS_{tr}) were heterologously expressed in *E. coli*. Proper base modification was only obtained when both *hsd*S subunits were expressed in *E. coli* (*hsd*SMS), as the deletion of the short subunit (*hsd*MS) resulted in low scores and instable base modification. We propose to classify the newly discovered type I variant as a new family within type I RM systems.

Importance

Restriction modification systems are known to provide efficient barriers against exogenous DNA entering the cell and are furthermore involved in epigenetic regulation and phase-variable expression of prokaryotic phenotypes. Understanding the distribution, gene arrangement and function of RM systems are important foundations for the understanding of evolution and ecology of prokaryotes. In this study, we present a newly discovered Type I restriction modification system, with a hitherto unknown gene arrangement, requiring two specificity units instead of one. The system is distributed among several important species of the genus Staphylococcus and provides new insights into the variety of RM systems occurring in *Staphylococcus spp*.

1 Introduction

Staphylococcus xylosus is a Gram-positive commensal of mammalian skin with a high biotechnological value, as it is commonly used in food fermentations (1,2). However, over the past years, studies have associated *S. xylosus* with infections, i.e. bovine mastitis infections, as well (3,4). Being of an industrial and medical importance, the species represents an ideal model organism for different kind of studies addressing e.g. the competing potential of the organism during food fermentations, the role of commensal staphylococci in infections as well as the interface between strains nominated to achieve qualified presumption of safety status (QPS) because of their extensive and historic usage in food fermentations and others harboring virulence associated genes such as antibiotic resistance genes. To work on these scientific questions, microbiological studies need to be able to perform gene replacement studies on the organism, being able to work with wildtype strains as well, which are usually much harder to genetically modify than laboratory strains. Furthermore, it is important to understand the chances and extent of natural horizontal gene transfer (HGT) occurring especially when considering that spread of virulence and acquisition of antibiotic resistance genes are emerging topics nowadays (5–7). One way, bacteria protect themselves from the uptake of exogenous, foreign DNA is by restriction modification (RM) systems. Active RM systems have been shown to be one of the major factors preventing inter- and intraspecies HGT (8–10). The basic principle of distinguishing between foreign and own DNA is the site-specific modification of the individual DNA by methyltransferases combined with the expression of effective restriction endonucleases that recognize and cleave any unmodified foreign DNA (11,12). Four major types of bacterial restriction (modification) systems (Type I - IV) have been described to date. They are distinguished based on their enzymatic subunits, mechanism of action, DNA specificity / sequence recognition motifs as well as co-factor requirements and reaction conditions (12–15). Type I systems are heterooligomeric complexes composed of three subunits, a methyltransferase (*hsd*M), modifying the host DNA by adding a methyl group to a defined base, a restriction endonuclease cleaving non-modified DNA (*hsd*R) and a specificity unit (*hsd*S) determining the recognition sequence of the system (15–17).

Hereby, *hsd*M and *hsd*S are usually transcribed from a common promoter, while *hsd*R is under the control of its own promoter (17). Currently, type I RM systems are subdivided into five families (IA – IE) based on sequence homologies and genetic complementation (18,19). While *hsd*M and *hsd*R are very conserved within one family, with sequence similarity values reported between 70 up to 90%, *hsd*S consist of two highly variable regions (19–21,17). These variable regions encode the target recognition domains (TRDs) of HsdS, each of them specifying one half of the bipartite target recognition motif (TRM) (15,17,22). The TRM comprises two specific 3 to 4 bp long sequences, separated by a 5 to 8 bp long non-specific spacer sequence, consisting of random nucleotides (22,9,15). Since individual TRDs can shuffle and rearrange between different *hsd*S subunits, an extensive variety of different target recognition motifs exists (23,19,15). Furthermore, halfsize HsdS subunits, encompassing only one TRD, have been reported to be functional as well, as they can still dimerize and form a stable complex with HsdM and HsdR. Typical for such halfsize HsdS' is their palindromic, symmetric recognition sequence (24–26). In contrast to the polycistronic organisation of type I systems, type II systems include two independent enzymes, a site-specific methyltransferase and a restriction endonuclease that cleaves DNA either precisely within the recognition sequence or at a defined position nearby. Recognition motifs of type II systems are usually 4 - 8 bp in length and palindromic (27). Type III systems are heterooligomeric complexes consisting of a methyltransferase that also determines sequence specificity (*mod*) and an endonuclease (*res*), again responsible for restriction of unmodified DNA (28). Type III systems usually recognize short (5 - 6 bp), asymmetric motifs and have been reported to occur only rarely in staphylococci such as *S. aureus* (29,11). Type IV systems are only composed of one to two endonucleases and distinguish themselves from type I to III systems as they are not associated with a respective methyltransferase. Hereby, Type IV restriction enzymes solely digest modified motifs (30).

For more detailed information on the functionality of the different types of RM systems, including required co- factors and complex assembly, extensive overviews are provided in the respective reviews (17,15,27,28,30). Moreover, RM systems also address other functions of

DNA methylation, which include epigenetic mechanisms such as controlling replication and the expression of phenotypes such as biofilm formation and host colonization as well as regulating phase variable expression of genes and thereby enabling cells to flexibly change between different physiological states (14,9,23).

In this study we established the methylome, thus all methyl-modified DNA sequences in eight *S. xylosus* strains using single molecule real-time (SMRT) sequencing in order to obtain more information on the presence of RM among the species *S. xylosus.*

2 Materials and Methods

Bacterial strains, growth conditions, reagents

All bacterial strains, oligonucleotides and plasmids used in this study are listed in Table 1. *Escherichia coli* and *Staphylococcus sp*. were routinely cultured at 37 °C, 200 rpm in Lysogeny Broth (LB, 10 tryptone 10 g/l, yeast extract 5 g/l, NaCl 5 g/l) and Trypticase soy broth (TSB, casein peptone 15 g/L, soy peptone 15 g/L, yeast extract 3 g/L), respectively, unless required otherwise. For the respective agar plates, liquid media were solidified with 1.5% agar. Antibiotics were purchased from Carl Roth and used at the following concentrations: chloramphenicol (10 µg/ml), ampicillin (100 µg/ml), kanamycin (20 µg/ml). Oligonucleotides were obtained from Eurofins Genomics, Germany. Restriction enzymes, Gibson assembly mix, T4 DNA ligase as well as PCR components (Q5 high fidelity PCR kit) were obtained from New England Biolabs (NEB). For plasmid isolation, DNA gel extractions and PCR product purification, the NEB Monarch Plasmid Miniprep, DNA gel extraction and PCR & DNA Cleanup kits were used, respectively.

Table 1: bacterial strains, plasmids and oligonucleotides used within this study. Underlined are overhangs for restriction sites. NCBI accession numbers are provided for whole genome sequenced strains.

Primer	Sequence (5'-3')	Source
vec_pBla_1F	GGATCGGAATTCGAGCTCGGTACTCTACATCTAAACTAAATACTATTGAG	this study
Bla_Mtase_1R	TTCACAATATTCCACCTCATACTCTTCCTTTTTCAATATTATTG	this study
Bla_Mtase_2F	AATATTGAAAAAGGAAGAGTATGAGGTGGAATATTGTG	this study
Mtase_186_2R	CATGCATCTCGAGGCATGCCTGCATTAATAGTTAGTTATTAGTACTTCATG	this study
Pn25_F	CATAAAAAATTTATTTGCTTTCAGGAAAATTTTTCTGTATAATAGATTCATAAATTTGAGAGAGGAGTT	this study
Pn25_R	AACTCCTCTCTCAAATTTATGAATCTATTATACAGAAAAATTTTCCTGAAAGCAAATAAATTTTTTG	this study
SacI_PN25_F	CGAGCTCGCATAAAAAATTTATTTGC	this study
PN25_MT_F	CATAAATTTGAGAGAGGAGTTATGAGGTGGAATATTGTG	this study
RS_MT_R	CCAATGCATTGGTTCTGCAGTTTTAATAGTTAGTTATTAGTACTTCATG	this study
RS_PN25_F	GGGGTACCCCCATAAAAAATTTATTTGC	this study
PN25_hsdSMS_F	GTATAATAGATTCATAAATTTGAGAGAGGAGTTATGTTAAAAGATTATGTTAATTATC	this study
PN25_hsdMS_F	GTATAATAGATTCATAAATTTGAGAGAGGAGTTATGTCTATTACGGAAAAACAAC	this study
RS_hsdS_R	GATCAGCATGCCTACACAAACATCTTCTG	this study
RS_hsdS_tr_R	GATCAGCATGCTTATGCCATTGACTGG	this study
186_1_P1	CTCATTCGAAACCACCCACCG	(33)
186_1_P2	ACTTAACGGCTGACATGG	(33)
186_1_P3	ACGAGTATCGAGATGGCA	(33)
186_1_P4	GATCATCATGTTTATTGCGTGG	(33)
186_2_P1	TCCGGAATGCCTGCATTG	(33)
186_2_P2	ACTTAACGGCTGACATGG	(33)
186_2_P3	ACGAGTATCGAGATGGCA	(33)
186_2_P4	CCCTGGAGCCAAAATATCC	(33)
Lambda_P1	GGCATCACGGCAATATAC	(33)
Lambda_P2	ACTTAACGGCTGACATGG	(33)
Lambda_P3	GGGAATTAATTCTTGAAGACG	(33)
Lambda_P4	TCTGGTCTGGTAGCAATG	(33)

strains	Description	Source, Accession
DC10B	*E. coli* DH10B (K12 derivate), Δ*dcm*	(47)
CM56	*E. coli* DC10B with 2.1023 hsdSMS integrated at 186-2 (Promotor: P_{N25})	this study
CM13	*E. coli* DC10B with 2.1324 hsdSMS integrated at 186-1 and 2.1324 MT integrated at λ (Promotor: P_{N25})	this study
CM57	*E. coli* DC10B with 2.1023 hsdMS integrated at 186-2 (Promotor: P_{N25})	this study
CM19	*E. coli* DC10B with 2.1324 hsdMS integrated at 186-1 and 2.1324 MT integrated at λ (Promotor: P_{N25})	this study
CM5	*E. coli* DC10B with 2.1324 hsdSMS integrated at 186-1 (Promotor: P_{N25})	this study
CM30	*E. coli* DC10B with 2.1324 hsdM*S_tr* integrated at 186-2, 2.1324 MT integrated at λ (Promotor: P_{N25})	this study
CM93	*E. coli* DC10B with 2.1324 MT integrated at λ (Promotor: P_{N25})	this study
CM2	*E. coli* DC10B with 2.1324 MT integrated at 186-1 (Promotor: P_{bla})	this study
DC3.1	*E. coli* resistant to ccdB	(33)
E811	*E. coli* (P2 lysogen) in which the strong promotor pE is repressed	(33)
Newman	*S. aureus*, ST8, CC8, commonly used laboratory strain	Newman AP009351
TMW 2.1023	*S. xylosus* isolated from raw fermented sausages	this study, JAEMUG000000000
TMW 2.1324	*S. xylosus* isolated from raw fermented sausages	this study, CP066726-CP066729
TMW 2.1521	*S. xylosus* isolated from raw fermented sausages	this study, JAEMUF000000000
TMW 2.1523	*S. xylosus* isolated from raw fermented sausages	this study, CP066721-CP066725
TMW 2.1602	*S. xylosus* isolated from raw fermented sausages	this study, CP066719-CP066720
TMW 2.1693	*S. xylosus* isolated from bovine mastitis	this study, JAJAGM000000000
TMW 2.1704	*S. xylosus* isolated from bovine mastitis	this study, JAJAGL000000000
TMW 2.1780	*S. xylosus* isolated from raw fermented sausages	this study, JAJAGN000000000

plasmids	Description	Reference
pIMAY*	temperature-sensitive, low copy plasmid, designed for allelic exchange in staphylococci, CM^R	(46)
pE-FLP	plasmid expressing a flippase gene from the constitutive promotor pE from phage P2, AMP^R	(33)
pOSIP-KO	plasmid expressing 186-integrase, KAN^R	(33)
pOSIP-KL	plasmid expressing Lambda-integrase, KAN^R	(33)

Transformation protocols

Transformation of *E. coli* strains was performed by washing *E. coli* cells electrocompetent using standard protocols. Basically, 100 ml of cells was harvested during mid-exponential phase (OD_{600} 0.5 - 0.7), placed on ice for 10 minutes and centrifuged at 5000 x g, 4 °C for 10 minutes. The supernatant was poured off and the pellet was resuspended in 100 ml 10% glycerol. Centrifugation and resuspension steps were repeated twice more with decelerating volumes of resuspension buffer and cells were finally resuspended in approximately 500 µl of 10% glycerol. Transformation of *E. coli* cells by electroporation was performed in a 0.1 cm cuvette at 1.8 kV. For transformation of *S. aureus* and *S. xylosus* we followed the protocol described by Schiffer *et al.* (31) and Monk and Stinear (32). All staphylococcal cells were electroporated in a 0.2 cm cuvette at 2.5 kV, using 50 µl of competent cells and 1.5 µg of plasmid DNA.

Expression of Type I and Type II modification enzymes in *E. coli*

To mimic and determine the methylation profile of *S. xylosus*, the respective methyltransferases were heterologously expressed in *E. coli*. Therefore, the respective genes were integrated into *E. coli* strain DC10B at site-specific locations of the chromosome, in a single cloning and chromosomal integration step (33). The expression of modification genes from the chromosome rather than multicopy plasmid, should result in less metabolic burden for the cell, a stable expression and subsequent complete modification. The applied method is based on bacteriophage integrases mediating site-specific insertions of the genes of interest into prokaryotic chromosomes (*att*B sites). Within this study, the integrases of coliphages λ (pOSIP-KL) and 186 (pOSIP-KO) were used. The type II methyltransferase of *S. xylosus* TMW 2.1324 was amplified using primers PN25_MT_F and RS_MT_R at first, followed by a subsequent PCR reaction complemented with the dimerized oligosaccharides of promoter P_{N25} and primers PN25_MT_F and RS_MT_R. The promoter-gene construct was excised from an agarose gel, purified and ligated into the linearized (SacI/PstI) vector pOSIP-KL. The different variants of type I systems of TMW 2.1023 and TMW 2.1324 (*hsd*SMS/*hsd*MS/*hsd*MS_{tr}) were ligated into vector pOSIP-KO (KpnI/SphI) the same way, using primer pairs PN25_*hsd*SMS_F

/ PN25_*hsd*MS_F and RS_*hsd*S_R / RS_*hsd*S_tr_R at first, followed by overamplification with RS_PN25_F and RS_*hsd*S_R / RS_*hsd*S_tr_R, respectively. Integration of the pBla-MTase construct was performed by amplifying the promoter from plasmid pE-Flp using primers vec_pBla_1F and Bla_Mtase_1R and the methyltransferase of TMW 2.1324 using Bla_Mtase_2F and Mtase_186_2R with subsequent Gibson assembly of all PCR products into the linearized vector pOSIP-KO (KpnI/PstI).

Assembled vectors were transformed into *E. coli* by electroporation, and FLP-mediated excision of the backbone was achieved by transforming cells with plasmid pE-FLP. Integration, screening for successful transformants, excision and final screening for successful integrants were performed according to the step-by-step protocol provided by Cui and Shearwin (34).

SMRT sequencing

Single molecule real-time (SMRT) sequencing was performed to identify modified bases of *S. xylosus* and genetically modified *E. coli* strains. DNA isolation was performed using the E.Z.N.A Bacterial DNA-kit (Omega bio-tek) according to the manufacture's instruction, yet lysostaphin (0.5mg/ml) was included into the lysis buffer to weaken the cell wall. Library construction and sequencing (PacBio RS II) of *S. xylosus* followed the protocol described by Schiffer *et al*. (35). *E. coli* sequencing was performed on a PacBio Sequel instrument (SMRT cell 1M), partly at the functional genomics center Zurich (ETH Zürich), partly at the research unit for environmental genomics Munich (Helmholtz Zentrum München). Therefore, the Sequel® Binding Kit 3.0 (Pacific Biosciences) was used and libraries were size selected to around 6 to 7 kb. SMRT Analysis version 7.0 (Pacific Biosciences) was used for assembly (HGAP4), base modification and motif analysis of *S. xylosus*, SMRT Link version 10.1 for assembly, base modification and motif analysis of *E. coli*. For *S. xylosus* the assembled genomes were used as their own reference, for *E. coli*, the assembly of strain DH10B available on NCBI (NC_010473) was used as a reference.

Bioinformatic analysis and data availability

Sequence alignments were made using CLC main workbench 8.1.4 (https://digitalinsights.qiagen.com/) with the built-in Clustal Omega plugin and subsequent construction of pairwise comparison matrices and phylogenetic trees (neighbor-joining). Blasting against two databases (NCBI's conserved domain database (36) as well as the restriction enzyme database REBASE (37)) were used to confirm the affiliation of the identified enzymes to one of the restriction modification families, to identify enzymatic domains and to determine RM systems with the same DNA target sequence. The Blast Diagnostic Gene finder tool (BADGE) was used for comparative genomics in order to match the corresponding RM genes and modification patterns (38). The online available NCBI blastn and blastp tool was used to search for RM components besides the ones already annotated. The protein fold recognition server PHYRE^2 (39) helped in predicting secondary structure conformation of the identified polypeptides. The CRISPRCasFinder online tool was used to screen the genomes for the respective CRISPR and cas genes (40). Identified spacer sequences were blasted (blastn) against the pIMAY* vector sequence manually. In a previous study, a full proteome dataset was generated for *S. xylosus* TMW 2.1023 and TMW 2.1523 (31), which was taken into account in this study to verify the expression of single genes. The dataset is available under the identifier PXD029728 at the ProteomeXchange Consortium via the PRIDE partner repository (41). All *S. xylosus* genome sequences have been deposited at GenBank under the accession numbers provided in Table 1. The assemblies of the whole genome sequenced *E. coli* strains (CMx strains) are supplied in fasta format as supplementary files.

3 Results

Analyzing the Methylome of *S. xylosus*

We determined the DNA methylation profile of eight different *S. xylosus* strains using PacBio SMRT sequencing technology (42) and further explored the occurrence of restriction modification systems by detailed bioinformatic analysis of the genomes. Hereby, we were able to assign the respective modification and restriction enzymes to the identified methylated DNA

sequences with a high degree of certainty as mostly not more than one respective open reading frame was available for choice. Table 2 provides an overview of identified RM systems and the assigned modification patterns. Table S1 displays the full base modification output of the sequenced TMW strains. Seven other strains of *S. xylosus* listed on Rebase (37) were included into the overview to provide a better overview of the prevalence of RM systems within the species. Out of the 15 strains analyzed, seven carry a complete type I restriction modification system in their genome (presence of *hsd*M, *hsd*S and *hsd*R). None of the *S. xylosus* strains harbors more than one type I RM system, nor any orphan *hsd*S genes. All type I systems are organized as a contiguous three (*hsd*MSR) or four (*hsd*RSMS) gene operon. Despite base modifications typical for type I systems, very common type II motifs were also identified such as GCATC in TMW 2.1324, a motif with more than 600 hits on Rebase, present across a wide range of species such as *Mycoplasma bovis, Mannheimia haemolytica* and *Streptococcus pneuomoniae.* Interestingly, three strains (TMW 2.1521, 2.1523 and 2.1780) possess a type IIG system, which comprises a single enzyme, mediating methyltransferase as well as endonuclease activity. The detected type IIG systems are all associated with the same modification pattern (GGGTNA) and sequence analysis did not reveal any frameshifts in the sequences. Furthermore, data derived from whole proteome analysis (31) confirmed the expression of a functional type IIG system in TMW 2.1523 (Table S2). Blasting of methyltransferase genes against the Rebase database also revealed the presence of type III systems in the strains TMW 2.1693 (LHJ66_13490-95) and DMSX03 (DMSX03_RS00135-40). The only strain, for which no respective methyltransferase could be assigned to the determined modification pattern is TMW 2.1602. According to its kinetic signature during sequencing, the strain modifies the motif CACCG, which could be a type II or type III motif. Nevertheless, using comparative genomics no strain specific methyltransferases or endonucleases were identifiable for this strain. The motif is not listed on Rebase either, therefore no further conclusions about which kind of modification system this strain possesses can be made at the time.

Table 2: overview of restriction modification systems (type I to III) in selected *S. xylosus* strains as well as the corresponding base modification motifs derived from SMRT sequencing whenever motifs could be assigned to the respective modification genes. Also indicated are strain number, NCBI locustag, location on chromosome (chrm) or plasmid (pL), NCBI-based annotation, length of the gene (nt) and RM system class (I-III). Bases in bold correspond to the methylation sites if known.

S. xylosus	Locustag	location	annotation	length (nt)	class	assigned motif
TMW 2.1023	JGY91_01640	chrm	type I restriction modification subunit M	198_*trunc.*	I	none
	JGY91_13160	Pl	type I restriction endonuclease subunit S	1170	I	
	JGY91_13165	Pl	type I restriction modification system subunit M	1557	I	TC**A**N_6CTC/ G**A**GN_6TGA
	JGY91_13170	Pl	type I restriction endonuclease subunit S	576	I	
	JGY91_13175	Pl	type I restriction endonuclease subunit R	2787	I	
TMW 2.1324	JGY90_00145	chrm	AlwI family type II restriction endonuclease	2121	II	GC**A**TC/G**A**TGC
	JGY90_00150	chrm	DNA-(adenine-N6)-methyltransferase	2127	II	
	JGY90_14115	Pl	type I restriction endonuclease subunit S	1185	I	
	JGY90_14120	Pl	type I restriction modification subunit M	1557	I	**A**CCN$_5$RTGT/ AC**A**YN$_5$GGT
	JGY90_14125	Pl	type I restriction endonuclease subunit S	576	I	
	JGY90_14130	Pl	type I restriction endonuclease subunit R	2787	I	
TMW 2.1521	JGY89_12325	chrm	DEAD/DEAH box helicase	4737	II G	GGGTN**A**
	JGY89_12080	chrm	type I restriction modification subunit M	198_*trunc.*	I	
TMW 2.1523	JGY88_00145	chrm	DEAD/DEAH box helicase	4728	II G	GGGTN**A**
TMW 2.1602	none found					CAC**C**G
TMW 2.1693	LHJ66_02060	chrm	type I restriction modification subunit M	1515	I	
	LHJ66_02065	chrm	type I restriction endonuclease subunit S	1215	I	G**A**CN$_5$TGT/ AC**A**N$_5$GTC
	LHJ66_02070	chrm	type I restriction endonuclease subunit R	3123	I	
	LHJ66_02820	chrm	DNA cytosine methyltransferase	1287	II	
	LHJ66_13490	Pl?	site-specific DNA methyltransferase	2001	III	GCTC**A**
	LHJ66_13495	Pl?	DEAD/DEAH box helicase family protein	2700	III	
TMW 2.1704	LHJ68_05155	chrm	DNA cytosine methyltransferase	1047	II	
	LHJ68_05160	chrm	DNA cytosine methyltransferase	1080	II	
	LHJ68_05170	chrm	DNA cytosine methyltransferase	1188	II	
TMW 2.1780	LHJ67_11845	chrm	DEAD_DEAH box helicase family protein	4737	II G	GGGTN**A**
2	DWB98_00235	chrm	type I restriction modification subunit M	1464	I	
	DWB98_00240	chrm	type I restriction endonuclease subunit S	1164	I	
	DWB98_00245	chrm	type I restriction endonuclease subunit R	3354	I	
DMSX03	DMSX03_RS00135	chrm	site-specific DNA-methyltransferase	1923	III	
	DMSX03_RS00140	chrm	restriction endonuclease	2967	III	
HKUOPL8	BE24_RS11845	chrm	type I restriction modification subunit M	1515	I	
	BE24_RS11850	chrm	type I restriction endonuclease subunit S	1251	I	
	BE24_RS11855	chrm	type I restriction endonuclease subunit R	3123	I	
	BE24_RS11615	chrm	cytosine methyltransferase	1080	II	CCCGT
	BE24_RS11620	chrm	DNA methyltransferase	1047	II	CCCGT
	BE24_RS13495	chrm	AAA family ATPase	1473	II	
	BE24_RS11635	chrm	LlaJI family restriction endonuclease	1122	II	
	BE24_RS05200	chrm	DNA methyltransferase (C5)	957	II	
S04010	sxy10ORFAMP	chrm	DNA-cytosine methyltransferase	1077	II	CCCGT
	sxy10ORFAMP	chrm	DNA-cytosine methyltransferase	1044	II	CCCGT
S170	AWC37_RS12155	chrm	type I restriction modification subunit M	1515	I	
	AWC37_RS12160	chrm	type I restriction endonuclease subunit S	1263	I	
	AWC37_RS12165	chrm	type I restriction endonuclease subunit R	3123	I	
SMQ-121	SXYLSMQ121_RS00165	chrm	type I restriction modification subunit M	1515	I	
	SXYLSMQ121_RS00160	chrm	type I restriction endonuclease subunit S	1266	I	C**A**CN$_4$RTTG/ GTGNNNNY**A**AC
	SXYLSMQ121_RS00155	chrm	type I restriction endonuclease subunit R	3123	I	
C2a	SXYL_RS00155	chrm	restriction endonuclease subunit R	423	I	

Whole genome sequencing analysis additionally revealed, that some *S. xylosus* strains encode cytosine methyltransferases, probably mediating 5-methylcytosine (m5C) modification, yet

checking whether these enzymes are active or which motifs they modify is difficult since it is challenging to use SMRT sequencing technology to distinguish m5C from cytosine (42,15). Of note is, that type IV systems were spared within the scope of this work as focus was laid on methyltransferases and modification patterns not endonucleases.

In silico **analysis of type I RM systems reveals a new family**

Type I restriction modification systems were identified in seven out of the 15 analyzed *S. xylosus* strains, making their presence within the species non-ubiquitous. While a common gene order of the *hsd* operon (*hsd*RSM/*hsd*MSR) was identified in the strains TMW 2.1693, 2, HKUOPL8, S170 and SMQ-121, an unusual gene arrangement (*hsd*RSMS) was found for TMW 2.1023 and TMW 2.1324, with two genes of different lengths, both annotated as *hsd*S surrounding the methyltransferase (*hsd*M). To confirm that none of the *hsd*S subunits is truncated, the proteomic dataset obtained from a previous study was consulted again, confirming the expression of both *hsd*S subunits in TMW 2.1023 (Table S2). The first *hsd*S (*hsd*S_short) subunit of the system is 191 aa in length and the second one (*hsd*S_long) around 390 - 400 aa. Furthermore, the 3' end of *hsd*M overlaps by 8 bp the 5' end of the second *hsd*S_long subunit. Because of the organization of the ORFs directly to one another (*hsd*S-*hsd*M-*hsd*S), with the *hsd*M-*hsd*S 8 bp overlap and a conserved Shine-Dalgarno binding site preceding each ORF, it can be assumed that genes are co-transcribed under the control of a single promoter in both *S. xylosus* strains. We also note that putative promoter sequences (canonical consensus σ70 -35/-10) are present in front of *hsd*R and *hsd*S_short. Polycistronic gene organization facilitates enhanced regulatory control through translational coupling between genes of related functional partners to control subunit stoichiometry and was previously described for type I restriction systems (43,44). Interestingly, *Hsd*RSMS systems are part of a large plasmid in both *S. xylosus* strains. Blasting the individual genes of the operon reveals that the system is located on at least eleven further staphylococcal plasmids (*hsd*RSMS$_{PL}$) as well as it was found that some staphylococcal species also carry the system on their chromosome (*hsd*RSMS$_{CHRM}$). Yet, it appears as if *hsd*RSMS$_{CHRM}$ is mostly encoded on mobile genetic elements (MGEs) on the chromosome, often being part of staphylococcal

cassette chromosome (SCC) genomic islands as well as recombinases are frequently encoded just a few genes up-or downstream from the operon. Table 3 lists all plasmid encoding *hsd*RSMS operons as well as a selection of strains that carry the operon on their chromosome.

Table 3: overview of organisms harboring the *hsd*RSMS systeme either on a plasmid (pL) or on the chromosome (chrm). Note: in *S. pseudoxylosus* 14AME *hsd*S_long is truncated and the *hsd*RSMS systems of *S. aureus* UP966 is truncated by a transposon. Genes indicating a localization on a mobile genetic element (MGE), identified in the surrounding of the operon, are listed when found.

Organism	Strain	pL/chrm	Located on MGE	Accession (Genbank)
Staphylococcus xylosus	TMW 2.1023	pL1	-	JAEMUG010000002
Staphylococcus xylosus	TMW 2.1324	pL1	-	CP066727.1
Staphylococcus aureus	SA01	pSA01-tet	-	CP053076.1
Staphylococcus aureus	55-100-016	pL1	-	CP076840.1
Staphylococcus aureus	UP_966	pL1	-	CP047831.1
Staphylococcus aureus	HUV05	pHUV05-03	-	CP007679.1
Staphylococcus equorum	C2014	pC2014-2	-	CP013716.1
Staphylococcus hominis	FDAARGOS_762	pL3	-	CP054008.1
Staphylococcus nepalensis	JS1	pSNJS101	-	CP017461.1
Staphylococcus pseudoxylosus	14AME19	p14AME19-2	-	CP068714.1
Staphylococcus saprophyticus	UTI-045	pUTI-045-1	-	CP054832.1
Staphylococcus aureus	45394F	chrm	SCC	GU122149.1
Staphylococcus aureus	ER02693.3	chrm	recombinase	CP030605.1
Staphylococcus caprae	SY333	chrm		CP051643.1
Staphylococcus carnosus	FDAARGOS_1147	chrm	recombinase	CP068079.1
Staphylococcus condimenti	FDAARGOS_1205	chrm	recombinase x 2	CP069567.1
Staphylococcus epidermidis	RP62A	chrm	yes (see Lee et al., (29))	CP000029.1
Staphylococcus epidermidis	FDAARGOS_161	chrm	transposase	CP014132.1
Staphylococcus equorum	FDAARGOS_1149	chrm	recombinase, transposase	CP068069.1
Staphylococcus hominis	TFGsh1	chrm	SCC	AB930126.1
Staphylococcus saprophyticus	UTI-042y	chrm	recombinase	CP054438.1
Staphylococcus schleiferi	OT1-1	chrm		CP035007.1
Mammaliicoccus fleurettii	FDAARGOS_682	chrm		CP046351.1

Alignments and gene topology analysis was performed to classify all discovered *S. xylosus* type I RM systems into one of the five existing type I families (A-E). Percent identity and distant values for alignments of *hsd*R and *hsd*M with the reference genes are provided in the comparison matrix of Figure S1. Hereby, *hsd*M and *hsd*R of *S. xylosus* chromosomal *hsd*MSR operons are closest to the reference genes of type ID RM systems (*Sty*SBLI) with 50% (*hsd*M) and 40% (*hsd*R) percent identity, respectively. An exception is *S. xylosus* strain 2, which cannot clearly be categorized as it carries a *hsd*MSR system with identity values below 30% to any of the reference genes. Methyltransferases and endonucleases of *hsd*RSMS systems display as little as 7% identity to family IB (M.*Eco*AI) and ID (M.*Sty*SBLI) and a maximum of 48% (*hsd*M) and 40% (*hsd*R) identity to the type IC reference genes (*Eco*R124I). Interestingly, intraspecies percent identity values of *hsd*M genes, namely *hsd*M of *hsd*RSMS operons and

*hsd*M of *hsd*MSR operons were all below 10%. When referring to the phylogenetic trees provided in Figure 1 (*hsd*M) and Figure S2 (*hsd*R), *hsd*R and *hsd*M of *hsd*RSMS cluster with none of the reference genes, neither do *hsd*R and *hsd*M of *S. xylosus* 2.

Figure 1: neighbor joining tree displaying the phylogenetic topology of *hsd*M from type I RM systems of different bacterial organisms and strains. The turquoise group represents *hsd*M genes of *hsd*RSMS$_{PL}$ systems, the green group belongs to *S. xylosus* chromosomal *hsd*MSR systems and the group in rose encompasses *hsd*M genes of *hsd*RSMS$_{CHRM}$ systems. The only outlier is *hsd*M of *S. equorum* FDAARGOS_1149 which is chromosomally encoded but clusters with the plasmid-based group. Reference genes of type I systems (A-E) were included into the Figure. The bar indicates 60% sequence divergence.

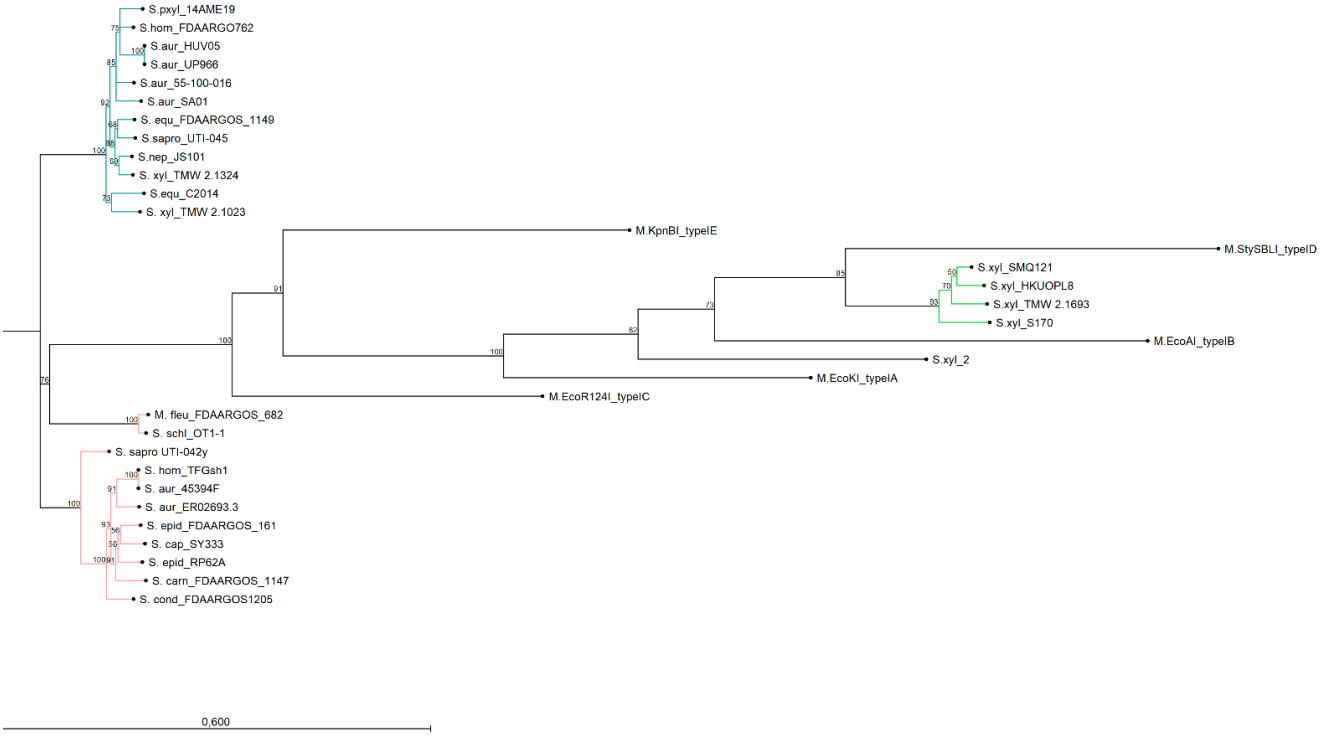

On the contrary, the phylogenetic distance of the other *S. xylosus* strains encoding a chromosomal *hsd*MSR system to type ID systems is smaller and they somehow group together. Interesting is that *hsd*M and *hsd*R of *hsd*RSMS$_{PL}$ systems also show a phylogenetic distance to *hsd*RSMS$_{CHRM}$ systems. The only exception is *S. equorum* FDAARGOS_1149, that carries a *hsd*RSMS$_{CHRM}$ system clustering together with the *hsd*RSMS$_{PL}$ systems. Alignments of each gene of *hsd*RSMS$_{PL}$ separately revealed that *hsd*M, *hsd*R and *hsd*S_short are well conserved along the entire sequence (Figure 2A). Alignments of *hsd*S_long resulted in a typical conservation plot often seen for *hsd*S subunits, with three conserved regions (N-, C -terminal, central) flanking two variable regions, each dedicated as one TRD (Figure 2B and C).

Figure 2: A. conservation plots based on amino acid alignments of HsdR, HsdM *and* HsdS_short derived from *hsd*RSMS$_{PL}$ systems (11 sequences each were aligned). **B***.* gene arrangement of type I RM systems occurring in *S. xylosus*: *hsd*RSMS$_{PL}$ and *hsd*MSR$_{CHR}$. *hsd*S_s = *hsd*S_short, *hsd*S_l = *hsd*S_long. *Hsd*S_long is composed of two variable regions (V1 and V2) as well as an N-terminal (N-CR), C-terminal (C-CR) and central conserved region (cCR). All conserved regions are marked in turquoise. Other repeating sequences are marked in red, blue and yellow respectively. Note the frameshift at the junction between coding regions: in *hsd*RSMS$_{PL}$**,** *hsd*M overlaps *hsd*S_long by 8 bp; in hsdMSR$_{CHR,}$ *hsd*M overlaps *hsd*S by 11 bp and *hsd*S overlaps *hsd*R by 17bp **C**. HsdS_long subunit alignment on amino acid level of all plasmid-derived *hsd*RSMS systems. Conservation plot shows the low conservation among the variable region as well as the repeating sections (blue, yellow, red) of the conserved (turquoise) regions. **D.** protein fold prediction based on PHYRE for HsdS_short and HsdS_long from strains TMW 2.1023 and TMW 2.1324. The coiled coil region (red/green) displays the conserved region connecting the two TRDs which are colored in blue and yellow to orange (99.9% modelling confidence).

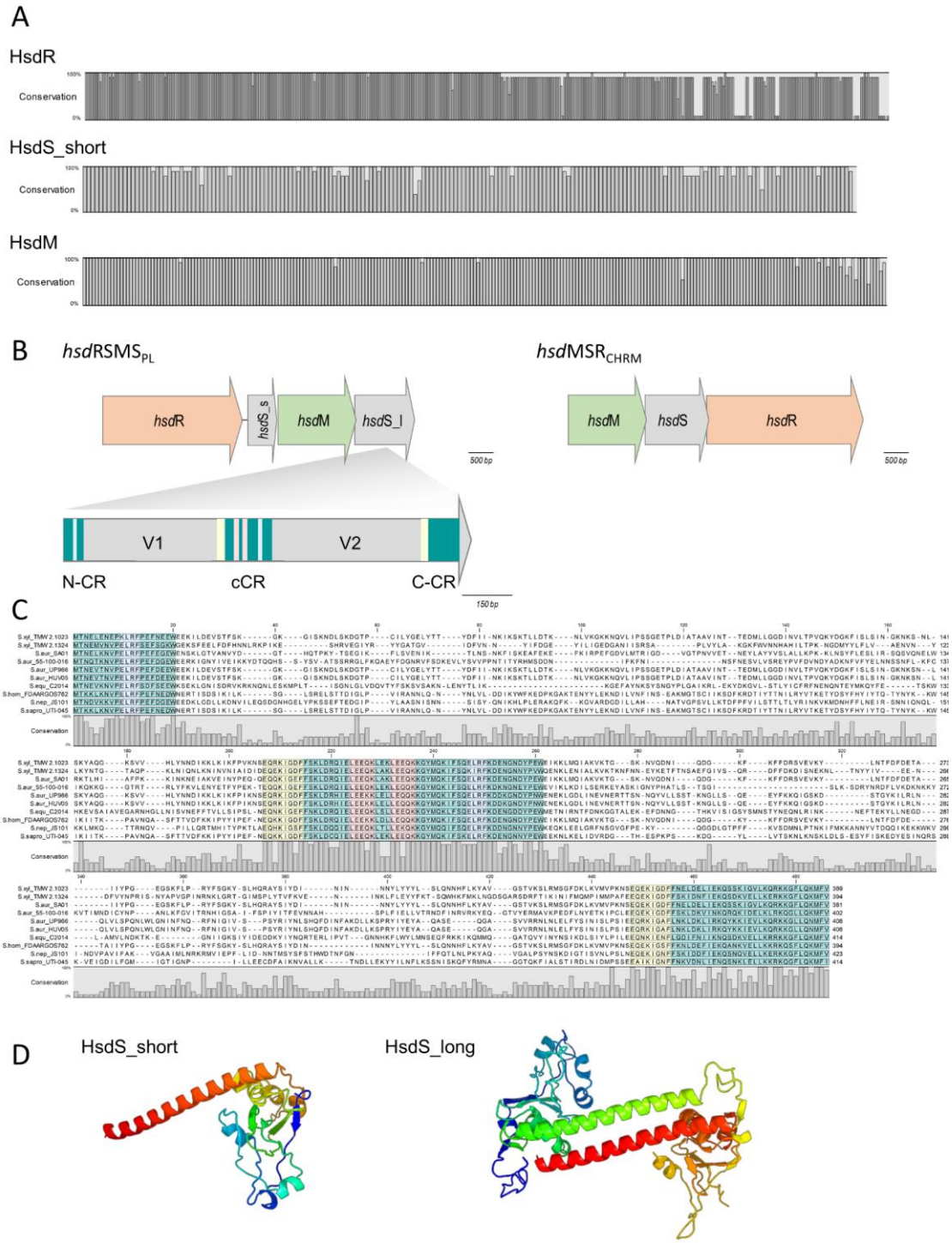

No tetra amino acid repeats as previously described for type IC *hsd*S subunits (45) could be identified in the central conserved region. We did identify two short repeating stretches in the central region though (2x LEEQK), as well as part of the central sequence is repeated in the N- and C- terminal conserved regions, respectively (Figure 2C). To mention is that long and short *hsd*S subunits of one *hsd*RSMS operon don't share any common, homologous regions. Further, the repeats found in the long *hsd*S subunits do not exist in the short ones. Taking secondary structure into consideration a typical protein fold was predicted by PHYRE (39) for *hsd*S_long with the two TRDs connected by alpha helices / coiled coil structures in an antiparallel order (Figure 2D), whereas for *hsd*S_short, a strikingly similar structure to a halfsize *hsd*S subunit is predicted. Referring to the NCBI Conserved Domain Database (36), *hsd*S_long subunits consist of two TRDs and *hsd*S_short of one. However, while this result is consistent for *hsd*S_long genes as they comprise two variable regions flanked by conserved regions, it is less clear for *hsd*S_short as the entire sequence is conserved, not harboring any variable parts. Furthermore, when blasting single TRD of *hsdS*_long, it yields hits on other *hsd*S subunits, emphasizing the dynamic, interallelic recombination of single TRDs between *hsd*S subunits. On the contrary, according to the results obtained upon blasting *hsd*S_short against the NCBI database, the short subunit does not exist as part of a long subunit, substantiating the theory that *hsd*S_short is not a halfsize or truncated *hsd*S subunit but rather an individual gene with a specific function, not flipping and recombining with *hsd*S_long subunits. One last noteworthy fact is, that it has been reported previously that *hsd*S genes, even if they are not part of the same family, share high homology (> 50%) among their variable regions determining the TRDs, if they recognize the same nucleotide motif (17). According to REBASE, the type I system of numerous *E. coli* strains (e.g. NCTC9029) as well as *Anaerobiospirillum thomasii* NCTC12467 recognize the same motif as TMW 2.1023 as well as certain *S. aureus* strains (AUS0325, WBG8366, MRSA - AMRF 6, MRSA - AMRF 4, ER09113.3) and TMW 2.1324 share a type I system specifying the same target DNA sequence. When aligning the TRDs accordingly, percent identity values of 69% (N-TRD) and 63% (C-TRD), respectively were obtained for TMW 2.1324 and the HsdS subunits of the *S. aureus* strains, compared to 20%

amino acid sequence identity when aligning the TMW 2.1023 TRDs with HsdS of the *S. aureus* strains. In contrast, the TRDs of TMW 2.1023 did not show any significant similarity to neither the HsdS subunits of *A. thomasii* NCTC12467 nor *E. coli* NCTC9029, despite recognizing the same sequence motif (percent identity values around 21%).

Expression of Modification systems in *E. coli*

To confirm the specificity of selected methyltransferases and to characterize the function of the newly detected *hsd*RSMS system in more detail, methyltransferases and specificity units were heterologously expressed in *E. coli*. As expression host functioned *E. coli* DC10B, a *dcm* - negative K12 derivate, unable to methylate cytosine. Modification enzymes were integrated into and expressed from the chromosome as expression on a plasmid has previously been associated with instability and inadequate base modification (29). In terms of choosing an adequate promoter, which provides a complete methylation of the target DNA but does not pose a too heavy burden for the cell, the less complex type II system of TMW 2.1324 was used as a test system. Therefore, the corresponding methyltransferase gene (motif GATGC/GCATC) was integrated into the *E. coli* chromosome including two different constitutive promoters, the β-lactamase promoter P_{bla} as well as the T5 coliphage promoter P_{N25}. Subsequent sequencing and base modification analysis revealed that only 42 - 76% of the available motifs are modified when P_{bla} was used (Table 4, *E. coli* CM2) compared to 99.7% modification when under the control of P_{N25} (*E. coli* CM93). The difference in methylation propensity is also clear when digesting isolated plasmid DNA from these two strains with SfaNI. SfaNI recognizes the same motif as the type II system of TMW 2.1324, thus, proper modification by the respective methyltransferase should protect the plasmid from restriction. While a complete restriction digest was visible on the gel when plasmid of *E. coli* DC10B was used, an incomplete digest was detectable for plasmids isolated from *E. coli* CM2 (P_{bla}) and no digestion was visible when plasmid isolated from *E. coli* CM93 (P_{N25}) was digested and applied to the gel (Figure S3).

Table 4: base modification and analysis results of heterologous gene expression of *S. xylosus* methyltransferases in *E. coli* using different gene combinations and promotors. GATC is an *E. coli* motif, controlled by *dam*. As for CM45 it is to note, that the whole sequencing quality was insufficient as even the intrinsic motif (GATC) shows lower scores (fraction methylated) than in the other strains. *hsd*S_short is colored in violet, *hsd*M in yellow, *hsd*S_long in turquoise (conserved regions) and grey (variable regions).

strain	integrated MT	promotor	motifs	centerPos	mod	fraction	nDetected	nGenome	meanScore	meanCov	integrated typeI version
CM56	*hsd*SMS_023 (186-2)	P_{N25}	GATC	2	m6A	1.00	38556	38594	141	81.3	
			TCANNNNNNCTC	3	m6A	0.82	1004	1225	128	84.3	
			GAGNNNNNNTGA	2	m6A	0.69	845	1225	128	85.2	
CM57	*hsd*MS_023 (186-2)	P_{N25}	GATC	2	m6A	1.00	38560	38594	289	185.3	
			HTCANNNNNACTCD	4	m6A	0.49	99	203	172	187.8	
			HGAGNRNNNNTGAD	3	m6A	0.32	129	399	158	187.0	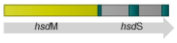
			TCABTNNBNCTC	3	m6A	0.44	89	202	168	185.8	
			GAGNNNNAVTGAND	2	m6A	0.36	72	198	162	185.9	
CM5	*hsd*SMS_324 (186-1)	P_{N25}	GATC	2	m6A	1.00	38557	38594	277	176.8	
			ACAYNNNNNGGT	3	m6A	0.98	652	664	231	176.9	
			ACCNNNNNRTGT	1	m6A	0.98	649	664	219	176.6	
CM13	*hsd*SMS_MT_324 (λ, 186-1)	P_{N25}	GATC	2	m6A	1.00	38555	38594	243	152.8	
			GATGC	2	m6A	1.00	14345	14382	224	152.5	
			ACAYNNNNNGGT	3	m6A	0.98	648	664	203	152.1	
			ACCNNNNNRTGT	1	m6A	0.97	645	664	194	151.4	
			GCNBGGATGC	2	m4C	0.17	32	189	134	148.3	
CM19	*hsd*MS_MT_324 (186-1)	P_{N25}	GATC	2	m6A	1.00	38515	38594	202	124.6	
			GATGC	2	m6A	0.99	14279	14382	187	124.5	
			GCATC	3	m6A	1.00	14333	14382	185	124.5	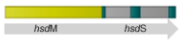
			ANNNNNNHNGCATGCV	12	m6A	0.19	36	189	149	128.5	
CM30	*hsd*MS$_{tr}$_MT_324 (λ, 186-2)	P_{N25}	GATC	2	m6A	0.98	37771	38594	206	118.2	
			GATGC	2	m6A	0.97	13916	14382	193	118.7	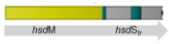
			GCATC	3	m6A	0.97	13899	14382	188	118.6	
CM93	MT_324 (λ)	P_{N25}	GATC	2	m6A	1.00	38524	38594	251	147.7	
			GATGC	2	m6A	1.00	14333	14382	233	148.0	
			GCATC	3	m6A	1.00	14340	14382	229	147.8	
CM2	MT_324 (186-1)	P_{bla}	GATC	2	m6A	1.00	38508	38594	256	150.4	
			GATGC	2	m6A	0.76	10930	14382	156	156.1	
			GCATC	3	m6A	0.42	6025	14382	134	164.2	

Expressing from promoter P_{N25}, other variants of modification enzymes were integrated into the chromosome of *E. coli*, namely the full *hsd*SMS system of *S. xylosus* strains TMW 2.1023 (*E. coli*_CM56) and 2.1324 (*E. coli* CM5 and CM13), respectively, as well as *hsd*MS only, neglecting *hsd*S_short (*E. coli* CM57 and CM19). Results are listed in Table 4. In both cases, the expected motif was only methylated when the full *hsd*SMS operon was expressed in *E. coli* (CM56, CM13 / CM5). On the contrary, if *hsd*S_short was missing, random motifs and/or modified motifs with a changed specificity and low modification scores appear (CM57, CM19). The function of *hsd*S_long as well as the influence of the presence of *hsd*S_short was further characterized in another experiment. Usually, the deletion of one half of the specificity unit *hsd*S does not impair the function of the whole type I system, it only results in a change of the TRM to a symmetric, palindrome specificity (25,26). We decided, to express only the N-terminal part (TRD1 and central conserved region) of TMW 2.1324 *hsd*S_long in *E. coli* (CM30) to see whether we could obtain a similar effect. This experiment resulted in no modification

patterns at all. This also indicates that *hsd*S_short is essential for successful base modification and that *hsd*S_long operates differently to *hsd*S subunits of other type I families.

Transformation efficiency of *S. xylosus*

As plasmid pIMAY* (and it's variants pIMAY-Z and pIMAY) represents an *E. coli/staphylococcal* temperature-sensitive plasmid widely used for allelic exchange in *Staphylococcus aureus* (20,32,46,47), which has also been shown to work for *S. xylosus* (31), we used it as a target for plasmid artificial modification (PAM) studies. Potential changes in the transformation efficiency of *S. xylosus* strains TMW 2.1023 and 2.1324 were determined, after the plasmid had been methylated in one of the *E. coli* strains expressing the target's strains base modification genes. As a control *S. aureus* strain Newman was included into the experiments as it has previously been successfully transformed with DNA isolated from *E. coli* DC10B (47). Transformation efficiencies of 37 ± 6 cfu/µg could be obtained for Newman. For TMW 2.1023, transformation efficiencies varied between 10 ± 2 cfu/µg when pIMAY* was isolated from DC10B and 8 ± 1 cfu/µg when pIMAY* originated from *E. coli* strain CM56. As expected, the transformation efficiency of TMW 2.1023 did not differ significantly between the different *E. coli* host strains, since pIMAY* vector does not possess any restriction sites of the type I RM system of TMW 2.1023. Regarding *S. xylosus* TMW 2.1324, any attempts to transform this strain remained unsuccessful. In contrast to TMW 2.1023, TMW 2.1324 RM systems do possess restriction sites in the empty pIMAY* vector, namely one site for the type I system and five sites for the type II system. In this context, the genomes of TMW 2.1023 and 2.1324 were also screened for clustered regularly interspaced short palindromic repeat (CRISPR) loci, as they can confer a barrier to horizontal gene transfer as well (5). The identified spacer sequences of the CRISPR loci were blasted against the sequence of pIMAY* but no homologies were found, making it unlikely that CIRSPR systems account for the low transformation efficiency of the two *S. xylosus* strains when using pIMAY*. Table S3 provides an overview of the CRISPR-cas systems identified in *S. xylosus* TMW 2.1023 and TMW 2.1324.

4 Discussion

In this study we describe the prevalence of RM systems among the species *Staphylococcus xylosus* as well as we discovered a new variant of type I RM systems. We found, that *S. xylosus* harbors a variety of RM systems, including systems that have been reported as rarely existing (type III) or inactive (type IIG) in other staphylococcal species such as *S. aureus* before (48,11). In *S. xylosus* on the contrary, both systems appear to be active and more common as proven in this study by methylome, bioinformatic and proteomic analysis. Special emphasis of this work was laid on Type I RM systems, which we could identify in seven out of the 15 investigated *S. xylosus* strains. This finding is consistent with data for other coagulase-negative staphylococci, which reported around 38% of *S. epidermidis* genomes to contain no functional type I RM systems (29). Further in accordance with data for *S. epidermidis* is the prevalence of a single type I RM system in the remaining strains, while on the contrary in *S. aureus*, up to three functional type I RM systems per genome have been reported (29,20). Among the type I positive *S. xylosus* isolates, we found two different types of *hsd*-operons. Firstly, chromosomally encoded *hsd*MSR operons, resembling in their gene and sequence structure other type I systems described for staphylococci but also other Gram-positive bacteria in the past (29,49,50). Namely, they are arranged in an operon like structure, in the order of transcription, including the three typical genes, *hsd*R, *hsd*M, *hsd*S. Secondly, we identified a hitherto undescribed variant of type I systems, *hsd*RSMS. The operon shares some common features with other staphylococcal type I systems such as the localization on mobile genetic elements (MGEs) of the chromosome and on plasmids (29) as well as the usual gene arrangement with *hsd*SMS all being transcribed from a mutual promoter and *hsd*R being associated with its own promoter (17). Yet, in contrast to other type I systems, *hsd*RSMS requires two specificity units for proper and stable base modification, a long and a short subunit. While *hsd*S_long resembles known specificity units in its composition consisting of variable regions (TRDs) flanked by conserved regions, for *hsd*S_short such typical structure is not evident, as it is lacking any variable regions. This makes it unlikely that *hsd*S_short is involved in target sequence recognition nor being a remnant, truncated halfsize *hsd*S

polypeptide. Fragmented *hsd*S genes have been reported for other type IC systems (e.g. *Ngo*AV, *Eco*DXXI, *Eco*R124I (24–26)) with the C-terminal domain of the long *hsd*S peptide usually missing, resulting in palindromic recognition motifs. Our data showed that *hsd*S_short does not exist as part of a long *hsd*S subunit though. It is functionally expressed as well as it contributes to specific base modification of non-palindromic motifs. We therefore rule out, that *hsd*S_short is a truncated halfsize subunit of *hsd*S_long. Upon methylation of DNA, type I methyltransferases usually form a M_2S trimer, whereas for restriction a pentamer consisting of either $R_2M_2S_1$ or $R_1M_2S_1$ is formed (16). One could speculate that *hsd*S_short might have a stabilizing role in these complexes, somehow promoting binding of *hsd*S_long to *hsd*M since missing *hsd*S_short resulted in DNA target motifs with a modified specificity and low modification scores. Further studies are needed to determine the exact role of *hsd*S_short during complex assembly of the newly discovered type I RM system.

Classification of type I RM systems into one of the five existing families is based on sequence similarity values of *hsd*R and *hsd*M genes, as they are usually well conserved. However, clear cutoff values have not been determined so far and values specified in the literature vary strongly. Yet in trying to find consent, one could conclude that *hsd*M and *hsd*R share usually over 70% sequence similarity when they are members of the same family and < 30% when they are part of different families (16–19,21). *Hsd*R and *hsd*M of the *hsd*RSMS system share highest percent identity values with the reference gene of Type IC systems (EcoR124I), namely 40 and 48%, respectively. Thereby, they are just at the interface between classifying them into the type IC family or establishing a new family for them. Voting for classifying them into the family of type IC systems is their occurrence on plasmids and MGEs which is characteristic for members of the type IC family (15,51). Moreover, according to Gao *et al.,* (16), HsdM of Type IC families is composed of three domains, namely a N-terminal (aa 11 – 190), a catalytic (aa 198 – 473) and a C-terminal (aa 481 – 510) domain. HsdM of $HsdRSMS_{PL}$ systems displays 33% protein sequence identity to the N-terminal, 44% to the catalytic and 13-23% to the C-terminal domain of M.EcoR124I (data not shown). Thus, even though both methyltransferases are arranged into a similar domain structure, single domains are not reaching sequence identity

values over 44%. Therefore, voting against grouping the new operon into the family of Type IC systems is not just the overall comparatively low sequence homology (~40%) of *hsd*R and *hsd*M with the respective Type I reference genes but also that *hsd*S is lacking some important structural and functional characteristics. Most importantly the long subunit is not able to function independently without the presence of *hsd*S_short. Additionally, type IC *hsd*S subunits usually harbor characteristic tandem tetra amino acid repeats (e.g. TAEL, LEAT, SEAL or TSEL (45)) in their central conserved region. These repeats define among others, the spacer length between the two TRDs, with two and three repeats correlating with a 6 and 7 bp spacer, respectively (24,45). No such tetra amino acid repeats were identified in the central conserved region of *hsdS* from the *hsd*RSMS system, though we did find two short repeating amino acid stretches in the central conserved region (2x LEEQK). However, they are separated by 3 random amino acids, thus not arranged in tandem and they do not seem to influence spacer length, as both *hsd*S_long subunits investigated in this study harbor two of such repeats but the TRDs of the TMW 2.1023 motif are divided by a 6 bp spacer compared to a 5 bp spacer in the motif of TMW 2.1324.

Plasmid artificial modification (PAM) is a method that mimics the host target strains methylation profile by passaging plasmid DNA through modified *E. coli* strains. The method has been shown to increase transformation efficiency in staphylococci but also in other organisms such as *Lactococcus lactis* and *Bifidobacterium adolescentis* in the past (20,29,43,52). In this study we were unable to introduce plasmid DNA into *S. xylosus* TMW 2.1324, even when the DNA had been passed through an *E. coli* host expressing the respective modification genes of TMW 2.1324. Furthermore, low transformation rates were obtained with TMW 2.1023, indicating that introducing xenogeneic DNA into *S. xylosus* wildtype strains is a challenge for itself, involving some barriers that go past restriction modification systems. Especially since pIMAY* does not contain any restriction sites for the type I system of TMW 2.1023, thus the strain should be transformable using this plasmid. Speculations on which factors could provide an additional barrier to transformation include phenotypic characteristics such as capsule formation, membrane composition and presence of teichoic acids, as well as bacteria might also possess

other restriction and defense systems such as CRISPR-cas, BREX- or phosphorothioate modification systems (5,53–55). Moreover, Type IV restriction modification systems, which have been reported to pose a strong barrier to transformation in *S. aureus*, have hitherto not been characterized in *S. xylosus*. Even though, we tried to evade them by using cytosine methylation deficient *E. coli* strains as most type IV systems address cytosine modified motifs (30), it remains possible that *S. xylosus* Type IV systems address adenine rather than cytosine methylated residues which might then interfere with *dam*-mediated methylation of *E. coli*. Additionally, it is just as likely that the plasmid used for transformation in this study is not well compatible with *S. xylosus*, as it was originally designed to transform *S. aureus*. We observed repeatedly that *S. xylosus* TMW 2.1023 lost one of its intrinsic plasmids after transformation with pIMAY*, indicating plasmid incompatibility (data not shown). Therefore, we conclude that using a plasmid with a different replication protein and controlling elements as well as to increase plasmid concentrations subjecting to transformation might improve the outcome.

Within this study, we provide new insights into the variety of restriction modification systems encoded by *S. xylosus*, a species, which has so far not been addressed in methylome analyses. We thereby revealed the presence of a new variant of type I restriction modification systems, which requires two specificity units for specific and thorough DNA methylation. This result is another piece in the mosaic of how bacteria can protect themselves from foreign DNA attacks or even generate prokaryotic phenotypic heterogeneity. We furthermore propose that *hsd*RSMS systems might need to be classified into a new family of type I restriction modification systems. Additional approaches such as subunit complementation tests or antibody cross reactivity assays could confirm the family affiliation in future.

Acknowledgement

We thank Dr. Barbara Fösel from Helmholtz Zentrum Munich as well as Weihong Qi and Simon Grüter from ETH Zurich for their support of sequencing and bioinformatic analysis of the CMx *E. coli* strains.

References

1. Ravyts, F., Vuyst, L.D. and Leroy, F. (2012) Bacterial diversity and functionalities in food fermentations, *Eng. Life Sci.,* **12,** 356–367.
2. Leroy, S., Vermassen, A., Ras, G. and Talon, R. (2017) Insight into the genome of *Staphylococcus xylosus*, a ubiquitous species well adapted to meat products, *Microorganisms,* **5**.
3. Condas, L.A.Z., Buck, J. de, Nobrega, D.B., Carson, D.A., Roy, J.-P., Keefe, G.P., DeVries, T.J., Middleton, J.R., Dufour, S. and Barkema, H.W. (2017) Distribution of non-aureus staphylococci species in udder quarters with low and high somatic cell count, and clinical mastitis, *Journal of dairy science,* **100,** 5613–5627. First published on Apr 27, 2017.
4. Supré, K., Haesebrouck, F., Zadoks, R.N., Vaneechoutte, M., Piepers, S. and Vliegher, S. de (2011) Some coagulase-negative Staphylococcus species affect udder health more than others, *Journal of dairy science,* **94,** 2329–2340.
5. Lindsay, J.A. (2019) Staphylococci: Evolving Genomes, *Microbiology spectrum,* **7**.
6. Karkman, A., Do, T.T., Walsh, F. and Virta, M.P.J. (2018) Antibiotic-Resistance Genes in Waste Water, *Trends in microbiology,* **26,** 220–228. First published on Oct 13, 2017.
7. Heilmann, C., Ziebuhr, W. and Becker, K. (2019) Are coagulase-negative staphylococci virulent?, *Clinical microbiology and infection : the official publication of the European Society of Clinical Microbiology and Infectious Diseases,* **25,** 1071–1080. First published on Nov 29, 2018.
8. Tock, M.R. and Dryden, D.T.F. (2005) The biology of restriction and anti-restriction, *Current opinion in microbiology,* **8,** 466–472.
9. Atack, J.M., Tan, A., Lo Bakaletz, Jennings, M.P. and Seib, K.L. (2018) Phasevarions of Bacterial Pathogens: Methylomics Sheds New Light on Old Enemies, *Trends in microbiology,* **26,** https://pubmed.ncbi.nlm.nih.gov/29452952/.
10. Lindsay, J.A. (2014) *Staphylococcus aureus* genomics and the impact of horizontal gene transfer, *International Journal of Medical Microbiology,* **304,** 103–109.
11. Sadykov, M.R. (2016) Restriction-Modification Systems as a Barrier for Genetic Manipulation of *Staphylococcus aureus*, *Methods in molecular biology (Clifton, N.J.),* **1373,** 9–23.
12. Wilson, G.G. and Murray, N.E. (1991) Restriction and modification systems, *Annual review of genetics,* **25,** 585–627.
13. Ste Croix, M. de, Vacca, I., Kwun, M.J., Ralph, J.D., Bentley, S.D., Haigh, R., Croucher, N.J. and Oggioni, M.R. (2017) Phase-variable methylation and epigenetic regulation by type I restriction-modification systems, *FEMS microbiology reviews,* **41,** S3-S15.
14. Oliveira, P.H. and Fang, G. (2021) Conserved DNA Methyltransferases: A Window into Fundamental Mechanisms of Epigenetic Regulation in Bacteria, *Trends in microbiology,* **29,** 28–40. First published on May 13, 2020.
15. Loenen, W.A.M., Dryden, D.T.F., Raleigh, E.A. and Wilson, G.G. (2014) Type I restriction enzymes and their relatives, *Nucleic Acids Research,* **42,** 20–44. First published on Sep 24, 2013.
16. Gao, Y., Cao, D., Zhu, J., Feng, H., Luo, X., Liu, S., Yan, X.-X., Zhang, X. and Gao, P. (2020) Structural insights into assembly, operation and inhibition of a type I restriction-modification system, *Nature Microbiology,* **5,** 1107–1118. First published on Jun 1, 2020.
17. Murray, N.E. (2000) Type I restriction systems: sophisticated molecular machines (a legacy of Bertani and Weigle), *Microbiology and Molecular Biology Reviews,* **64,** 412–434.
18. Titheradge, A.J., King, J., Ryu, J. and Murray, N.E. (2001) Families of restriction enzymes: an analysis prompted by molecular and genetic data for type ID restriction and modification systems, *Nucleic Acids Research,* **29,** 4195–4205.
19. Cooper, L.P., Roberts, G.A., White, J.H., Luyten, Y.A., Bower, E.K.M., Morgan, R.D., Roberts, R.J., Lindsay, J.A. and Dryden, D.T.F. (2017) DNA target recognition domains in the Type I restriction and modification systems of *Staphylococcus aureus*, *Nucleic Acids Research,* **45,** 3395–3406.

20. Monk, I.R., Tree, J.J., Howden, B.P., Stinear, T.P. and Foster, T.J. (2015) Complete Bypass of Restriction Systems for Major *Staphylococcus aureus* Lineages, *mBio,* **6,** ://mbio.asm.org/content/mbio/6/3/e00308-15.full.pdf.

21. Chin, V., Valinluck, V., Magaki, S. and Ryu, J. (2004) KpnBI is the prototype of a new family (IE) of bacterial type I restriction-modification system, *Nucleic Acids Research,* **32,** e138.

22. Costa, S.K., Donegan, N.P., Corvaglia, A.-R., François, P. and Cheung, A.L. (2017) Bypassing the Restriction System To Improve Transformation of *Staphylococcus epidermidis*, *Journal of bacteriology,* **199**.

23. Atack, J.M., Guo, C., Yang, L., Zhou, Y. and Jennings, M.P. (2020) DNA sequence repeats identify numerous Type I restriction-modification systems that are potential epigenetic regulators controlling phase-variable regulons; phasevarions, *FASEB journal : official publication of the Federation of American Societies for Experimental Biology,* **34,** 1038–1051. First published on Nov 28, 2019.

24. Piekarowicz, A., Kłyz, A., Kwiatek, A. and Stein, D.C. (2001) Analysis of type I restriction modification systems in the Neisseriaceae: genetic organization and properties of the gene products, *Molecular microbiology,* **41,** 1199–1210.

25. Abadjieva, A., Patel, J., Webb, M., Zinkevich, V. and Firman, K. (1993) A deletion mutant of the type IC restriction endonuclease EcoR1241 expressing a novel DNA specificity, *Nucleic Acids Research,* **21,** 4435–4443.

26. MacWilliams, M.P. and Bickle, T.A. (1996) Generation of new DNA binding specificity by truncation of the type IC EcoDXXI hsdS gene, *The EMBO journal,* **15,** 4775–4783.

27. Pingoud, A., Wilson, G.G. and Wende, W. (2014) Type II restriction endonucleases--a historical perspective and more, *Nucleic Acids Research,* **42,** 7489–7527.

28. Rao, D.N., Dryden, D.T.F. and Bheemanaik, S. (2014) Type III restriction-modification enzymes: a historical perspective, *Nucleic Acids Research,* **42,** 45–55. First published on Jul 17, 2013.

29. Lee, J.Y.H., Carter, G.P., Pidot, S.J., Guérillot, R., Seemann, T., Silva, A.G.d., Foster, T.J., Howden, B.P., Stinear, T.P. and Monk, I.R. (2019) Mining the Methylome Reveals Extensive Diversity in *Staphylococcus epidermidis* Restriction Modification, *mBio,* **10**.

30. Loenen, W.A.M. and Raleigh, E.A. (2014) The other face of restriction: modification-dependent enzymes, *Nucleic Acids Research,* **42,** 56–69. First published on Aug 29, 2013.

31. Schiffer, C.J., Abele, M., Ehrmann, M.A. and Vogel, R.F. (2021) Bap-Independent Biofilm Formation in *Staphylococcus xylosus*, *Microorganisms,* **9,** 2610.

32. Monk, I.R. and Stinear, T.P. (2021) From cloning to mutant in 5 days: rapid allelic exchange in *Staphylococcus aureus*, *Access Microbiology,* **3**.

33. St-Pierre, F., Cui, L., Priest, D.G., Endy, D., Dodd, I.B. and Shearwin, K.E. (2013) One-step cloning and chromosomal integration of DNA, *ACS synthetic biology,* **2,** 537–541.

34. Cui, L. and Shearwin, K.E. (2017) Clonetegration Using OSIP Plasmids: One-Step DNA Assembly and Site-Specific Genomic Integration in Bacteria, *Methods in molecular biology (Clifton, N.J.),* **1472,** 139–155.

35. Schiffer, C., Hilgarth, M., Ehrmann, M. and Vogel, R.F. (2019) Bap and cell surface hydrophobicity are important factors in *Staphylococcus xylosus* biofilm formation, *Front. Microbiol.,* **10,** 1387, https://www.frontiersin.org/articles/10.3389/fmicb.2019.01387/pdf.

36. Marchler-Bauer, A., Derbyshire, M.K., Gonzales, N.R., Lu, S., Chitsaz, F., Geer, L.Y., Geer, R.C., He, J., Gwadz, M. and Hurwitz, D.I. *et al.* (2015) CDD: NCBI's conserved domain database, *Nucleic Acids Research,* **43,** D222-6. First published on Nov 20, 2014.

37. Roberts, R.J., Vincze, T., Posfai, J. and Macelis, D. (2015) REBASE--a database for DNA restriction and modification: enzymes, genes and genomes, *Nucleic Acids Research,* **43,** D298-9. First published on Nov 5, 2014.

38. Behr, J., Geissler, A.J., Schmid, J., Zehe, A. and Vogel, R.F. (2016) The Identification of Novel Diagnostic Marker Genes for the Detection of Beer Spoiling *Pediococcus damnosus* Strains Using the BlAst Diagnostic Gene findEr, *PloS one,* **11,** e0152747.

39. Kelley, L.A., Mezulis, S., Yates, C.M., Wass, M.N. and Sternberg, M.J.E. (2015) The Phyre2 web portal for protein modeling, prediction and analysis, *nprot,* **10,** 845–858.

40. Couvin, D., Bernheim, A., Toffano-Nioche, C., Touchon, M., Michalik, J., Néron, B., Rocha, E.P.C., Vergnaud, G., Gautheret, D. and Pourcel, C. (2018) CRISPRCasFinder, an update of CRISRFinder, includes a portable version, enhanced performance and integrates search for Cas proteins, *Nucleic Acids Research,* **46,** W246-W251.

41. Perez-Riverol, Y., Csordas, A., Bai, J., Bernal-Llinares, M., Hewapathirana, S., Kundu, D.J., Inuganti, A., Griss, J., Mayer, G. and Eisenacher, M. *et al.* (2019) The PRIDE database and related tools and resources in 2019: improving support for quantification data, *Nucleic Acids Research,* **47,** D442-D450.

42. Clark, T.A., Murray, I.A., Morgan, R.D., Kislyuk, A.O., Spittle, K.E., Boitano, M., Fomenkov, A., Roberts, R.J. and Korlach, J. (2012) Characterization of DNA methyltransferase specificities using single-molecule, real-time DNA sequencing, *Nucleic Acids Research,* **40,** e29.

43. Deng, Y.M., Liu, C.Q. and Dunn, N.W. (2000) LldI, a plasmid-encoded type I restriction and modification system in *Lactococcus lactis*, *DNA sequence : the journal of DNA sequencing and mapping,* **11,** 239–245.

44. Roberts, G.A., Chen, K., Cooper, L.P., White, J.H., Blakely, G.W. and Dryden, D.T.F. (2012) Removal of a frameshift between the hsdM and hsdS genes of the EcoKI Type IA DNA restriction and modification system produces a new type of system and links the different families of Type I systems, *Nucleic Acids Research,* **40,** 10916–10924. First published on Sep 23, 2012.

45. Adamczyk-Popławska, M., Kondrzycka, A., Urbanek, K. and Piekarowicz, A. (2003) Tetra-amino-acid tandem repeats are involved in HsdS complementation in type IC restriction-modification systems, *Microbiology,* **149,** 3311–3319.

46. Schuster, C.F., Howard, S.A. and Gründling, A. (2019) Use of the counter selectable marker PheS* for genome engineering in *Staphylococcus aureus*, *Microbiology,* **165,** 572–584. First published on Apr 3, 2019.

47. Monk, I.R., Shah, I.M., Xu, M., Tan, M.-W. and Foster, T.J. (2012) Transforming the Untransformable: Application of Direct Transformation To Manipulate Genetically *Staphylococcus aureus* and *Staphylococcus epidermidis*, *mBio,* **3,** e00277-11.

48. Jones, M.J., Donegan, N.P., Mikheyeva, I.V. and Cheung, A.L. (2015) Improving transformation of *Staphylococcus aureus* belonging to the CC1, CC5 and CC8 clonal complexes, *PloS one,* **10,** e0119487.

49. Finn, M.B., Ramsey, K.M., Tolliver, H.J., Dove, S.L. and Wessels, M.R. (2021) Improved transformation efficiency of group A Streptococcus by inactivation of a type I restriction modification system, *PloS one,* **16,** e0248201. First published on Apr 29, 2021.

50. Reva, O.N., Swanevelder, D.Z.H., Mwita, L.A., Mwakilili, A.D., Muzondiwa, D., Joubert, M., Chan, W.Y., Lutz, S., Ahrens, C.H. and Avdeeva, L.V. *et al.* (2019) Genetic, Epigenetic and Phenotypic Diversity of Four *Bacillus velezensis* Strains Used for Plant Protection or as Probiotics, *Front. Microbiol.,* **10,** 2610. First published on Nov 15, 2019.

51. Youell, J. and Firman, K. (2008) EcoR124I: from plasmid-encoded restriction-modification system to nanodevice, *Microbiology and Molecular Biology Reviews : MMBR,* **72,** 365-77, table of contents.

52. Suzuki, T. and Yasui, K. (2011) Plasmid Artificial Modification: A Novel Method for Efficient DNA Transfer into Bacteria. In Williams, J.A. (ed.), *Strain engineering. Methods and protocols.* Humana Press, Totowa, N.J. Vol. 765, pp. 309–326.

53. Nye, T.M., Fernandez, N.L. and Simmons, L.A. (2020) A positive perspective on DNA methylation: regulatory functions of DNA methylation outside of host defense in Gram-positive bacteria, *Critical reviews in biochemistry and molecular biology,* **55,** 576–591. First published on Oct 15, 2020.

54. Wang, L., Jiang, S., Deng, Z., Dedon, P.C. and Chen, S. (2019) DNA phosphorothioate modification-a new multi-functional epigenetic system in bacteria, *FEMS microbiology reviews,* **43,** 109–122.

55. Thomas, C.M. and Nielsen, K.M. (2005) Mechanisms of, and barriers to, horizontal gene transfer between bacteria, *Nature reviews. Microbiology,* **3,** 711–721.

4.5 Proteomic analysis of *Staphylococcus xylosus* cells grown under planktonic and sessile conditions

Preface

The idea of this study was to identify physiological differences and possibly new adaptive changes involved in *S. xylosus* biofilm formation. Therefore, cells were grown at two different physical states, namely planktonic *versus* sessile conditions and their proteomes were subsequently analyzed and compared.

According to the literature, only one study has been published so far, addressing changes in protein expression between sessile and planktonic cells of *S. xylosus* (Planchon et al., 2009). Hereby, to reveal changes in the proteome, the authors used two-dimensional gel electrophoresis and a protocol that tried to include both cytoplasmic and cell envelope proteins. Still, the method has its typical restrictions regarding general resolution and an increased focus on cytoplasmic proteins. The aim of our study was to better understand the molecular processes and adaptive changes involved in *S. xylosus* biofilm formation, thereby using recently available high-resolution liquid chromatography mass spectrometry (LC-MS) that enables the generation of a full proteome, including the proteins abundant in the extracellular biofilm matrix and a higher proportion of membrane-associated proteins.

The detected changes in the proteome of biofilm cells were primarily related to the production of detoxifying components and a switch to anaerobic metabolism. Furthermore, phage-related proteins were identified in samples of strains that carry intact prophages in their genomes. These findings help to unravel the metabolic routes of *S. xylosus* cells living in a biofilm.

Author contribution: Carolin Schiffer was responsible for the design of the study. She performed all experiments in the lab as well as bioinformatic analysis of the proteins differentially expressed between the two physiological stages. Carolin Schiffer is currently working on the original draft of the manuscript.

Note: Although this paragraph is not yet a finished manuscript the following data is included into this work as a chapter as it assists the interpretation of molecular mechanisms of the planktonic *versus* biofilm lifestyle of *S. xylosus*.

Experimental setup of the study

A detailed description of the experimental setup is given in the methods section (chapter 3.15 and 3.16). Basically, cells were grown either in Erlenmeyer-flasks under constant agitation or under static conditions in petri-discs favoring the formation of an adhesive biofilm. Glucose supplemented (1%) TSB acidified to pH 6 (Lac^+) was chosen as a growth medium because all investigated strains form sufficient amounts of biofilm in this medium (Schiffer et al., 2019). After 24 hours of growth, medium proteins were removed and the whole proteome of planktonic cells as well as of the entire biofilm was analyzed via LC-MS. Of note is, that the growth medium used causes cells to clump, also during planktonic growth, heavily. Therefore, the strongest biofilm-producing strain (TMW 2.1523) was also sampled in TSB_N, a medium not causing such strong multicellular effects.

Results and Discussion

Within this study, the whole proteome profile of four different *S. xylosus* strains, previously characterized for their ability to form biofilm (Schiffer et al., 2019), was investigated by growing them in planktonic and in sessile mode. Statistically significant differentially expressed proteins (log_2 fold change ≥ 2) are listed in the following tables. Since each strain displays a different set of differentially expressed proteins, the data was decided not to be summarized and shall be described for each strain separately at first.

For TMW 2.1023, whole proteome analysis reproducibly identified 1390 proteins (53% of total encoded (2625) proteins). Out of these, 35 proteins, were differentially expressed between planktonic and sessile growth. Comparing the proteomic profile of planktonic *versus* sessile cells of TMW 2.1023 revealed that planktonic cells overexpressed only very few proteins, mostly related to basic cellular biosynthesis processes such as pyrimidine and amino acid biosynthesis. In biofilm cells on the other hand, higher amounts of proteins related to heme biosynthesis (ferrochelatase, protoporphyrinogen oxidase), nitrogen metabolism (nitrate reductase) and stress response (small heat shock protein, Ohr family peroxiredoxin) were found. Results are listed in Table 2.

Table 2: Differentially represented proteins in TMW 2.1023 planktonic *vs*. sessile samples (pairwise comparison) when grown in glucose supplemented medium acidified to pH6 with lactic acid (Lac^+). Proteins in the upper part of the table were identified in higher intensities in planktonic cells and proteins in the lower part of the table are more abundant in sessile compared to planktonic samples. (p-value < 0.05; log_2 fold change > 2.0, p-values were adjusted using Benjamini-Hochberg method).

Locustag	Annotation	log2	p.adj	Associated with
JGY91_04800	2-hydroxyacid dehydrogenase family protein	6.9	0.00	Glyoxylate reductase, Glycerate metabolism
JGY91_08080	aminopeptidase P family protein	2.8	0.02	Protein modification, degradation and repair
JGY91_05560	amidohydrolase	2.7	0.03	Degradation of proteins, peptides, and glycopeptides
JGY91_05930	ketol-acid reductoisomerase	2.5	0.02	Amino acid biosynthesis, Pyruvat family
JGY91_09880	glutamine-hydrolyzing carbamoyl phosphate synthase small subunit	2.4	0.01	De Novo Pyrimidine Synthesis
JGY91_00685	NDxxF motif lipoprotein	2.2	0.01	Protein and peptide secretion and trafficking
JGY91_12935	CDP-glycerol glycerophosphotransferase family protein	2.2	0.01	Teichoic and lipoteichoic acids biosynthesis
JGY91_07495	DUF4930 family protein	2.1	0.01	- none -
JGY91_06990	TIGR01212 family radical SAM protein	2.1	0.00	- none -
JGY91_02675	NAD-dependent succinate-semialdehyde dehydrogenase	2.0	0.00	Central intermediary metabolism
JGY91_03135	universal stress protein	2.0	0.00	Stress response
JGY91_04275	nitrate reductase subunit alpha	- 5.2	0.03	Energy metabolism; Denitrifying reductase gene clusters
JGY91_03850	pyridoxal kinase	- 4.5	0.00	Biosynthesis of cofactors, prosthetic groups, and carriers
JGY91_06775	protoporphyrinogen oxidase	- 4.3	0.00	Heme, porphyrin, and cobalamin
JGY91_04505	transcription factor S	- 4.2	0.01	Transcription factors
JGY91_00190	16S rRNA (cytidine(1402)-2-O)-methyltransferase	- 4.1	0.00	tRNA and rRNA base modification
JGY91_03510	D-ribitol-5-phosphate cytidylyltransferase	- 4.0	0.00	Biosynthesis of cofactors, prosthetic groups, and carriers
JGY91_13230	glycerol-3-phosphate transporter	- 3.3	0.03	Glycerol and Glycerol-3-phosphate Uptake and Utilization
JGY91_06770	ferrochelatase	- 3.3	0.00	Heme, porphyrin, and cobalamin
JGY91_09125	Exonuclease SbcC	- 3.1	0.00	DNA replication, recombination, and repair
JGY91_09940	cell division protein SepF	- 3.1	0.00	Cell division
JGY91_06835	PepSY domain-containing protein	- 3.0	0.00	Sporulation and germination
JGY91_10085	excinuclease ABC subunit UvrC	- 2.9	0.04	DNA replication, recombination, and repair
JGY91_04315	Hsp20/alpha crystallin family, small heat shock protein	- 2.6	0.00	Stress response
JGY91_12105	dihydroxyacetone kinase subunit DhaK	- 2.5	0.00	Dihydroxyacetone kinases
JGY91_09865	orotate phosphoribosyltransferase	- 2.5	0.00	De Novo Pyrimidine Synthesis
JGY91_05650	TIGR01440 family protein	- 2.3	0.02	- none -
JGY91_02725	CDP-glycerol:glycerophosphate transferase	- 2.3	0.00	Teichoic and lipoteichoic acids biosynthesis
JGY91_10440	phosphoribosylformylglycinamidine synthase I	- 2.2	0.02	De Novo Purine Biosynthesis
JGY91_09180	30S ribosomal protein S14	- 2.1	0.05	Ribosome SSU bacterial
JGY91_03740	antibiotic biosynthesis monooxygenase	- 2.1	0.00	- none -
JGY91_09285	Ohr family peroxiredoxin	- 2.1	0.01	Response to oxidative stress
JGY91_06980	Sar: staphylococcal accessory regulator family	- 2.0	0.00	Regulatory functions
-	hypothetical proteins (2)	-	-	-

For TMW 2.1324, 1322 proteins could be identified using whole proteome analysis (48% of total proteins (2736)). Thereof, 31 were found differentially expressed between planktonic and sessile samples (Table 3). This is again a relatively low amount. In planktonic cells of TMW 2.1324 particularly beta-class phenol-soluble modulins were highly abundant compared to their sessile counterparts with log_2 fold differences of 7.0. On the contrary, sessile cells overexpressed proteins associated with anaerobic growth (formate C-acetlytransferase, L-lactate dehydrogenase, acetolactate decarboxylase) as well as proteins related to nitrosative stress (nitric oxide dioxygenase). Similar to TMW 2.1023, sessile samples contained higher amounts of a staphylococcal accessory regulator (Sar) family protein and heme associated proteins (IsdE: heme binding protein).

Table 3: Differentially represented proteins in TMW 2.1324 planktonic *vs.* sessile samples. Proteins that were found in significantly higher amounts in planktonic samples are listed in the upper half of the table and proteins that were found in higher concentrations in sessile samples are listed in the lower half of the table (p-value < 0.05; log2 fold change > 2.0, p-values were adjusted using Benjamini-Hochberg method).

Locustag	Annotation	log2	p.adj	Associated with
JGY90_08925	beta-class phenol-soluble modulin	7.0	0.03	- none -
JGY90_08915	beta-class phenol-soluble modulin	6.9	0.02	- none -
JGY90_12060	class A beta-lactamase	4.5	0.03	Antibiotic resistance
JGY90_05855	3.4-dihydroxy-2-butanone-4-phosphate synthase/GTP cyclohydrolase II	3.9	0.01	Riboflavin, FMN and FAD metabolism
JGY90_09805	glycerophosphodiester phosphodiesterase	2.8	0.02	- none -
JGY90_04055	DUF393 domain-containing protein	2.6	0.01	- none -
JGY90_05190	response regulator transcription factor	2.5	0.02	- none -
JGY90_06995	acetyl-CoA carboxylase biotin carboxyl carrier protein	2.4	0.03	Fatty acid and phospholipid metabolism
JGY90_01630	ABC transporter ATP-binding protein	2.2	0.03	Cations and iron carrying compounds
JGY90_01075	alpha-keto acid decarboxylase family protein	2.1	0.03	Pyruvate metabolism II: acetogenesis from pyruvate
JGY90_09915	YuzD family protein	2.1	0.02	- none -
-	hypothetical proteins (2)	-	-	-
JGY90_05230	formate C-acetyltransferase	- 8.5	0.00	Fermentation: Butanol Biosynthesis
JGY90_05875	L-lactate dehydrogenase	- 7.8	0.00	Fermentation: Anaerobic Glycolysis/gluconeogenesis
JGY90_06875	50S ribosomal protein L33	- 7.4	0.00	Ribosomal proteins: synthesis and modification
JGY90_00220	DUF2648 domain-containing protein	- 6.5	0.00	- none -
JGY90_09375	nitric oxide dioxygenase	- 6.3	0.00	Response to nitrosative stress
JGY90_02725	zinc transporter substrate-binding lipoprotein AdcA	- 6.0	0.01	Transport and binding proteins
JGY90_09795	argininosuccinate synthase	- 5.5	0.00	Amino acid biosynthesis, Glutamate family
JGY90_08085	50S ribosomal protein L33.1	- 4.3	0.05	Ribosomal proteins: synthesis and modification
JGY90_13110	PepSY domain-containing protein	- 4.2	0.01	Sporulation and germination
JGY90_10885	IsdE: heme ABC transporter, heme-binding protein	- 3.0	0.03	Heme, hemin uptake and utilization systems
JGY90_00435	antibiotic biosynthesis monooxygenase	- 2.8	0.02	- none -
JGY90_13105	DUF4889 domain-containing protein	- 2.7	0.01	- none -
JGY90_13575	nitric oxide dioxygenase	- 2.6	0.01	Response to nitrosative stress
JGY90_13085	NDxxF motif lipoprotein	- 2.3	0.02	Protein and peptide secretion and trafficking
JGY90_00235	acetolactate decarboxylase	- 2.0	0.02	Acetoin, butanediol metabolism, fermentation
JGY90_05880	Sar: staphylococcal accessory regulator family	- 2.0	0.04	Regulatory functions
-	hypothetical proteins (2)	-	-	-

Using the same experimental setup, 1367 proteins (49% of total proteins (2782)) of TMW 2.1521 were identified, of which 70 were found significantly differentially expressed. This time, higher amounts of proteins related to pyrimidine and purine ribonucleotide biosynthesis as well as proteins associated with DNA replication, recombination and repair were found in planktonic cells, indicating higher rates of cell division and active metabolism in planktonic compared to sessile cells. Other than that, a higher number of proteins associated with detoxification processes was measured in planktonic samples (Table 4).

Table 4: Differentially represented proteins in TMW 2.1521 planktonic samples (planktonic vs. sessile, grown in Lac^+, pairwise comparison, $p < 0.05$, log_2 fold change > 2)

Locustag	Annotation	log2	p.adj	Associated with
JGY89_02645	D-alanine--poly(phosphoribitol) ligase subunit 2	4.8	0.01	Biosynthesis and degradation of murein sacculus and peptidoglycan
JGY89_13935	CDP-glycerol glycerophosphotransferase family protein	4.4	0.01	Teichoic and lipoteichoic acids biosynthesis
JGY89_07770	tRNA-threonylcarbamoyltransferase complex ATPase subunit type 1 TsaE	3.7	0.01	tRNA and rRNA base modification
JGY89_11370	anaerobic ribonucleoside-triphosphate reductase	3.6	0.01	2-Deoxyribonucleotide metabolism
JGY89_03845	carbamoyl-phosphate synthase large subunit	3.6	0.01	Pyrimidine ribonucleotide biosynthesis
JGY89_14125	DJ-1/PfpI family protein	3.3	0.01	- none -
JGY89_03310	phosphoribosylamine--glycine ligase	2.9	0.01	Purine ribonucleotide biosynthesis
JGY89_13385	PH domain-containing protein	2.9	0.03	- none -
JGY89_07310	ABC transporter ATP-binding protein	2.8	0.03	Cell envelope Transport and binding proteins
JGY89_04655	AI-2E family transporter	2.8	0.01	Sporulation and germination
JGY89_04595	SMC family ATPase	2.8	0.01	DNA replication, recombination, and repair
JGY89_09265	CDP-glycerol glycerophosphotransferase family protein	2.7	0.01	Teichoic and lipoteichoic acids biosynthesis
JGY89_12025	persulfide response sulfurtransferase CstA	2.7	0.01	Detoxification
JGY89_13055	DUF2309 family protein	2.6	0.04	- none -
JGY89_03280	phosphoribosylformylglycinamidine synthase I	2.6	0.01	Purine ribonucleotide biosynthesis
JGY89_03265	5-(carboxyamino)imidazole ribonucleotide synthase	2.5	0.02	Purine ribonucleotide biosynthesis
JGY89_04060	tRNA (guanosine(37)-N1)-methyltransferase TrmD	2.5	0.04	tRNA and rRNA base modification
JGY89_03285	phosphoribosylformylglycinamidine synthase subunit	2.5	0.01	Purine ribonucleotide biosynthesis
JGY89_05735	rhomboid family intramembrane serine protease	2.5	0.03	Peptidyl-prolyl cis-trans isomerase containing cluster
JGY89_04640	alanine:cation symporter family protein	2.4	0.02	- none -
JGY89_13310	xanthine phosphoribosyltransferase	2.3	0.03	Salvage of nucleotides/xanthine metabolism
JGY89_05770	metal ABC transporter ATP-binding protein	2.3	0.05	Transport and binding proteins
JGY89_05225	5-3 exonuclease	2.3	0.02	DNA replication, recombination, and repair
JGY89_12020	persulfide dioxygenase-sulfurtransferase CstB	2.2	0.03	Detoxification
JGY89_11285	oxidoreductase	2.2	0.01	Pantothenate and coenzyme A biosynthesis
JGY89_12915	ABC transporter ATP-binding protein	2.1	0.04	- none -
JGY89_07625	ABC transporter ATP-binding protein	2.1	0.02	- none -
JGY89_10485	ABC transporter ATP-binding protein	2.1	0.04	- none -
JGY89_08145	type II pantothenate kinase	2.1	0.02	Pantothenate and coenzyme A biosynthesis
JGY89_12010	arsenate reductase (thioredoxin)	2.0	0.04	Detoxification
JGY89_01275	ABC transporter ATP-binding protein	2.0	0.04	- none -
JGY89_12400	DHH family phosphoesterase	2.0	0.01	- none -
JGY89_04365	DNA mismatch repair endonuclease MutL	2.0	0.04	DNA replication, recombination, and repair
-	hypothetical protein	-	-	-

Comparing the proteomic profile of TMW 2.1521 sessile cells with that of planktonic cells (Table 5) showed once more the overexpression of proteins related to anaerobic growth in biofilms (L-lactate dehydrogenase, pyruvate formate lyase-activating protein, acetolactate synthase AlsS, nitrate reductase subunit alpha). In TMW 2.1521 sessile cells, a higher number of phage-related proteins (phage major capsid protein, phage tail protein) compared to planktonic cells was also found. Furthermore, sessile samples show a clear stress response to osmotic and nitrosative stress (betaine aldehyde dehydrogenase, nitric oxide dioxygenase)

Table 5: Differentially represented proteins in TMW 2.1521 sessile samples (planktonic vs. sessile, grown in Lac^+, pairwise comparison, $p < 0.05$, log_2 fold change > 2)

Locustag	Annotation	log2	p.adj	Associated with
JGY89_06745	L-lactate dehydrogenase	- 8.0	0.01	Fermentation; Anaerobic Glycolysis/gluconeogenesis
JGY89_04535	50S ribosomal protein L33	- 6.9	0.00	Ribosomal proteins: synthesis and modification
JGY89_07030	formate C-acetyltransferase	- 6.2	0.00	Butanol Biosynthesis; Fermentation
JGY89_06095	CsbD family protein	- 5.9	0.01	- none -
JGY89_09445	nitrate reductase subunit alpha	- 5.3	0.01	Denitrifying reductase gene clusters;Anaerobic
JGY89_12110	DUF2648 domain-containing protein	- 4.2	0.02	- none -
JGY89_02410	phage major capsid protein	- 3.8	0.02	Prophage functions
JGY89_02030	CsbD family protein	- 3.5	0.01	- none -
JGY89_07035	pyruvate formate lyase-activating protein	- 3.0	0.01	Fermentation: Anaerobic Protein modification,repair
JGY89_00945	C1q-binding complement inhibitor VraX	- 2.9	0.01	- none -
JGY89_11010	betaine-aldehyde dehydrogenase	- 2.9	0.01	Choline and Betaine Uptake, Betaine Biosynthesis
JGY89_03250	nitric oxide dioxygenase	- 2.8	0.01	Response to nitrosative stress
JGY89_02435	phage tail protein	- 2.8	0.01	Prophage functions
JGY89_10055	N-acetyltransferase	- 2.7	0.01	- none -
JGY89_09520	DNA-binding protein	- 2.7	0.03	Transcription
JGY89_03630	thioredoxin	- 2.7	0.01	Electron transport
JGY89_13745	GNAT family N-acetyltransferase	- 2.6	0.02	- none -
JGY89_02695	hotdog fold thioesterase	- 2.5	0.02	- none -
JGY89_02295	ERF family protein	- 2.4	0.01	- none -
JGY89_08160	M20 family metallopeptidase	- 2.4	0.02	Degradation of proteins, peptides, and glycopeptides
JGY89_10045	aldehyde dehydrogenase	- 2.4	0.01	Central intermediary metabolism
JGY89_12040	DUF1541 domain-containing protein	- 2.3	0.02	Sporulation and germination
JGY89_03190	SH3-like domain-containing protein	- 2.3	0.01	Adhesins in Staphylococcus
JGY89_04565	DUF896 domain-containing protein	- 2.2	0.02	- none -
JGY89_09365	magnesium transporter CorA family protein	- 2.2	0.03	Magnesium transport
JGY89_06885	PepSY domain-containing protein	- 2.2	0.01	Sporulation and germination
JGY89_12100	acetolactate synthase AlsS	- 2.1	0.01	Fermentation: Acetoin, butanediol metabolism
JGY89_11155	general stress protein	- 2.1	0.04	Stress response
JGY89_05745	50S ribosomal protein L33	- 2.1	0.01	Ribosomal proteins: synthesis and modification
JGY89_08540	translation initiation factor IF-1	- 2.1	0.01	Translation initiation factors bacterial
JGY89_01465	ABC transporter ATP-binding protein/permease	- 2.1	0.02	- none -
-	hypothetical proteins (5)	-	-	-

To analyze the proteome of TMW 2.1523 cells were grown in two different media. Glucose supplemented, lactic acid - acidified medium (Lac^+) like the other strains and, additionally, TSB_N, a protein-rich but monosaccharide - scarce medium, in which cells start to aggregate in a slower and reduced rate. In total 1583 proteins (57% (total encoded proteins: 2771)) were identified. Hereof, 95 proteins were differentially expressed between Lac^+ planktonic and sessile samples and 192 between the two growth stages in TSB_N.

In planktonic Lac^+ samples, higher amounts of proteins related to pyrimidine and purine ribonucleotide biosynthesis were found as well as ribosomal proteins and proteins related to cell division, DNA replication, recombination and repair. Furthermore, proteins involved in vitamin (thiamine, folate) and amino acid (tryptophan, aromatic amino acids, cysteine) biosynthesis were identified in higher quantities, implicating all in all an active cell metabolism, including active transcription and translation processes in the cells. Also, beta-class phenol-soluble modulins were found highly abundant in planktonic cells again (Table 6).

Table 6: Differentially represented proteins in TMW 2.1523 planktonic samples (planktonic vs. sessile, grown in Lac^+, pairwise comparison, $p < 0.05$, log_2 fold change > 2)

Locustag	Annotation	log2	p.adj	Associated with
JGY88_08490	carbamoyl-phosphate synthase large subunit	7.4	0.00	Pyrimidine ribonucleotide biosynthesis
JGY88_10220	glycine cleavage system protein GcvH	6.1	0.00	Energy metabolism; Amino acids and amines
JGY88_08485	orotidine-5-phosphate decarboxylase	6.1	0.00	Pyrimidine ribonucleotide biosynthesis
JGY88_10025	D-alanine--poly(phosphoribitol) ligase subunit 2	5.6	0.00	Biosynthesis/degradation of murein sacculus/peptidoglyc.
JGY88_08500	dihydroorotase	5.1	0.00	Pyrimidine ribonucleotide biosynthesis
JGY88_08640	beta-class phenol-soluble modulin	5.1	0.00	- none -
JGY88_08495	glutamine-hydrolyzing carbamoyl-phosphate synthase small subunit	4.9	0.00	Pyrimidine ribonucleotide biosynthesis
JGY88_08480	orotate phosphoribosyltransferase	4.4	0.00	Pyrimidine ribonucleotide biosynthesis
JGY88_08630	beta-class phenol-soluble modulin	4.4	0.00	- none -
JGY88_08505	aspartate carbamoyltransferase catalytic subunit	4.3	0.00	Pyrimidine ribonucleotide biosynthesis
JGY88_11365	ABC transporter substrate-binding protein	4.1	0.00	- none -
JGY88_00015	S4 domain-containing protein YaaA	3.7	0.03	DNA replication, recombination, and repair
JGY88_14285	plasmid mobilization relaxosome protein MobC	3.5	0.00	- none -
JGY88_04435	copper-sensing transcriptional repressor CsoR	3.5	0.01	Copper Transport System
JGY88_13695	SulP family inorganic anion transporter	3.3	0.01	Cysteine Biosynthesis
JGY88_12265	septum formation initiator family protein	3.2	0.01	Cell division
JGY88_05660	TIGR01212 family radical SAM protein	3.2	0.00	Enzymes of unknown specificity
JGY88_03590	GbsR/MarR family transcriptional regulator	3.1	0.00	- none -
JGY88_04440	heavy-metal-associated domain-containing protein	3.1	0.02	Cations and iron carrying compounds
JGY88_07515	indole-3-glycerol phosphate synthase TrpC	3.0	0.00	Tryptophan synthesis
JGY88_04985	YtxH domain-containing protein	2.9	0.00	- none -
JGY88_12045	50S ribosomal protein L33	2.8	0.01	Ribosomal proteins: synthesis and modification
JGY88_12225	dihydroneopterin aldolase	2.8	0.00	Folate Biosynthesis;
JGY88_14155	replication initiator protein A	2.8	0.01	- none -
JGY88_14235	thioredoxin domain-containing protein	2.8	0.00	- none -
JGY88_08515	uracil phosphoribosyltransferase PyrR, regulator	2.8	0.00	Salvage of nucleosides and nucleotides
JGY88_05535	phosphoenolpyruvate carboxykinase (ATP)	2.8	0.00	Energy metabolism; Pyruvate metabolism I: anaplerotic R.
JGY88_00775	putative glycoside hydrolase	2.7	0.04	- none -
JGY88_14190	zinc ABC transporter substrate-binding protein	2.7	0.00	Transport and binding proteins
JGY88_11070	DUF402 domain-containing protein	2.7	0.00	- none -
JGY88_08510	uracil permease	2.7	0.01	Nucleosides, purines and pyrimidines
JGY88_07615	DUF2089 family protein	2.7	0.00	- none -
JGY88_06635	penicillin-binding protein 2	2.6	0.00	Cell envelope
JGY88_04240	DNA-directed RNA polymerase subunit delta	2.5	0.00	DNA-dependent RNA polymerase
JGY88_14260	Txe/YoeB family addiction module toxin	2.5	0.02	Other Toxin production and resistance
JGY88_04850	NETI motif-containing protein	2.5	0.00	- none -
JGY88_14130	DJ-1/PfpI family protein	2.4	0.00	- none -
JGY88_00640	WXG100 family type VII secretion effector EsxA	2.4	0.00	- none -
JGY88_09120	phosphoribosylformylglycinamidine synthase I	2.4	0.00	Purine ribonucleotide biosynthesis
JGY88_08465	VOC family protein	2.3	0.03	- none -
JGY88_03280	formimidoylglutamase	2.3	0.00	Energy metabolism; Histidine Degradation
JGY88_09130	phosphoribosylaminoimidazolesuccinocarboxamide synthase	2.3	0.01	Purine ribonucleotide biosynthesis
JGY88_03925	DUF2273 domain-containing protein	2.3	0.01	- none -
JGY88_03820	50S ribosomal protein L15	2.2	0.00	Ribosomal proteins: synthesis and modification
JGY88_08115	30S ribosome-binding factor RbfA	2.2	0.00	Transcription
JGY88_07980	RicAFT regulatory complex protein RicA protein	2.2	0.00	- none -
JGY88_04410	hydroxyethylthiazole kinase	2.1	0.01	Biosynthesis of cofactors; Thiamine
JGY88_07505	tryptophan synthase subunit beta	2.1	0.00	Aromatic amino acid biosynthesis
JGY88_10810	ABC transporter permease/substrate-binding protein	2.0	0.01	Choline and Betaine Uptake, Betaine Biosynthesis
JGY88_09155	DUF5011 domain-containing protein	2.0	0.02	- none -
-	hypothetical proteins (11)	-	-	-

Sessile-grown cells again expressed higher amounts of proteins related to anaerobic growth conditions as well as phage-related proteins were found, too. Moreover, stress response-related proteins were highly abundant in sessile cells (nitrosative and oxidative stress). Interestingly, the highest log_2 fold change between sessile compared to planktonic cells was found for a member of the family of general bacterial stress proteins, CsbD (Table 7).

Table 7: Differentially represented proteins in TMW 2.1523 sessile samples (planktonic vs. sessile, grown in Lac+, pairwise comparison, $p < 0.05$, log2 fold change > 2)

Locustag	Annotation	log2	p.adj	Associated with
JGY88_06295	CsbD family protein	-9.5	0.00	- none -
JGY88_06640	50S ribosomal protein L33	-8.1	0.00	Ribosomal proteins: synthesis and modification
JGY88_09405	phage major capsid protein	-4.6	0.01	Prophage functions
JGY88_13180	CoA transferase	-3.9	0.03	Detoxification / Coenzyme A / oxidative stress
JGY88_09380	phage tail protein	-3.8	0.00	Prophage functions
JGY88_05645	L-lactate dehydrogenase	-3.4	0.00	Energy metabolism; Fermentation; Anaerobic Glycolysis/gluconeogenesis
JGY88_09975	hotdog fold thioesterase	-3.4	0.00	- none -
JGY88_10990	ABC transporter ATP-binding protein/permease	-3.3	0.00	- none -
JGY88_04830	nitric oxide synthase oxygenase	-3.3	0.00	- none -
JGY88_03125	L-lactate permease	-3.2	0.00	Transport and binding;
JGY88_14060	excinuclease ABC subunit UvrA	-3.1	0.03	DNA replication, recombination, and repair
JGY88_05345	formate C-acetyltransferase	-3.1	0.00	Energy metabolism; Fermentation; Butanol Biosynthesis;
JGY88_10985	thiol reductant ABC exporter subunit CydC	-2.8	0.03	- none -
JGY88_01400	betaine-aldehyde dehydrogenase	-2.7	0.00	Choline and Betaine Uptake and Betaine Biosynthesis;
JGY88_09150	nitric oxide dioxygenase	-2.7	0.00	Response to nitrosative stress
JGY88_02105	pyruvate oxidase	-2.7	0.00	Energy metabolism, aerobic
JGY88_13215	amidohydrolase	-2.6	0.01	Degradation of proteins, peptides, glycopeptides
JGY88_03310	amidohydrolase	-2.5	0.00	Degradation of proteins, peptides, glycopeptides
JGY88_00955	phenolic acid decarboxylase	-2.4	0.04	- none -
JGY88_09560	phage antirepressor KilAC domain-containing protein	-2.4	0.00	- none -
JGY88_07000	HU family DNA-binding protein	-2.4	0.00	DNA metabolism
JGY88_09540	DUF1071 domain-containing protein	-2.3	0.02	- none -
JGY88_11735	NtaA/DmoA family FMN-dependent monooxygenase	-2.2	0.04	- none -
JGY88_02255	N-acetylmannosamine-6-phosphate 2-epimerase	-2.1	0.01	Sialic Acid Metabolism
JGY88_10355	CsbD family protein	-2.1	0.00	- none -
JGY88_00265	amidase domain-containing protein	-2.1	0.05	- none -
JGY88_09890	argininosuccinate synthase	-2.0	0.00	Amino acid biosynthesis; Glutamate family
JGY88_12860	DUF4889 domain-containing protein	-2.0	0.02	- none -
JGY88_00215	acetolactate synthase AlsS	-2.0	0.00	Fermentation; Acetoin, butanediol metabolism;
JGY88_05340	pyruvate formate lyase-activating protein	-2.0	0.01	Energy metabolism; anaerobic Protein mod. and repair
JGY88_04075	phosphoglucosamine mutase	-2.0	0.00	Biosynthesis and degradation of murein sacculus and peptidoglycan
-	hypothetical proteins (3)	-	-	-

In carbohydrate-low, protein-rich TSB_N medium, planktonic cells expressed higher amounts of beta-class phenol-soluble modulins compared to their sessile counterparts. Also, ribosomal proteins and further proteins involved in active metabolism were identified in higher quantities than in sessile samples. Moreover, a wide range of staphylococcal surface proteins, some of them related to adhesion (SxsA, G-related albumin-binding module containing proteins, fibrinogen binding adhesin) appeared as more abundant in planktonic compared to sessile samples (Tables 8 and 9).

Table 8: Differentially represented proteins in TMW 2.1523 planktonic samples grown in TSB_N (planktonic vs. sessile, pairwise comparison, $p < 0.05$, log2 fold change > 2)

Locustag	Annotation	log2	p.adj	Associated with
JGY88_08640	beta-class phenol-soluble modulin	9.4	0.00	- none -
JGY88_08630	beta-class phenol-soluble modulin	7.4	0.00	- none -
JGY88_08380	50S ribosomal protein L28	5.8	0.00	Ribosomal proteins: synthesis and modification
JGY88_10640	CHAP domain-containing protein	5.7	0.00	Sporulation and germination
JGY88_11875	class A beta-lactamase	5.5	0.00	- none -
JGY88_03790	type Z 30S ribosomal protein S14	5.4	0.00	Ribosome SSU bacterial;
JGY88_10545	immunodominant antigen B	5.3	0.00	- none -
JGY88_12550	YSIRK-type signal peptide-containing protein	5.2	0.00	YSIRK family
JGY88_02080	CHAP domain-containing protein	5.1	0.00	- none -
JGY88_01140	YSIRK-type signal peptide-containing protein_bap	5.1	0.00	YSIRK family
JGY88_08900	YlaN family protein	4.5	0.00	- none -
JGY88_09900	glycerophosphodiester phosphodiesterase	4.5	0.00	- none -
JGY88_00885	transglycosylase family protein	4.4	0.00	- none -
JGY88_00265	amidase domain-containing protein	4.4	0.00	- none -
JGY88_11760	fibrinogen-binding adhesin SdrG	4.2	0.00	YSIRK family
JGY88_01880	transglycosylase	4.0	0.00	- none -
JGY88_01050	YSIRK-type signal peptide-containing protein_sxsA	3.8	0.00	YSIRK family
JGY88_14295	ribbon-helix-helix domain-containing protein	3.7	0.00	- none -
JGY88_08910	DUF2197 domain-containing protein	3.7	0.00	- none -
JGY88_12265	septum formation initiator family protein	3.6	0.00	Cell division
JGY88_07810	30S ribosomal protein S14	3.4	0.02	Ribosome SSU bacterial;
JGY88_00260	GA module-containing protein_GA2	3.4	0.00	Adhesins in Staphylococcus, LPxTG
JGY88_04435	copper-sensing transcriptional repressor CsoR	3.3	0.00	Copper Transport System
JGY88_13900	helix-turn-helix transcriptional regulator	3.3	0.00	Regulatory functions
JGY88_01895	copper chaperone CopZ	3.3	0.00	Copper Transport System
JGY88_13950	GA module-containing protein_GA1	3.1	0.00	Adhesins in Staphylococcus, LPxTG
JGY88_08820	50S ribosomal protein L32	3.1	0.00	Ribosomal proteins: synthesis and modification
JGY88_02350	N-acetyltransferase	3.1	0.00	Ribosomal proteins: synthesis and modification
JGY88_12530	LysM peptidoglycan-binding domain-containing protein	3.1	0.00	Sporulation and germination
JGY88_14025	protein rep	3.1	0.03	- none -
JGY88_13995	arsenate reductase (thioredoxin)	3.1	0.02	Detoxification / oxidative stress
JGY88_14115	recombinase family protein	3.0	0.01	- none -
JGY88_02450	DUF2188 domain-containing protein	3.0	0.01	- none -
JGY88_04260	helix-turn-helix transcriptional regulator	3.0	0.00	- none -
JGY88_00485	antibiotic biosynthesis monooxygenase	3.0	0.00	- none -
JGY88_00865	DM13 domain-containing protein	3.0	0.00	- none -
JGY88_02995	DUF3139 domain-containing protein	3.0	0.00	- none -
JGY88_14285	plasmid mobilization relaxosome protein MobC	2.9	0.00	- none -
JGY88_00615	melibiose:sodium transporter MelB	2.9	0.00	Carbohydrates, organic alcohols, and acids
JGY88_12045	50S ribosomal protein L33	2.8	0.01	Ribosomal proteins: synthesis and modification
JGY88_13020	DUF951 domain-containing protein	2.8	0.00	- none -
JGY88_07550	helix-turn-helix transcriptional regulator	2.7	0.00	- none -
JGY88_10835	polyglycerol-phosphate lipoteichoic acid synthase LtaS	2.7	0.00	Polyglycerolphosphate lipoteichoic acid biosynthesis
JGY88_09555	DUF771 domain-containing protein	2.7	0.01	- none -
JGY88_07640	4-oxalocrotonate tautomerase	2.6	0.00	Energy metabolism
JGY88_14130	DJ-1/PfpI family protein	2.6	0.00	- none -
JGY88_03815	50S ribosomal protein L30	2.6	0.00	Ribosomal proteins: synthesis and modification
JGY88_07615	DUF2089 family protein	2.6	0.00	- none -
JGY88_08450	DNA-directed RNA polymerase subunit omega	2.6	0.00	DNA-dependent RNA polymerase
JGY88_02540	DUF1413 domain-containing protein	2.6	0.00	- none -
JGY88_12955	LysM peptidoglycan-binding domain-containing protein	2.5	0.00	Adhesin in Staphylococcus
JGY88_02045	helix-turn-helix transcriptional regulator	2.5	0.00	- none -
JGY88_13580	replication initiator protein A	2.5	0.01	- none -

Table 9: Continued. Differentially represented proteins in TMW 2.1523 planktonic samples grown in TSB_N (planktonic vs. sessile, pairwise comparison, $p < 0.05$, log2 fold change > 2)

Locustag	Annotation	log2	p.adj	Associated with
JGY88_10160	DUF1433 domain-containing protein	2.4	0.02	- none -
JGY88_09055	DUF697 domain-containing protein	2.4	0.00	- none -
JGY88_09210	glucosaminidase domain-containing protein	2.4	0.00	Adhesin in Staphylococcus
JGY88_14015	helix-turn-helix transcriptional regulator	2.3	0.03	Regulatory functions
JGY88_06520	30S ribosomal protein S21	2.2	0.00	Ribosomal proteins: synthesis and modification
JGY88_04985	YtxH domain-containing protein	2.2	0.00	- none -
JGY88_10015	NifU family protein	2.2	0.00	- none -
JGY88_00745	helix-turn-helix transcriptional regulator	2.2	0.00	DNA interactions
JGY88_08265	50S ribosomal protein L19	2.2	0.00	Ribosomal proteins: synthesis and modification
JGY88_06655	YqgQ family protein	2.2	0.00	- none -
JGY88_05505	PepSY domain-containing protein	2.2	0.00	Sporulation and germination
JGY88_14235	thioredoxin domain-containing protein	2.1	0.00	- none -
JGY88_09050	phosphocarrier protein HPr	2.1	0.00	Fructose utilization; PTS
JGY88_06065	50S ribosomal protein L20	2.1	0.00	Ribosomal proteins: synthesis and modification
JGY88_07180	NifU N-terminal domain-containing protein	2.1	0.00	- none -
JGY88_01785	winged helix DNA-binding protein	2.1	0.00	Regulatory functions
JGY88_00520	5-nucleotidase lipoprotein e(P4) family	2.1	0.00	Other Pyridine nucleotides
JGY88_08305	putative DNA-binding protein	2.1	0.05	- none -
JGY88_08055	helix-turn-helix domain-containing protein	2.0	0.00	- none -
JGY88_00240	TIR domain-containing protein	2.0	0.00	- none -
JGY88_03840	50S ribosomal protein L36	2.0	0.03	Ribosomal proteins: synthesis and modification
JGY88_14255	type II toxin-antitoxin system Phd/YefM family antitoxin	2.0	0.00	Toxin-antitoxin replicon stabilization systems
JGY88_03150	MarR family transcriptional regulator	2.0	0.01	- none -
JGY88_05660	TIGR01212 family radical SAM protein	2.0	0.01	- none -
JGY88_06615	metal ABC transporter ATP-binding protein	2.0	0.04	- none -
JGY88_03130	glycosyltransferase family 4 protein	2.0	0.00	Glutathione and analogs
JGY88_09620	DUF2187 family protein	2.0	0.00	- none -
-	hypothetical proteins (23)	-	-	-

On the contrary, sessile samples showed a clear fermentative metabolism again. Furthermore, a high number of enzymes generally related to energy metabolism as well as a high amount of amino acid synthases, was detected (Tables 10 and 11).

Table 10: Differentially represented proteins in TMW 2.1523 sessile samples grown in TSB_N (planktonic vs. sessile, pairwise comparison, $p < 0.05$, log2 fold change > 2)

Locustag	Annotation	log2	p.adj	Associated with
JGY88_05345	formate C-acetyltransferase	-9.7	0.00	Energy metabolism, Fermentation; Butanol Biosynthesis;
JGY88_00640	WXG100 family type VII secretion effector EsxA	-6.6	0.00	- none -
JGY88_07855	aspartate kinase	-5.2	0.00	Amino acid biosynthesis; Aspartate family
JGY88_06395	acetyl-CoA carboxylase biotin carboxylase subunit	-4.9	0.00	Fatty acid and phospholipid metabolism
JGY88_05645	L-lactate dehydrogenase	-4.8	0.00	Fermentation; Anaerobic Glycolysis/gluconeogenesis
JGY88_00835	glucose 1-dehydrogenase	-4.6	0.00	- none -
JGY88_13455	CDP-glycerol glycerophosphotransferase family protein	-4.6	0.01	Biosynthesis and degradation of surface polysaccharides and lipopolysaccharides
JGY88_04590	acetolactate synthase small subunit	-4.4	0.00	Amino acid biosynthesis; Pyruvate family
JGY88_09150	nitric oxide dioxygenase	-4.3	0.00	Energy metabolism
JGY88_00845	NAD-dependent succinate-semialdehyde dehydrogenase	-4.2	0.00	Central intermediary metabolism
JGY88_03125	L-lactate permease	-4.2	0.00	Transport and binding proteins;
JGY88_06805	dihydrolipoyl dehydrogenase	-4.2	0.00	Dehydrogenase complexes;
JGY88_13215	amidohydrolase	-4.2	0.00	Degradation of proteins, peptides, and glycopeptides
JGY88_04585	ketol-acid reductoisomerase	-4.2	0.00	Amino acid biosynthesis; Pyruvate family
JGY88_01310	pyruvate phosphate dikinase	-4.1	0.00	Energy metabolism; Glycolysis and Gluconeogenesis;
JGY88_11245	metal ABC transporter ATP-binding protein	-4.0	0.00	- none -
JGY88_01160	DsbA family protein	-4.0	0.05	- none -
JGY88_01315	kinase/pyrophosphorylase	-3.9	0.00	- none -
JGY88_03300	imidazolonepropionase	-3.9	0.00	Energy metabolism; Histidine Degradation
JGY88_11255	zinc ABC transporter substrate-binding protein	-3.9	0.00	- none -
JGY88_12995	amino acid adenylation domain-containing protein	-3.9	0.01	- none -
JGY88_06385	biotin-dependent carboxyltransferase family protein	-3.9	0.00	- none -
JGY88_02310	glycoside hydrolase family 1 protein	-3.9	0.00	- none -
JGY88_06350	DUF1292 domain-containing protein	-3.8	0.01	- none -
JGY88_13880	AbrB/MazE/SpoVT family DNA-binding domain-containing protein	-3.6	0.00	DNA interactions; regulatory functions
JGY88_14085	3-hexulose-6-phosphate synthase	-3.6	0.01	- none -
JGY88_02760	M20/M25/M40 family metallo-hydrolase	-3.5	0.01	Arginine and Ornithine Degradation
JGY88_10945	DNA-binding protein	-3.5	0.02	- none -
JGY88_14180	metal ABC transporter ATP-binding protein	-3.5	0.00	- none -
JGY88_10985	thiol reductant ABC exporter subunit CydC	-3.4	0.01	- none -
JGY88_02505	glycoside hydrolase family 3 protein	-3.3	0.00	- none -
JGY88_00840	glutamine synthetase	-3.3	0.00	Amino acid biosynthesis; Glutamate family
JGY88_04830	nitric oxide synthase oxygenase	-3.2	0.00	- none -
JGY88_11800	ribulokinase	-3.2	0.00	Energy metabolism, sugars
JGY88_01745	urease subunit gamma	-3.2	0.01	Nitrogen metabolism
JGY88_05340	pyruvate formate lyase-activating protein	-3.1	0.00	Fermentations; Anaerobic Protein modification and repair
JGY88_13155	efflux RND transporter periplasmic adaptor subunit	-3.0	0.00	Transport and binding proteins
JGY88_01780	ABC transporter substrate-binding protein	-3.0	0.00	- none -
JGY88_11415	sugar phosphate isomerase/epimerase	-3.0	0.01	- none -
JGY88_13265	adenosine deaminase	-2.9	0.00	Purine conversions
JGY88_07980	RicAFT regulatory complex protein RicA	-2.9	0.00	- none -
JGY88_00215	acetolactate synthase AlsS	-2.7	0.00	Fermentation; Acetoin, butanediol metabolism;
JGY88_03310	amidohydrolase	-2.7	0.00	Protein fate
JGY88_07410	4-hydroxy-tetrahydrodipicolinate synthase	-2.7	0.00	Amino acid biosynthesis; Aspartate family
JGY88_04580	2-isopropylmalate synthase	-2.6	0.01	Amino acid biosynthesis; Pyruvate family
JGY88_04440	heavy-metal-associated domain-containing protein	-2.6	0.03	- none -
JGY88_10990	ABC transporter ATP-binding protein/permease	-2.6	0.00	- none -
JGY88_11075	5-methyltetrahydropteroyltriglutamate- homocysteine S-methyltransferase	-2.6	0.00	Amino acid biosynthesis; Aspartate family
JGY88_06400	5-oxoprolinase subunit PxpA	-2.6	0.02	- none -
JGY88_12805	L-serine ammonia-lyase iron-sulfur-dependent subunit β	-2.5	0.01	Energy metabolism; Glycine and Serine Utilization;
JGY88_10955	malate dehydrogenase	-2.5	0.00	Energy metabolism; TCA cycle
JGY88_14190	zinc ABC transporter substrate-binding protein	-2.5	0.00	Transport and binding proteins
JGY88_00220	acetolactate decarboxylase	-2.5	0.00	Fermentation; Acetoin, butanediol metabolism;
JGY88_02295	NAD(P)H-dependent oxidoreductase	-2.5	0.00	Flavodoxin;
JGY88_08505	aspartate carbamoyltransferase catalytic subunit	-2.4	0.01	Pyrimidine ribonucleotide biosynthesis

Table 11: Continued. Differentially represented proteins in TMW 2.1523 sessile samples grown in TSB_N (planktonic vs. sessile, pairwise comparison, $p < 0.05$, log2 fold change > 2)

Locustag	Annotation	log2	p.adj	Associated with
JGY88_10805	histidinol-phosphate transaminase	-2.4	0.00	Amino acid biosynthesis; histidine family
JGY88_13425	acyl-CoA thioesterase	-2.4	0.00	- none -
JGY88_01910	ABC transporter ATP-binding protein	-2.4	0.00	Protein fate
JGY88_03355	HAD-IA family hydrolase	-2.4	0.00	- none -
JGY88_13150	ABC transporter ATP-binding protein	-2.4	0.00	Protein fate
JGY88_00555	nickel ABC transporter nickel/metallophore periplasmic binding protein	-2.4	0.00	Cations and iron carrying compounds
JGY88_11080	cupin domain-containing protein	-2.3	0.04	- none -
JGY88_04060	arginase	-2.3	0.00	Arginine and Ornithine Degradation
JGY88_09735	truncated hemoglobin	-2.3	0.00	Bacterial hemoglobins
JGY88_04595	biosynthetic-type acetolactate synthase large subunit	-2.3	0.00	Acetoin, butanediol metabolism;pyruvate family
JGY88_13050	alpha-glucosidase/alpha-galactosidase	-2.3	0.00	- none -
JGY88_11780	agmatinase family protein	-2.2	0.00	- none -
JGY88_07465	oligoendopeptidase F	-2.2	0.00	Degradation of proteins, peptides, and glycopeptides
JGY88_01125	3-methyl-2-oxobutanoate hydroxymethyltransferase	-2.2	0.00	Pantothenate and coenzyme A biosynthesis
JGY88_07740	aconitate hydratase AcnA	-2.2	0.00	Energy metabolism; TCA cycle
JGY88_03670	efflux RND transporter permease subunit	-2.2	0.03	- none -
JGY88_12685	allantoinase AllB	-2.2	0.02	- none -
JGY88_12580	ketoacyl-ACP synthase III	-2.2	0.00	- none -
JGY88_10785	peptide MFS transporter	-2.1	0.01	- none -
JGY88_06390	acetyl-CoA carboxylase biotin carboxyl carrier protein subunit	-2.1	0.01	Fatty acid and phospholipid metabolism
JGY88_13145	ABC transporter permease	-2.1	0.02	- none -
JGY88_08750	succinate dehydrogenase iron-sulfur subunit	-2.1	0.00	Aerobic Anaerobic TCA cycle
JGY88_04720	bacillithiol transferase BstA	-2.1	0.02	- none -
JGY88_03570	UDP-glucose--hexose-1-phosphate uridylyltransferase	-2.1	0.00	Energy metabolism; Lactose, Galactose Uptake, Utilization
JGY88_00040	histidine ammonia-lyase	-2.1	0.03	Energy metabolism; Amino acids and amines
JGY88_04825	prephenate dehydratase	-2.1	0.02	Phenylalanine and Tyrosine Branches from Chorismate
JGY88_05930	aminopeptidase P family protein	-2.1	0.00	- none -
JGY88_03495	DoxX family protein	-2.1	0.04	- none -
JGY88_05925	copper homeostasis protein CutC	-2.1	0.00	Copper homeostasis: copper tolerance
JGY88_03040	glucose 1-dehydrogenase	-2.0	0.00	- none -
JGY88_04185	purine-nucleoside phosphorylase	-2.0	0.00	Salvage of nucleosides and nucleotides
-	hypothetical proteins (3)	-	-	-

Cells within a biofilm encounter different growth conditions than cells grown planktonically. In biofilms, oxygen and nutrient concentrations are scarce, forcing cells to lower their metabolic activity and down-regulate the biosynthesis of DNA, proteins and cell components (Otto, 2008; Schilcher and Horswill, 2020). This dormant-like, persistent state is an ideal response of bacteria to unfavorable or stressful environmental conditions and results in cells being less susceptible to e.g., starvation and the hosts immune response as well as less targetable for antibiotics, antibacterial peptides and other antimicrobial substances (Yao et al., 2005; Jones and Lennon, 2010). Nevertheless, biofilms remain dynamic structures, with steady cell accumulation and detachment processes. Furthermore, the higher oxygen and nutrient availability in the outer parts of a biofilm results in heterogenic populations, with different physiological states causing distinct gene expression patterns of the various subpopulations (Stewart, 2002).

One of the main metabolic changes usually reported in biofilm cells is the switch to fermentative energy gain due to the low oxygen concentrations, inducing metabolic pathways associated with fermentation such as acetoin metabolism (Beenken et al., 2004; Otto, 2008). Subsequently,

staphylococci try to conquer the low pH resulting from fermentative acid accumulation by up-regulating genes involved in the urease and arginine deiminase pathway (Beenken et al., 2004).

Facing and responding to unfavorable environmental conditions is again done in a species-specific way. A good example is the response of two different CoNS to nutrient deficiency. Hereby, *S. haemolyticus* was found to use phosphatidylglycerol and diglucosyl-diacylglycerol to build a lipidome, *S. epidermidis* on the other hand responded by accumulating cardiolipin and / or lyso-cardiolipin (Luo et al., 2018).

We also found strain-specific protein expression profiles in planktonic and sessile cells, demonstrated by the description of the proteomic profiles of each sample as well as seen by the varying amount of differentially expressed proteins found for each strain. Nonetheless, taken together, across samples, we observed higher amounts of proteins related to purine and pyrimidine ribonucleotide biosynthesis, cell division, replication and repair in planktonic cells. The reason for this is that such active cell processes are usually downregulated in sessile cells therefore levels of proteins related to fast-growing cells are higher in planktonic samples (Leroy et al., 2021). Additionally, one of the most evident results was the significantly higher amount of beta-class phenol-soluble modulins (PSMs) in planktonic compared to sessile samples. PSMs are short, amphipathic peptides, which are important for biofilm structuring (e.g. channel formation) and cell dispersal (Otto, 2014; Schilcher and Horswill, 2020). They are directly controlled by the quorum-sensing system Agr with the absence of Agr resulting in low PSM concentrations and thick biofilms (Le et al., 2019). Of note, gene expression of the *agr* operon is reported to be lower in biofilms (Yao et al., 2005). PSMs are usually expressed in very high quantities as one of their leading physiological roles is to enable cells to grow at oil/water interfaces (e.g. skin) due to their surfactant-like properties (Peschel and Otto, 2013; Otto, 2014). Therefore, we speculate that the high discrepancy measured between planktonic and sessile samples is most likely due to a much lower abundance of PSMs in sessile samples compared to their planktonic counterparts. Such differences have been reported by others as well (Yao et al., 2005). One could suggest that the PSM downregulation in “young” biofilms (in this study, the biofilm was 24 hours old, far away from being mature) is due to their putative biofilm-inhibitory properties as well as to protect the biofilm from the destructive properties of PSMs that lead to a dispersal of mature biofilms during later stages (Otto, 2014). Interestingly, in TMW 2.1523 planktonic cells (TSB_N), a wide range of surface adhesins was found in significantly higher amounts than in their sessile counterparts. The expression of surface proteins is known to be highly dependent on growth stage and growth conditions (Foster et al., 2014), underlining again that the cell aims

for adherence and colonization of new niches during planktonic growth. Other authors reported the downregulation of surface adhesins like Aap in biofilms as well, referring to the fact that surface adhesins, especially those involved in initial attachment, are not required in established biofilms anymore (Yao et al., 2005).

On the contrary, in sessile samples, many proteins involved in anaerobic energy metabolism (fermentation) were identified in higher intensities than in planktonic samples, with formate C-acetyltransferase, acetolactate decarboxylase and synthase, as well as L-lactate dehydrogenase being prominently represented in the data. Their presence indicates a partial glucose metabolism with pyruvate most likely being catabolized to lactate, acetoin and formate through lactate dehydrogenase, butanediol and formate-lyase pathways, similar as reported for *S. aureus* USA200 and USA300 (Zhu et al., 2007). Furthermore, nitrate instead of oxygen might serve as terminal electron acceptor during anaerobic growth since nitrate reductase subunits were found in high quantities in sessile samples of TMW 2.1023 and TMW 2.1521. This is in complete concordance with the literature that reported a switch to fermentation pathways in sessile samples for other staphylococci such as *S. aureus* and *S. epidermidis* as well (Yao et al., 2005; Uribe-Alvarez et al., 2016; Martínez-García et al., 2021; Piras et al., 2021). Despite the presence of nitrate reductase subunit alpha, TMW 2.1023 sessile cells were the only ones in which switch to fermentative energy gain was not as prominently represented by the respective enzymes as in the other strains. An explanation could be that TMW 2.1023 is the lowest biofilm producer of all measured strains, forming only thin layers of biofilm on abiotic surfaces. Such a thin biofilm layer might still provide enough oxygen to the cells to continue the more efficient aerobic energy metabolism. Sessile cells also overexpressed proteins related to stress responses therefore higher levels of proteins involved in detoxification and osmoprotectant synthesis were identified. Nitric oxide dioxygenase (nitrosative stress), betaine-aldehyde dehydrogenase (osmotic stress), CoA transferase (oxidative stress) and general stress proteins were overrepresented in many of the sessile samples. This is in concordance with other proteomic studies that reported the upregulation of genes associated with osmoprotection, detoxification and resistance in sessile samples (Leroy et al., 2021; Yao et al., 2005; Planchon et al., 2009). In biofilms, cells experience scarce oxygen and nutrient availability, high cell densities, decreased pH and high levels of metabolic waste products as well as reactive oxygen and nitrogen species (Fey and Olson, 2010). Staphylococci therefore seem to upregulate a global stress response so that cells can adapt to the closed environment encountered in biofilms. Here it should be noted that while biofilms protect cells from external stressors (immune system, antimicrobials), they also pose a challenge to the bacterium, to which it reacts with multiple stress responses. Also,

more prevalent in sessile samples than their planktonic counterparts were proteins associated to bacteriophages. Phage-related proteins were found in sessile samples of two strains, TMW 2.1521 and TMW 2.1523. Both strains harbor intact prophages in their genome (Figure 7). Phage-release is commonly occurring in *S. aureus* biofilms (Resch et al., 2005) but also in *S. xylosus* biofilms, where phage-mediated lysis results in nutrient and eDNA release, thereby contributing to persistence, cell survival and biofilm integrity (Leroy et al., 2021). It would be interesting to test the eDNA content of the biofilms of these two strains compared to the others. In general, proteomic differences were more pronounced and in total more proteins were differentially expressed in the strong biofilm-producing strain TMW 2.1523. This is most likely because the high biofilm mass enables an increased protein mass to be subjected to analysis, resulting in better resolved and more accurate results. Yet, the study's experimental design had its weaknesses, which are hard to overcome. Strains other than TMW 2.1523 do not adhere well to surfaces in $TSB_{N,}$ therefore they could not be sampled in this less autoaggregation inducing medium. These strains seem to be dependent on the presence of fermentation induced acidosis instead. A drop in pH causes almost all staphylococcal cells to aggregate, thereby favoring biofilm formation. This in turn is reflected in the proteomic analyses, as the cells in planktonic culture obviously start to aggregate in the same way as they do in sessile samples, just not adhering to surfaces. Noteworthy here is a study by Bottagisio et al., (2019), elucidating the effect of shear forces that trigger the expression of cell aggregating proteins, which results in a biofilm-like behavior of planktonic cells. Therefore, one should keep in mind that one is comparing floating biofilms to adherent biofilms to a large extent. Nevertheless, planktonic samples represent an artificial system in which bacteria are unnaturally grown, primarily due to the high shear forces acting on them through vigorous agitation. Furthermore, as mentioned above, biofilms express heterogeneous phenotypes, with differential gene expression of the single cells, especially between outer and inner layers of the biofilm (Stewart and Franklin, 2008). Thus, when sampling biofilm cells, one scrapes off the entire film. Therefore, a proteomic profile of the entire heterogenic population is created, which complicates data analysis.

In conclusion, we were able to identify differences in metabolism between sessile and planktonic growth, mostly related to oxygen availability and stress response. When such studies are interpreted with care, always keeping in mind the difficulties in appropriate experimental design, they can provide valuable knowledge on the physiological adjustments of biofilms cells and the understanding of strain-dependent cellular mechanisms responding to environmental *stimuli*, also illustrated by the heterogenic protein profiles we obtained. Such studies emphasize again that the favored lifestyle of staphylococci is to form aggregates and colonize habitats.

5 Discussion

Resuming the original hypotheses made for this thesis, presented in chapter 2, one can conclude that biofilm formation by *S. xylosus* is indeed strain-specific and dependent on surface hydrophobicity of cells and matrices as well as heavily influenced by environmental factors in particular (fermentation induced-) acidity, which however stops at values of around pH 5. Additionally, the presence of calcium is essential for biofilm development of *S. xylosus*. Genes mediating biofilm formation of *S. xylosus* can be identified using bioinformatic screenings, yet the sheer presence of genes and their homologs have to be considered with care. This thesis shows that the function of Bap in *S. xylosus* differs from that described for *S. aureus*, which reminds us that gene functions cannot easily be extrapolated to their homologs in other species. The discovery of the novel *Staphylococcus xylosus* surface protein A (SxsA) shows that different mechanisms encompassing different proteins can be effective in biofilm formation of different species. Thus, simply screening for the presence or absence of genes could lead to incorrect predictions of phenotypes, especially as one should also bear in mind that TMW 2.1602 is SxsA-positive but still biofilm negative. In this context, it needs to be stressed again that each strain carries a slightly different set of genes and transcriptional regulators mediating biofilm formation, which again influences the adherence behavior and response to environmental changes. Generic approaches, such as those used in this work, which employ functional gene modules rather than just gene homologies, can open up the view on "homology searches" also beyond staphylococci or biofilm formation.

Using the transformation system, optimized in this work, allows to transform at least some of the *S. xylosus* wildtype strains, despite low transformation efficiencies, and subsequently genetically manipulate to elucidate biofilm formation mechanisms of the species further and identify new genes involved. When applying whole proteome analysis to investigate physiological differences between planktonic and sessile cells, the complexity of generating an appropriate experimental setup needs to be kept in mind. This is because *S. xylosus* prefers to reside in aggregates, even when living a "planktonic" lifestyle, especially when exposed to high shear forces and pH values below 6. Still, differences in metabolism related to the conditions prevailing in biofilms, in particular low oxygen availability were identified. Within strain-specific differential proteomes, overlapping responses were observed in all strains, predicting enhanced fermentative metabolism in large cell aggregates and biofilms. At the same time, phenol-soluble modulins were much more abundant in planktonic than in sessile samples, most likely related to their biofilm-destructive properties. Finally, this work underlines how coping with stress

factors provided by the natural and man-made habitats forced staphylococci including *S. xylosus* to express a strongly adhesive and biofilm forming phenotype. Hereby the organism retains the abundance of multiple, supposedly redundant mechanisms in order to ensure colonization and thereby protecting the cells from physical and chemical environmental factors.

5.1 Biofilm formation by *S. xylosus* is strain-specific and influenced by environmental factors

Staphylococci have taken on the mantra to "stick to surfaces at all costs" (Zapotoczna et al., 2016). The ability to adhere and form biofilms is well established within the genus with a remarkable variety of adhesion and biofilm forming mechanisms. The reason why they exhibit such a strong adhesion behavior can be found when considering their natural habitat. *Staphylococcus spp.* are mostly commensals of the epithelia of (mammal) skin, with different species preferring different niches on the body (Vos et al., 2009; Byrd et al., 2018). Here they have to cope with stress factors such as mechanical stress e.g. by epithelial turnover, UV radiation, relatively high NaCl concentration, mostly low water availability, reduced pH values between 4 - 6 (depending on body site) as well as the hosts immune system (Otto, 2014). Strong adherence as well as embedding their cells into a thick, protective exopolymer matrix, helps them to conquer the environmental adversities (Donlan, 2002). Staphylococci, in particular CoNS, are known for their extraordinary ability to colonize surfaces (Otto, 2009). Therefore, as already mentioned, they encode a whole set of genes enabling them to colonize a surface and form a biofilm (Götz, 2002; Otto, 2008; An and Friedman, 2010; Schiffer et al., 2019). Mechanisms and intensity with which they adhere to a surface and start to form a biofilm differ between species and strains and are further influenced by the type of surface (abiotic vs. biotic, hydrophobic vs. hydrophilic) as well as environmental factors, e.g. pH and osmotic pressure (Moretro et al., 2003; Planchon et al., 2006; Karatan and Watnick, 2009; Lawal et al., 2021). In Schiffer et al., (2019) we confirmed that *S. xylosus* forms biofilm with strain-specific differences in intensities and that strains react differently to growth medium composition with regard to glucose availability, pH values and presence of sodium chloride or lactic acid. Such environmental influences are in concordance with published data for other staphylococci as already discussed in Schiffer et al., (2019) and are mostly related to growth conditions influencing cell surface charge, thereby affecting hydrophobic and electrostatic interactions. Additionally, factors such as mechanical signals, oxygen, iron and nutrient availability regulate gene expression (Karatan and Watnick, 2009). Next to the described factors presented in the paper, we have also tested biofilm formation under other growth conditions derived from the environment encountered by

S. xylosus when it is used as a meat starter, such as meat simulation medium or TSB complemented with 2% glucose or 5 mmol nitrite. Yet their addition did not affect biofilm formation to the extent that glucose, sodium chloride and lactic acid did and were therefore excluded from the respective manuscript. Still, nitrite is a good example to show how the environment influences biofilm formation in a strain/species specific manner. Nitrite addition has been previously reported to successfully inhibit biofilm formation of *S. aureus* and *S. epidermidis* (Schlag et al., 2007). The inhibiting effect was attributed to nitrite interfering with the expression of the *ica* operon, responsible for polysaccharide (PIA) - mediated biofilm formation of the organisms. Since the here studied *S. xylosus* strains are all *ica* negative (Schiffer et al., 2019), a similar inhibiting effect was unlikely to occur. The example of nitrite also demonstrates how differences in strain-specific adherence behavior are often attributed to different genomic backgrounds. To increase our understanding of the distribution of biofilm-associated genes within the species *S. xylosus*, we screened five different strains for the presence of biofilm mediating genes previously described for *S. aureus* and *S. epidermidis* (Schiffer et al., 2019). Yet, the screening revealed that only a few homologs were present in *S. xylosus*. Particularly noticeable was that some of the well-known proteins belonging to the microbial surface components recognizing adhesive matrix molecules (MSCRAMMs) that mediate attachment to host matrix proteins were missing in *S. xylosus*. For example, no homologs to SD-repeat containing proteins (Josefsson et al., 1998; McCrea et al., 2000), the collagen adhesin (Patti et al., 1992) or clumping factors A and B (McDevitt et al., 1994; Ní Eidhin et al., 1998) were identified. Since *S. xylosus* is able to colonize surfaces and biotic materials successfully, the genetic screening implicates that the organism must encode a different set of genes enabling the same function. In terms of MSCRAMMs, genome screening identified proteins with fibrinogen/fibronectin, elastin, laminin, and albumin binding domains among the selected *S. xylosus* strains (Schiffer et al., 2019 + unpublished results). Basically, it underlines the importance of adherence for the genus again, but also the complexity of screening for genetic determinants as the phenotype is ensured by a variety of genes/mechanisms i.e. different genes having the same function among different species of the genus. Furthermore, even when gene homologs are found, they might not fulfill the same role in different species, as we could demonstrate with the example of Bap, a major contributor to biofilm formation of selected *S. aureus* and *S. epidermidis* strains (Cucarella et al., 2001; Tormo et al., 2005) but not contributing to biofilm formation of *S. xylosus* (Schiffer et al., 2021). That is because many biofilm-associated genes often have different primary functions, e.g. a catalytic activity (major autolysin Atl, Nega et al., 2020). Another function of Bap

has not yet been found, and it might just not be relevant to the species after all, as discussed later on.

Generally, all staphylococci share the contribution of polysaccharides, eDNA and proteins to adherence and biofilm formation (Schilcher and Horswill, 2020). With respect to proteins, surface proteins are one of the main players. Most of them are covalently bound to the cell surface, yet non-covalently bound and secreted proteins (Eap, Sbp) have been associated with adherence and biofilm formation as well (Decker et al., 2015; Yonemoto et al., 2019). Covalently bound proteins differ in their sequence and the presence of specific binding domains but most of them share an LPxTG cell wall anchor, an YSIRK-G/S motif signal peptide and the sequence arrangement into several domains including a repeat region. These characteristics mostly apply to SxsA as well, a novel surface protein mediating biofilm formation in *S. xylosus* discovered in this work (Schiffer et al., 2022a). Until now, the importance of SxsA has been characterized only in terms of intercellular adhesion and attachment to abiotic surfaces. The role of the protein in attachment to host matrices remains to be investigated. In contrast to surface proteins e.g. of the MSCRAMM family, no matrix protein binding domain has been localized in the SxsA sequence. Moreover, Aap a key protein for adhesion in *S. epidermidis*, binds to glycan structures of skin cells (corneocytes) via its N-terminal lectin domain (Rahmdel and Götz, 2021; Roy et al., 2021). Such type of lectin binding domain was not identified in SxsA either. Additionally, SxsA is missing key characteristics of MSCRAMM proteins (no Ig-like folds, no ligand binding domains), all in all suggesting that the protein has no specific ECM-binding activities but is rather involved in intercellular adhesion and attachment to abiotic surfaces.

One way to learn more about the regulation and mechanism of (SxsA-mediated) biofilm formation in *S. xylosus* is by taking a closer look at *S. xylosus* TMW 2.1602. The strain was found to be a non-biofilm producer, carrying a truncated version of Bap, which we first assumed was the reason for the biofilm negative phenotype (Schiffer et al., 2019). In a subsequent study, we revealed that Bap deletion does not impair the species' biofilm formation, moreover many other *S. xylosus* strains (e.g. C2a, 2, HKUOPL8) also carry a naturally truncated version of the protein on their chromosome (Schiffer et al., 2021). This suggests that Bap is neither essential for the species nor for the expression of a biofilm positive phenotype.

Interestingly, TMW 2.1602 does carry an intact version of SxsA, which is functionally expressed, as confirmed by proteomic analysis (compare Table 12). Intensity values for the protein are lower compared to the other strains, though, which could be explained by the fact that TMW 2.1602 encodes the shortest SxsA version and the protein is therefore digested into fewer

peptides causing reduced intensity values. Nevertheless, we do not want to exclude at this point that the protein in TMW 2.1602 is just very little expressed compared to TMW 2.1523, for example, which might harbor a much higher number of SxsA proteins on its cell surface.

Table 12: SxsA expression analysed by full proteome analysis of the listed strains. Determined IBAQ values (log2) are shown for each strain. Some strains were only sampled in Lac^+ but not in TSB_N. Others were not determined under certain conditions (n.d.). Since TMW 2.1602 is biofilm negative, it was only sampled in planktonic (P) not in sessile (S) growth.

	Lac^+_P	**Lac^+_S**	**TSB_N_P**	**TSB_N_S**
TMW 2.1023	21.95	18.66	n.d.	n.d.
TMW 2.1324	20.32	17.92	n.d.	n.d.
TMW 2.1521	20.12	17.19	n.d.	n.d.
TMW 2.1523	23.09	22.51	25.12	23.35
TMW 2.1602	19.81	n.d.	19.76	n.d.

In Schiffer et al., (2022a) we speculated that the amyloidprone B-region of the protein could mediate biofilm formation by SxsA. In the case of Aap and Bap, amyloid-based cell aggregation can only occur if the protein has previously been proteolytically processed. With Bap, this occurs by a mechanism that has not yet been fully characterized (likely by unknown protease(s) (Taglialegna et al., 2016a)). For Aap, the protease responsible has been identified (SepA), Paharik et al., 2017). It is possible that SxsA has to undergo proteolytic cleavage as well in order for cell aggregation and adhesion to occur. That process could be impaired in TMW 2.1602, if the respective (putative) protease were truncated. To estimate whether SxsA is processed in general, we used the available proteomic dataset, mapped all identified peptides onto the SxsA sequence and examined whether peptides mapping on the protein differed between planktonic and sessile samples. As shown in Figure 5 exemplarily for SxsA of TMW 2.1023 and 2.1523 (both Lac^+ samples), peptides mapping onto the entire protein sequence length were measured in similar intensities under planktonic and sessile growth conditions in TMW 2.1523. In TMW 2.1023 however, peptides mapping to the sequence were identified less frequently under sessile conditions. These controversial statistics make it hard to judge whether SxsA is proteolytically processed or not.

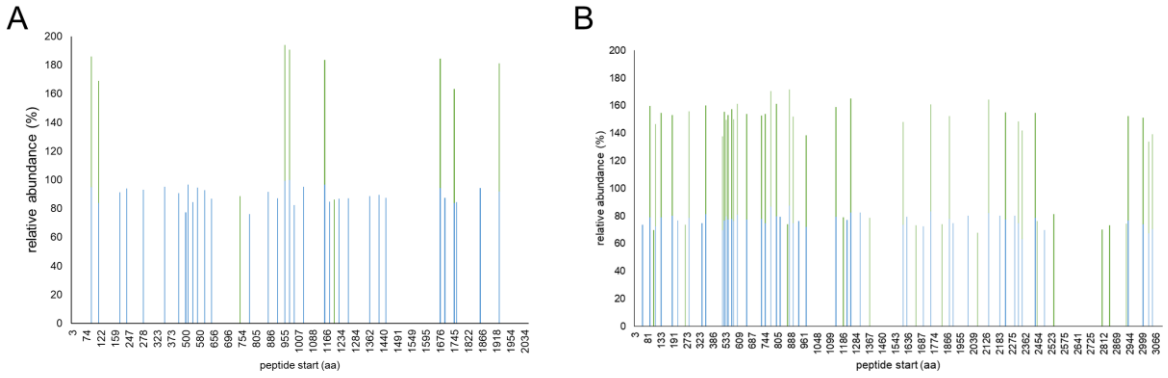

Figure 5: Peptide map of peptides mapping on SxsA of *S. xylosus* TMW 2.1023 (A) and TMW 2.1523 (B) sampled after grown for 24 h in Lac$^+$. Positions of trypsin cleavage sites / peptide start are indicated on the x-axis. Relative abundance is indicated as the intensity of peptides in relation to the most abundant peptide of the sample. In blue: peptides identified in planktonic samples, in green: peptide identified in sessile samples.

Impaired biofilm formation caused by sequence differences in the supposedly important B-region can most likely be excluded, as TMW 2.1023, TMW 2.1523 and TMW 2.1602 share almost 100% sequence identity in their B-region and the sequence of TMW 2.1602 differs by one amino acid only (asparagine instead of aspartic acid at position 458). Yet, this part of the sequence is not encoding for one of the identified, conserved amyloid peptides within the B-region of the protein. Other hypotheses to why the function of SxsA could be impaired in TMW 2.1602 include that SxsA might mediate cell aggregation by heterophilic interactions with other surface proteins on neighboring cells or with other components of the biofilm matrix such as eDNA (Campoccia et al., 2021). Such a counterpart or ligand could be truncated in TMW 2.1602. Using the comparative genomic pipeline BADGE (Behr et al., 2016) we were able to identify 111 proteins that are encoded in biofilm positive strains TMW 2.1023, 2.1324, 2.1521 and 2.1523 but missing in TMW 2.1602 (see Appendix 1). Interestingly, a large number of transcriptional regulators (helix-turn-helix, LysR, TetR/AcrR, AbrB, MarR, MurR/RpiR family transcriptional regulators) is missing in TMW 2.1602. Biofilm formation and adhesion of *Staphylococcus spp*. are tightly regulated by global regulators such as the *agr* QS system, the autoinducer-2 (AI-2) QS system and factors such as the staphylococcal accessory regulator A (SarA) and the alternative sigma factor Sigma B (Knobloch et al., 2001; Trotonda et al., 2005; Karatan and Watnick, 2009). Some of the regulators missing in TMW 2.1602 have been reported in the context of biofilm formation as well, such as LysR regulators like CidR being involved in controlled cell death and subsequent eDNA release (Sadykov and Bayles, 2012) and TetR/AcrR family regulators influencing *ica*-expression (Yu et al., 2017).

In Schiffer et al., (2022a) we also suggested that the C-repeats of SxsA could contribute to intercellular aggregation by homophilic interactions with C-repeats on neighboring cells. As

TMW 2.1602 holds the lowest number of C-repeats (12) among our tested isolates, one could speculate that the number of C-repeats must overcome a critical threshold to contribute to biofilm formation effectively. In SxsA almost every C-repeat is composed of an EF-hand binding motif, known to bind divalent cations, such as calcium (Lewit-Bentley and Réty, 2000). Therefore, we hypothesized that SxsA-mediated cell aggregation might involve crosslinking of cells by calcium binding to the EF-hand domains. Interestingly, we observed an increase in biofilm formation by calcium addition in a strain- and medium-dependent matter (compare Schiffer et al., 2022a and Figure 6). Furthermore, EDTA addition completely abolished biofilm formation of TMW 2.1023 and TMW 2.1523 (Schiffer et al., 2022a). Since zinc was reported to be essential for Aap-mediated biofilm formation in *S. epidermidis* and SasG-mediated biofilm formation of *S. aureus* (Conrady et al., 2008; Geoghegan et al., 2010; Yarawsky et al., 2020), its addition (40 µM $ZnCl_2$) was also tested for TMW 2.1023 and TMW 2.152 but did not change the biofilm intensity in neither of the strains. Also noteworthy, neither zinc nor calcium were able to induce biofilm formation in 2.1602, the strain remained biofilm negative.

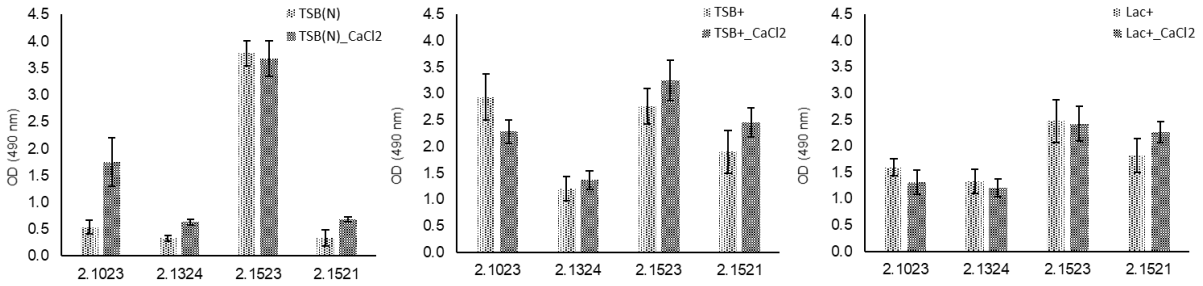

Figure 6: Biofilm formation of *S. xylosus* on hydrophobic support in three different growth media (w / w/o addition of 20 mM CaCl2). Mean ± SE.

TMW 2.1023 appears to have a different mechanism for biofilm formation than for example TMW 2.1523. This is indicated not only by its more pronounced response to calcium but also because this strain was only conditionally hindered in its ability to form biofilm upon the deletion of SxsA (Schiffer et al., 2022a). Reasons for this can be surmised by looking into the genome of the strain. It is striking that TMW 2.1023 encodes a surface protein on its largest plasmid, which is very similar in its structure and key characteristics to the usual biofilm mediating surface proteins. The protein was named *Staphylococcus xylosus surface protein* B (Schiffer et al., 2022a). SxsB is a high molecular weight protein (1187 aa, 278 kDA in TMW 2.1023) which is also encoded by TMW 2.1324 and TMW 2.1521. BLASTp searches against the NCBI database indicate the presence of SxsB in further staphylococci such as *S. saprophyticus*. SxsB has a YSIRK-G/S motif signal peptide, an LPxTG cell wall anchor, and the typical sequence

structure, which can be divided into a C-terminal repeat region (tandem SESLSTSESLSE repeats) as well as an amyloidprone region in the N-terminal part of the protein (predicted for aa 340 to 570). Interestingly, SxsB does not contain any EF-hand motifs. To sum it up, even though the contribution of SxsB to biofilm formation needs to be confirmed by gene deletion experiments, one can speculate at the time that the protein might reduce the effect of SxsA deletion in TMW 2.1023. These analyses highlight again how the biofilm behavior of different strains is influenced by their genetic background beyond the selected protein studied in detail.

This work focused mainly on the protein part of *S. xylosus* biofilm formation. Nevertheless, we do not want to exclude that other components such as polysaccharides and eDNA also contribute to biofilm formation of the species. The importance of eDNA in *S. xylosus* biofilms was investigated by the group of Régine Talon in strain C2a in the past year (Leroy et al., 2021). They suggested that eDNA is predominantly released by phage and *cid*ABC mediated lysis into the matrix. All biofilm positive isolates investigated in this study, carry prophages in their genome, yet some of them only incomplete fragments (Figure 7). Furthermore, the proteomic analysis found higher amounts of phage-associated proteins in sessile samples of strains TMW 2.1521 and TMW 2.1523 (compare Chapter 4.5). Moreover, as part of the work for this thesis, we observed that *S. xylosus* biofilms were sensitive to externally added DNAseI, resulting in complete degradation of the matrix (data not shown). This is in concordance with other studies that have observed heavy degradation effects of DNAseI treatment on mature biofilms of other staphylococci such as *S. saprophyticus* as well (Lawal et al., 2021). Additionally, we found the biofilm matrix of TMW 2.1523 to respond to Bobo-3 staining (data not shown), confirming that eDNA is another important structural component of the *S. xylosus* biofilm matrix.

Not much is known yet in terms of polysaccharides contributing to *S. xylosus* biofilm formation. In the scope of this study, some minor experiments were performed, e.g. lectin-based polysaccharide (WGA) staining of the TMW 2.1523 matrix, resulting in positive signals (data not shown). The most important exopolysaccharide contributing to biofilm formation of *Staphylococcus spp.* is PIA, encoded by *ica*ADBCR (Heilmann et al., 1996b). The few studies that exist on *S. xylosus* biofilm formation mainly report *S. xylosus* to be *ica*-negative (Planchon et al., 2006; Schiffer et al., 2019), with only a couple of studies reporting *ica*A-positive *S. xylosus* isolates (Tremblay et al., 2013). However, such positive results were based on PCR-based presence/absence screening of one gene (*ica*A) of the operon and as we have shown in Schiffer et al., (2019) some strains carry incomplete *ica* operons (only *ica*D missing in TMW 2.1602). When, screening the NCBI *S. xylosus* genome database for the presence of *ica* positive strains

it yields at least two positive hits, both strains encoding the entire operon (strains NCTC11043 and 47-83). These analyses demonstrate the multifactorial nature of biofilm forming mechanisms again and that *S. xylosus* adherence surely does not depend on SxsA only but can also be complemented by polysaccharides, (lipo)teichoic acids, eDNA and other proteins in a strain-dependent matter.

5.2 The role of biofilm formation in the persistence of *S. xylosus* in natural and man-made environments

After discussing all these different mechanisms of adherence and biofilm formation in *S. xylosus*, one should go back to where this discussion initially started off. Why and how do these adherence mechanisms favor and contribute to the behavior of *S. xylosus* in its habitats and why does the species retain the ability to express different biofilm mechanisms.

Defining the natural ecological niche of the species is not easy since the organism has been isolated from a whole range of different environments. According to its discoverers Schleifer and Kloos, *S. xylosus* was first isolated from human skin (Schleifer and Kloos, 1975). Over the years, especially since species identification became more accurate, *S. xylosus* has been categorized to being mainly associated with warm blooded animals (Becker et al., 2014) as it has been isolated from horses, dogs, lower primates, rodents, mice, cattle, sheep and rabbits (Kloos et al., 1976; Nagase et al., 2002; Huerta et al., 2016; Kim et al., 2017; Kaspar et al., 2018). However, studies examining the microbiota of human skin frequently identify *S. xylosus* in low percentages as well (Luqman et al., 2020). Whole genome sequenced strains deposited on NCBI name a wide range of isolation sources from the just named animal-associated sources to environmental sources and vegetable-based fermented products like fermented soybeans (compare table S5, Schiffer et al., 2022a). Studies of our laboratory were also able to identify *S. xylosus* as the predominant species in rabbit feces. Interestingly, *S. xylosus* has also been sampled from the feces of mice (Kaur et al., 2016) and giant pandas (Ma et al., 2014) before. Thus, it is hard to define “the” natural habitat of the species, but one can summarize that the species is frequently found as a commensal of mammal skin, hereby probably preferring glandular tissue / mucous body sites. Moreover, udder quarters and teats are also very frequently colonized by *S. xylosus* (Condas et al., 2017; Buck et al., 2021). They display a challenging environment, with high cell proliferation rates particularly during dry periods and close to parturition (Sorensen et al., 2006). Furthermore, mammary glands are a very calcium-rich environment, which could explain why *S. xylosus* adherence is partly increased and highly dependent on the

presence of calcium. Firm adherence is hereby likely associated with increased permanent colonization, allowing the strains to better compete with other organisms and cope with the harsh environmental conditions exposed to when residing on mammal skin. In this regard, it is particularly interesting that biofilm formation of Bap-positive *S. aureus* strains, which share an ecological niche with *S. xylosus* (bovine mammary gland) is inhibited by calcium while the adherence of *S. xylosus* is promoted / dependent on calcium (Arrizubieta et al., 2004; Cucarella et al., 2004; Schiffer et al., 2022a). Whether factors similar to those in humans play a role here, wherein a complex interplay the skin commensal *S. epidermidis*, contributes to controlling the colonization of *S. aureus*, remains speculative (Iwase et al., 2010). However, a recently published study by Leroy and colleagues should not go unmentioned here, who were able to find first indicators of a potential inhibition of *S. aureus* biofilms by *S. xylosus* (Leroy et al., 2020). This may even cast a different light on reports of *S. xylosus* accompanying mastitis infections.

S. xylosus not only occurs in its natural habitats but also has a dominating role in fermented foods, such as raw fermented sausages (Greppi et al., 2015) and cheese (Coton et al., 2010). Once more, biofilm formation plays a role, as *S. xylosus* has been shown to rapidly colonize the production environment of processing plants, depending on the strain's ability to form a biofilm (Leroy et al., 2010). Furthermore, the ability to colonize surfaces might increase the persistence of the species in such man-made habitats. In this respect, one could speculate that strains that are heavy biofilm formers are able to adhere quickly to the matrix of the fermented products, thereby colonizing the niche and contributing to competitive exclusion of the potentially spoiling autochthonous microbiota (Laranjo et al., 2019). Moreover, entering a sessile growth stage during fermentation could help *S. xylosus* to persist over the fermentation process in which the organism has to cope with low pH values (dropping to 5.0 - 5.3 (Corbiere Morot-Bizot et al., 2007)), osmo- and nitrosative stress (Vermassen et al., 2016). Proteomic analysis (chapter 4.5) revealed that the metabolism of *S. xylosus* is reduced once they grow in a biofilm. Furthermore, fermentative energy gain is activated. The latter is beneficial for *S. xylosus* as raw fermented sausages display a microaerophilic environment (Leroy et al., 2017). Experiments conducted by our lab and other studies (Corbiere Morot-Bizot et al., 2007) usually report staphylococci colony forming units per gram increasing by factor $10^1 – 10^2$ during sausage ripening. It suggests that the organism rather persists than actively grows during the fermentation. Therefore, cells might enter a sessile stage to protect themselves from environmental stress factors during fermentation. The herewith associated occupation of the food matrix can be advantageous for a strain's performance, as it could reduce the risk of autochthonous microorganisms with unknown risk potential (e.g. biogenic amine formation or transmissible antibiotic resistance). The

fermentation process could thereby be dominated by concomitant induction of colonization resistance similarly as it has been reported in other systems such as the gut microbiota and *Clostridium difficile* (Pérez-Cobas et al., 2015). As proteomics has shown, important technological enzymes, such as nitrate reductase, are still active in sessile cells, since they are also involved in fermentative energy production. We therefore speculate that a biofilm positive phenotype could have an adaptive advantage in food fermentations because attachment to matrix proteins and subsequent embedding in a protective polymeric matrix could give the cells a fitness advantage.

5.3 Restriction modification systems in *S. xylosus* and the likelihood of HGT

This thesis also addresses restriction modification (RM) systems. RM systems have been studied extensively since the 1980s and besides the original described function in providing a barrier to exogenous DNA, particularly bacteriophage attacks, they are now known to provide an essential contribution to procaryotic epigenetics as well (Atack et al., 2018; Oliveira and Fang, 2021). Studies over the past years revealed that many phenotypes are expressed in a phase variable manner, regulated by the methylation of DNA sequences, thereby allowing a cell population to generate a phenotypic diversity within a population. Among such regulated phenotypes are expression of bacterial surface-structures, biofilm formation, pathogenesis, antibiotic resistance and general host-adaption (Atack et al., 2018; Atack et al., 2020; Nye et al., 2020; Oliveira and Fang, 2021). In Schiffer et al., (2022b), we identified a novel type I restriction modification system, requiring two specificity units instead of one, for proper base modification. The system is associated with the occurrence on mobile genetic elements (MGE) and was only identified in *Staphylococcus spp*. to date.

Some staphylococcal species are known to be very resistant to horizontal gene transfer and the uptake of exogenous DNA. Among them is *S. lugdunensis*, which encompasses a highly conserved, closed pan-genome with only very few acquired genes (Argemi et al., 2018). In other staphylococci, such as *S. aureus* HGT is more common. Hereby, natural transformation is suggested to occur rarely and inefficiently. However, one should keep in mind that conditions under which bacteria become naturally competent are difficult to determine in the lab (Otto, 2013a; Lindsay, 2019). Conjugation on the other hand works effectively in staphylococci but the number of conjugative transfer genes is constrained. Therefore, the main driver for HGT seems to be transduction, as bacteriophages occur widely among staphylococci (Haaber et al., 2017; Lindsay, 2019).

In the lab, many researchers experience that staphylococci are very resistant to transformation, and for a long time, they struggled to modify clinical wildtype isolates genetically but rather had to work with a few well-characterized laboratory strains (Monk et al., 2012; Lee et al., 2019). Yet, thanks to a method developed by Monk and his colleagues the restriction barrier of *S. aureus* and *S. epidermidis* could finally be circumvented by mimicking the strain's DNA methylation profile (Monk et al., 2015). This method, also known as plasmid artificial modification, did not yield higher transformation efficiencies in selected *S. xylosus* strains (Schiffer et al., 2022b). Possible explanations addressing the role of other restriction systems and physical factors like capsule formation interfering with transformation have already been discussed extensively in Schiffer et al., (2022b). They shall be complemented with some additional information on one of the hypotheses in the following. Furthermore, the extent and possibility of HGT occurring in *S. xylosus* is discussed.

In general, the exchange of genetic material in *S. aureus* within each lineage is facilitated due to the presence of similar RM systems compared to the exchange between members of different lineages (Waldron and Lindsay, 2006; Monk et al., 2015). Mobile genetic elements can therefore be found quite frequently in *Staphylococcus spp.* genomes. Almost all natural isolates have phages inserted into their chromosome and pathogenicity islands, staphylococcal cassette chromosomes (SCCs), transposons and other integrative elements, as well as a large number of plasmids are commonly distributed within the genus (McCarthy et al., 2014).

The core genome of *S. xylosus* accounts for up to 50% of the species pangenome as shown in Figure 7. Moreover, many strains carry strain-specific genes, prophages and genomic islands in their genome, as well as they harbor different numbers of high- and low copy mega- and small plasmids. Also, *S. xylosus* does not display a strictly conserved antibiotic sensitivity profile, as is has been associated multiple times with acquired not intrinsic resistances to different antibiotics (França et al., 2021).

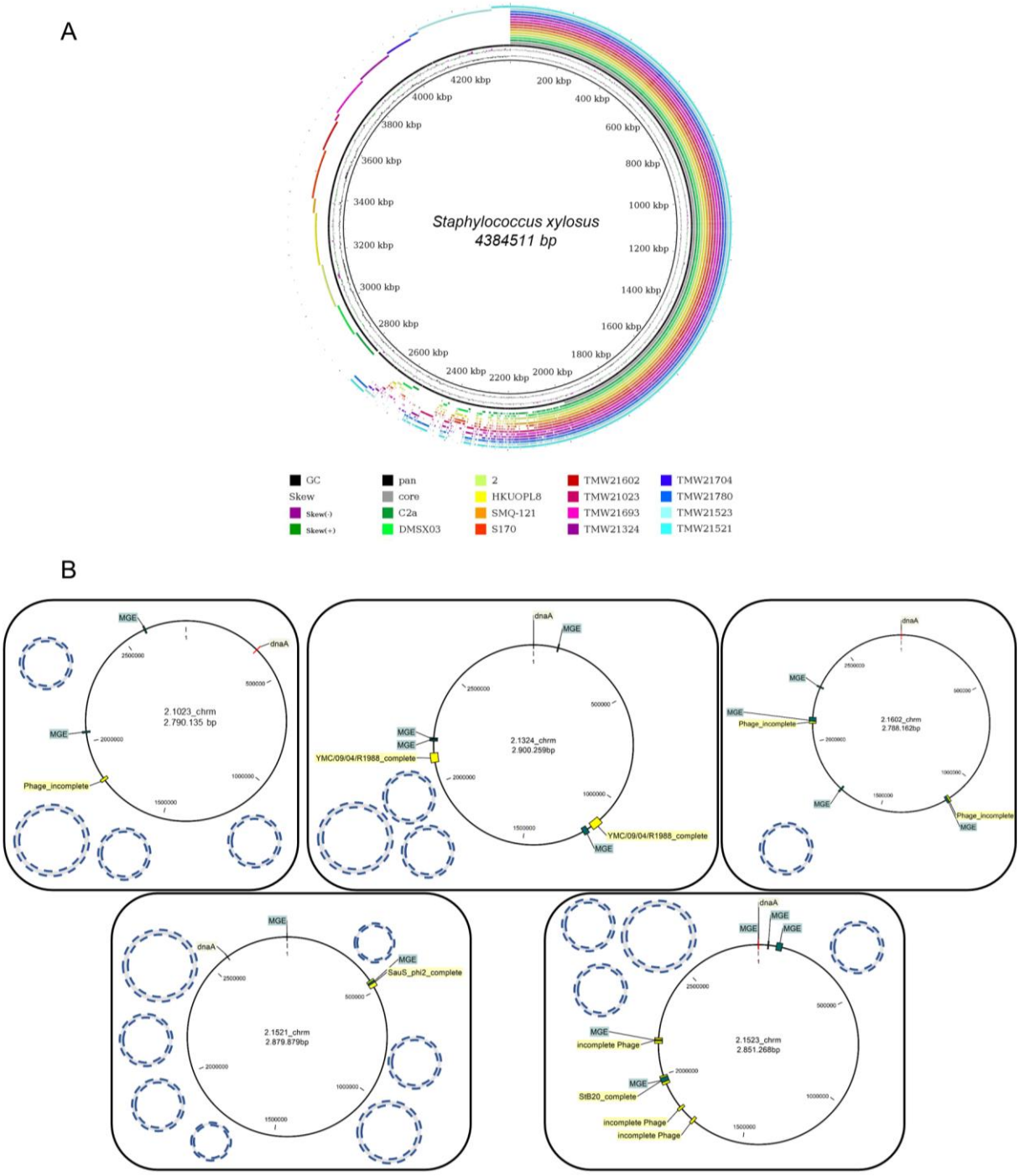

Figure 7: Core, pan- and accessory- genome prediction for *S. xylosus*. **A**. Imaging was performed using BRIG, the cut-off was set to 0.95% sequence identity. **B**. *S. xylosus* mobilome: chromosome (black circle) including position of predicted prophages and mobile genetic elements (MGE) as well as number of plasmids carried by each strain is depicted (blue circles).

Therefore, *S. xylosus* does not seem to be a species generally unable to take up exogenous DNA even though general genome stability seems to be ensured by the presence of genetic barriers to HGT (RM systems, CRISPR/Cas systems, (Schiffer et al., 2022b)). It rather appears that the species is inefficiently transformed but again conjugation and transduction probably work efficiently. Among other reasons, we suggested in Schiffer et al., (2022b) that a Type IV present

in *S. xylosus* could oppose a barrier to transformation not being circumventable by using *dcm* negative *E. coli* host strains. Indeed, we could identify a Type IV system in many of the analyzed *S. xylosus* strains, different from the well-described Type IV SauUSI system of *S. aureus* (Xu et al., 2011). The main difference is that the *S. xylosus* Type IV system comprises two subsequent endonucleases as outlined in Figure 8 using TMW 2.1023 as an example.

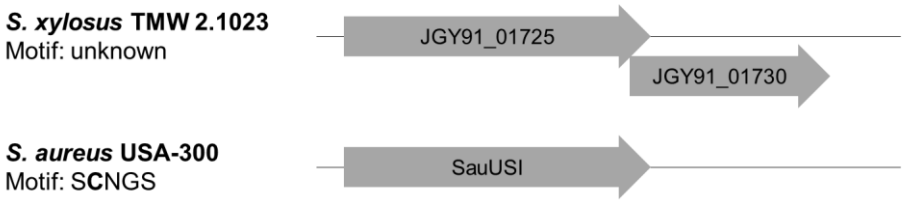

Figure 8: Gene arrangement of the type IV RM system of *S. xylosus* TMW 2.1023 with unknown restriction motif and the type IV system of *S. aureus* USA 300 which is known to restrict methylated SCNGS motifs.

This system has not been described or characterized so far in the literature; therefore, we can only speculate at the time which kind of methylation the system recognizes and restricts. Most type IV systems, including SauUSI, recognize and restrict cytosine methylated motifs (Xu et al., 2011; Loenen and Raleigh, 2014). However, type IV systems that respond to adenine methylated motifs are also known (Loenen and Raleigh, 2014). Therefore, without further characterization of the *S. xylosus* type IV system, we cannot exclude that it might recognize adenine-modified motifs rather than cytosine-modified ones. Unfortunately, the use of *dam- E. coli* strains in transformation experiments is unfavorable because proper base modification by the *dam* methyltransferase and the resulting adenine methylation are essential for DNA replication and mismatch repair (Boye and Løbner-Olesen, 1990; Nye et al., 2020).

In summary, a more comprehensive analysis of the restriction systems distributed within *S. xylosus* might make it possible to define genetic lineages for *S. xylosus*, similarly as already described for other staphylococci (*S. lugdunensis*, *S. aureus* (Lindsay, 2010; Argemi et al., 2018)) which could increase the knowledge on evolution and HGT occurring in the species.

6 Conclusion and outlook

In summary, the present work provided novel insights into biofilm formation mechanisms of staphylococcal species other than the well-characterized, clinically most relevant examples *S. epidermidis* and *S. aureus*. By identifying species- and strain-specific differences in regulating factors and mechanisms of adhesion, the importance of species- and strain-directed research was emphasized. Using the example of Bap, the present work showed that gene functions cannot easily be extrapolated from one species to another. Moreover, the new characterization of the *Staphylococcus xylosus* surface protein SxsA proved that not all biofilm-mediating mechanisms within the genus *Staphylococcus spp*. are fully known and understood yet. Thus, there is room for more, especially when focusing on coagulase-negative staphylococci other than *S. epidermidis*. Based on the presented results, it would be interesting to find out how *S. xylosus* attaches to biotic surfaces, which adhesins are involved and, in particular, how SxsA affects the colonization of biological matrices. Therefore, it would be highly appreciable to further characterize the behavior of wildtype and mutants in stepwise more complex systems from *in situ* conditions to models close to *in vivo* systems. One could simply start by using protein-coated microtiter plates and proceed by using meat as a matrix. This could be an ideal starting point to characterize MSCRAMMs and other adhesins that bind to host matrix proteins. Furthermore, raw fermented sausages oppose a useful example to substantiate primary hypotheses on mechanisms of coping with stress, transiently acidified environments, passive protection and adherence. Hereby, the contribution of SxsA on the behavior of *S. xylosus* during sausage fermentation could also be tested.

To further characterize the impact of *sxs*A on multicellular behavior, the gene should be expressed in a surrogate host as functional redundancy can make it challenging to evaluate a reduction in multicellular behavior in a mutant that is defective for a single gene. Heterologous expression of the protein in strains with a biofilm negative background such as in *Lactococcus lactis* MG1363 or in other staphylococci like *S. carnosus* TM300, *S. epidermidis* ATCC 12228 or *S. aureus* Newman (all biofilm negative) would be conceivable. Furthermore, it would be interesting to characterize the role of the C-repeats, the amyloidogenic potential of the B-region, and the role of potential proteases processing SxsA in more detail.

This work also shows that SxsA is not the only protein that might play a crucial role in biofilms and adhesion. Genome mining revealed that other surface proteins such as SxsB of

TMW 2.1023 may have a putative function and are worth investigating as well. Biofilm formation depends on environmental conditions and is regulated e.g. by peptide-based QS systems in *Staphylococcus spp.* (Schilcher and Horswill, 2020). Based on the repeatedly observed species differences, it seems reasonable to investigate whether regulatory differences follow the same rules or whether biofilm-associated proteins are under the control of other regulators in the species.

Another research gap is the influence of ions on biofilm formation of *S. xylosus*. We have reported that EDTA inhibited the species' biofilm formation, while calcium enhanced the phenotypes in some strains. Zinc addition had no effect but an interesting fact we observed was that growth of *S. xylosus* was completely abolished upon addition of micromolar levels of the zinc chelator diethylenetriaminepentaacetic acid (DTPA). Concentrations of 30 µM, which have been reported to be easily tolerated by other staphylococci such as *S. epidermidis* (Conrady et al., 2008), were already cytotoxic for *S. xylosus*. Such observations again prove the heterogenicity of the whole genus. The addition of other divalent cations and their respective chelators could provide further insights in that respect.

A last aspect to add to the characterization of biofilm formation of *S. xylosus* is that we have focused strongly on the protein part of the species' biofilm. Data on other components such as eDNA and polysaccharides is mostly missing. In *S. aureus* and *S. epidermidis*, the major autolysin Atl is responsible for cell wall remodeling but has been reported multiple times to be involved in initial adhesion and eDNA release (Heilmann et al., 1997; Bose et al., 2012). First analyses conducted by our lab showed that the respective Autolysin-homolog in *S. xylosus* might act differently again, having for example a much larger propeptide than reported for the other two staphylococci (Figure 9) as well as we have observed that *S. xylosus* behaved differently to *S. epidermidis* in Triton-X induced autolysis assays (data not shown).

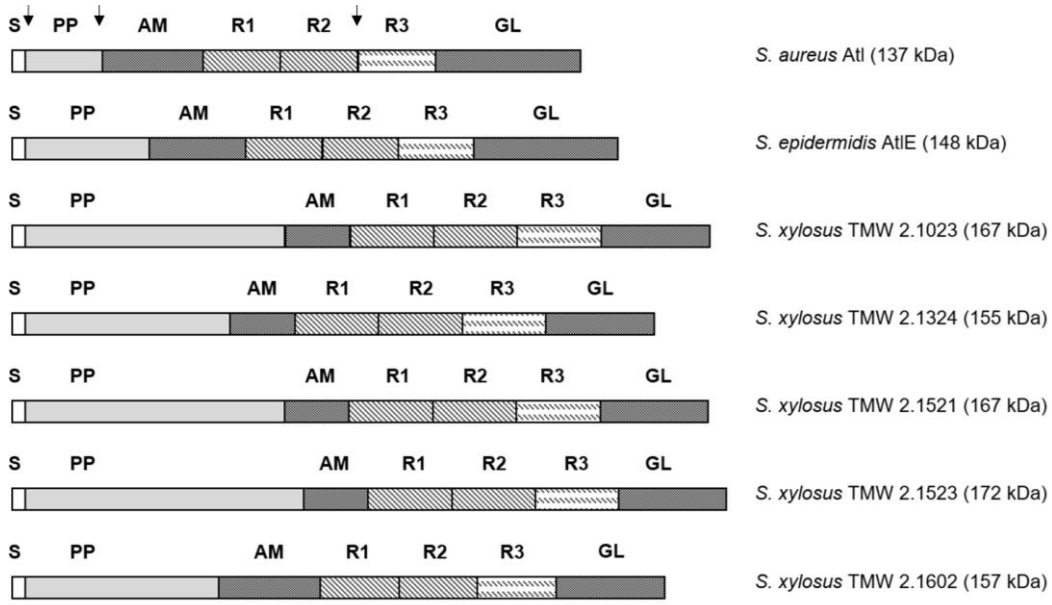

Figure 9: Gene structure organization of the major autolysin in staphylococci. Signal peptide (S), propeptide (PP), amidase (AM) and glucosaminidase (GL) domain are shown as well as repeats (R1, R2, R2), of which R1 and R2 are associated with the amidase domain and R3 with the glucosaminidase domain. Post-translational processing of Atl occurs at the respective cleavage sites, which are indicated by arrows. The figure is inspired by Götz *et al*., (2014) and was supplemented by the multidomain organization of the *S. xylosus* autolysin.

To fill these research gaps, simplified genetic manipulation experiments are crucial. Knowledge of the functionality of the type IV RM system of *S. xylosus* still needs to be expanded and other factors limiting genetic accessibility need to be addressed, e.g. plasmid incompatibility in wildtype strains.

7 References

Abe, K., Nomura, N., and Suzuki, S. (2020). Biofilms: hot spots of horizontal gene transfer (HGT) in aquatic environments, with a focus on a new HGT mechanism. *FEMS Microbiol Ecol* 96. doi: 10.1093/femsec/fiaa031

Alikhan, N.-F., Petty, N. K., Ben Zakour, N. L., and Beatson, S. A. (2011). BLAST Ring Image Generator (BRIG): simple prokaryote genome comparisons. *BMC Genomics* 12, 402. doi: 10.1186/1471-2164-12-402

An, Y. H., and Friedman, R. J., eds (2010). *Handbook of bacterial adhesion: Principles, methods, and applications*. Totowa, NJ: Humana Press.

Anton, B. P., and Roberts, R. J. (2021). Beyond Restriction Modification: Epigenomic Roles of DNA Methylation in Prokaryotes. *Annu Rev Microbiol* 75, 129–149. doi: 10.1146/annurev-micro-040521-035040

Argemi, X., Matelska, D., Ginalski, K., Riegel, P., Hansmann, Y., Bloom, J., et al. (2018). Comparative genomic analysis of *Staphylococcus lugdunensis shows* a closed pan-genome and multiple barriers to horizontal gene transfer. *BMC Genomics* 19. doi: 10.1186/s12864-018-4978-1

Arndt, D., Grant, J. R., Marcu, A., Sajed, T., Pon, A., Liang, Y., et al. (2016). PHASTER: a better, faster version of the PHAST phage search tool. *Nucleic Acids Research* 44, W16-21. doi: 10.1093/nar/gkw387

Arrizubieta, M. J., Toledo-Arana, A., Amorena, B., Penadés, J. R., and Lasa, I. (2004). Calcium inhibits Bap-dependent multicellular behavior in *Staphylococcus aureus*. *J. Bacteriol.* 186, 7490–7498. doi: 10.1128/JB.186.22.7490-7498.2004

Atack, J. M., Guo, C., Yang, L., Zhou, Y., and Jennings, M. P. (2020). DNA sequence repeats identify numerous Type I restriction-modification systems that are potential epigenetic regulators controlling phase-variable regulons; phasevarions. *FASEB J* 34, 1038–1051. doi: 10.1096/fj.201901536RR

Atack, J. M., Tan, A., Lo Bakaletz, Jennings, M. P., and Seib, K. L. (2018). Phasevarions of Bacterial Pathogens: Methylomics Sheds New Light on Old Enemies. *Trends Microbiol* 26. doi: 10.1016/j.tim.2018.01.008

Aziz, R. K., Bartels, D., Best, A. A., DeJongh, M., Disz, T., Edwards, R. A., et al. (2008). The RAST Server: Rapid annotations using subsystems technology. *BMC Genomics* 9, 75. doi: 10.1186/1471-2164-9-75

Barrière, C., Brückner, R., Centeno, D., and Talon, R. (2002). Characterisation of the katA gene encoding a catalase and evidence for at least a second catalase activity in *Staphylococcus xylosus*, bacteria used in food fermentation. *FEMS Microbiol Lett* 216, 277–283. doi: 10.1111/j.1574-6968.2002.tb11447.x

Becker, K., Both, A., Weißelberg, S., Heilmann, C., and Rohde, H. (2020). Emergence of coagulase-negative staphylococci. *Expert Review of Anti-infective Therapy* 18, 349–366. doi: 10.1080/14787210.2020.1730813

Becker, K., Heilmann, C., and Peters, G. (2014). Coagulase-negative staphylococci. *Clin Microbiol Rev* 27, 870–926. doi: 10.1128/CMR.00109-13

Beenken, K. E., Dunman, P. M., McAleese, F., Macapagal, D., Murphy, E., Projan, S. J., et al. (2004). Global gene expression in *Staphylococcus aureus* biofilms. *J. Bacteriol.* 186, 4665–4684. doi: 10.1128/JB.186.14.4665-4684.2004

Behr, J., Geissler, A. J., Schmid, J., Zehe, A., and Vogel, R. F. (2016). The Identification of Novel Diagnostic Marker Genes for the Detection of Beer Spoiling *Pediococcus damnosus* Strains Using the BlAst Diagnostic Gene findEr. *PLoS ONE* 11, e0152747. doi: 10.1371/journal.pone.0152747

Bertelli, C., Laird, M. R., Williams, K. P., Lau, B. Y., Hoad, G., Winsor, G. L., et al. (2017). IslandViewer 4: expanded prediction of genomic islands for larger-scale datasets. *Nucleic Acids Research* 45, W30-W35. doi: 10.1093/nar/gkx343

Biswas, R., Voggu, L., Simon, U. K., Hentschel, P., Thumm, G., and Götz, F. (2006). Activity of the major staphylococcal autolysin Atl. *FEMS Microbiol Lett* 259, 260–268. doi: 10.1111/j.1574-6968.2006.00281.x

Bose, J. L., Lehman, M. K., Fey, P. D., and Bayles, K. W. (2012). Contribution of the *Staphylococcus aureus* Atl AM and GL murein hydrolase activities in cell division, autolysis, and biofilm formation. *PLoS ONE* 7, e42244. doi: 10.1371/journal.pone.0042244

Bottagisio, M., Soggiu, A., Piras, C., Bidossi, A., Greco, V., Pieroni, L., et al. (2019). Proteomic Analysis Reveals a Biofilm-Like Behavior of Planktonic Aggregates of *Staphylococcus epidermidis* Grown Under Environmental Pressure/Stress. *Front. Microbiol.* 10, 1909. doi: 10.3389/fmicb.2019.01909

Boye, E., and Løbner-Olesen, A. (1990). The role of dam methyltransferase in the control of DNA replication in E. coli. *Cell* 62, 981–989. doi: 10.1016/0092-8674(90)90272-G

Brand, Y. E., and Rufer, B. (2021). Late prosthetic knee joint infection with *Staphylococcus xylosus*. *IDCases* 24, e01160. doi: 10.1016/j.idcr.2021.e01160

Brückner, R. (1997). Gene replacement *in Staphylococcus carnosus* and *Staphylococcus xylosus*. *FEMS Microbiology Letters* 151, 1–8.

Buck, J. de, Ha, V., Naushad, S., Nobrega, D. B., Luby, C., Middleton, J. R., et al. (2021). Non-aureus Staphylococci and Bovine Udder Health: Current Understanding and Knowledge Gaps. *Front Vet Sci* 8, 658031. doi: 10.3389/fvets.2021.658031

Byrd, A. L., Belkaid, Y., and Segre, J. A. (2018). The human skin microbiome. *Nat Rev Microbiol* 16, 143–155. doi: 10.1038/nrmicro.2017.157

Campoccia, D., Montanaro, L., and Arciola, C. R. (2021). Extracellular DNA (eDNA). A Major Ubiquitous Element of the Bacterial Biofilm Architecture. *Int J Mol Sci* 22. doi: 10.3390/ijms22169100

Carneiro, C. R. W., Postol, E., Nomizo, R., Reis, L. F. L., and Brentani, R. R. (2004). Identification of enolase as a laminin-binding protein on the surface of *Staphylococcus aureus*. *Microbes Infect* 6, 604–608. doi: 10.1016/j.micinf.2004.02.003

Christensen, G. D., Simpson, W. A., Younger, J. J., Baddour, L. M., Barrett, F. F., Melton, D. M., et al. (1985). Adherence of coagulase-negative staphylococci to plastic tissue culture plates: A quantitative model for the adherence of staphylococci to medical devices. *J Clin Microbiol* 22, 996–1006.

Clark, T. A., Murray, I. A., Morgan, R. D., Kislyuk, A. O., Spittle, K. E., Boitano, M., et al. (2012). Characterization of DNA methyltransferase specificities using single-molecule, real-time DNA sequencing. *Nucleic Acids Research* 40, e29. doi: 10.1093/nar/gkr1146

Condas, L. A. Z., Buck, J. de, Nobrega, D. B., Carson, D. A., Roy, J.-P., Keefe, G. P., et al. (2017). Distribution of non-aureus staphylococci species in udder quarters with low and high somatic cell count, and clinical mastitis. *J Dairy Sci* 100, 5613–5627. doi: 10.3168/jds.2016-12479

Conlon, B. P., Geoghegan, J. A., Waters, E. M., McCarthy, H., Rowe, S. E., Davies, J. R., et al. (2014). Role for the A domain of unprocessed accumulation-associated protein (Aap) in the attachment phase of the *Staphylococcus epidermidis* biofilm phenotype. *J Bacteriol* 196, 4268–4275. doi: 10.1128/JB.01946-14

Conrady, D. G., Brescia, C. C., Horii, K., Weiss, A. A., Hassett, D. J., and Herr, A. B. (2008). A zinc-dependent adhesion module is responsible for intercellular adhesion in staphylococcal biofilms. *PNAS* 105, 19456–19461. doi: 10.1073/pnas.0807717105

Corbiere Morot-Bizot, S., Leroy, S., and Talon, R. (2007). Monitoring of staphylococcal starters in two French processing plants manufacturing dry fermented sausages. *J Appl Microbiol* 102, 238–244. doi: 10.1111/j.1365-2672.2006.03041.x

Corrigan, R. M., Rigby, D., Handley, P., and Foster, T. J. (2007). The role of *Staphylococcus aureus* surface protein SasG in adherence and biofilm formation. *Microbiology (Reading, Engl)* 153, 2435–2446. doi: 10.1099/mic.0.2007/006676-0

Costa, S. K., Donegan, N. P., Corvaglia, A.-R., François, P., and Cheung, A. L. (2017). Bypassing the Restriction System To Improve Transformation of *Staphylococcus epidermidis*. *J Bacteriol* 199. doi: 10.1128/JB.00271-17

Costerton, J. W., Geesey, G. G., and Cheng, K. J. (1978). How bacteria stick. *Sci Am* 238, 86–95. doi: 10.1038/scientificamerican0178-86

Coton, E., Desmonts, M.-H., Leroy, S., Coton, M., Jamet, E., Christieans, S., et al. (2010). Biodiversity of coagulase-negative Staphylococci in French cheeses, dry fermented sausages, processing environments and clinical samples. *Int J Food Microbiol* 137, 221–229. doi: 10.1016/j.ijfoodmicro.2009.11.023

Couvin, D., Bernheim, A., Toffano-Nioche, C., Touchon, M., Michalik, J., Néron, B., et al. (2018). CRISPRCasFinder, an update of CRISRFinder, includes a portable version, enhanced performance and integrates search for Cas proteins. *Nucleic Acids Research* 46, W246-W251. doi: 10.1093/nar/gky425

Cox, J., Neuhauser, N., Michalski, A., Scheltema, R. A., Olsen, J. V., and Mann, M. (2011). Andromeda: a peptide search engine integrated into the MaxQuant environment. *J Proteome Res* 10, 1794–1805. doi: 10.1021/pr101065j

Cucarella, C., Solano, C., Valle, J., Amorena, B., Lasa, I., and Penadés, J. R. (2001). Bap, a *Staphylococcus aureus* surface protein involved in biofilm formation. *J Bacteriol* 183, 2888–2896. doi: 10.1128/JB.183.9.2888-2896.2001

Cucarella, C., Tormo, M. A., Ubeda, C., Trotonda, M. P., Monzon, M., Peris, C., et al. (2004). Role of biofilm-associated protein Bap in the pathogenesis of bovine *Staphylococcus aureus*. *Infection and Immunity* 72, 2177–2185. doi: 10.1128/IAI.72.4.2177-2185.2004

Cui, L., and Shearwin, K. E. (2017). Clonetegration Using OSIP Plasmids: One-Step DNA Assembly and Site-Specific Genomic Integration in Bacteria. *Methods Mol Biol* 1472, 139–155. doi: 10.1007/978-1-4939-6343-0_11

Decker, R., Burdelski, C., Zobiak, M., Büttner, H., Franke, G., Christner, M., et al. (2015). An 18 kDa scaffold protein is critical for *Staphylococcus epidermidis* biofilm formation. *PLOS Pathogens* 11, e1004735. doi: 10.1371/journal.ppat.1004735

Delorenzi, M., and Speed, T. (2002). An HMM model for coiled-coil domains and a comparison with PSSM-based predictions. *Bioinformatics* 18, 617–625. doi: 10.1093/bioinformatics/18.4.617.

Donlan, R. M. (2002). Biofilms: Microbial life on surfaces. *Emerging Infect Dis* 8, 881–890. doi: 10.3201/eid0809.020063

Donlan, R. M., and Costerton, J. W. (2002). Biofilms: Survival Mechanisms of Clinically Relevant Microorganisms. *Clin Microbiol Rev* 15, 167–193. doi: 10.1128/CMR.15.2.167-193.2002

Downer, R., Roche, F., Park, P. W., Mecham, R. P., and Foster, T. J. (2002). The elastin-binding protein of *Staphylococcus aureus* (EbpS) is expressed at the cell surface as an integral membrane protein and not as a cell wall-associated protein. *J Biol Chem* 277, 243–250. doi: 10.1074/jbc.M107621200

Duthie E. S., and Lorenz, L. L. (1952). Staphylococcal coagulase; mode of action and antigenicity. *J Gen Microbiol* 6, 95–107. doi: 10.1099/00221287-6-1-2-95

Eisenbach, L., Geissler, A. J., Ehrmann, M. A., and Vogel, R. F. (2019). Comparative genomics of *Lactobacillus sakei* supports the development of starter strain combinations. *Microbiol Res* 221, 1–9. doi: 10.1016/j.micres.2019.01.001

Erskine, E., MacPhee, C. E., and Stanley-Wall, N. R. (2018). Functional Amyloid and Other Protein Fibers in the Biofilm Matrix. *Journal of Molecular Biology* 430, 3642–3656. doi: 10.1016/j.jmb.2018.07.026

Even, S., Leroy, S., Charlier, C., Zakour, N. B., Chacornac, J.-P., Lebert, I., et al. (2010). Low occurrence of safety hazards in coagulase negative staphylococci isolated from fermented foodstuffs. *Int J Food Microbiol* 139, 87–95. doi: 10.1016/j.ijfoodmicro.2010.02.019

Falkow, S. (1988). Molecular Koch's postulates applied to microbial pathogenicity. *Rev Infect Dis* 10 Suppl 2, S274-6. doi: 10.1093/cid/10.supplement_2.s274

Fernandez-Escamilla, A.-M., Rousseau, F., Schymkowitz, J., and Serrano, L. (2004). Prediction of sequence-dependent and mutational effects on the aggregation of peptides and proteins. *Nat Biotechnol* 22, 1302–1306. doi: 10.1038/nbt1012

Fey, P. D., and Olson, M. E. (2010). Current concepts in biofilm formation of *Staphylococcus epidermidis*. *Future Microbiol* 5, 917–933. doi: 10.2217/fmb.10.56

Flemming, H.-C., and Wingender, J. (2010). The biofilm matrix. *Nature Reviews Microbiology* 8, 623–633. doi: 10.1038/nrmicro2415

Foster, T. J. (2019). The MSCRAMM Family of Cell-Wall-Anchored Surface Proteins of Gram-Positive Cocci. *Trends Microbiol* 27, 927–941. doi: 10.1016/j.tim.2019.06.007

Foster, T. J. (2020). Surface Proteins of *Staphylococcus epidermidis*. *Front. Microbiol.* 11, 1829. doi: 10.3389/fmicb.2020.01829

Foster, T. J., Geoghegan, J. A., Ganesh, V. K., and Höök, M. (2014). Adhesion, invasion and evasion: the many functions of the surface proteins of *Staphylococcus aureus*. *Nature Reviews Microbiology* 12, 49–62. doi: 10.1038/nrmicro3161

França, A., Gaio, V., Lopes, N., and Melo, L. D. R. (2021). Virulence Factors in Coagulase-Negative Staphylococci. *Pathogens* 10. doi: 10.3390/pathogens10020170

Freeman, D. J., Falkiner, F. R., and Keane, C. T. (1989). New method for detecting slime production by coagulase negative staphylococci. *J Clin Pathol*, 872–874.

Gabler, F., Nam, S.-Z., Till, S., Mirdita, M., Steinegger, M., Söding, J., et al. (2020). Protein Sequence Analysis Using the MPI Bioinformatics Toolkit. *Curr Protoc Bioinformatics* 72, e108. doi: 10.1002/cpbi.108.

Garbuzynskiy, S. O., Lobanov, M. Y., and Galzitskaya, O. V. (2010). FoldAmyloid: a method of prediction of amyloidogenic regions from protein sequence. *Bioinformatics* 26, 326–332. doi: 10.1093/bioinformatics/btp691

Geoghegan, J. A., Corrigan, R. M., Gruszka, D. T., Speziale, P., O'Gara, J. P., Potts, J. R., et al. (2010). Role of surface protein SasG in biofilm formation by *Staphylococcus aureus*. *J Bacteriol* 192, 5663–5673. doi: 10.1128/JB.00628-10

Gill, S. R., Fouts, D. E., Archer, G. L., Mongodin, E. F., Deboy, R. T., Ravel, J., et al. (2005). Insights on evolution of virulence and resistance from the complete genome analysis of an early methicillin-resistant *Staphylococcus aureus* strain and a biofilm-producing methicillin-resistant *Staphylococcus epidermidis* strain. *J. Bacteriol.* 187, 2426–2438. doi: 10.1128/JB.187.7.2426-2438.2005

Goldfarb, T., Sberro, H., Weinstock, E., Cohen, O., Doron, S., Charpak-Amikam, Y., et al. (2015). BREX is a novel phage resistance system widespread in microbial genomes. *EMBO J* 34, 169–183. doi: 10.15252/embj.201489455

Goris, J., Konstantinidis, K. T., Klappenbach, J. A., Coenye, T., Vandamme, P., and Tiedje, J. M. (2007). DNA-DNA hybridization values and their relationship to whole-genome sequence similarities. *Int J Syst Evol Microbiol* 57, 81–91. doi: 10.1099/ijs.0.64483-0

Gøtterup, J., Olsen, K., Knöchel, S., Tjener, K., Stahnke, L. H., and Møller, J. K. S. (2007). Relationship between nitrate/nitrite reductase activities in meat associated staphylococci and nitrosylmyoglobin formation in a cured meat model system. *Int J Food Microbiol* 120, 303–310. doi: 10.1016/j.ijfoodmicro.2007.08.034

Götz, F. (2002). Staphylococcus and biofilms. *Mol Microbiol* 43, 1367–1378. doi: 10.1046/j.1365-2958.2002.02827.x

Götz, F., Heilmann, C., and Stehle, T. (2014). Functional and structural analysis of the major amidase (Atl) in *Staphylococcus*. *Int J Med Microbiol* 304, 156–163. doi: 10.1016/j.ijmm.2013.11.006

Götz, F., Zabielski, J., Philipson, L., and Lindberg, M. (1983). DNA homology between the arsenate resistance plasmid pSX267 from *Staphylococcus xylosus* and the penicillinase plasmid pI258 from *Staphylococcus aureus*. *Plasmid* 9, 126–137. doi: 10.1016/0147-619X(83)90015-X

Gozalo, A. S., Hoffmann, V. J., Brinster, L. R., Elkins, W. R., Ding, L., and Holland, S. M. (2010). Spontaneous *Staphylococcus xylosus* infection in mice deficient in NADPH oxidase and comparison with other laboratory mouse strains. *J Am Assoc Lab Anim Sci* 49, 480–486.

Greppi, A., Ferrocino, I., La Storia, A., Rantsiou, K., Ercolini, D., and Cocolin, L. (2015). Monitoring of the microbiota of fermented sausages by culture independent rRNA-based approaches. *Int J Food Microbiol* 212, 67–75. doi: 10.1016/j.ijfoodmicro.2015.01.016

Groot, N. S. de, Castillo, V., Graña-Montes, R., and Ventura, S. (2012). AGGRESCAN: method, application, and perspectives for drug design. *Methods Mol Biol* 819, 199–220. doi: 10.1007/978-1-61779-465-0_14

Gross, M., Cramton, S. E., Götz, F., and Peschel, A. (2001). Key role of teichoic acid net charge in *Staphylococcus aureus* colonization of artificial surfaces. *Infection and Immunity* 69, 3423–3426. doi: 10.1128/IAI.69.5.3423-3426.2001

Haaber, J., Penadés, J. R., and Ingmer, H. (2017). Transfer of Antibiotic Resistance in *Staphylococcus aureus*. *Trends Microbiol* 25, 893–905. doi: 10.1016/j.tim.2017.05.011

Haft, D. H., Selengut, J. D., and White, O. (2003). The TIGRFAMs database of protein families. *Nucleic Acids Research* 31, 371–373. doi: 10.1093/nar/gkg128

Hall, R. J., Whelan, F. J., McInerney, J. O., Ou, Y., and Domingo-Sananes, M. R. (2020). Horizontal Gene Transfer as a Source of Conflict and Cooperation in Prokaryotes. *Front. Microbiol.* 11, 1569. doi: 10.3389/fmicb.2020.01569

Hartford, O., O'Brien, L., Schofield, K., Wells, J., and Foster, T. J. (2001). The Fbe (SdrG) protein of *Staphylococcus epidermidis* HB promotes bacterial adherence to fibrinogen. *Microbiology (Reading, Engl)* 147, 2545–2552. doi: 10.1099/00221287-147-9-2545

Heilmann, C., Gerke, C., Perdreau-Remington, F., and Götz, F. (1996a). Characterization of Tn917 insertion mutants of *Staphylococcus epidermidis* affected in biofilm formation. *Infection and Immunity* 64, 277–282.

Heilmann, C., and Götz, F. (1998). Further characterization of *Staphylococcus epidermidis* transposon mutants deficient in primary attachment or intercellular adhesion. *Zentralblatt für Bakteriologie* 287, 69–83. doi: 10.1016/S0934-8840(98)80149-7

Heilmann, C., Hussain, M., Peters, G., and Götz, F. (1997). Evidence for autolysin-mediated primary attachment of *Staphylococcus epidermidis* to a polystyrene surface. *Mol Microbiol* 24, 1013–1024. doi: 10.1046/j.1365-2958.1997.4101774.x

Heilmann, C., Schweitzer, O., Gerke, C., Vanittanakom, N., Mack, D., and Götz, F. (1996b). Molecular basis of intercellular adhesion in the biofilm-forming *Staphylococcus epidermidis*. *Mol Microbiol* 20, 1083–1091. doi: 10.1111/j.1365-2958.1996.tb02548.x

Heilmann, C., Ziebuhr, W., and Becker, K. (2019). Are coagulase-negative staphylococci virulent? *Clin Microbiol Infect* 25, 1071–1080. doi: 10.1016/j.cmi.2018.11.012

Hilgarth, M. (2018). *Spoilage-associated psychrotrophic and psychrophilic microbiota on modified atmosphere packaged beef*. München: Universitätsbibliothek der TU München.

Huerta, B., Barrero-Dominguez, B., Galan-Relaño, A., Tarradas, C., Maldonado, A., and Luque, I. (2016). Essential Oils in the Control of Infections by *Staphylococcus xylosus* in Horses. *Journal of Equine Veterinary Science* 38, 19–23. doi: 10.1016/j.jevs.2015.11.011

Hutkins, R. W. (2006). *Microbiology and technology of fermented foods*. Ames, Iowa: Blackwell.

Iwase, T., Uehara, Y., Shinji, H., Tajima, A., Seo, H., Takada, K., et al. (2010). *Staphylococcus epidermidis* Esp inhibits *Staphylococcus aureus* biofilm formation and nasal colonization. *Nature* 465, 346. doi: 10.1038/nature09074

Janßen, D., Dworschak, L., Ludwig, C., Ehrmann, M. A., and Vogel, R. F. (2020). Interspecies assertiveness of *Lactobacillus curvatus* and *Lactobacillus sakei* in sausage fermentations. *Int J Food Microbiol* 331, 108689. doi: 10.1016/j.ijfoodmicro.2020.108689

Janßen, D., Eisenbach, L., Ehrmann, M. A., and Vogel, R. F. (2018). Assertiveness of *Lactobacillus sakei* and *Lactobacillus curvatus* in a fermented sausage model. *Int J Food Microbiol* 285, 188–197. doi: 10.1016/j.ijfoodmicro.2018.04.030

Jeong, H., Arif, B., Caetano-Anollés, G., Kim, K. M., and Nasir, A. (2019). Horizontal gene transfer in human-associated microorganisms inferred by phylogenetic reconstruction and reconciliation. *Sci Rep* 9, 5953. doi: 10.1038/s41598-019-42227-5

Jones, S. E., and Lennon, J. T. (2010). Dormancy contributes to the maintenance of microbial diversity. *PNAS* 107, 5881–5886. doi: 10.1073/pnas.0912765107

Jönsson, K., Signas, C., Müller, H.-P., and Lindberg, M. (1991). Two different genes encode fibronectin binding proteins in *Staphylococcus aureus*. The complete nucleotide sequence and characterization of the second gene. *European Journal of Biochemistry* 202, 1041–1048. doi: 10.1111/j.1432-1033.1991.tb16468.x

Josefsson, E., McCrea, K. W., Ní Eidhin, D., O'Connell, D., Cox, J., Höök, M., et al. (1998). Three new members of the serine-aspartate repeat protein multigene family of *Staphylococcus aureus*. *Microbiology (Reading, Engl)* 144 (Pt 12), 3387–3395. doi: 10.1099/00221287-144-12-3387

Kamens, J. (2015). The Addgene repository: an international nonprofit plasmid and data resource. *Nucleic Acids Research* 43, D1152-7. doi: 10.1093/nar/gku893

Karatan, E., and Watnick, P. (2009). Signals, regulatory networks, and materials that build and break bacterial biofilms. *Microbiol Mol Biol Rev* 73, 310–347. doi: 10.1128/MMBR.00041-08

Kaspar, U., Lützau, A. von, Schlattmann, A., Roesler, U., Köck, R., and Becker, K. (2018). Zoonotic multidrug-resistant microorganisms among small companion animals in Germany. *PLoS ONE* 13, e0208364. doi: 10.1371/journal.pone.0208364

Kaur, G., Arora, A., Sathyabama, S., Mubin, N., Verma, S., Mayilraj, S., et al. (2016). Genome sequencing, assembly, annotation and analysis of *Staphylococcus xylosus* strain DMB3-Bh1 reveals genes responsible for pathogenicity. *Gut Pathog* 8, 55. doi: 10.1186/s13099-016-0139-8

Kelley, L. A., Mezulis, S., Yates, C. M., Wass, M. N., and Sternberg, M. J. E. (2015). The Phyre2 web portal for protein modeling, prediction and analysis. *nprot* 10, 845–858. doi: 10.1038/nprot.2015.053

Kim, Y., Lee, Y.-S., Yang, J.-Y., Lee, S.-H., Park, Y.-Y., and Kweon, M.-N. (2017). The resident pathobiont *Staphylococcus xylosus* in Nfkbiz-deficient skin accelerates spontaneous skin inflammation. *Sci Rep* 7, 6348. doi: 10.1038/s41598-017-05740-z

Kloos, W. E., Zimmerman, R. J., and Smith, R. F. (1976). Preliminary studies on the characterization and distribution of *Staphylococcus* and *Micrococcus* species on animal skin. *Applied and Environmental Microbiology* 31, 53–59. doi: 10.1128/aem.31.1.53-59.1976

Knobloch, J. K., Bartscht, K., Sabottke, A., Rohde, H., Feucht, H. H., and Mack, D. (2001). Biofilm formation by *Staphylococcus epidermidis* depends on functional RsbU, an activator of the sigB operon: differential activation mechanisms due to ethanol and salt stress. *J Bacteriol* 183, 2624–2633. doi: 10.1128/JB.183.8.2624-2633.2001

Knobloch, J. K.-M., Horstkotte, M. A., Rohde, H., and Mack, D. (2002). Evaluation of different detection methods of biofilm formation in *Staphylococcus aureus*. *Med Microbiol Immunol* 191, 101–106. doi: 10.1007/s00430-002-0124-3

Koonin, E. V., Makarova, K. S., and Aravind, L. (2001). Horizontal gene transfer in prokaryotes: quantification and classification. *Annu Rev Microbiol* 55, 709–742. doi: 10.1146/annurev.micro.55.1.709

Kumar, S., Stecher, G., and Tamura, K. (2016). MEGA7: Molecular Evolutionary Genetics Analysis Version 7.0 for Bigger Datasets. *Mol Biol Evol* 33, 1870–1874. doi: 10.1093/molbev/msw054

Lamret, F., Varin-Simon, J., Velard, F., Terryn, C., Mongaret, C., Colin, M., et al. (2021*). Staphylococcus aureus* Strain-Dependent Biofilm Formation in Bone-Like Environment. *Front. Microbiol.* 12, 714994. doi: 10.3389/fmicb.2021.714994

Laranjo, M., Potes, M. E., and Elias, M. (2019). Role of Starter Cultures on the Safety of Fermented Meat Products. *Front. Microbiol.* 10, 853. doi: 10.3389/fmicb.2019.00853

Lawal, O. U., Barata, M., Fraqueza, M. J., Worning, P., Bartels, M. D., Goncalves, L., et al. (2021). *Staphylococcus saprophyticus* from clinical and environmental origins have distinct biofilm composition. *Front. Microbiol.* 12, 663768. doi: 10.3389/fmicb.2021.663768

Lawley, T. D., and Walker, A. W. (2013). Intestinal colonization resistance. *Immunology* 138, 1–11. doi: 10.1111/j.1365-2567.2012.03616.x

Le, K. Y., Villaruz, A. E., Zheng, Y., He, L., Fisher, E. L., Nguyen, T. H., et al. (2019). Role of Phenol-Soluble Modulins in *Staphylococcus epidermidis* Biofilm Formation and Infection of Indwelling Medical Devices. *Journal of Molecular Biology* 431, 3015–3027. doi: 10.1016/j.jmb.2019.03.030

Lee, J. Y. H., Carter, G. P., Pidot, S. J., Guérillot, R., Seemann, T., Silva, A. G. d., et al. (2019). Mining the Methylome Reveals Extensive Diversity in *Staphylococcus epidermidis* Restriction Modification. *MBio* 10. doi: 10.1128/mBio.02451-19

Leroy, F., Verluyten, J., and Vuyst, L. D. (2006). Functional meat starter cultures for improved sausage fermentation. *Int J Food Microbiol* 106, 270–285. doi: 10.1016/j.ijfoodmicro.2005.06.027

Leroy, S., Christieans, S., and Talon, R. (2019). Tetracycline Gene Transfer in *Staphylococcus xylosus* in situ During Sausage Fermentation. *Front. Microbiol.* 10, 392. doi: 10.3389/fmicb.2019.00392

Leroy, S., Giammarinaro, P., Chacornac, J.-P., Lebert, I., and Talon, R. (2010). Biodiversity of indigenous staphylococci of naturally fermented dry sausages and manufacturing environments of small-scale processing units. *Food Microbiol* 27, 294–301. doi: 10.1016/j.fm.2009.11.005

Leroy, S., Lebert, I., Andant, C., Micheau, P., and Talon, R. (2021). Investigating Extracellular DNA Release in *Staphylococcus xylosus* Biofilm In Vitro. *Microorganisms* 9, 2192. doi: 10.3390/microorganisms9112192

Leroy, S., Lebert, I., Andant, C., and Talon, R. (2020). Interaction in dual species biofilms between *Staphylococcus xylosus* and *Staphylococcus aureus*. *Int J Food Microbiol* 326, 108653. doi: 10.1016/j.ijfoodmicro.2020.108653

Leroy, S., Vermassen, A., Ras, G., and Talon, R. (2017). Insight into the genome of *Staphylococcus xylosus*, a ubiquitous species well adapted to meat products. *Microorganisms* 5. doi: 10.3390/microorganisms5030052

Lewit-Bentley, A., and Réty, S. (2000). EF-hand calcium-binding proteins. *Current Opinion in Structural Biology* 10, 637–643. doi: 10.1016/S0959-440X(00)00142-1

Liljeqvist, S., Samuelson, P., Hansson, M., Nguyen, T. N., Binz, H., and Ståhl, S. (1997). Surface display of the cholera toxin B subunit on *Staphylococcus xylosus* and *Staphylococcus carnosus*. *Applied and Environmental Microbiology* 63, 2481–2488. doi: 10.1128/aem.63.7.2481-2488.1997

Lindsay, J. A. (2010). Genomic variation and evolution of *Staphylococcus aureus*. *International Journal of Medical Microbiology* 300, 98–103. doi: 10.1016/j.ijmm.2009.08.013

Lindsay, J. A. (2014). *Staphylococcus aureus* genomics and the impact of horizontal gene transfer. *International Journal of Medical Microbiology* 304, 103–109. doi: 10.1016/j.ijmm.2013.11.010

Lindsay, J. A. (2019). Staphylococci: Evolving Genomes. *Microbiol Spectr* 7. doi: 10.1128/microbiolspec.GPP3-0071-2019

Loenen, W. A. M., Dryden, D. T. F., Raleigh, E. A., and Wilson, G. G. (2014). Type I restriction enzymes and their relatives. *Nucleic Acids Research* 42, 20–44. doi: 10.1093/nar/gkt847

Loenen, W. A. M., and Raleigh, E. A. (2014). The other face of restriction: modification-dependent enzymes. *Nucleic Acids Research* 42, 56–69. doi: 10.1093/nar/gkt747

Louros, N., Konstantoulea, K., Vleeschouwer, M. de, Ramakers, M., Schymkowitz, J., and Rousseau, F. (2020). WALTZ-DB 2.0: an updated database containing structural information of experimentally determined amyloid-forming peptides. *Nucleic Acids Research* 48, D389-D393. doi: 10.1093/nar/gkz758

Luo, Y., Javed, M. A., and Deneer, H. (2018). Comparative study on nutrient depletion-induced lipidome adaptations in *Staphylococcus haemolyticus* and *Staphylococcus epidermidis*. *Sci Rep* 8, 2356. doi: 10.1038/s41598-018-20801-7

Luqman, A., Zabel, S., Rahmdel, S., Merz, B., Gruenheit, N., Harter, J., et al. (2020). The Neuromodulator-Encoding sadA Gene Is Widely Distributed in the Human Skin Microbiome. *Front. Microbiol.* 11, 573679. doi: 10.3389/fmicb.2020.573679

Ma, A. P. Y., Jiang, J., Tun, H. M., Mauroo, N. F., Yuen, C. S., and Leung, F. C.-C. (2014). Complete genome sequence of *Staphylococcus xylosus* HKUOPL8, a potential opportunistic pathogen of mammals. *Genome Announc* 2. doi: 10.1128/genomeA.00653-14

Mack, D., Nedelmann, M., Krokotsch, A., Schwarzkopf, A., Heesemann, J., and Laufs, R. (1994). Characterization of transposon mutants of biofilm-producing *Staphylococcus epidermidis* impaired in the accumulative phase of biofilm production: genetic identification of a hexosamine-containing polysaccharide intercellular adhesin. *Infection and Immunity* 62, 3244–3253.

Marchler-Bauer, A., Derbyshire, M. K., Gonzales, N. R., Lu, S., Chitsaz, F., Geer, L. Y., et al. (2015). CDD: NCBI's conserved domain database. *Nucleic Acids Research* 43, D222-6. doi: 10.1093/nar/gku1221

Martín, B., Garriga, M., Hugas, M., Bover-Cid, S., Veciana-Nogués, M. T., and Aymerich, T. (2006). Molecular, technological and safety characterization of Gram-positive catalase-positive cocci from slightly fermented sausages. *Int J Food Microbiol* 107, 148–158. doi: 10.1016/j.ijfoodmicro.2005.08.024

Martínez-García, S., Peralta, H., Betanzos-Cabrera, G., Chavez-Galan, L., Rodríguez-Martínez, S., Cancino-Diaz, M. E., et al. (2021). Proteomic comparison of biofilm vs. *planktonic Staphylococcus epidermidis* cells suggests key metabolic differences between these conditions. *Res Microbiol* 172, 103796. doi: 10.1016/j.resmic.2020.103796

McCarthy, A. J., Loeffler, A., Witney, A. A., Gould, K. A., Lloyd, D. H., and Lindsay, J. A. (2014). Extensive horizontal gene transfer during *Staphylococcus aureus* co-colonization in vivo. *Genome Biol Evol* 6, 2697–2708. doi: 10.1093/gbe/evu214

McCourt, J., O'Halloran, D. P., McCarthy, H., O'Gara, J. P., and Geoghegan, J. A. (2014). Fibronectin-binding proteins are required for biofilm formation by community-associated methicillin-resistant *Staphylococcus aureus* strain LAC. *FEMS Microbiol Lett* 353, 157–164. doi: 10.1111/1574-6968.12424

McCrea, K. W., Hartford, O., Davis, S., Eidhin, D. N., Lina, G., Speziale, P., et al. (2000). The serine-aspartate repeat (Sdr) protein family in *Staphylococcus epidermidis*. *Microbiology (Reading, Engl)* 146 (Pt 7), 1535–1546. doi: 10.1099/00221287-146-7-1535

McDevitt, D., Francois, P., Vaudaux, P., and Foster, T. J. (1994). Molecular characterization of the clumping factor (fibrinogen receptor) of *Staphylococcus aureus*. *Mol Microbiol* 11, 237–248.

Monk, I. R., and Foster, T. J. (2012). Genetic manipulation of Staphylococci—breaking through the barrier. *Front Cell Infect Microbiol* 2. doi: 10.3389/fcimb.2012.00049

Monk, I. R., Shah, I. M., Xu, M., Tan, M.-W., and Foster, T. J. (2012). Transforming the Untransformable: Application of Direct Transformation To Manipulate Genetically *Staphylococcus aureus* and *Staphylococcus epidermidis*. *MBio* 3, e00277-11. doi: 10.1128/mBio.00277-11

Monk, I. R., and Stinear, T. P. (2021). From cloning to mutant in 5 days: rapid allelic exchange in *Staphylococcus aureus*. *Access Microbiology* 3. doi: 10.1099/acmi.0.000193

Monk, I. R., Tree, J. J., Howden, B. P., Stinear, T. P., and Foster, T. J. (2015). Complete Bypass of Restriction Systems for Major *Staphylococcus aureus* Lineages. *MBio* 6. doi: 10.1128/mBio.00308-15

Moretro, T., Hermansen, L., Holck, A. L., Sidhu, M. S., Rudi, K., and Langsrud, S. (2003). Biofilm formation and the presence of the intercellular adhesion locus *ica* among staphylococci from food and food processing environments. *Applied and Environmental Microbiology* 69, 5648–5655. doi: 10.1128/AEM.69.9.5648-5655.2003

Murray, N. E. (2000). Type I restriction systems: sophisticated molecular machines (a legacy of Bertani and Weigle). *Microbiology and Molecular Biology Reviews* 64, 412–434. doi: 10.1128/MMBR.64.2.412-434.2000

Nagase, N., Sasaki, A., Yamashita, K., Shimizu, A., Wakita, Y., Kitai, S., et al. (2002). Isolation and species distribution of staphylococci from animal and human skin. *J Vet Med Sci* 64, 245–250. doi: 10.1292/jvms.64.245

Nega, M., Tribelli, P. M., Hipp, K., Stahl, M., and Götz, F. (2020). New insights in the coordinated amidase and glucosaminidase activity of the major autolysin (Atl) in *Staphylococcus aureus*. *Commun Biol* 3, 695. doi: 10.1038/s42003-020-01405-2

Ní Eidhin, D., Perkins, S., Francois, P., Vaudaux, P., Höök, M., and Foster, T. J. (1998). Clumping factor B (ClfB), a new surface-located fibrinogen-binding adhesin of *Staphylococcus aureus*. *Mol Microbiol* 30, 245–257. doi: 10.1046/j.1365-2958.1998.01050.x

Nye, T. M., Fernandez, N. L., and Simmons, L. A. (2020). A positive perspective on DNA methylation: regulatory functions of DNA methylation outside of host defense in Gram-positive bacteria. *Crit Rev Biochem Mol Biol* 55, 576–591. doi: 10.1080/10409238.2020.1828257

Okshevsky, M., and Meyer, R. L. (2015). The role of extracellular DNA in the establishment, maintenance and perpetuation of bacterial biofilms. *Crit Rev Microbiol* 41, 341–352. doi: 10.3109/1040841X.2013.841639

Oliveira, P. H., and Fang, G. (2021). Conserved DNA Methyltransferases: A Window into Fundamental Mechanisms of Epigenetic Regulation in Bacteria. *Trends Microbiol* 29, 28–40. doi: 10.1016/j.tim.2020.04.007

Ommen, P., Zobek, N., and Meyer, R. L. (2017). Quantification of biofilm biomass by staining: Non-toxic safranin can replace the popular crystal violet. *J Microbiol Methods* 141, 87–89. doi: 10.1016/j.mimet.2017.08.003

Otto, M. (2004). Virulence factors of the coagulase-negative staphylococci. *Front Biosci* 9, 841–863. doi: 10.2741/1295

Otto, M. (2006). Bacterial evasion of antimicrobial peptides by biofilm formation. *Curr Top Microbiol Immunol* 306, 251–258. doi: 10.1007/3-540-29916-5_10

Otto, M. (2008). Staphylococcal Biofilms. *Curr Top Microbiol Immunol* 322, 207–228.

Otto, M. (2009). *Staphylococcus epidermidis* – the "accidental" pathogen. *Nat Rev Microbiol* 7, 555–567. doi: 10.1038/nrmicro2182

Otto, M. (2013a). Coagulase-negative staphylococci as reservoirs of genes facilitating MRSA infection: Staphylococcal commensal species such as *Staphylococcus epidermidis* are being recognized as important sources of genes promoting MRSA colonization and virulence. *Bioessays* 35, 4–11. doi: 10.1002/bies.201200112

Otto, M. (2013b). Staphylococcal infections: mechanisms of biofilm maturation and detachment as critical determinants of pathogenicity. *Annu Rev Med* 64, 175–188. doi: 10.1146/annurev-med-042711-140023

Otto, M. (2014). Physical stress and bacterial colonization. *FEMS Microbiol Rev* 38, 1250–1270. doi: 10.1111/1574-6976.12088

Overbeek, R., Olson, R., Pusch, G. D., Olsen, G. J., Davis, J. J., Disz, T., et al. (2014). The SEED and the Rapid Annotation of microbial genomes using Subsystems Technology (RAST). *Nucleic Acids Research* 42, D206-14. doi: 10.1093/nar/gkt1226

Paharik, A. E., Kotasinska, M., Both, A., Hoang, T.-M. N., Büttner, H., Roy, P., et al. (2017). The metalloprotease SepA governs processing of accumulation-associated protein and shapes intercellular adhesive surface properties in *Staphylococcus epidermidis*. *Mol Microbiol* 103, 860–874. doi: 10.1111/mmi.13594

Patti, J. M., Jonsson, H., Guss, B., Switalski, L. M., Wiberg, K., Lindberg, M., et al. (1992). Molecular characterization and expression of a gene encoding a *Staphylococcus aureus* collagen adhesin. *J Biol Chem* 267, 4766–4772.

Pérez-Cobas, A. E., Moya, A., Gosalbes, M. J., and Latorre, A. (2015). Colonization Resistance of the Gut Microbiota against Clostridium difficile. *Antibiotics (Basel)* 4, 337–357. doi: 10.3390/antibiotics4030337

Perez-Riverol, Y., Csordas, A., Bai, J., Bernal-Llinares, M., Hewapathirana, S., Kundu, D. J., et al. (2019). The PRIDE database and related tools and resources in 2019: improving support for quantification data. *Nucleic Acids Research* 47, D442-D450. doi: 10.1093/nar/gky1106

Peschel, A., and Otto, M. (2013). Phenol-soluble modulins and staphylococcal infection. *Nat Rev Microbiol* 11, 667–673. doi: 10.1038/nrmicro3110

Piras, C., Di Ciccio, P. A., Soggiu, A., Greco, V., Tilocca, B., Costanzo, N., et al. (2021). S. aureus Biofilm Protein Expression Linked to Antimicrobial Resistance: A Proteomic Study. *Animals (Basel)* 11. doi: 10.3390/ani11040966

Planchon, S., Desvaux, M., Chafsey, I., Chambon, C., Leroy, S., Hébraud, M., et al. (2009). Comparative subproteome analyses of planktonic and sessile *Staphylococcus xylosus* C2a: New insight in cell physiology of a coagulase-negative *Staphylococcus* in biofilm. *J Proteome Res* 8, 1797–1809. doi: 10.1021/pr8004056

Planchon, S., Gaillard-Martinie, B., Dordet-Frisoni, E., Bellon-Fontaine, M. N., Leroy, S., Labadie, J., et al. (2006). Formation of biofilm by *Staphylococcus xylosus*. *Int J Food Microbiol* 109, 88–96. doi: 10.1016/j.ijfoodmicro.2006.01.016

Qin, Z., Ou, Y., Yang, L., Zhu, Y., Tolker-Nielsen, T., Molin, S., et al. (2007). Role of autolysin-mediated DNA release in biofilm formation of *Staphylococcus epidermidis*. *Microbiology (Reading, Engl)* 153, 2083–2092. doi: 10.1099/mic.0.2007/006031-0

Rachid, S., Ohlsen, K., Wallner, U., Hacker, J., Hecker, M., and Ziebuhr, W. (2000a). Alternative transcription factor sigma B is involved in regulation of biofilm expression in a *Staphylococcus aureus* mucosal isolate. *J Bacteriol* 182, 6824–6826. doi: 10.1128/JB.182.23.6824-6826.2000

Rachid, S., Ohlsen, K., Witte, W., Hacker, J., and Ziebuhr, W. (2000b). Effect of subinhibitory antibiotic concentrations on polysaccharide intercellular adhesin expression in biofilm-forming *Staphylococcus epidermidis*. *Antimicrob Agents Chemother* 44, 3357–3363. doi: 10.1128/AAC.44.12.3357-3363.2000

Rahmdel, S., and Götz, F. (2021). The Multitasking Surface Protein of Staphylococcus epidermidis: Accumulation-Associated Protein (Aap). *MBio* 12, e0198921. doi: 10.1128/mBio.01989-21

Resch, A., Fehrenbacher, B., Eisele, K., Schaller, M., and Götz, F. (2005). Phage release from biofilm and planktonic *Staphylococcus aureus* cells. *FEMS Microbiol Lett* 252, 89–96. doi: 10.1016/j.femsle.2005.08.048

Resch, M., Nagel, V., and Hertel, C. (2008). Antibiotic resistance of coagulase-negative staphylococci associated with food and used in starter cultures. *Int J Food Microbiol* 127, 99–104. doi: 10.1016/j.ijfoodmicro.2008.06.013

Richter, M., Rosselló-Móra, R., Oliver Glöckner, F., and Peplies, J. (2016). JSpeciesWS: a web server for prokaryotic species circumscription based on pairwise genome comparison. *Bioinformatics* 32, 929–931. doi: 10.1093/bioinformatics/btv681

Roche, F. M., Massey, R., Peacock, S. J., Day, N. P. J., Visai, L., Speziale, P., et al. (2003). Characterization of novel LPXTG-containing proteins of *Staphylococcus aureus* identified from genome sequences. *Microbiology* 149, 643–654. doi: 10.1099/mic.0.25996-0

Rogers, K. L., Fey, P. D., and Rupp, M. E. (2009). Coagulase-negative staphylococcal infections. *Infect Dis Clin North Am* 23, 73–98. doi: 10.1016/j.idc.2008.10.001

Rohde, H., Burdelski, C., Bartscht, K., Hussain, M., Buck, F., Horstkotte, M. A., et al. (2005). Induction of *Staphylococcus epidermidis* biofilm formation via proteolytic processing of the accumulation-associated protein by staphylococcal and host proteases. *Mol Microbiol* 55, 1883–1895. doi: 10.1111/j.1365-2958.2005.04515.x

Rossi, C. C., Souza-Silva, T., Araújo-Alves, A. V., and Giambiagi-Demarval, M. (2017). CRISPR-Cas Systems Features and the Gene-Reservoir Role of Coagulase-Negative Staphylococci. *Front. Microbiol.* 8, 1545. doi: 10.3389/fmicb.2017.01545

Roy, P., Horswill, A. R., and Fey, P. D. (2021). Glycan-Dependent Corneocyte Adherence of *Staphylococcus epidermidis* Mediated by the Lectin Subdomain of Aap. *MBio* 12, e0290820. doi: 10.1128/mBio.02908-20

Sadykov, M. R., and Bayles, K. W. (2012). The control of death and lysis in staphylococcal biofilms: a coordination of physiological signals. *Curr Opin Microbiol* 15, 211–215. doi: 10.1016/j.mib.2011.12.010

Samuelson, P., Wernérus, H., Svedberg, M., and Ståhl, S. (2000). Staphylococcal surface display of metal-binding polyhistidyl peptides. *Applied and Environmental Microbiology* 66, 1243–1248. doi: 10.1128/aem.66.3.1243-1248.2000

Schiffer, C., Hilgarth, M., Ehrmann, M., and Vogel, R. F. (2019). Bap and cell surface hydrophobicity are important factors in *Staphylococcus xylosus* biofilm formation. *Front. Microbiol.* 10, 1387. doi: 10.3389/fmicb.2019.01387

Schiffer, C. J., Abele, M., Ehrmann, M. A., and Vogel, R. F. (2021). Bap-Independent Biofilm Formation in *Staphylococcus xylosus*. *Microorganisms* 9, 2610. doi: 10.3390/microorganisms9122610

Schiffer, C. J., Schaudinn, C., Ehrmann, M. A., and Vogel, R. F. (2022a). SxsA, a novel surface protein mediating cell aggregation and adhesive biofilm formation of *Staphylococcus xylosus*. *Mol Microbiol*. doi: 10.1111/mmi.14884

Schiffer, C. J., Vogel, R. F., and Ehrmann, M. A. (2022b). Characterization of the *Staphylococcus xylosus* methylome reveals a new variant of Type I restriction modification system. Currently under Review.

Schilcher, K., and Horswill, A. R. (2020). Staphylococcal Biofilm Development: Structure, Regulation, and Treatment Strategies. *Microbiol Mol Biol Rev* 84. doi: 10.1128/MMBR.00026-19

Schlag, S., Nerz, C., Birkenstock, T. A., Altenberend, F., and Götz, F. (2007). Inhibition of Staphylococcal Biofilm Formation by Nitrite. *J Bacteriol* 189, 7911–7919. doi: 10.1128/JB.00598-07

Schleifer, K. H., and Kloos, W. E. (1975). Isolation and Characterization of Staphylococci from Human Skin I. Amended Descriptions of *Staphylococcus epidermidis* and *Staphylococcus saprophyticus* and Descriptions of Three New Species: *Staphylococcus cohnii*, *Staphylococcus haemolyticus*, and *Staphylococcus xylosus*. *International Journal of Systematic Bacteriology* 25, 50–61. doi: 10.1099/00207713-25-1-50

Schuster, C. F., Howard, S. A., and Gründling, A. (2019). Use of the counter selectable marker PheS* for genome engineering in *Staphylococcus aureus*. *Microbiology* 165, 572–584. doi: 10.1099/mic.0.000791

Seitter, M., Geng, B., and Hertel, C. (2011). Binding to extracellular matrix proteins and formation of biogenic amines by food-associated coagulase-negative staphylococci. *Int J Food Microbiol* 145, 483–487. doi: 10.1016/j.ijfoodmicro.2011.01.026

Shah, A. D., Goode, R. J. A., Huang, C., Powell, D. R., and Schittenhelm, R. B. (2020). LFQ-Analyst: An Easy-To-Use Interactive Web Platform To Analyze and Visualize Label-Free Proteomics Data Preprocessed with MaxQuant. *J Proteome Res* 19, 204–211. doi: 10.1021/acs.jproteome.9b00496

Sizemore, C., Wieland, B., Götz, F., and Hillen, W. (1992). Regulation of *Staphylococcus xylosus* xylose utilization genes at the molecular level. *J. Bacteriol.* 174, 3042–3048. doi: 10.1128/jb.174.9.3042-3048.1992

Sorensen, M. T., Nørgaard, J. V., Theil, P. K., Vestergaard, M., and Sejrsen, K. (2006). Cell turnover and activity in mammary tissue during lactation and the dry period in dairy cows. *J Dairy Sci* 89, 4632–4639. doi: 10.3168/jds.S0022-0302(06)72513-9

Speziale, P., Pietrocola, G., Foster, T. J., and Geoghegan, J. A. (2014). Protein-based biofilm matrices in Staphylococci. *Front Cell Infect Microbiol* 4, 171. doi: 10.3389/fcimb.2014.00171

Stahnke, L. H. (1994). Aroma components from dried sausages fermented with *Staphylococcus xylosus*. *Meat Sci* 38, 39–53. doi: 10.1016/0309-1740(94)90094-9

Stalder, T., and Top, E. (2016). Plasmid transfer in biofilms: a perspective on limitations and opportunities. *npj Biofilms Microbiomes* 2. doi: 10.1038/npjbiofilms.2016.22

Stewart, P. S. (2002). Mechanisms of antibiotic resistance in bacterial biofilms. *International Journal of Medical Microbiology* 292, 107–113. doi: 10.1078/1438-4221-00196

Stewart, P. S., and Franklin, M. J. (2008). Physiological heterogeneity in biofilms. *Nat Rev Microbiol* 6, 199–210. doi: 10.1038/nrmicro1838

St-Pierre, F., Cui, L., Priest, D. G., Endy, D., Dodd, I. B., and Shearwin, K. E. (2013). One-step cloning and chromosomal integration of DNA. *ACS Synth Biol* 2, 537–541. doi: 10.1021/sb400021j

Supré, K., Haesebrouck, F., Zadoks, R. N., Vaneechoutte, M., Piepers, S., and Vliegher, S. de (2011). Some coagulase-negative *Staphylococcus* species affect udder health more than others. *J Dairy Sci* 94, 2329–2340. doi: 10.3168/jds.2010-3741

Suzuki, T., and Yasui, K. (2011). "Plasmid Artificial Modification: A Novel Method for Efficient DNA Transfer into Bacteria," in *Strain engineering: Methods and protocols*, ed. J. A. Williams (Totowa, N.J. Humana Press), 309–326.

Taglialegna, A., Lasa, I., and Valle, J. (2016a). Amyloid structures as biofilm matrix scaffolds. *J Bacteriol* 198, 2579–2588. doi: 10.1128/JB.00122-16

Taglialegna, A., Navarro, S., Ventura, S., Garnett, J. A., Matthews, S., Penades, J. R., et al. (2016b). Staphylococcal Bap proteins build amyloid scaffold biofilm matrices in response to environmental signals. *PLOS Pathogens* 12, e1005711. doi: 10.1371/journal.ppat.1005711

Talon, R., and Leroy, S. (2011). Diversity and safety hazards of bacteria involved in meat fermentations. *Meat Sci* 89, 303–309. doi: 10.1016/j.meatsci.2011.04.029

Tatusova, T., DiCuccio, M., Badretdin, A., Chetvernin, V., Nawrocki, E. P., Zaslavsky, L., et al. (2016). NCBI prokaryotic genome annotation pipeline. *Nucleic Acids Research* 44, 6614–6624. doi: 10.1093/nar/gkw569

Thomas, C. M., and Nielsen, K. M. (2005). Mechanisms of, and barriers to, horizontal gene transfer between bacteria. *Nat Rev Microbiol* 3, 711–721. doi: 10.1038/nrmicro1234

Toldrá, F. (2015). *Handbook of fermented meat and poultry*. Chichester, West Sussex, UK: Wiley Blackwell.

Tormo, M. A., Knecht, E., Götz, F., Lasa, I., and Penades, J. R. (2005). Bap-dependent biofilm formation by pathogenic species of *Staphylococcus*: evidence of horizontal gene transfer? *Microbiology (Reading, Engl)* 151, 2465–2475. doi: 10.1099/mic.0.27865-0

Tremblay, Y. D. N., Caron, V., Blondeau, A., Messier, S., and Jacques, M. (2014). Biofilm formation by coagulase-negative staphylococci: impact on the efficacy of antimicrobials and disinfectants commonly used on dairy farms. *Vet Microbiol* 172, 511–518. doi: 10.1016/j.vetmic.2014.06.007

Tremblay, Y. D. N., Lamarche, D., Chever, P., Haine, D., Messier, S., and Jacques, M. (2013). Characterization of the ability of coagulase-negative staphylococci isolated from the milk of Canadian farms to form biofilms. *J Dairy Sci* 96, 234–246. doi: 10.3168/jds.2012-5795

Trotonda, M. P., Manna, A. C., Cheung, A. L., Lasa, I., and Penadés, J. R. (2005). SarA positively controls bap-dependent biofilm formation in *Staphylococcus aureus. J. Bacteriol.* 187, 5790–5798. doi: 10.1128/JB.187.16.5790-5798.2005

Tyanova, S., Temu, T., Sinitcyn, P., Carlson, A., Hein, M. Y., Geiger, T., et al. (2016). The Perseus computational platform for comprehensive analysis of (prote)omics data. *Nat Methods* 13, 731–740. doi: 10.1038/nmeth.3901

Uribe-Alvarez, C., Chiquete-Félix, N., Contreras-Zentella, M., Guerrero-Castillo, S., Peña, A., and Uribe-Carvajal, S. (2016). *Staphylococcus epidermidis:* metabolic adaptation and biofilm formation in response to different oxygen concentrations. *Pathog Dis* 74, ftv111. doi: 10.1093/femspd/ftv111

Vermassen, A., Dordet-Frisoni, E., La Foye, A. de, Micheau, P., Laroute, V., Leroy, S., et al. (2016). Adaptation of *Staphylococcus xylosus* to Nutrients and Osmotic Stress in a Salted Meat Model. *Front Microbiol* 7, 87. doi: 10.3389/fmicb.2016.00087

Vermassen, A., La Foye, A. de, Loux, V., Talon, R., and Leroy, S. (2014). Transcriptomic analysis of *Staphylococcus xylosus* in the presence of nitrate and nitrite in meat reveals its response to nitrosative stress. *Front Microbiol* 5, 691. doi: 10.3389/fmicb.2014.00691

Vos, P. de, Garrity, G. M., and Jones, D., eds (2009). *Bergey's manual of systematic bacteriology: Volume 3: The firmicutes*. Dordrecht, London: Springer.

Vuong, C., Voyich, J. M., Fischer, E. R., Braughton, K. R., Whitney, A. R., DeLeo, F. R., et al. (2004). Polysaccharide intercellular adhesin (PIA) protects *Staphylococcus epidermidis* against major components of the human innate immune system. *Cellular Microbiology* 6, 269–275. doi: 10.1046/j.1462-5822.2004.00367.x

Waldron, D. E., and Lindsay, J. A. (2006). Sau1: a Novel Lineage-Specific Type I Restriction-Modification System That Blocks Horizontal Gene Transfer into *Staphylococcus aureus* and *between S. aureus* Isolates of Different Lineages. *J Bacteriol* 188, 5578–5585. doi: 10.1128/JB.00418-06

Wang, L., Jiang, S., Deng, Z., Dedon, P. C., and Chen, S. (2019). DNA phosphorothioate modification-a new multi-functional epigenetic system in bacteria. *FEMS Microbiol Rev* 43, 109–122. doi: 10.1093/femsre/fuy036

Wick, R. R., Judd, L. M., Gorrie, C. L., and Holt, K. E. (2016). *Unicycler: resolving bacterial genome assemblies from short and long sequencing reads*.

Widenmann, A., Schiffer, C. J., Ehrmann, M. A., and Vogel, R. F. (2022). Impact of different sugars and glycosyltransferases on the assertiveness of *Latilactobacillus sakei* in raw sausage fermentations. *Int J Food Microbiol*. Submitted, minor revision pending.

Wu, Y.-F., Lee, T.-Y., Liao, W.-T., Chuan, H.-H., Cheng, N.-C., and Cheng, C.-M. (2020). Rapid detection of biofilm with modified alcian blue staining: In-vitro protocol improvement and validation with clinical cases. *Wound Repair Regen* 28, 834–843. doi: 10.1111/wrr.12845

Xu, C.-G., Yang, Y.-B., Zhou, Y.-H., Hao, M.-Q., Ren, Y.-Z., Wang, X.-T., et al. (2017). Comparative proteomic analysis provides insight into the key proteins as possible targets involved in aspirin inhibiting biofilm formation of *Staphylococcus xylosus*. *Frontiers in Pharmacology* 8. doi: 10.3389/fphar.2017.00543

Xu, S.-Y., Corvaglia, A. R., Chan, S.-H., Zheng, Y., and Linder, P. (2011). A type IV modification-dependent restriction enzyme SauUSI from *Staphylococcus aureus* subsp. aureus USA300. *Nucleic Acids Research* 39, 5597–5610. doi: 10.1093/nar/gkr098

Yao, Y., Sturdevant, D. E., and Otto, M. (2005). Genomewide analysis of gene expression in *Staphylococcus epidermidis* biofilms: insights into the pathophysiology of S. epidermidis biofilms and the role of phenol-soluble modulins in formation of biofilms. *J Infect Dis* 191, 289–298. doi: 10.1086/426945

Yarawsky, A. E., Johns, S. L., Schuck, P., and Herr, A. B. (2020). The biofilm adhesion protein Aap from *Staphylococcus epidermidis* forms zinc-dependent amyloid fibers. *J. Biol. Chem.* 295, 4411–4427. doi: 10.1074/jbc.RA119.010874

Yonemoto, K., Chiba, A., Sugimoto, S., Sato, C., Saito, M., Kinjo, Y., et al. (2019). Redundant and Distinct Roles of Secreted Protein Eap and Cell Wall-Anchored Protein SasG in Biofilm Formation and Pathogenicity of *Staphylococcus aureus*. *Infection and Immunity* 87. doi: 10.1128/IAI.00894-18

Yu, L., Hisatsune, J., Hayashi, I., Tatsukawa, N., Sato'o, Y., Mizumachi, E., et al. (2017). A Novel Repressor of the *ica* Locus Discovered in Clinically Isolated Super-Biofilm-Elaborating *Staphylococcus aureus*. *MBio* 8. doi: 10.1128/mBio.02282-16

Zapotoczna, M., O'Neill, E., and O'Gara, J. P. (2016). Untangling the Diverse and Redundant Mechanisms of *Staphylococcus aureus* Biofilm Formation. *PLOS Pathogens* 12, e1005671. doi: 10.1371/journal.ppat.1005671

Zell, C., Resch, M., Rosenstein, R., Albrecht, T., Hertel, C., and Götz, F. (2008). Characterization of toxin production of coagulase-negative staphylococci isolated from food and starter cultures. *Int J Food Microbiol* 127, 246–251. doi: 10.1016/j.ijfoodmicro.2008.07.016

Zhou, Y.-H., Xu, C.-G., Yang, Y.-B., Xing, X.-X., Liu, X., Qu, Q.-W., et al. (2018). Histidine Metabolism and IGPD Play a Key Role in Cefquinome Inhibiting Biofilm Formation of *Staphylococcus xylosus*. *Front Microbiol* 9, 665. doi: 10.3389/fmicb.2018.00665

Zhu, Y., Weiss, E. C., Otto, M., Fey, P. D., Smeltzer, M. S., and Somerville, G. A. (2007). *Staphylococcus aureus* Biofilm Metabolism and the Influence of Arginine on Polysaccharide Intercellular Adhesin Synthesis, Biofilm Formation, and Pathogenesis. *Infection and Immunity* 75, 4219–4226. doi: 10.1128/IAI.00509-07

8 Appendix

Appendix A 1 | Table A1: Overview of ORFs encoded in TMW 2.1023, 2.1324, 2.1521 and 2.1523 but not in 2.1602. Output was generated using the BADGE pipeline with 0.95% sequence identity cutoff.

TMW 2.1023	TMW 2.1324	TMW 2.1521	TMW 2.1523	TMW 2.1602	Annotation (PGAP based)
1	1	1	1	0	**LysR family transcriptional regulator**
1	1	1	1	0	MFS transporter
1	1	1	1	0	hypothetical protein
1	1	1	1	0	amino acid adenylation domain-containing protein
1	1	1	1	0	gluconate permease
1	1	1	1	0	TIM barrel protein
1	1	1	1	0	2-hydroxy-3-oxopropionate reductase
1	1	1	1	0	DUF805 domain-containing protein
1	1	1	1	0	membrane protein insertase YidC
1	1	1	1	0	**helix-turn-helix transcriptional regulator**
1	1	1	1	0	nitronate monooxygenase
1	1	1	1	0	**helix-turn-helix transcriptional regulator**
1	1	1	1	0	NAD(P)-binding domain-containing protein
1	1	1	1	0	hypothetical protein
1	1	1	1	0	zinc ribbon domain-containing protein
1	1	1	1	0	nitric oxide dioxygenase
1	1	1	1	0	DUF3021 domain-containing protein
1	1	1	1	0	DUF4188 domain-containing protein
1	1	1	1	0	ABC transporter substrate-binding protein
1	1	1	1	0	**helix-turn-helix transcriptional regulator**
1	1	1	1	0	MFS transporter
1	1	1	1	0	right-handed parallel beta-helix repeat-containing protein
1	1	1	1	0	DUF2648 domain-containing protein
1	1	1	1	0	malate dehydrogenase (quinone)
1	1	1	1	0	acetolactate synthase AlsS
1	1	1	1	0	acetolactate decarboxylase
1	1	1	1	0	hypothetical protein
1	1	1	1	0	flavin reductase family protein
1	1	1	1	0	LLM class flavin-dependent oxidoreductase
1	1	1	1	0	solute:sodium symporter family transporter
1	1	1	1	0	transglycosylase family protein
1	1	1	1	0	beta-class phenol-soluble modulin
1	1	1	1	0	DUF418 domain-containing protein
1	1	1	1	0	alanine:cation symporter family protein
1	1	1	1	0	sulfite exporter TauE/SafE family protein
1	1	1	1	0	3-methyl-2-oxobutanoate hydroxymethyltransferase
1	1	1	1	0	pantoate--beta-alanine ligase
1	1	1	1	0	NAD(+)--rifampin ADP-ribosyltransferase
1	1	1	1	0	**helix-turn-helix transcriptional regulator**
2	2	2	6	0	IS3 family transposase
1	1	1	1	0	hypothetical protein
1	1	1	1	0	ABC transporter permease
1	1	1	1	0	ABC transporter permease
1	1	1	1	0	ABC transporter ATP-binding protein
1	1	1	1	0	**TetR/AcrR family transcriptional regulator**
1	1	1	1	0	hypothetical protein
1	1	1	1	0	N-acyl homoserine lactonase family protein
1	1	1	1	0	zinc-dependent alcohol dehydrogenase family protein
1	1	1	1	0	universal stress protein
1	1	1	1	0	ABC transporter ATP-binding protein
1	1	1	1	0	ATP-binding cassette domain-containing protein
1	1	1	1	0	YxeA family protein
1	1	1	1	0	DUF1430 domain-containing protein
1	1	1	1	0	lactococcin 972 family bacteriocin
1	1	1	1	0	sugar O-acetyltransferase
1	1	1	1	0	ABC transporter substrate-binding protein
1	1	1	1	0	**TetR/AcrR family transcriptional regulator**
1	1	1	1	0	HD domain-containing protein
1	1	1	1	0	SLC13/DASS family transporter

TMW 2.1023	TMW 2.1324	TMW 2.1521	TMW 2.1523	TMW 2.1602	Annotation (PGAP based)
1	1	1	1	0	S9 family peptidase
1	1	1	1	0	**AbrB family transcriptional regulator**
1	1	1	1	0	DNA internalization-related competence protein ComEC/Rec2
1	1	1	1	0	molecular chaperone DnaJ
1	1	1	1	0	hypothetical protein
1	1	1	1	0	hypothetical protein
1	1	1	1	0	DMT family transporter
1	1	1	1	0	DMT family transporter
1	1	1	1	0	**helix-turn-helix transcriptional regulator**
1	1	1	1	0	LysE family translocator
1	1	1	1	0	YqcI/YcgG family protein
1	1	1	1	0	rhodanese-like domain-containing protein
1	1	1	1	0	MarR family transcriptional regulator
1	1	1	1	0	DUF4865 family protein
1	1	1	1	0	**LysR family transcriptional regulator**
1	1	1	1	0	zinc ribbon domain-containing protein
1	1	1	1	0	HAD family hydrolase
1	1	1	1	0	DUF402 domain-containing protein
1	1	1	1	0	sugar phosphate isomerase/epimerase
1	1	1	1	0	Gfo/Idh/MocA family oxidoreductase
1	1	1	1	0	ThuA domain-containing protein
1	1	1	1	0	Gfo/Idh/MocA family oxidoreductase
1	1	1	1	0	**MurR/RpiR family transcriptional regulator**
1	1	1	1	0	PTS transporter subunit EIIC
1	1	1	1	0	threonine/serine exporter family protein
1	1	1	1	0	ASCH domain-containing protein
1	1	1	1	0	carboxymuconolactone decarboxylase family protein
1	1	1	1	0	DMT family transporter
1	1	1	1	0	PLP-dependent aminotransferase family protein
1	1	1	1	0	threonine--tRNA ligase
1	1	1	1	0	hypothetical protein
1	1	1	1	0	hypothetical protein
1	1	1	1	0	NmrA family protein
1	1	1	1	0	6-phospho-3-hexuloisomerase
1	1	1	1	0	3-hexulose-6-phosphate synthase
1	1	1	1	0	**helix-turn-helix transcriptional regulator**
1	1	1	1	0	PLP-dependent aminotransferase family protein
1	1	1	1	0	EamA family transporter
1	1	1	1	0	alcohol dehydrogenase catalytic domain-containing protein
1	1	1	1	0	excinuclease ABC subunit UvrA
1	1	1	1	0	type 1 glutamine amidotransferase
1	1	1	2	0	**MarR family transcriptional regulator**
1	1	1	2	0	YhgE/Pip domain-containing protein
1	1	1	2	0	amidase domain-containing protein
1	1	1	2	0	GA module-containing protein
1	1	1	1	0	type I toxin-antitoxin system Fst family toxin
1	1	3	1	0	plasmid mobilization relaxosome protein MobC
1	1	2	1	0	YitT family protein
1	1	1	1	0	replication initiator protein A
1	1	2	1	0	recombinase family protein
1	2	4	6	0	IS6-like element IS257 family transposase, partial

Appendix A 2 | Supplementary material corresponding to the publication of Schiffer *et al.* (2019): Bap and cell surface hydrophobicity are important factors in *Staphylococcus xylosus* biofilm formation

Table S1: General genome features of the chromosomes in *S. xylosus* | Note: this table has been updated, with information obtained from hybrid genomes, which have been assembled from long (PacBio) and short (Illumina) sequencing reads.

***S. xylosus* strain**	**TMW 2.1023**	**TMW 2.1324**	**TMW 2.1521**	**TMW 2.1523**	**TMW 2.1602**
total size [bp]	2,875,771	2,974,797	3,005,360	2,983,043	2,791,217
chromosome size [bp]	2,790,135	2,900,259	2,879,879	2,851,286	2,788,162
No. of plasmids	4	3	7	4	1
GC content [%]	32.75	32.88	32.66	32.68	32.88
Number of CDS	2,625	2,736	2,782	2,771	2,538
tRNA	59	60	59	59	59
rRNA (5S, 16S, 23S)	8, 7, 7	12, 11, 11	7, 6, 6	9, 8, 8	8, 7, 7
Coding density [%]	83.7	83.1	84.1	85.8	83.7
Isolation source	sausage	sausage	sausage	sausage	sausage

Table S2: relative comparison analysis of biofilm formation of *S. xylosus* shows whether biofilm intensity in a supplemented medium is inferior, equal or superior to the medium compared to. Statistically significant differences of means are marked by *. TSB^+ = TSB + 1% glucose, $NaCl^+$ = TSB + 1% glucose + 3% NaCl, $Lactate^+$ = TSB acidified to pH 6 by Lactate + 1% glucose.

strain	TMW 2.1023		TMW 2.1324		TMW 2.1521		TMW 2.1523		RP62A	
support	H.phob	H.phil	H.phob	H.phil	H.phob	H.phil	H.phob	H.phil	H.phob	H.phil
TSB:TSB^+	↓	↑	↑*	↑*	↑*	↑*	↓	↓*	↑*	↑*
TSB:$NaCl^+$	↓*	↑	↑*	↑*	↑*	↑*	↑*	↑	↑*	↑*
TSB:$Lactate^+$	↓*	↓	↑*	↑*	↑*	↑*	↑	↑	↓*	↓*
TSB^+:$NaCl^+$	↓	↓	↑	↓*	↑*	↓	↑*	↑*	↓*	↓*
TSB^+:$Lactate^+$	↓*	↓	↑	↓	↑*	↑*	↑	↑*	↓*	↓*
$NaCl^+$:$Lactate^+$	↓	↓	↓	↑	↑*	↑*	↓	↑	↓*	↓*

Figure S1: Phylogenetic tree of all available whole genome sequenced *S. xylosus* isolates based on their ANI values. Nucleotide substitutions per site are indicated by the bar.

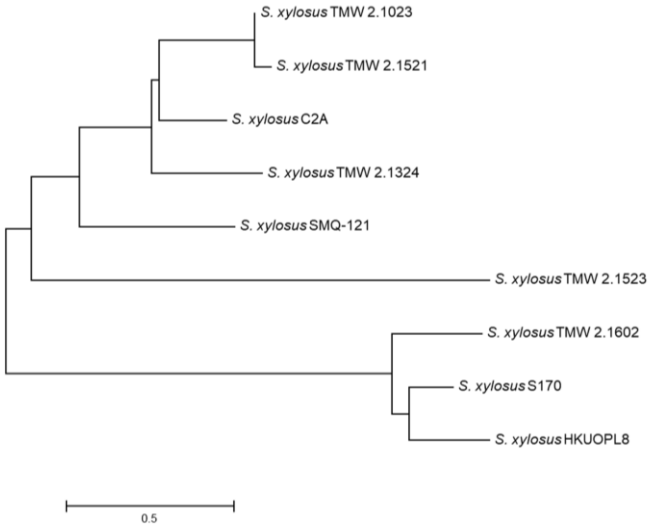

Appendix A 3 | Supplementary material corresponding to the publication Schiffer *et al.* (2021): Bap-Independent Biofilm Formation in *Staphylococcus xylosus*

Figure S1: Bap sequence alignment of selected *S. xylosus* strains with two Bap-dependent biofilm formers: *S. epidermidis* C533 and *S. aureus* V329. Only functionally important parts of the alignment are shown. A. shows the YSIRK-G/S signal peptide sequence as well the difference in A-region repeat length between *S. epidermidis*/*S. aureus* and *S. xylosus*. B. shows the sequence differences between the two amyloidprone peptides (defined by Taglialegna et al., [8]) of Bap Region B (marked in yellow). C. displays the conservation across species of EF hand domains 2 and 3 (pink). D. shows the differences in D-repeats between the species. While *S. aureus* and *S. epidermidis* region D is rich in SD repeats, *S. xylosus* encodes G-rich repeats.

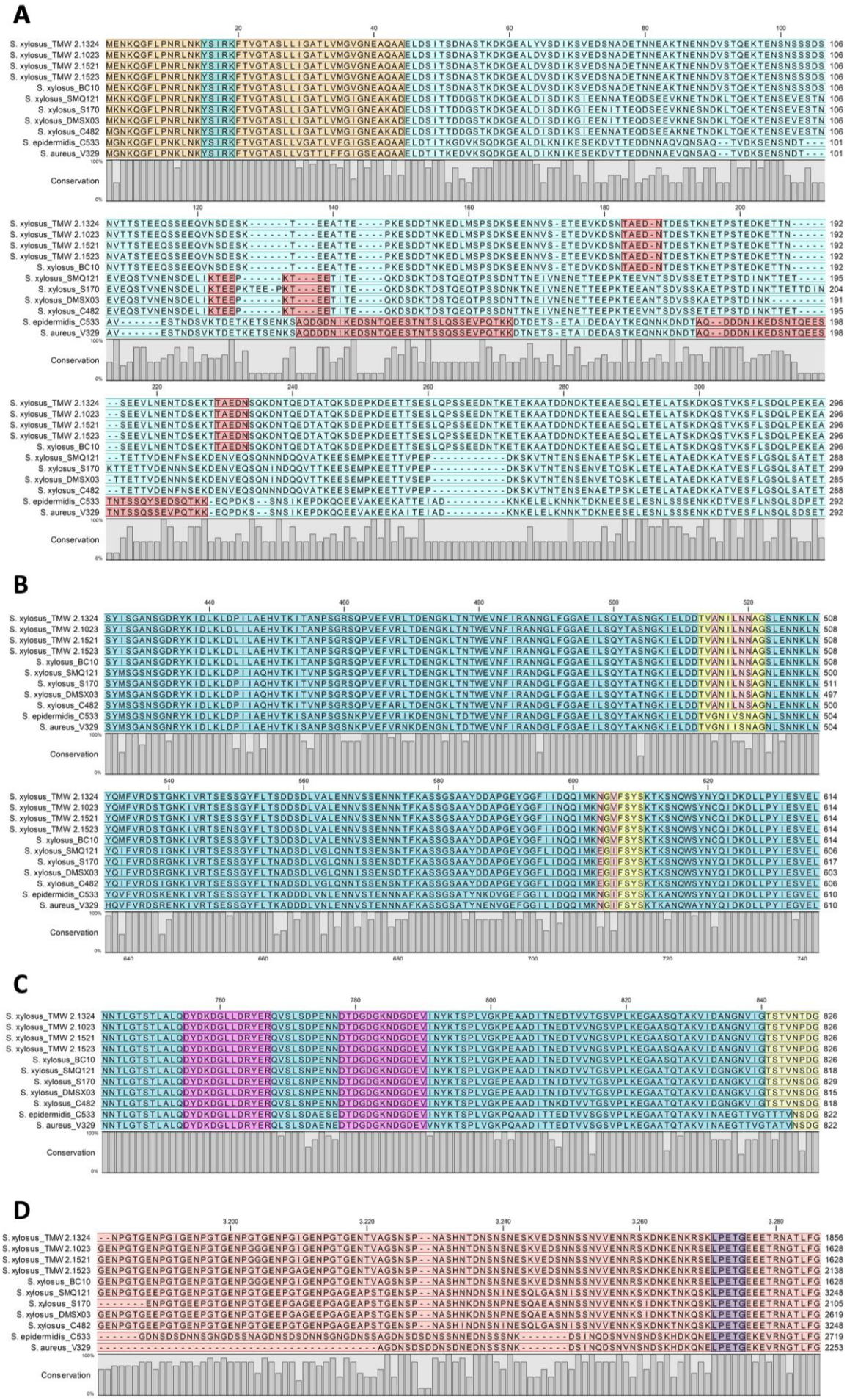
A
B
C
D
Conservation

Figure S2: Analysis of cell extract protein preparations on SDS-PAGE. Left: TMW 2.1523 wildtype (Wt) and mutant (Mt) strain, Right: TMW 2.1023 Wt and Mt. The black arrow indicates a possible location of Bap in TMW 2.1523 - Wt.

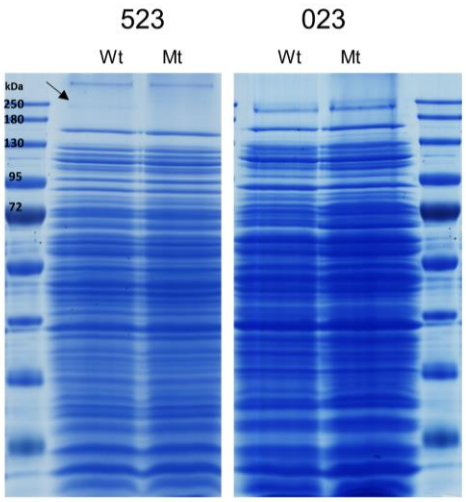

Figure S3: pH changes of *S. xylosus* TMW 2.1023 (grey) and 2.1523 (black) incubated in TSB$^+$ aerobically at 37 °C. Changes in pH were recorded over 12 hours, OD_{600} at t_0 was set to 0.1. Curves display the mean of 3 biological replicates.

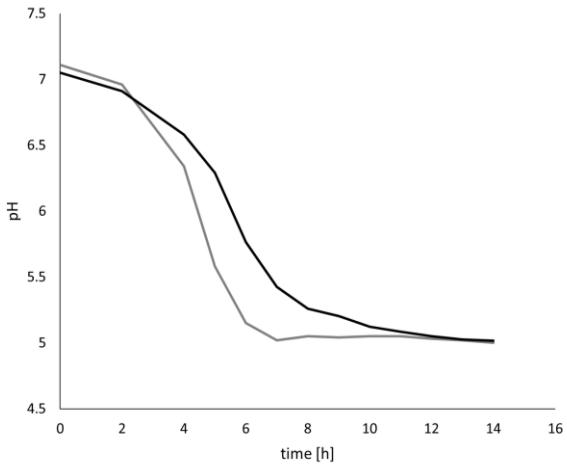

Figure S4: Calcium (20 mM) does not impair biofilm formation of selected *S. xylosus* strains (incubated in TSB$^+$, 24h, 37 °C, stained with safranin-O)

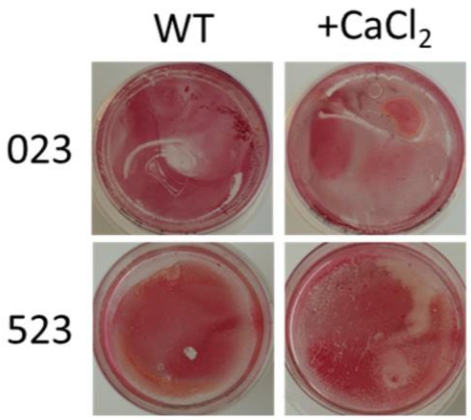

Figure S5: Boxplot of log_2 transformed LFQ-intensities measured for Bap in TMW 2.1023 (A) under planktonic and sessile conditions in Lac^+, for TMW 2.1523 (B) under planktonic and sessile conditions in Lac^+ and TSB_N.

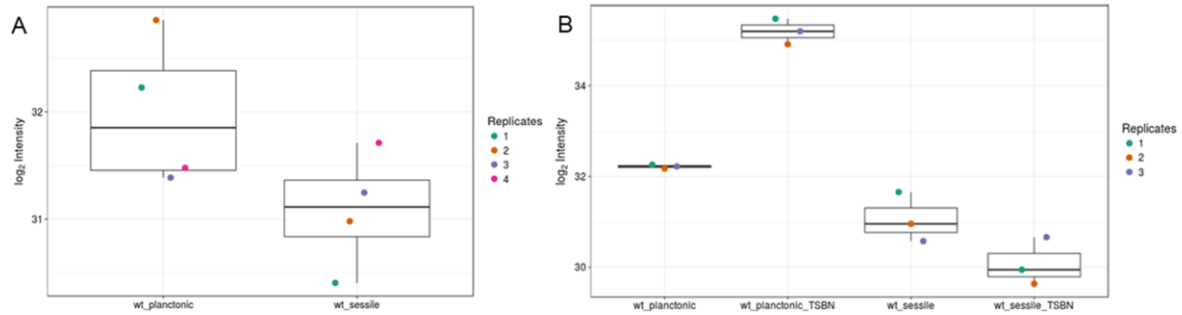

Figure S6: iBAQ-intensities of proteins expressed in TMW 2.1023 under planktonic (A) or sessile (B) conditions and TMW 2.1523 under planktonic Lac^+ (A), sessile Lac^+ (B), planktonic TSB_N (C) and sessile TSB_N (D) conditions. Bap is marked in red, highly abundant ribosomal proteins (50S) are marked in green for comparison.

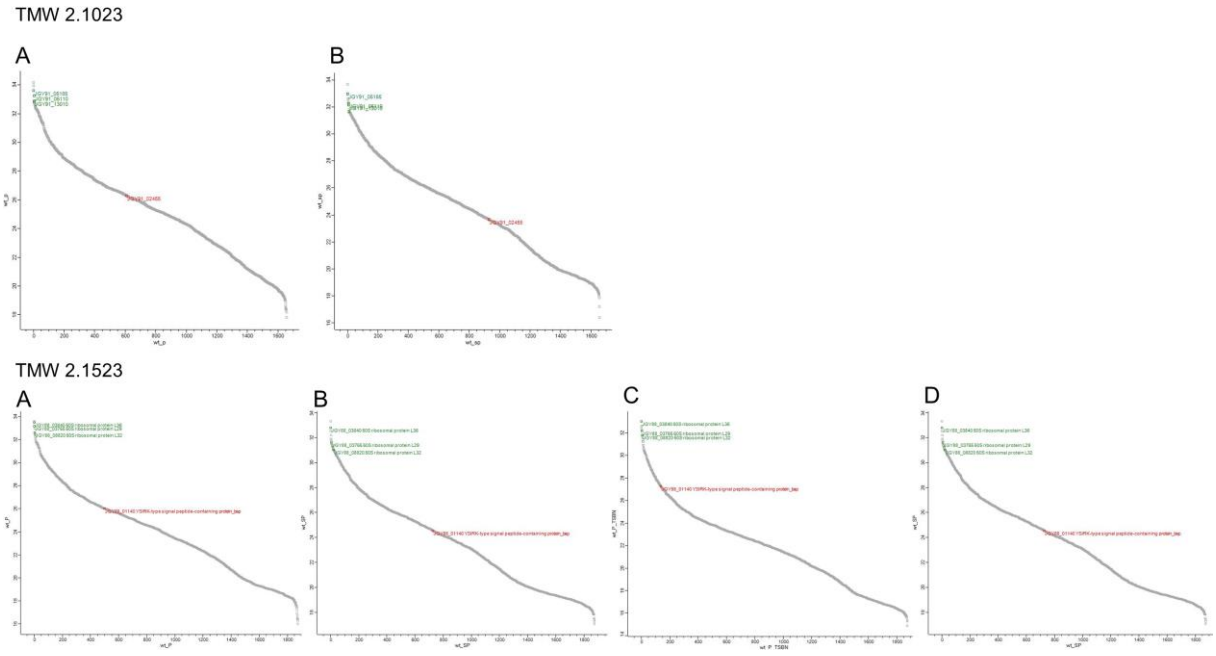

Table S1: Identified peptide sequences (intensity values) mapping on Bap in wildtype and mutant strains of TWW strains 2.1023 and 2.1523

identified peptide sequences mapping on Bap	start	end	WT_.023 Intensity	Mut_.023 Intensity	WT_.523 Intensity	Mut_.523 Intensity
AATDDNDKTEEAESQLETELATSK	254	277	437230000		825520000	
AEPNSSVTVGFPGGGK	970	985			32081000	
AMATPTALAAAADQSEEVEK	347	366	208800000		327180000	
ASLIELVNDQESAK	322	335			629790000	
DAEYDDQGNLIR	686	697	168230000		437700000	
DEETTSESLQPSSEEDNTK	231	249			11131000	
DKGEALDVSDIK	58	69	442310000		834900000	
DLLPYIESVELHK	604	616			39975000	
DLLPYIESVELHKYDYQGLSGFDK	604	627			51671000	
ESDDTNKEDLMSPSDK	137	152	51506000		95708000	
GLLINNTLGTSTLALQDYDKDGLLDR	717	742			390300000	
GLLINNTLGTSTLALQDYDKDGLLDRYER	717	745	592080000		655690000	
IELDDTVANILNNAGSLENNK	486	506	51193000		146510000	
IELDDTVANILNNAGSLENNKLNYQMFVR	486	514	177740000		218030000	
LDLILAEHVTK	420	430	280790000		363530000	
LIEFNNLLPETIGVR	656	670	310470000			
LNQSVNNILTK	675	685	137520000	75044000	269420000	
LTNTWEVNFIR	454	464	196220000		340010000	
NETPSTEDKETTNSEEVLNENTDSEK	180	205			51684000	
NGVFSYSK	582	589	76472000		112630000	
QKEDFTFAGYLTDSK	702	716	171600000		181760000	
QVSLSDPENNDTDGDGKNDGDEVINYK	746	772	242550000		377590000	
SDEPKDEETTSESLQPSSEEDNTK	226	249	97864000		173990000	
SDEPKDEETTSESLQPSSEEDNTKETEK	226	253	242560000		265260000	
SFLSDQLPEK	285	294	211740000			
SNQWSYNCQIDK	592	603			31703000	
SNQWSYNCQIDKDLLPYIESVELHK	592	616			58891000	
SNQWSYNCQIDKDLLPYIESVELHKYDYQGLSGFDK	592	627	119000000		212380000	
SQPVEFVR	439	446	174800000			
SVEDSNADETNNEAK	70	84	219120000		318450000	
TLATPTR	336	342	12563000		26559000	
TSPLVGKPEAADITNEDTVVNGSVPLK	773	799	46138000		190040000	
TSPLVGKPEAADITNEDTVVNGSVPLKEGAASQAAK	773	808			596210000	
TSPLVGKPEAADITNEDTVVNGSVPLKEGAASQTAK	773	808	392440000			
TTAEDNSQKDNTQEDTATQK	206	225	394100000		544760000	
VADLTLDDIGNGSITSDNLNK	635	655	110330000		213300000	
VEDSNNSSNVVENNR	2097	2111	36659000		28438000	
YDYQGLSGFDK	617	627	96400000		180680000	

Appendix A 4 | Supplementary material corresponding to the publication Schiffer *et al.* (2022a): SxsA, a novel surface protein mediating cell aggregation and adhesive biofilm formation of *Staphylococcus xylosus*

Figure S1: Growth dynamics recorded for TMW 2.1023 and TMW 2.1523 and their respective *sxsA* and *bap* mutant strains over a period of 33 hours. The curves display the mean of three independent replicates. For comparison reasons, the results for wildtype and bap mutant, already published in Schiffer et al., (2021), were included into the figures. ●wildtype, ● Δ*bap*, ● Δ*sxs*A, ● Δ*bap*,*sxs*A.

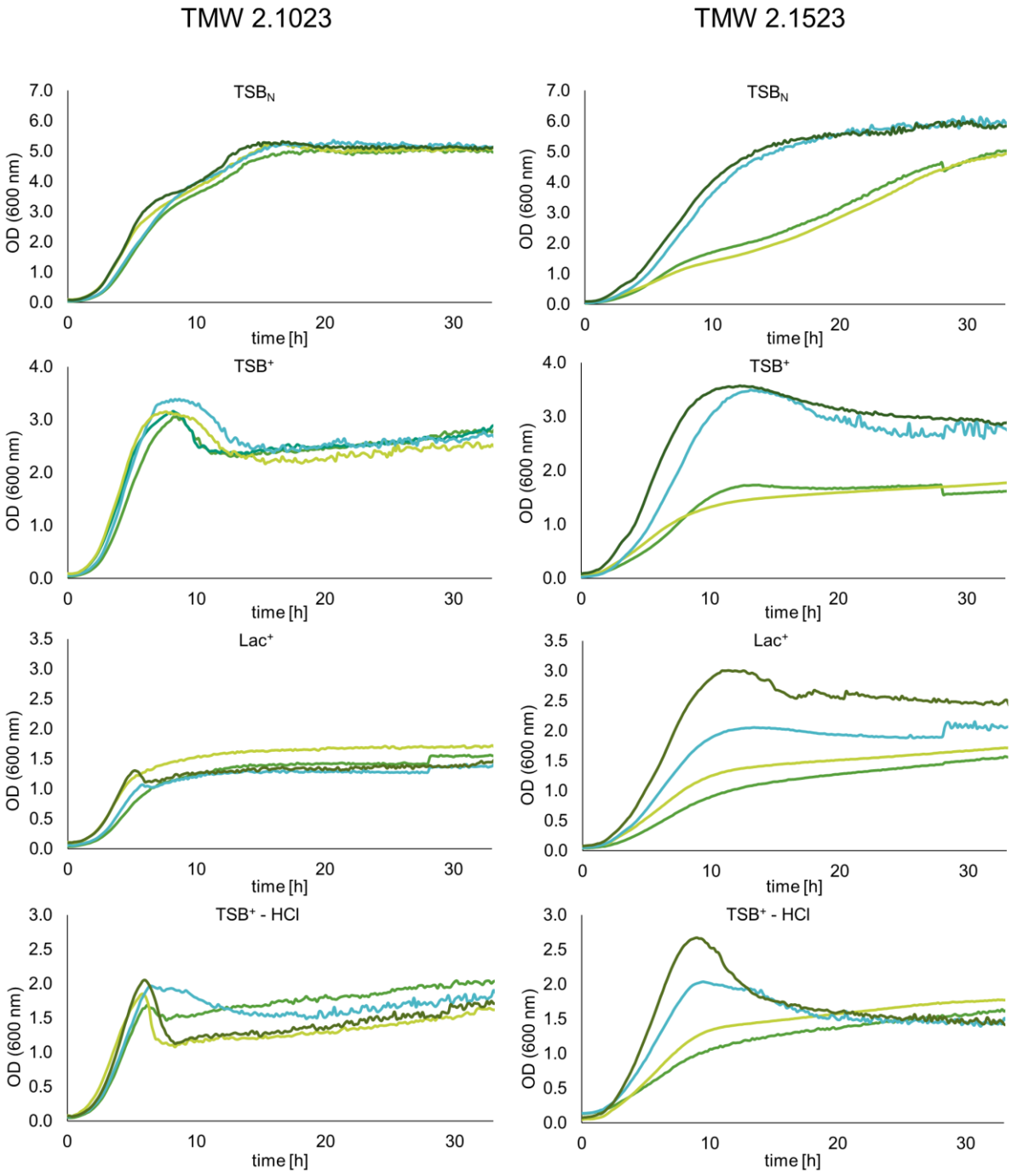

Figure S2: Biofilm formation on petridiscs of wildtype and mutant strains, incubated for 24 hours, stained with safranin-O.

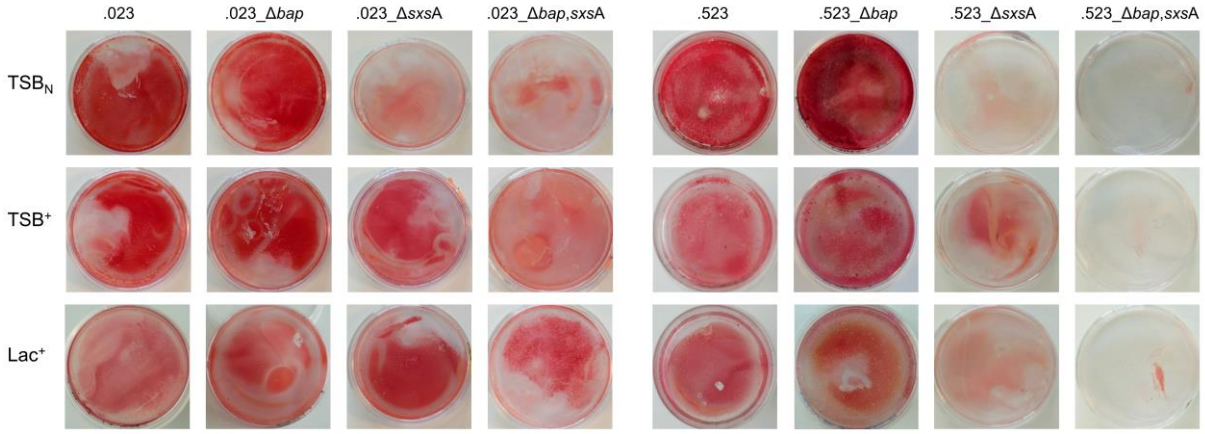

Figure S3: **Sedimentation assay for strain TMW 2.1023**. Macroscopic observation of cell settlement at different time points.

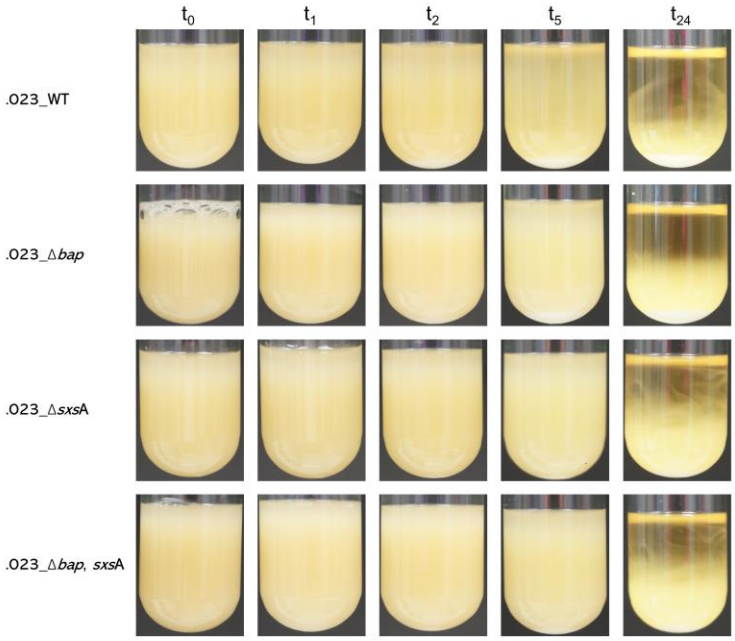

Figure S4: Planktonic growth of TMW 2.1023 and its *sxs*A deficient mutant in TSB_N and TSB^+ at two different growth stages.

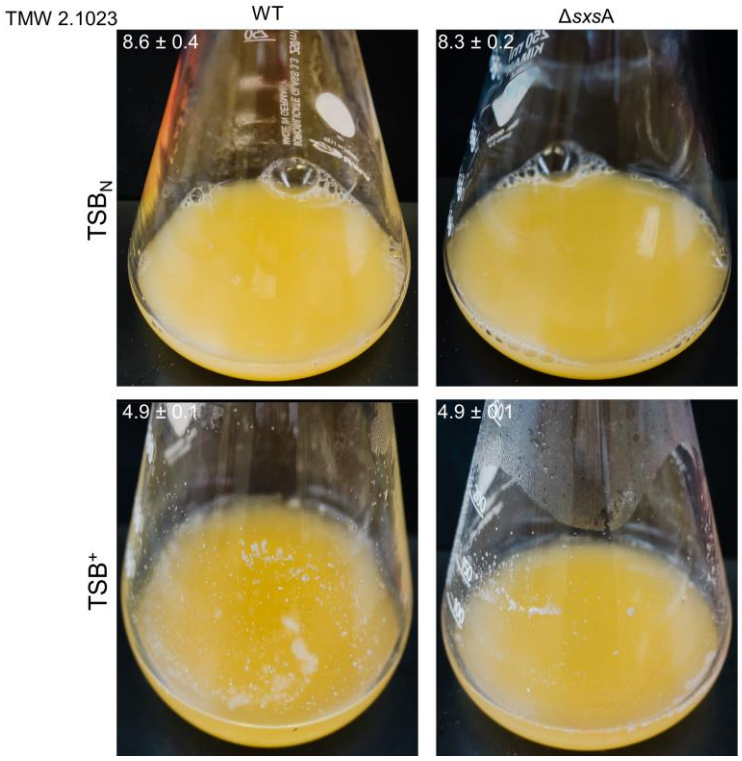

Figure S5: Colony morphology of wildtype and mutant strains on modified CRA, containing no glucose.

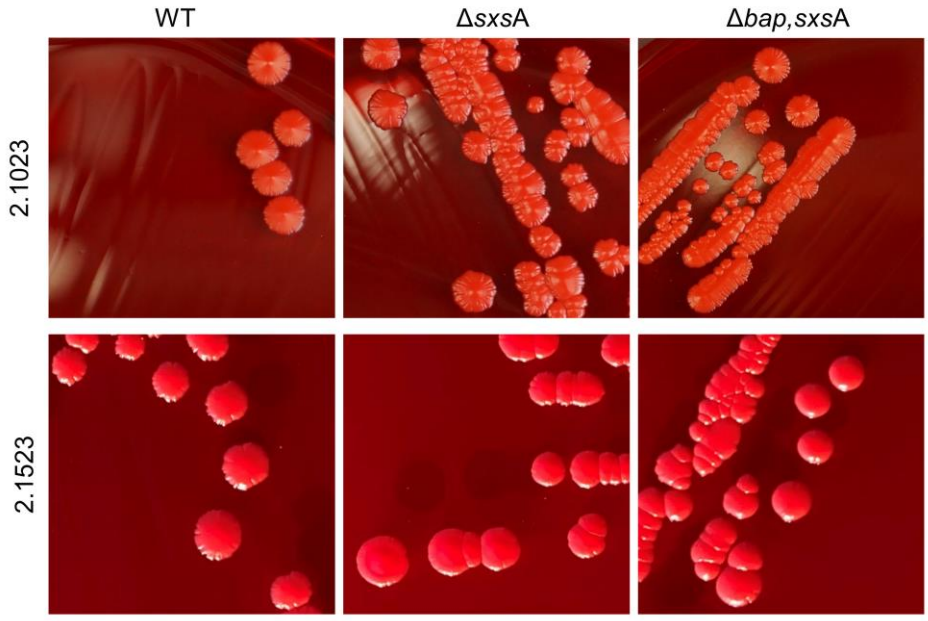

Figure S6: Pairwise comparison based on ClustalO alignment between SxsA and other well-known staphylococcal surface proteins (species, strain, protein name are stated in the labelling). Upper matrix (green) displays percentage identity between the protein sequences, lower matrix (red) shows the distance between the proteins.

		1	2	3	4	5	6	7	8	9	10	11	12	13
XYL_.523_sxsA	1		63,72	36,78	60,28	39,21	8,33	3,86	4,07	8,03	10,75	8,54	7,51	5,83
XYL_.023_sxsA	2	0,03		19,92	38,26	24,59	6,13	3,37	2,80	4,37	7,67	6,29	5,89	5,31
PXYL_S04009_sxsA	3	0,42	0,41		29,33	19,94	5,67	6,38	6,68	6,82	7,52	8,05	5,76	5,77
NEP_JS1_sxsA	4	0,44	0,46	0,58		42,88	7,93	3,87	3,72	8,38	12,02	9,92	7,40	5,54
COH_SNUC2486_sxsA	5	0,57	0,60	0,67	0,54		5,77	3,00	3,15	6,04	8,65	7,38	5,18	3,91
AUR_V329_bap	6	1,90	1,98	2,10	1,96	2,03		5,90	7,36	19,64	7,06	6,36	57,91	44,04
XYL_.023_sxsB	7	2,15	2,03	2,16	2,06	2,04	1,82		8,64	6,46	2,83	2,42	5,64	7,03
EPID_RP62A_aap	8	2,08	2,20	2,09	2,14	2,00	1,66	2,09		8,45	3,44	4,12	8,26	10,33
EPID_RP62A_bhp	9	1,94	2,11	1,99	1,94	2,02	1,19	1,85	1,55		6,86	7,10	19,41	14,59
AUR_Newman_fmtB	10	1,76	1,73	1,92	1,68	1,75	2,10	2,37	2,22	2,09		28,18	6,50	5,12
AUR_Col_SasC	11	1,91	1,87	1,91	1,79	1,82	2,17	2,75	2,13	2,00	1,13		6,46	5,50
XYL_.523_bap	12	1,95	1,96	2,13	1,97	2,10	0,47	1,96	1,58	1,22	2,15	2,15		73,28
XYL_.023_bap	13	1,97	1,95	2,02	2,03	2,13	0,47	1,97	1,59	1,26	2,16	2,02	0,04	

Figure S7: Overview of *sxs*A neighboring genes in different organisms. The transposase located close to *sxs*A in *S. cohnii* SNUC 2486 seems to be an exception as no nearby located transposase was found in any of the other *S. cohnii* genomes analyzed.

***S. xylosus* 2.1023**

Name	Description	Size (aa)
JGY91_02315	AEC family transporter	307
JGY91_02320	xylulokinase	495
JGY91_02325	thiamine phosphate synthase	194
JGY91_02330	FAD-dependent oxidoreductase	366
JGY91_02335	sulfur carrier protein ThiS	66
JGY91_02340	thiazole synthase	255
JGY91_02345	ThiF family adenylyltransferase	332
JGY91_02350	anaerobic ribonucleoside-triphosphate reductase	616
JGY91_02355	anaerobic ribonucleoside-triphosphate reductase ac	178
JGY91_02360	cholylglycine hydrolase family protein	327
JGY91_02365	**YSIRK-type signal peptide-containing protein sxsA**	2044
JGY91_02370	NAD(P)H-dependent oxidoreductase	188
JGY91_02375	LLM class flavin-dependent oxidoreductase	353
JGY91_02380	VOC family protein	308
JGY91_02385	GntR family transcriptional regulator	205
JGY91_02390	NAD-binding protein	291
JGY91_02395	hypothetical protein	458
JGY91_02400	gluconate permease	453
JGY91_02405	LysE family transporter	191

***S. xylosus* 2.1324**

Name	Description	Size (aa)
JGY90_00855	AEC family transporter	307
JGY90_00860	xylulokinase	495
JGY90_00865	thiamine phosphate synthase	194
JGY90_00870	FAD-dependent oxidoreductase	366
JGY90_00875	sulfur carrier protein ThiS	66
JGY90_00880	thiazole synthase	255
JGY90_00885	ThiF family adenylyltransferase	332
JGY90_00890	anaerobic ribonucleoside-triphosphate reductase	616
JGY90_00895	anaerobic ribonucleoside-triphosphate reductase ac	178
JGY90_00900	cholylglycine hydrolase family protein	327
JGY90_00905	**YSIRK-type signal peptide-containing protein sxsA**	2528
JGY90_00910	NAD(P)H-dependent oxidoreductase	188
JGY90_00915	LLM class flavin-dependent oxidoreductase	353
JGY90_00920	VOC family protein	308
JGY90_00925	GntR family transcriptional regulator	205
JGY90_00930	NAD-binding protein	291
JGY90_00935	hypothetical protein	458
JGY90_00940	gluconate permease	453
JGY90_00945	LysE family transporter	191

***S. paraxylosus* S04009**

Name	Description	Size (aa)
D9V42_RS029	LysE family transporter	191
D9V42_RS029	gluconate permease	453
D9V42_RS029	hypothetical protein	458
D9V42_RS029	NAD-binding protein	291
D9V42_RS029	GntR family transcriptional regulator	205
D9V42_RS029	VOC family protein	308
D9V42_RS029	LLM class flavin-dependent oxidoreductase	353
D9V42_RS029	NAD(P)H-dependent oxidoreductase	189
D9V42_RS029	**YSIRK-type signal peptide-containing protein_sxsA**	1752
D9V42_RS029	cholylglycine hydrolase family protein	327
D9V42_RS029	anaerobic ribonucleoside-triphosphate reductase ac	178
D9V42_RS029	anaerobic ribonucleoside-triphosphate reductase	616
D9V42_RS029	ThiF family adenylyltransferase	332
D9V42_RS029	thiazole synthase	255
D9V42_RS029	sulfur carrier protein ThiS	66
D9V42_RS029	FAD-dependent oxidoreductase	370
D9V42_RS030	thiamine phosphate synthase	194
D9V42_RS030	xylulokinase	495

***S. nepalensis* J51**

Name	Description	Size (aa)
BJD96_RS01090	DUF4064 domain-containing protein	188
BJD96_RS01095	helix-turn-helix domain-containing protein	273
BJD96_RS14540	hypothetical protein	55
BJD96_RS01100	AEC family transporter	307
BJD96_RS01105	anaerobic ribonucleoside-triphosphate reductase	616
BJD96_RS01110	anaerobic ribonucleoside-triphosphate reductase activating protein	176
BJD96_RS01115	cholylglycine hydrolase family protein	327
BJD96_RS01120	**YSIRK-type signal peptide-containing protein_sxsA**	3316
BJD96_RS01125	NAD(P)H-dependent oxidoreductase	188
BJD96_RS01130	LLM class flavin-dependent oxidoreductase	352
BJD96_RS01135	VOC family protein	308
BJD96_RS01140	ABC transporter ATP-binding protein	220
BJD96_RS01145	FtsX-like permease family protein	349
BJD96_RS01150	sulfite exporter TauE/SafE family protein	248
BJD96_RS01155	DUF2871 domain-containing protein	141
BJD96_RS01160	YSIRK-type signal peptide-containing protein	2141

***S. xylosus* 2.1521**

Name	Description	Size (aa)
JGY89_11315	LysE family transporter	191
JGY89_11320	gluconate permease	453
JGY89_11325	hypothetical protein	458
JGY89_11330	NAD-binding protein	291
JGY89_11335	GntR family transcriptional regulator	205
JGY89_11340	VOC family protein	308
JGY89_11345	LLM class flavin-dependent oxidoreductase	353
JGY89_11350	NAD(P)H-dependent oxidoreductase	188
JGY89_11355	**YSIRK-type signal peptide-containing protein sxsA**	2044
JGY89_11360	cholylglycine hydrolase family protein	327
JGY89_11365	anaerobic ribonucleoside-triphosphate reductase ac	178
JGY89_11370	anaerobic ribonucleoside-triphosphate reductase	616
JGY89_11375	ThiF family adenylyltransferase	332
JGY89_11380	thiazole synthase	255
JGY89_11385	sulfur carrier protein ThiS	66
JGY89_11390	FAD-dependent oxidoreductase	366
JGY89_11395	thiamine phosphate synthase	194
JGY89_11400	xylulokinase	495
JGY89_11405	AEC family transporter	307

***S. xylosus* 2.1523**

Name	Description	Size (aa)
JGY88_01000	AEC family transporter	307
JGY88_01005	xylulokinase	495
JGY88_01010	thiamine phosphate synthase	194
JGY88_01015	FAD-dependent oxidoreductase	366
JGY88_01020	sulfur carrier protein ThiS	66
JGY88_01025	thiazole synthase	255
JGY88_01030	ThiF family adenylyltransferase	332
JGY88_01035	anaerobic ribonucleoside-triphosphate reductase	616
JGY88_01040	anaerobic ribonucleoside-triphosphate reductase ac	178
JGY88_01045	cholylglycine hydrolase family protein	327
JGY88_01050	**YSIRK-type signal peptide-containing protein sxsA**	3123
JGY88_01055	NAD(P)H-dependent oxidoreductase	188
JGY88_01060	LLM class flavin-dependent oxidoreductase	353
JGY88_01065	VOC family protein	308
JGY88_01070	GntR family transcriptional regulator	205
JGY88_01075	NAD-binding protein	291
JGY88_01080	hypothetical protein	458
JGY88_01085	gluconate permease	453
JGY88_01090	LysE family transporter	191

***S. xylosus* 2.1602**

Name	Description	Size (aa)
JGY87_01040	AEC family transporter	307
JGY87_01045	xylulokinase	495
JGY87_01050	thiamine phosphate synthase	194
JGY87_01055	FAD-dependent oxidoreductase	366
JGY87_01060	sulfur carrier protein ThiS	66
JGY87_01065	thiazole synthase	255
JGY87_01070	ThiF family adenylyltransferase	332
JGY87_01075	anaerobic ribonucleoside-triphosphate reductase	616
JGY87_01080	anaerobic ribonucleoside-triphosphate reductase ac	178
JGY87_01085	cholylglycine hydrolase family protein	327
JGY87_01090	**YSIRK-type signal peptide-containing protein sxsA**	1946
JGY87_01095	NAD(P)H-dependent oxidoreductase	188
JGY87_01100	LLM class flavin-dependent oxidoreductase	353
JGY87_01105	VOC family protein	308
JGY87_01110	GntR family transcriptional regulator	205
JGY87_01115	NAD-binding protein	291
JGY87_01120	hypothetical protein	458
JGY87_01125	gluconate permease	453
JGY87_01130	LysE family transporter	191

***S. cohnii* SNUC 2486**

Name	Description	Size (aa)
BUY30_RS03950	thioredoxin family protein	106
BUY30_RS03955	transposase	141
BUY30_RS03960	nitroreductase	181
BUY30_RS03965	type I 3-dehydroquinate dehydratase	187
BUY30_RS03970	VOC family protein	308
BUY30_RS03975	LLM class flavin-dependent oxidoreductase	353
BUY30_RS03980	NAD(P)H-dependent oxidoreductase	188
BUY30_RS03985	**YSIRK-type signal peptide-containing protein_sxsA**	4467
BUY30_RS03990	cholylglycine hydrolase family protein	328
BUY30_RS03995	anaerobic ribonucleoside-triphosphate reductase activating protein	177
BUY30_RS04000	anaerobic ribonucleoside-triphosphate reductase	616
BUY30_RS04005	ThiF family adenylyltransferase	332
BUY30_RS04010	thiazole synthase	255
BUY30_RS04015	sulfur carrier protein ThiS	66
BUY30_RS04020	thiamine phosphate synthase	195
BUY30_RS04025	xylulokinase	495
BUY30_RS04030	winged helix-turn-helix transcriptional regulator	369

Figure S8: Neighbor joining tree showing the phylogenetic topology of all analyzed SxsA sequences (aa). Bap of *S. aureus* V329 was included as an outgroup. Species and Strain are stated, AUR = *S. aureus*, NEP = *S. nepalensis*, XYL = *S. xylosus*, PXYL = *S. pseudoxylosus*, COH = *S. cohnii*. Bar indicates 18% sequence divergence.

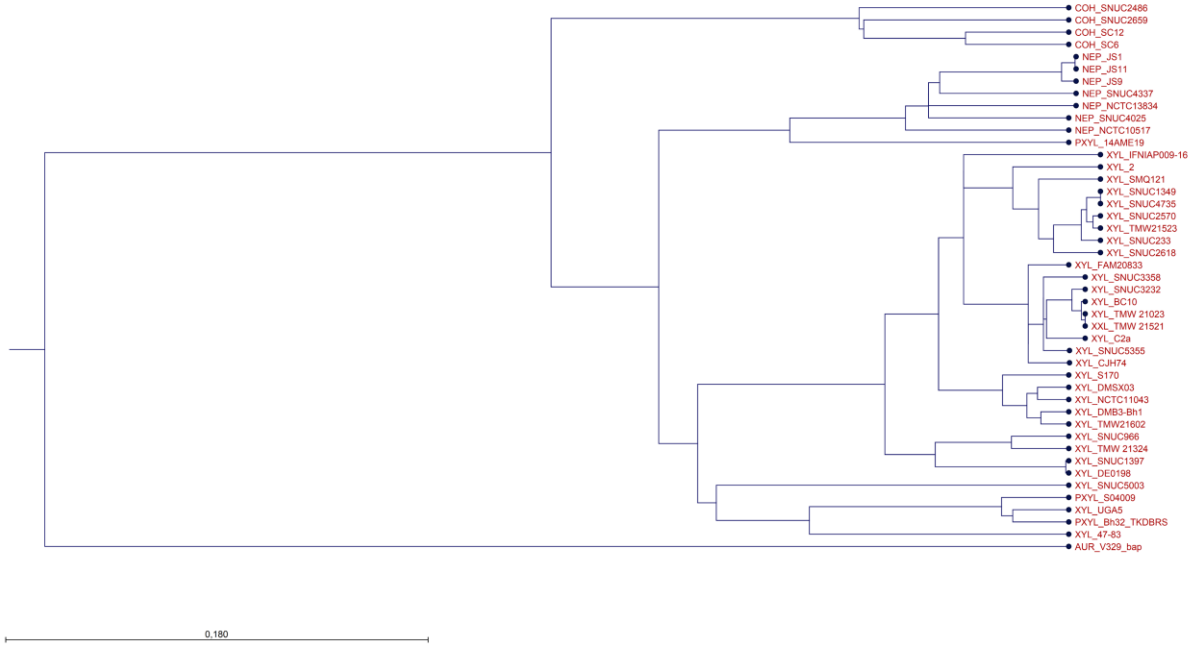

Figure S9: Overview of all analyzed SxsA sequences. Indicated are organism (XYL: *S. xylosus*, PXYL: *S. paraxylosus*, NEP: *S. nepalensis*, COH: *S. cohnii*), amyloid peptides (LGYYSY (red), LFGYILS (blue), EFVISFDASYYI (green), VKFYISFDA (violet), VLIATMVL (brightblue), C-region repeats (grey arrows), EF Hand motifs with > 80% sequence similarity (black arrow), YSIRK-G/S signal peptide and LPxTG cell wall anchor.

Figure S10: SxsA domain organization. Data which was used to predict structural division of SxsA genes for *S. xylosus* 2.1023, *S. pseudoxylosus* S04009, *S. nepalensis* JS1, *S. cohnii* SNUC2486. From left to right: Predicted, normalized amyloidogenic potential by four different algorithms, secondary structure prediction (α-helices (blue), β-sheet (red)) and predicted coiled-coil motifs.

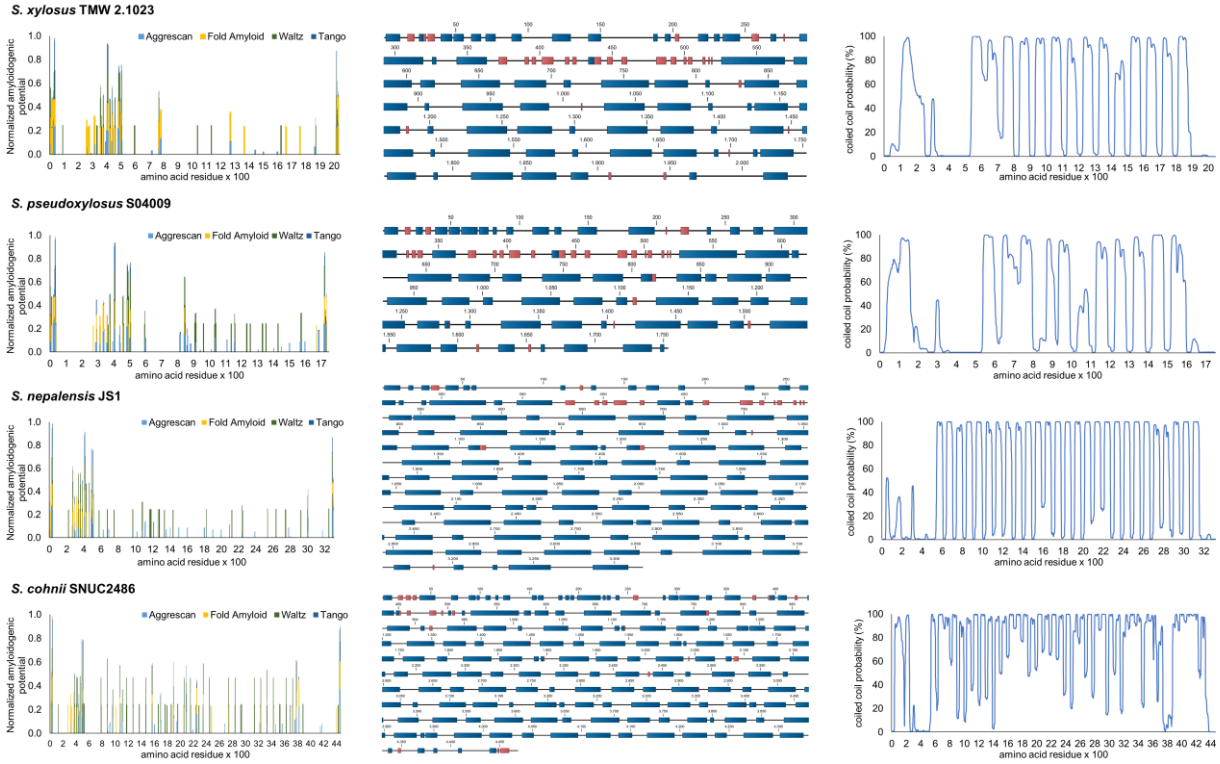

Table S1: LFQ intensities determined during full proteome analysis for two different *S. xylosus* strains in two different growth media (TSB_N and Lac^+). Indicated are gene identifier, log_2 fold change of intensity values, adjusted (Benjamini-Hochberg method) p-values and whether the change in expression between the compared conditions is considered as statistically significant ($\alpha = 0.05$, log_2 fold change > 1).

			SxsA	**Bap**
TMW 2.1023			JGY91_02365	JGY91_02455
	plankt. vs. sessile, Lac^+	log_2 fold change	2.51	0.901
		p.val (adj.)	0.06	0.16
		significant	FALSE	FALSE
TMW 2.1523			JGY88_01050	JGY88_01140-45
	plankt. vs. sessile, Lac^+	log_2 fold change	0.403	1.15
		p.val (adj.)	0.44	0.02
		significant	FALSE	***TRUE***
	plankt. vs. sessile, TSB_N	log_2 fold change	3.75	5.11
		p.val (adj.)	0.0002	0.00002
		significant	**TRUE**	**TRUE**
	Lac^+ vs TSB_N (plankt.)	log_2 fold change	-3.66	-2.97
		p.val (adj.)	0.0002	0.0001
		significant	**TRUE**	**TRUE**
	Lac^+ vs TSB_N (sessil)	log_2 fold change	-0.309	0.981
		p.val (adj.)	0.56	0.04
		significant	FALSE	FALSE

Table S2: In silico prediction of the largest proteins (size and MW) encoded by TMW 2.1023 and TMW 2.1523. Protein detection in whole proteome analysis of wildtype (W) and *sxs*A mutant strains (M) is further included into the Table. If the protein was detected, it is indicated as "y", if not as "n". "(y)" refers to Bap, which was measured in Δ*sxs*A samples, but not in Δ*sxs*A,*bap* mutants.

	Locustag	size (aa)	kDa	annotation	W	M
TMW 2.1023	JGY91_00830	5598	635	amino acid adenylation domain containing protein	n	n
	JGY91_02365	**2044**	**223**	**Staphylococcus xylosus surface protein A (SxsA)**	y	n
	JGY91_02455	1651	173	Biofilm-associated protein (Bap)	y	(y)
	JGY91_10530	1533	167	SH3-like domain containing protein	y	y
	JGY91_00330	1500	167	glutamate synthase large subunit	y	y
TMW 2.1523	JGY88_12995	5598	635	amino acid adenylation domain containing protein	n	n
	JGY88_01050	**3123**	**338**	**Staphylococcus xylosus surface protein A (SxsA)**	**y**	**n**
	JGY88_01140	2161	224	Biofilm-associated protein (Bap)	y	(y)
	JGY88_09360	1690	181	phage tail tape measure protein	n	n
	JGY88_00145	1575	180	DEAD/DEAH box helicase	y	y
	JGY88_09210	1574	171	glucosaminidase domain-containing protein	y	y

Table S3: Confirming deletion of the *sxs*A gene in TMW 2.1023 by full proteome analysis. Peptides mapping on SxsA are listed in wildtype as well as mutant strains.

Peptides on SxsA_2.1023	Start	End	WT	Δ*sxs*A_R1	Δ*sxs*A_R2	Δ*bap,sxs*A
LTESEETNK	96	104	28857000	0	33036000	33095000
GAQKHEQTSVNNEEEVK	105	121	7235100	0	0	0
GAQKHEQTSVNNEEEVKESQK	105	125	26553000	0	0	0
HEQTSVNNEEEVKESQK	109	125	24837000	0	0	0
SSDKITDNTNLKPEENDQYTVEQK	167	190	37253000	0	0	0
IESNSDINQANSLNLANLNNEIK	223	245	115810000	0	0	162370000
LSYDTVQSGDYITTALR	278	294	43756000	0	0	0
NRNELTEEERK	299	309	6648700	0	0	0
NELTEEERK	301	309	0	0	24744000	0
GVNITNQSVDIDDVAR	516	531	75514000	0	0	0
AEQAIEAAEQAK	545	556	20533000	0	0	0
IQEVIADGAVSPSEK	563	577	51308000	0	0	0
LSEVNSDGLITPSEKDEIDRLNQLLK	661	686	76388000	0	0	0
LSNVPEGTTGK	794	804	73428000	0	0	0
AIEAAEEAKR	1038	1047	8372500	0	0	0
LNNVTEGTTGK	1088	1098	43805000	0	0	0
LNNVPEGTTGK	1186	1196	89474000	0	0	0
LTEITSDGLVNPSEKVELDKLIE-ALDK	1445	1471	37733000	0	0	0
HTNINDHLDNSIR	1921	1933	46169000	0	0	0

Table S4: Confirming deletion of the sxsA gene in TMW 2.1523 by full proteome analysis. Peptides mapping on SxsA are listed in wildtype as well as mutant strains.

Peptides on SxsA_2.1523	Start	End	WT	Δ*sxs*A_R1	Δ*sxs*A_R2	Δ*bap,sxs*A
IDGNVSNIVNQK	84	95	101590000	0	0	0
LTESEETNK	96	104	23830000	40005000	99324000	51286000
GAQKHEQTSVNNEEEVKESQK	105	125	29945000	0	0	0
HEQTSVNNEEEVKESQK	109	125	44122000	0	0	0
SSDKITDNTNLKPEENDQYTVEQK	167	190	97155000	0	0	0
ITDNTNLKPEENDQYTVEQK	171	190	40046000	0	0	0
IESNSDINQANSLNLANLNNEIKK	223	246	64822000	0	0	0
YNSCFIDR	265	272	66360000	0	0	0
LSYDTVQSGDYITTALR	278	294	69788000	0	0	0
NRNELTEEERK	299	309	14824000	0	0	0
INQLLYK	352	358	71570000	0	0	0
FENYAIRPNPSLNKK	420	434	64176000	0	0	0
QVFAVYDGR	437	445	22393000	0	0	0
GVNITNQSVDIDDVAR	516	531	111410000	0	0	0
RINTALIK	532	539	55856000	0	0	0
INTALIK	533	539	29134000	0	0	0
KAEQAIEAAEQAK	544	556	27705000	0	0	0
IQEVIADGAVSPSEK	563	577	91179000	0	0	0
LSDVLDGASGK	598	608	98308000	0	0	0
AVQAAEEAQR	646	655	15777000	0	0	0
LSEVNSDGLITPSEK-DEIDRLNQLLK	661	686	122920000	0	0	0
ISTVTSPEVNDR	716	727	35484000	0	0	0
DGLINPSEK	765	773	93231000	0	0	0
DGLINPSEKGELDKLIEALDK	863	883	105480000	0	0	0
LIEALDK	877	883	55616000	0	0	0
LNNVPEGTTGK	892	902	232260000	0	0	0
LSNVPEGTTGK	990	1000	141590000	0	0	0
DGLINPR	1157	1163	50745000	0	0	0
EKDELDKLIEALDK	1164	1177	79462000	0	0	0
LTEITSDGLVNPR	1249	1261	99756000	0	0	0
EKAELDVLIEALDK	1262	1275	92904000	0	0	0
AELDKLIEALDK	1362	1373	103700000	0	0	0
LGNVPEGTAGK	1578	1588	27207000	0	0	0
LTEITSDGLVNPNEK	1935	1949	138080000	0	0	0
LDGIGTASSPEVNDK	1987	2001	36084000	0	0	0
AELDKLIEAVDK	2048	2059	25231000	0	0	0
EKAELDVLIEVLNDAK	2242	2257	18026000	0	0	0
DGLVNPSEKGELDVLIEALDK	2823	2843	38034000	0	0	0
HTNINDHLDNSIR	2999	3011	30829000	0	0	0

Table S5: Overview of SxsA sequences that were analyzed within the scope of this work. Information on originating species, NCBI-Locustag, size of the protein, signal peptide, cell wall anchor, number of EF hand motifs (cutoff 80%) and C-Repeats of SxsA are given. Of note is that only those strains are listed, in which *sxs*A was encoded as an entire ORF in the genome, not splitted on different contigs.

S. xylosus	**YSIRK**	**LPxTG**	**#EF hand motifs**	**# C-Repeats**	**Locustag**	**size (aa)**	**isolation source/host**
2	x	LPNTG	25	27	DWB98_RS00930	3416	Milker's hand, Brazil
47-83	x	LPDAG	9	8	BJT83_RS10880	1552	Bulk milk
BC10	x	LPNTG	11	12	AST17_RS11930	1848	Cheese rind
C2a	x	LPNTG	29	29	SXYL_RS00745	3612	human skin
CJH74	x	LPNTG	13	14	AST14_RS09025	2142	Raw cow's milk
DE0198	x	LPNAG	28	29	FS563_RS12705	3808	environmental
DMB3-Bh1	x	LPNTG	11	11	M920_RS0113465	1848	Meju, fermented soybean, s. korea
DMSX03	x	LPNTG	44	44	DMSX03_RS00850	5082	raw ham
FAM20833	x	LPNTG	30	31	FEZ53_RS09830	3808	Animal faecal matter (Panda)
INIFAP009-16	x	LPNAG	26	27	CW744_RS08425	3417	exudates from adult ticks
NCTC11043	x	LPNTG	22	22	DYA11_RS01025	2926	Homo sapiens,skin
S170	x	LPNTG	30	29	AWC37_RS11445	3612	leaf vegetable, south Korea
SMQ-121	x	LPNTG	12	13	SMQ121_RS00780	2044	meat starter, Canada
SNUC1349	x	LPNAG	6	6	BU104_RS08110	1359	Bos taurus,Herd 223
SNUC1397	x	LPNAG	27	28	BU105_RS03950	3504	Bos taurus,Herd 117
SNUC233	x	LPNAG	4	4	BU099_RS06820	1163	Bos taurus,Herd 108
SNUC2570	x	LPNAG	13	13	BU106_RS01075	2045	Bos taurus,Herd 303
SNUC2618	x	LPNTG	35	36	BU107_RS02600	4298	Bos taurus,Herd 315
SNUC3232	x	LPNTG	27	27	BU108_RS02500	3416	Bos taurus,Herd 226
SNUC3358	x	LPNTG	18	18	BU109_RS04910	2534	Bos taurus,Herd 318
SNUC4735	x	LPNAG	6	6	BU122_RS01375	1359	Bos taurus,Herd 226
SNUC5003	x	LPDTG	12	12	BU116_RS04320	1930	Bos taurus,Herd 306
SNUC5355	x	LPNTG	9	9	BU119_RS09800	1652	Bos taurus,Herd 314
SNUC966	x	LPNTG	12	11	BU102_RS02615	1842	Bos taurus,Herd 328
UGA5	x	LPDAG	16	19	CO206_RS11020	2534	Homo sapiens,pelvis
TMW21023	x	LPNTG	13	13	JGY91_02365	2044	raw fermented sausage
TMW21324	x	LPNTG	17	18	JGY90_00905	2528	raw fermented sausage
TMW21521	x	LPNTG	13	13	JGY89_11355	2044	raw fermented sausage
TMW21523	x	LPNAG	24	24	JGY88_01050	3123	raw fermented sausage
TMW21602	x	LPNTG	12	12	JGY87_01090	1946	raw fermented sausage
S. nepalensis							
NCTC10517	x	LPNTG	42	44	DX965_RS01105	5081	skin
SNUC4337	x	LPNTG	30	32	BUZ61_RS09615	3905	Bos taurus_Subclinical mastitis
SNUC4025	x	LPNTG	25	26	BUZ60_RS04215	3317	Bos taurus_Subclinical mastitis
NCTC13834	x	LPNTG	33	35	DYE02_RS01285	4199	Nepal: Chitwan; nasal mucosa
JS1	x	LPNTG	19	26	BJD96_RS01120	3317	Korean fermented food
JS11	x	LPNTG	22	29	BJG89_RS01480	3611	Korean fermented food
JS9	x	LPNTG	6	7	BJG88_RS01225	1455	Korean fermented food
S. cohnii							
SC12	x	LPYTG	35	33	HW365_RS10275	3537	Dairy farm
SC6	x	LPYTG	42	39	HW359_RS11815	4566	Dairy farm
SNUC2486	x	LPYTG	41	40	BUY30_RS03985	4468	Bos taurus_Subclinical mastitis
SNUC2659	x	LPYTG	42	40	BUY31_RS01485	4468	Bos taurus_Subclinical mastitis
S. pseudoxylosus							
14AME19	x	LPNTG	26	29	JMB28_RS01290	3614	Korean fermented soybean food
S04009	x	LPNSD	9	10	D9V42_RS02960	1753	bovine mastitis
Bh32_TKDBRS	x	LPDAG	6	6	HV358_RS09890	1361	milk

Appendix A 5 | Supplementary material corresponding to the publication Schiffer et al. (2022b): Characterization of the *Staphylococcus xylosus* methylome reveals a new variant of Type I restriction modification system

Figure S1: Pairwise comparison matrix based on Clustal-O alignments of *hsd*M (A) and *hsd*R (B) genes investigated in the scope of this study. Reference genes for type I family A - E were included. Percent identity (upper) and distance (lower matrix) values are shown in green and red, respectively.

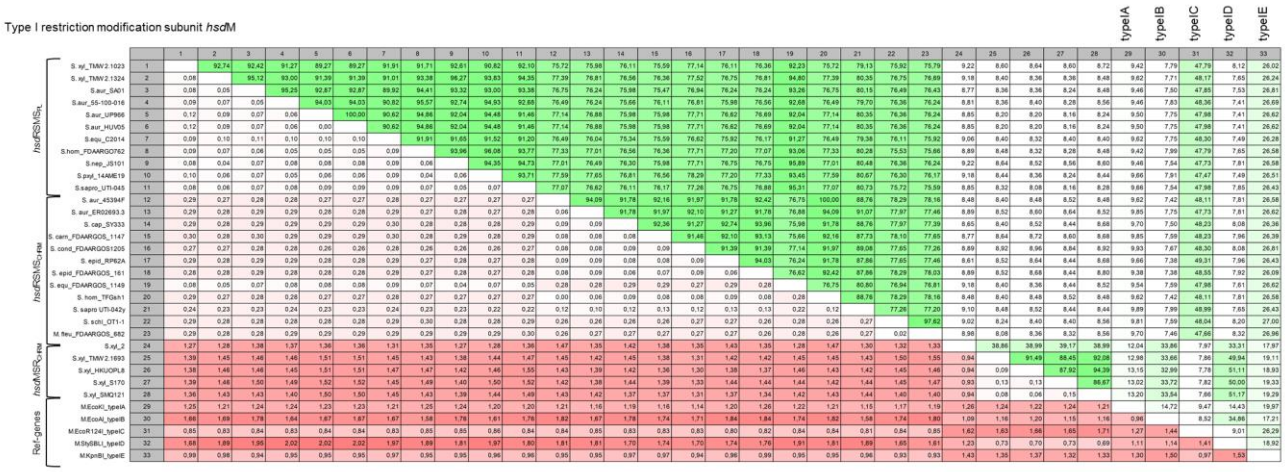

Figure S2: Neighbor joining tree of *hsd*R from type I RM systems of different bacterial organisms and strains. The turquoise group represents *hsd*R genes of *hsd*RMS$_{PL}$ systems, the green group belongs to *S. xylosus* chromosomal *hsd*MSR systems and the group in rose encompasses *hsd*R genes of *hsd*RMS$_{CHRM}$ systems. *Hsd*R of *S. equorum* FDAARGOS_1149 is chromosomally encoded but clusters with the plasmid-based group. Reference genes of type I systems (A-E) were included into the Figure. The bar indicates 50% sequence divergence.

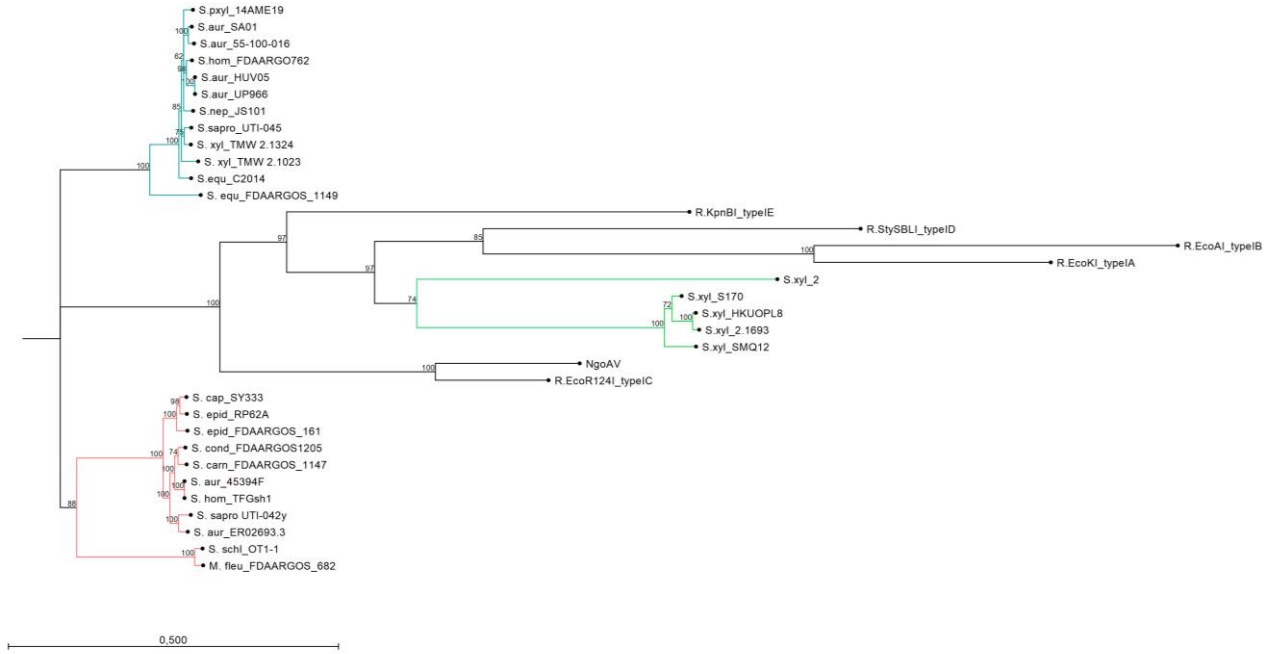

Figure S3: Restriction digest (SfaNI) of plasmid (pIMAY*) isolated from *E. coli* strain expressing the *S. xylosus* TMW 2.1324 Type II methyltransferase from different promotors (P_{bla}, P_{N25}).

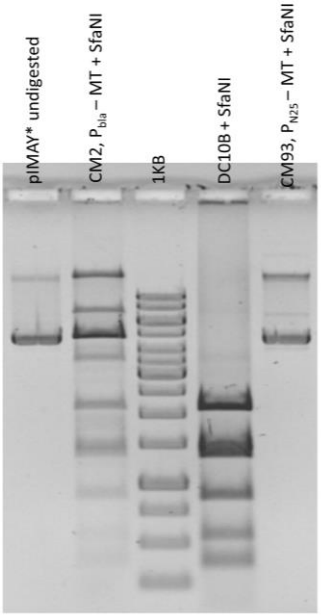

Table S1: Proteomic expression of methyltransferases and restriction enzymes in two selected *S. xylosus* strains (TMW 2.1023 and TMW 2.1523). Label free quantification (LFQ) intensity values in (log_2) and mean of 3 replicates determined under planktonic growth in TSB-Lac$^+$ (1% Glucose, acidified to pH 6 (lactic acid)) are indicated. The data was derived from a whole proteome analysis conducted by Schiffer et al. (31).

	Locus_Tag	annotation	LFQ intensity
TMW 2.1023	JGY91_01640	type I restriction modification subunit M	-
	JGY91_13160	type I restriction endonuclease subunit S	29.10
	JGY91_13165	type I restriction modification subunit M	32.20
	JGY91_13170	type I restriction endonuclease subunit S	27.65
	JGY91_13175	type I restriction endonuclease subunit R	29.51
TMW 2.1523	JGY88_00145	DEAD/DEAH box helicase (type IIG)	30.32

Table S2: Base modification and motif analysis output generated by SMRT link for whole genome sequenced *S. xylosus* strains. In grey are motifs that are probably artifacts / non-genuine as the mean modification QV values are mostly below 50.

strain	motifString	type	centerPos	modificationType	fraction	nDetected	nGenome	meanQV	Mean Coverage
TMW 2.1693	GCTCA	III	5	m6A	0.88	2779	3158	416.4	317.4
	GACN$_5$TGT	I	2	m6A	0.86	649	759	402.2	316.7
	ACAN$_5$GTC	I	3	m6A	0.86	656	759	391.1	314.1
TMW 2.1704	-								
TMW 2.1780	GGGTNA	II	6	m6A	0.91	2191	2410	326.4	239.7
TMW 2.1023	TCA N$_6$ CTC	I	3	m6A	1.00	652	652	84.1	51.6
	GAG N$_6$ TGA		2	m6A	1.00	651	652	79.3	49.4
TMW 2.1324	GCATC	II	3	m6A	0.99	4572	4595	132.7	91.6
	GATGC		2	m6A	0.99	4574	4595	128.9	91.6
	ACCN$_5$RTGT	I	1	m6A	1.00	597	597	122.3	90.5
	ACAYN$_5$GGT		3	m6A	0.98	586	597	126.0	91.6
	GATGCAVY		3		0.41	268	648	41.4	93.8
	SGGTAVYDNB		2		0.22	210	926	46.6	98.1
TMW 2.1521	GGGTNA	II	6	m6A	1.00	2354	2356	166.9	118.5
	GGGTRA		1		0.68	754	1114	62.3	122.4
	GGGTAAYD		2		0.55	142	257	49.9	122.2
	DNNNNNNGGGGTAM		8		0.63	94	149	51.5	127.2
	GGGTYA		1		0.19	241	1242	45.3	129.6
	GGGTYAAAW		2		0.61	57	93	50.3	130.0
	GGGTNAAV		7		0.25	140	558	40.1	122.8
	SGTATAVCR		3		0.28	61	221	47.9	124.2
	KTTTATACY		2		0.20	58	283	43.7	132.1
	AAATATANYA		2		0.16	78	495	39.9	122.5
TMW 2.1523	GGGTNA	II	6	m6A	0.81	1866	2300	160.5	113.8
	GGGTRA		1		0.57	610	1077	62.3	118.2
TMW 2.1602	CACCG	III ?	4	m4C (?)	0.92	1590	1728	64.5	95.2
	SGTRTAVCR		3		0.26	112	426	45.3	115.5

Table S3: CRISPR/Cas systems identified in *S. xylosus* TMW 2.1023 and TMW 2.1324.

CRISPR systems 2.1023

Start	End	Repeat consensus / cas genes	spacer
535371	535471	GGAAATCAACAAGTTACAGATGGTTT	GAAACAGTTAGAACCTGCAGTAGGACAGCCTGCACAACAGTTGATTTCA
1486240	1486321	ATATTTAATTTGTGAAATAAATCACA	AAATCATTGCAATTTTCTATATACCCTGTT
2282325	2282413	GTAAGAGTCACTAACTCAATTTATTG	TGAGTGATGGTTCGTTCACCTGAGCTTTCGCTCATGC

CISPPR systems 2.1324

191561	191661	GGAAATCAACAAGTTACAGATGGTTT	GAAACAGTTAGAACCTGCAGTAGGACAGCCTGCACAACAGTTGATTTCA
965691	965789	AAGCGACACTAATCCAAATAAATTTGGAAGTGT	ATAGAGGAACGCCTTAGCTTAAAGCCAAAGCAT
1193379	1193484	TATTTAATTTGTGAAATAAATCACA	TATTTAATTTGTGAAATAAATCACAAAATCATTGCAATTTTCTATATACCCTGTTA

9 Publications and supervised student projects

List of publications and presentations at academic symposia

Schiffer, C. J., Vogel, R. F., and Ehrmann, M. A. (2022). Characterization of the *Staphylococcus xylosus* methylome reveals a new variant of Type I restriction modification system. Submitted to *Journal of Bacteriology* on January 25th, currently under review.

Widenmann, A., **Schiffer, C. J.**, Ehrmann, M. A., and Vogel, R. F. (2022). Impact of different sugars and glycosyltransferases on the assertiveness of *Latilactobacillus sakei* in raw sausage fermentations. *Int J Food Microbiol*. 366, 109575.

Schiffer, C. J., Schaudinn, C., Ehrmann, M. A., and Vogel, R. F. (2022). SxsA, a novel surface protein mediating cell aggregation and adhesive biofilm formation of *Staphylococcus xylosus*. *Mol Microbiol*. 117, 986 - 1001.

Schiffer, C. J., Abele, M., Ehrmann, M. A., and Vogel, R. F. (2021). Bap-Independent Biofilm Formation in *Staphylococcus xylosus*. *Microorganisms* 9, 2610.

Schiffer, C., Hilgarth, M., Ehrmann, M., and Vogel, R. F. (2019). Bap and cell surface hydrophobicity are important factors in *Staphylococcus xylosus* biofilm formation. *Front. Microbiol.* 10, 1387.

Schiffer, C. (2019). Genomic and physiological characterization of biofilm formation in *Staphylococcus xylosus*; 26.05-30.05.2019, BAGECO, Lisbon. Poster presentation.

List of supervised student projects

Anna Widenmann (2020): Role of glycosyltransferases in the assertiveness of *Latilactobacillus sakei* in raw sausage fermentation [master's thesis]

Adrian Thaqi (2020): Establishment of a marker-free knockout system for *Staphylococcus xylosus* for the generation and characterization of *bap*- and *ure*- deficient *S. xylosus* mutant mutants [master's thesis]

Adrian Thaqi (2019): Study on the transformability of *Staphylococcus xylosus* [research internship]

Martina Dannecker (2019): Durchsetzungsfähigkeit von *Staphylococcus xylosus* während der Rohwurstfermentation [master's thesis]

Anna Widenmann (2020): Evaluierung der Virulenz von *Staphylococcus xylosus* [student seminar]

Nadine Skubala (2020): Evaluierung der Virulenz von *Staphylococcus warneri* [student seminar]

10 Acknowledgements

Die vorliegende Arbeit wurde durch Fördermittel des Forschungskreises der Ernährungsindustrie (FEI) unterstützt (Projekt AiF 19690 N).

Mein besonderer Dank gilt allen Personen, die mich während meiner Doktorarbeit unterstützt haben und insbesondere:

meinem Doktorvater Prof. Dr. Rudi Vogel für die Möglichkeit, diese Dissertation an seinem Institut durchzuführen. Vielen Dank für das stetige Vertrauen, die Geduld, die wissenschaftlichen Freiheiten, die viele Zeit und dafür, dass jede Diskussion mit einer positiven Botschaft endete. Danke, dass du auch in anstrengenden Zeiten die Übersicht behalten hast und dafür, dass du mich mit deiner „Vorwärtsgang"-Mentalität stets gefordert hast und wir dadurch viele spannende Entdeckungen machen konnten.

meinem Mentor, Prof. Dr. Matthias Ehrmann, dessen Tür ebenfalls immer offenstand und der mir in schwierigen Situationen stets unterstützend und tatkräftig zur Seite stand. Danke für jedes gemeinsame Experiment, all die Lehren im Labor, die Kreativität und die Freude am Forschen.

Ebenfalls möchte ich mich bei allen anderen Kollegen des Instituts bedanken, insbesondere auch Prof. Dr. Ludwig Niessen, Dr. Maik Hilgarth und Dr. Frank Jakob für ihre wissenschaftliche Unterstützung. Auch bedanke ich mich für die organisatorische Unterstützung und die Hilfe im Labor bei Margarethe Schreiber, Monika Engel, Johanna Hainzinger und Angela Seppeur.

Dr. Christoph Schaudinn möchte ich für den lehrreichen Austausch danken und die wunderbaren Mikroskop-Aufnahmen der Staphylokokken, die uns allen so viel Freude bereitet haben.

Allen Mitdoktoranden und Studenten aber insbesondere Max, Meike, Jonas, Alex, Luca, Juli, Manu, Anna, Lena und Esther danke ich für die vielen spaßigen Stunden im Büro und im Labor.

Außerhalb des Labors gilt mein größter Dank den Schiffers und den Buhmäns, meinen Freunden und meinem Freund. Danke, für all die schönen und lustigen gemeinsamen Zeiten, dafür, dass ich mich immer auf euch verlassen kann, ihr stets hinter mir steht und mich in allem unterstützt.